

INFORMATION TO USERS

This manuscript has been reproduced from the microfilm master. UMI films the text directly from the original or copy submitted. Thus, some thesis and dissertation copies are in typewriter face, while others may be from any type of computer printer.

The quality of this reproduction is dependent upon the quality of the copy submitted. Broken or indistinct print, colored or poor quality illustrations and photographs, print bleedthrough, substandard margins, and improper alignment can adversely affect reproduction.

In the unlikely event that the author did not send UMI a complete manuscript and there are missing pages, these will be noted. Also, if unauthorized copyright material had to be removed, a note will indicate the deletion.

Oversize materials (e.g., maps, drawings, charts) are reproduced by sectioning the original, beginning at the upper left-hand corner and continuing from left to right in equal sections with small overlaps. Each original is also photographed in one exposure and is included in reduced form at the back of the book.

Photographs included in the original manuscript have been reproduced xerographically in this copy. Higher quality 6" x 9" black and white photographic prints are available for any photographs or illustrations appearing in this copy for an additional charge. Contact UMI directly to order.

UMI

**A Bell & Howell Information Company
300 North Zeeb Road, Ann Arbor MI 48106-1346 USA
313/761-4700 800/521-0600**

RICE UNIVERSITY

**Vector Basis Function Solution of Maxwell's
Equations**

by

Dipankar Sarkar

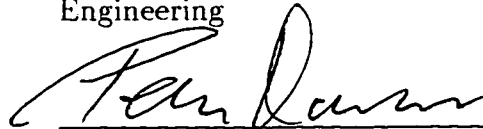
A THESIS SUBMITTED
IN PARTIAL FULFILLMENT OF THE
REQUIREMENTS FOR THE DEGREE

Doctor of Philosophy

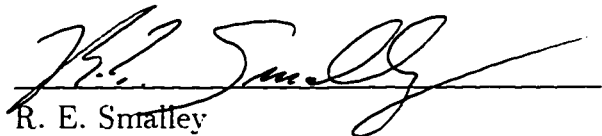
APPROVED. THESIS COMMITTEE:



Naomi J. Halas, Director
Associate Professor of Electrical
Engineering



Peter Nordlander
Associate Professor of Physics



R. E. Smalley
Professor of Chemistry and Physics

Houston, Texas

September, 1996

UMI Number: 9727599

UMI Microform 9727599
Copyright 1997, by UMI Company. All rights reserved.

**This microform edition is protected against unauthorized
copying under Title 17, United States Code.**

UMI
300 North Zeeb Road
Ann Arbor, MI 48103

Vector Basis Function Solution of Maxwell's Equations

Dipankar Sarkar

Abstract

A general technique for solving Maxwell's equations exactly, based on expansion of the solution in a complete set of vector basis functions has been developed. These vector eigenfunctions are derived from the complete set of separable solutions to the scalar Helmholtz equation in a particular coordinate system and are shown to form a complete set. The method is applicable to a variety of problems including the study of near and far field electromagnetic scattering from particles with arbitrary shapes, plasmon resonances in spherical nanoparticles with spherically concentric 'shells' and the calculation of plasmon resonances in the sphere-plane geometry. An exact method for solving the inhomogenous Maxwell's equations (i.e., in the presence of charges and currents) is also outlined.

Acknowledgments

The set of all words and phrases do not form a complete set. In other words, any arbitrary emotion/idea may not be expressible in a convergent sequence/series of sentences. Given the incompleteness of our linguistic universe, I may not succeed in expressing the total sense of my gratitude towards every person or thing who provided me with the opportunity and motivation to be a scientist. Furthermore, the process of enumeration of names is unfair, since it implies a hierarchical sequence which is strictly unintentional:

- Naomi Halas, and Peter Nordlander for providing me with the opportunity and motivation to work on this topic.
- My colleagues Richard Averitt, Kevin Kelly, Steve Oldenburg, Gregory Hale, Sarah Westcott, Scott Stokes, Daniel Wolfe and Tasshi Dennis, for all the help I ever required, including 'lending' computer accounts, debugging my codes, obtaining print-outs, or just plain listening to me!
- Terrence L. Graham and Bruce Brinson for keeping up with my odd requests at all sorts of odd times.

Finally, I would like to express my love and gratitude to my parents, my teachers, and 3D, who have always provided me the encouragement and inspiration to become a scientist.

Contents

Abstract	ii
Acknowledgments	iii
List of Illustrations	vii
Preface	xii
Dedication	xiii
1 Introduction	1
1.1 Historical Development	2
1.2 Outline of The Thesis	4
2 General Solution of Maxwell's Equations	6
2.1 Introduction	6
2.2 Linear Homogenous Isotropic Medium	7
2.3 Solution Space of Vector Helmholtz Equation	8
2.4 Completeness of Vector Eigenfunctions	11
2.4.1 Completeness of the L, M, N set	13
2.4.2 Zero Divergence Solutions	15
2.5 Boundary Conditions for Time-Varying Fields	15
3 Plane Wave Expansion in Basis Functions	20
3.1 Introduction	20
3.2 The L.M.N basis	20
3.3 Orthogonal Properties of L, M and N Functions	25
3.4 Plane Wave Expansion in L, M, N Basis	29
3.4.1 Deriving a_{mn}^z, b_{mn}^z and c_{mn}^z	30
3.4.2 Deriving a_{mn}^x, b_{mn}^x and c_{mn}^x	33
3.4.3 Deriving a_{mn}^y, b_{mn}^y and c_{mn}^y	35
3.4.4 Numerical Convergence of Basis Function Expansion	37
3.5 Numerical Evaluation of L_{mn}, M_{mn} and N_{mn}	39

4	Shell Problem	43
4.1	Introduction	43
4.2	The Model	43
4.3	Expansion Coefficients of the Scattered Wave	47
4.4	Poynting Vector Calculations	51
4.5	Numerical Calculations of Total Cross-Section	55
4.6	Test Dielectric Functions	56
	4.6.1 C60 Coated Gold Nanoparticles	58
4.7	Plasmon Resonance in Gold-Sulfide Systems	61
5	Scattering From Non-Spherical Objects	66
5.1	Introduction	66
5.2	The Model	67
	5.2.1 Convergence Consideration	68
5.3	Expansion in positive m only	69
5.4	Boundary Condition Equations	73
5.5	Solving the Boundary Condition Equations	76
5.6	The Sphere-Plane Model	80
	5.6.1 Fresnel's Formulae	87
	5.6.2 The Boundary Condition Matrix	89
	5.6.3 Field on the z -axis	90
	5.6.4 Plasmon Resonances in The Sphere-Plane Model	92
6	Conclusion	97
6.1	Transient Excitation	97
6.2	Related Problems	98
6.3	Antenna Problem	100
6.4	Final Remarks	103
	Bibliography	104
A	Helmholtz Equation in Spherical Polar Coordinates	108
A.1	Radial Equation	108
A.2	Angular Equations	109
A.3	Eigenfunctions of the Helmholtz Equation	110

B Spherical Bessel Functions	111
B.1 Recurrence Relations	112
B.2 Special Integrals of Spherical Bessel Functions	114
C Associated Legendre Functions	117
C.1 Legendre and Associated Legendre Functions	117
C.2 Recursion Relations of Associated Legendre Functions	118
C.3 Useful Integrals of Associated Legendre Functions	120
C.4 Additional Integrals	132
D Evaluating Inner Product Integrals	135
D.1 Introduction	135
D.2 Evaluation of $\langle \mathbf{E}_z \mathbf{M}_{mn} \rangle$	136
D.3 Evaluation of $\langle \mathbf{E}_z \mathbf{N}_{mn} \rangle$	138
D.4 Evaluation of $\langle \mathbf{E}_z \mathbf{L}_{mn} \rangle$	140
D.5 Evaluating $\langle \mathbf{E}_x \mathbf{N}_{mn} \rangle$	142
D.6 Evaluating $\langle \mathbf{E}_x \mathbf{M}_{mn} \rangle$	146
D.7 Evaluating $\langle \mathbf{E}_x \mathbf{L}_{mn} \rangle$	148
D.8 Evaluating $\langle \mathbf{E}_y \mathbf{N}_{mn} \rangle$, $\langle \mathbf{E}_y \mathbf{M}_{mn} \rangle$ and $\langle \mathbf{E}_y \mathbf{L}_{mn} \rangle$	151
D.9 Evaluating $\langle \mathbf{M}_{mn} \mathbf{M}_{mn} \rangle$, $\langle \mathbf{N}_{mn} \mathbf{N}_{mn} \rangle$ and $\langle \mathbf{L}_{mn} \mathbf{L}_{mn} \rangle$	153
D.10 Evaluating Inner Products when $m < 0$	154
E Scattering Cross-Section and Total Cross-Section	160
F A Vector Identity	170

Illustrations

2.1	Pillbox at an interface between two media. δz_1 and δz_2 are made to approach zero so that the only contribution to the surface integral occurs from the area ΔS only.	16
2.2	When the rectangular loop is made to shrink in height, the contribution to the line-integral will be dominated by only the lengths parallel to the interface.	18
3.1	Demonstrating completeness of basis function expansion. The expansion of an arbitrarily chosen wave in the L , M and N functions. The solid lines show exact values. The broken lines are computed from a truncated series in the basis functions. The above calculations are done with 15 terms ($n = 15$) for $kr \in [0, 12]$, $\theta = 37$ degrees, $\phi = 59$ degrees, $\alpha = 123$ degrees, $\beta = 83$ degrees, $\theta_e = 49$ degrees and $\phi_e = 21$ degrees. Convergence is very good for $ kr \leq 0.75n$. The horizontal axes are in units of $ kr $	38
3.2	Demonstrating completeness of basis function expansion when the specified wave vector is complex. The solid lines show exact values. The broken lines are computed from a truncated series in the basis functions. The above calculations are done with 15 terms ($n = 15$) for $kr_{max} = 10 + 8i$, $\theta = 35$ degrees, $\phi = 42$ degrees, $\alpha = 97$ degrees, $\beta = 82$ degrees, $\theta_e = 21$ degrees and $\phi_e = 79$ degrees. Convergence is very good for $ kr \leq 0.75n$. The horizontal axes are in units of $ kr $	40
4.1	Shell-geometry with single shell. There are three spherically concentric regions indicated. The core has dielectric constant ϵ_1 , the shell has dielectric constant ϵ_2 and the exterior has dielectric constant ϵ_3 . In general there can be more number of shells.	44

4.2	Scattering from glass sphere coated with a thin gold shell. The total diameter of the core-shell scatterer is 2λ . The thickness of the gold shell is reduced from 0.15λ (top-left) to zero (bottom-right). Incident light is directed from the bottom of the page with polarization pointing out of the page. White represents larger fields.	52
4.3	Poynting vector calculation for scattering from gold cluster. The incident light at 2.0eV is incident from $\theta = 0^\circ$, with the polarization directed out of the paper. Scattering from two cluster sizes. $R = 20\text{nm}$ and $R = 100\text{nm}$ are shown, where b is the radius of the observation points.	54
4.4	Plasmon Resonance in 12nm Gold Colloids in Aqueous Solution . . .	56
4.5	Total scattering cross section (in m^2) of gold nanoparticles, of 5nm diameter, coated with a shell of 1nm of a test dielectric whose refractive index, n , and the extinction, k , are also indicated. $k_{max} = 1$, $\gamma = 0.5\text{eV}$ and ν_0 is varied between 2.2eV and 1.2eV. . . .	59
4.6	Total scattering cross section (in m^2) of gold nanoparticles, of 5nm diameter, coated with a shell of varying thickness of a test dielectric specified by $k_{max} = 1$, $\gamma = 0.5\text{eV}$ and $\nu_0 = 1.5\text{eV}$. The peak positions and shapes change as a function shell thickness.	60
4.7	Total scattering cross section of gold nanoparticles, of 5nm diameter, coated with a shell of C_{60} . The peak at $\sim 520\text{nm}$ shifts towards longer wavelengths as the thickness of the shell is increased from 1nm to 10nm.	60
4.8	Absorbance of gold sulfide colloids coated with a shell of gold. The peak at $\sim 520\text{nm}$ corresponds to gold particles. The peak at longer wavelengths shifts initially towards the red ($1 \rightarrow 4$), but eventually shifts towards shorter wavelengths ($5 \rightarrow 10$).	62
4.9	Calculated Plasmon Resonance in core-shell model. The shell is of gold. The core is a dielectric with $\epsilon = 5$. The diameter of the core is increased from 1nm to 4nm, but the shell thickness is held constant at 0.5nm. The peak shifts towards the red.	62
4.10	Calculated Plasmon Resonance in core-shell model. The shell is gold. The core is a dielectric with $\epsilon = 5$. The total diameter of the core-shell is held constant at 20nm, but the shell increases in thickness from 2nm to 15nm. The peak shifts towards the blue. The absorption becomes more gold-like.	63

- 4.11 Calculated Plasmon Resonance in core-shell model. The shell is of gold. The core is a dielectric with $\epsilon = 5$. The diameter of the core is held constant at 10nm, but the shell increases in thickness from 1.5nm to 6nm. The peak shifts towards the blue. 64
- 5.1 (a) Geometry of ‘capsule’ shaped scattering object. Two hemispheres of radius R are attached to the end of a cylinder of length L . Letting $L \rightarrow 0$, the capsule degenerates to a sphere. (b) Approximating the azimuthally symmetrical surface by means of the discrete set of angles θ_i . r as a function of θ is specified by a piece-wise continuous function. \mathbf{n} indicates the normal and \mathbf{t} the tangent orthogonal to \mathbf{e}_ρ . 68
- 5.2 Defining the relative orientation of \mathbf{E} and \mathbf{k} for s and p polarization geometries. The definition assumes the presence of an interface at the xy-plane. 70
- 5.3 Structure of the matrix derived from the boundary condition equations for a specified m . We obtain $6p$ equations from specifying p points on the boundary to solve for the $4N$ unknown expansion coefficients. All the blocks corresponding to say θ_1 , represent the six boundary condition equations for point θ_1 . The unknown expansion coefficients of the scattered fields are obtained from the over determined system of equations by a linear least-square method (we require $6p \geq 6N$). 77
- 5.4 Comparing the method of linear least-square solution of the boundary-condition equations with the ‘exact’ solution for scattering from a glass sphere ($\epsilon = 2.5$) of radius $R = 1\lambda$. The optical field is focussed to ≥ 7 times the incident field by ‘lens-action’. The incident field is polarized normal to the plane of the figure. (a) $\theta_i = 0^\circ$ (top row) . (b) $\theta_i = 45^\circ$ (bottom row). Physically, the 45 degree incidence case should have been identical to the 0 degree incidence except for an overall rotation by 45 degrees. The differences are due to round-off errors in evaluation of the basis functions. 79

- 5.5 Field calculations by including higher orders of m , from $m = 0$ up to $m = 5$. Glass sphere ($\epsilon = 2.5$) of radius $R = 1\lambda$ and $\theta_i = 45^\circ$. Although $m = 1$ appears to be the ‘dominant’ term in this sequence, serving to establish the overall field distribution, the higher orders are necessary to obtain more accurate calculation of the field intensities. 81
- 5.6 Field calculations for different orders of m , from $m = 0$ up to $m = 5$. Glass sphere ($\epsilon = 2.5$) of radius $R = 1\lambda$ and $\theta_i = 45^\circ$. The $m = 1$ contribution appears to be the most ‘dominant’ term in this sequence. The contributions from $m = 4$ and $m = 5$ terms are going to be small. 82
- 5.7 Electromagnetic scattering from a ‘capsule’ scatterer. $R = 0.5\lambda$ and L is increased from zero (sphere) to 0.3λ . The dielectric constant of the scatterer is taken as 2.5 in these calculations. Light is incident from the bottom of the figure with the polarization directed out of the paper. 83
- 5.8 Electromagnetic scattering from a ‘capsule’ scatterer. The incident light approaches from different directions. From top-left to bottom-right the images are shown with θ_i changing by 22.5° between the images. Although the 0° and the 180° situations are computationally different (due to lack of symmetry about the origin), the fields evaluate identically, which is expected physically. The ‘focused’ spot achieves higher intensity for 22.5° incidence angle. . . 84
- 5.9 The Sphere-Plane model. The dielectric function of the sphere is ϵ_1 and that of the plane is ϵ_3 . The medium surrounding the sphere has non-dissipative dielectric function ϵ_2 . \mathbf{k} is the propagation vector of the incident radiation. Such a model is often used to do theoretical studies of plasmon resonances on roughened surfaces. 85
- 5.10 Plane wave incident at a planar interface. Reflection and refraction occurs. The plane is located at $z = d$. The phase must satisfy spatial invariance on the plane. 88
- 5.11 Structure of the matrix derived for the sphere-plane model from the boundary condition equations for a specified m . We obtain $6N$ equations in $6N$ unknowns by specifying $N/3$ points on the substrate. The equations for the sphere boundary (indicated by the dotted box) are exact. The matrix above is shown for $n = 6$ and so the number of points specified on the substrate. $N_{sub} = 2$ 91

- 5.12 Plasmon resonance in sphere-plane model. A Gold sphere of radius 30nm located 5nm from a gold substrate. the sphere are gold. (a) Theoretical calculation of plasmon resonance based on experimentally obtained bulk dielectric function for gold: the broken line shows the assumed detector response in the photoemission experiment in (c). (b) Multiplying the calculated spectrum in (a) by the detector response. (c) Experimentally obtained spectrum of photon emission from a tip-substrate geometry in the 'field-emission' regime. 93
- 5.13 Plasmon resonance in sphere-plane model. A Copper sphere of radius 30nm located 5nm from a copper substrate. the sphere are copper. (a) Theoretical calculation of plasmon resonance based on experimentally obtained bulk dielectric function for copper: the broken line shows the assumed detector response in the photoemission experiment in (c). (b) Multiplying the calculated spectrum in (a) by the detector response. (c) Experimentally obtained spectrum of photon emission from a tip-substrate geometry in the 'field-emission' regime. 94
- 5.14 Plasmon resonance in sphere-plane model. A silver sphere of radius 30nm located 5nm from a silver substrate. The sphere is silver. (a) Theoretical calculation of plasmon resonance based on experimentally obtained bulk dielectric function for silver: the broken line shows the assumed detector response in the photoemission experiment in (c). (b) Multiplying the calculated spectrum in (a) by the detector response. (c) Experimentally obtained spectrum of photon emission from a tip-substrate geometry in the 'field-emission' regime. Notice the field enhancement at resonance (by a factor of ~ 10). 95
- 5.15 Comparison of field enhancements with a silver sphere on a copper substrate and a copper sphere on a silver substrate. In this case, it is clear that the enhancements are contributed more by the nature of the sphere as compared to the substrate. 95

Preface

There are many classic problems that attract scientific interest for long periods of time. Over time, different researchers put in their fresh inputs and the subject continues to evolve. It is almost a team effort, except that it is distributed in time. Certain problems are sufficiently difficult in that it requires a few generations of scientists to finally solve them. The problem of solving Maxwell's equations is once such classic problem. The collective knowledge of many scientists and researchers of the past have contributed in significant ways to allow us to put together this work "Vector Basis Function Solution of Maxwell's Equations". This is certainly not the last word in such solution methods, just another important contributory step towards our goal of understanding nature. In other words, it is part of one of the greatest adventures known to humanity: the scientific endeavour.

With this in mind, we must continue to march towards progress. Specifically, the knowledge contained here or any of its derivatives may be employed for peaceful purposes only. **This knowledge is strictly forbidden for use by any military organization.**

Dipankar Sarkar
Rice University
Department of Physics
Houston, Texas
Sept 10, 1996

Dedication

**This work is dedicated to 3D
and all her polymorphic states.**

Chapter 1

Introduction

The subject of obtaining the solution of Maxwell's equations in a boundary value problem has kept scientists occupied for more than one hundred years [25]. It is one of the few 'classic' problems that continue to attract the attention of researchers. Many contemporary problems of interest involve our knowledge of the exact solution to these equations. However, the complexity of these equations has defied analytic solutions for all but the simplest cases.

To state the problem more correctly, one needs to understand the length-scales involved. In a scattering problem for example there are two lengths involved: d , the physical size of the scattering object and λ , the wavelength of electromagnetic waves in question. When $d \gg \lambda$, the problem is readily solved. The method of solution, called geometrical optics, has been known for at least a few hundred years. In fact we do not even need to invoke Maxwell's equations directly. The other limiting case is when $d \ll \lambda$. This regime is called the quasistatic limit or nano-optics. Although mathematically involved, the solution in the quasistatic limit is obtained by solving Laplace's equation. The problem is far more complicated when $d \sim \lambda$. It is in this regime that one is required to solve Maxwell's equations exactly.

The problem involves the solution of a set of partial differential equations (The Maxwell Equations) for the coupled vector fields for the electric field \mathbf{E} and the magnetic field \mathbf{H} . Although the general theoretical aspects of these equations are fairly well understood at the moment [25] [30], there are still some formidable mathematical or computational problems to overcome in the area of solving the time-varying boundary value problem. Whereas the problem of acoustic (scalar fields) diffraction has been solved in a number of cases such as the strip, elliptic cylinder, hyperbolic cylinder, wedge, prolate and oblate spheroids, etc. [13], the corresponding solution for the vector fields are still by and large unconquered. Often the solution is worked out only in the quasistatic approximation by solving Laplace's equation (homogenous case) [4] [3].

1.1 Historical Development

In the absence of sources, these coupled partial differential equations have been solved exactly, analytically, only for a few isolated cases. The method of solution involved in these cases requires the knowledge of certain ingenious transformations, suitable only for the problem in question. Usually these are dictated by the simple geometric shapes of the boundaries in question. Often these boundaries have to correspond to the coordinate surfaces in order for the boundary conditions to be separable. The simplest canonical case of scattering of plane waves reflecting/refracting at a planar interface [22] is commonly known by the name of Fresnel's Equations. The most celebrated analytic solution to the scattering problem is that of Mie scattering, the scattering of electromagnetic waves from a dielectric sphere [12], originally due to G. Mie (1908).

Immediately after Mie obtained the general solution to the sphere problem, Debye was able to formulate the same problem in terms of a pair of *coupled* scalar functions [27], in which the electric and magnetic fields were expressed. The method was again suitable for boundary value problems with spherical boundaries only. Hansen [19] [20] [18] developed a technique for addressing the problem of radiation from antennas using a special type of transformation. The subject was developed further by Stratton [38] who solved the problem of Mie scattering using a set of vector functions derived from the solutions of the scalar Helmholtz equation. Subsequently, Aden and Kerker [1] used the formalism to solve the problem of electromagnetic scattering from two concentric spheres. Although Stratton [38] had made considerable contributions to this area of basis function expansion, the method of solution was still considered as just another 'more elegant' way to solve the Mie problem, analogous to the approach of Debye. The crucial idea that was missing at this stage was the notion of mathematical completeness of basis function expansions. Furthermore, the algebraic difficulties one had to overcome restricted the Stratton approach to solving the spherical scatterer problem with incident light approaching along the z-axis only. Progress in this subject was negligible beyond this stage and the problem is reproduced in its original form even in contemporary text-books [40] [11].

The problem of diffraction of a plane wave at normal incidence on a circular cylinder was originally solved by Rayleigh and since then his solution has been generalized and extended to plane waves at oblique incidence [41]. The method of basis function expansion was again used in this problem. Similarly, the problems of electromagnetic

and acoustic scattering from a semi-infinite cone [36] and a semi-infinite body of revolution [35] were obtained by the method of basis function expansion. For the special case of the paraboloid, the solutions were ‘exact’. The generality of these approaches were not apparently proved (or even appreciated) beyond the specific geometries these earlier researchers were interested in.

In the mid 1960’s there began a growing interest in the study of Maxwell’s equations as a purely mathematical problem [25] [30]. Perhaps the growing use of sophisticated electromagnetic devices testified beyond doubt the correctness of these equations for macroscopic electromagnetic phenomena. The theory of Maxwell’s equations was now to go through the rigors of verifying its mathematical foundations. The mathematical apparatus of topology and modern analysis was available to study the mathematically interesting properties of these equations. For example, it was found that any electromagnetic response within a perfectly conducting cavity (resonator) could be expressed in a complete set of functions (that is, the existence of such functions was proved) [25] [30].

The Sphere-Plane model consisting of a dielectric sphere close to a semi-infinite half-space substrate has been used to model the effect of irregularities in a surface that can lead to high local field enhancements [3] [4] [33] [34] [39]. The problem has been solved in the quasistatic approximation except in the work of Takemori [39] who obtained the exact solution using a Greens function approach with higher orders of scattering from the sphere and the plane.

More recently, primarily due to the availability of increasingly powerful computers, our approach for solving the Maxwell equations have taken a rapid ‘numerical’ path. It is all too common to try to solve a boundary value problem entirely numerically. One uses finite difference equation approximations of the Maxwell equations on a (often non-linear) grid within a defined region of interest. Although such techniques are extremely powerful for solving problems with absolutely no symmetry, they are often very resource hungry in terms of memory(core) and computation time. Often researchers have to resort to solving the two-dimensional analogs (or some approximation of it) to try to understand the physics in a specific situation.

In the last decade there has been a rapid development in the area of scanning probe microscopies. As experiments have become more sophisticated, including the coupling of light at the active junction in a scanning probe microscope, considerable efforts have been directed towards modelling an illuminated tip-substrate geometry [14] [28] [10] [9] [8] [23]. Whereas the solution in the quasistatic limit is easy to solve [14],

it is difficult to justify. The use of complex dielectric functions and the fact that the tip and substrate boundaries (the scattering objects in this problem) extend to infinity (so the condition that the dimensions are much smaller than the wavelength of the optical field in question does not hold true) are not totally justified. Attempts are currently underway to obtain ‘exact’ solutions to these problems. At the present moment, the available techniques to solve this problem too have remained by and large unsatisfactory.

Some other notable geometries for which the exact solution of electromagnetic scattering have been obtained in three dimensions include the prolate and oblate ellipsoids. Certain two dimensional cases, such as the circular, parabolic and elliptic cylinders, are also amenable for exact solutions [13]. However, for arbitrary geometrical shapes one has to resort to solving the Maxwell equations by finite element numerical techniques.

Finally, the problem of solving the inhomogenous Maxwell equations in general have seen very little progress. The usual approach has been to reformulate the problem in terms of the scalar and the vector potentials in a given gauge. One uses Greens function techniques to solve for the vector potential, given the current densities. The scalar potential is similarly solved from the knowledge of the charge densities. The mathematical apparatus is not sufficiently developed in this area and the problem is by and large unsolved, exactly.

1.2 Outline of The Thesis

In Chapter 2 we introduce the notion of the vector basis functions and prove that they form a complete set in a given coordinate system. The proof on completeness is followed by a discussion on the relevant boundary conditions in a scattering problem. In Chapter 3 we go into the detailed algebra of trying to expand an arbitrary plane wave in the basis set. Only the key results are highlighted and the bulk of the algebra is carried out in the appendices. The chapter on the Shell-Problem is the first application we consider in which the basis functions are used to obtain the solution. Comparison of the calculations are made with several experiments that are published in the literature. The next chapter on ‘Scattering from non-spherical objects’ uses the same basis function technique to solve the problem of scattering from an elongated object whose boundaries do not conform to the coordinate surfaces. Previously, this kind of calculation could be done by using completely numerical techniques only. We

also look into the solution of the sphere-plane model and compare our calculations with experiments reported in the literature. Finally we conclude by highlighting the future directions in which this research could continue to establish itself as a powerful general technique for solving Maxwell's equations.

Chapter 2

General Solution of Maxwell's Equations

2.1 Introduction

Many macroscopic electromagnetic phenomena have been successfully described by Maxwell's Equations. Over the past one hundred years, it has been put to test through the rigors of scientific scrutiny. Strictly speaking, the theory is applicable in a macroscopic sense, where one can assume the knowledge of 'bulk' electromagnetic properties of materials such as the dielectric function. However, the theory has been so successful that scientist have often taken the liberty of extrapolating the region of applicability to the nanometer and sub-nanometer scales.

The electromagnetic field at a time t , and at any point \mathbf{r} in a medium characterized by a dielectric function $\epsilon(\mathbf{r}, t)$ and magnetic permeability $\mu(\mathbf{r}, t)$ is described by Maxwell's Equations. The differential form of the equations in terms of the electric field \mathbf{E} , the magnetic field \mathbf{H} , the electric displacement \mathbf{D} , the magnetic induction \mathbf{B} , and the sources: \mathbf{J} , the current density and ρ , the charge density, are defined below, for notational consistency within this thesis:

$$\nabla \cdot \mathbf{D}(\mathbf{r}, t) = \rho(\mathbf{r}, t) \quad (\text{Gauss's Law}) \quad (2.1)$$

$$\nabla \times \mathbf{E}(\mathbf{r}, t) = -\frac{\partial \mathbf{B}(\mathbf{r}, t)}{\partial t} \quad (\text{Faraday's Law}) \quad (2.2)$$

$$\nabla \cdot \mathbf{B}(\mathbf{r}, t) = 0 \quad (\text{No Magnetic Monopoles}) \quad (2.3)$$

$$\nabla \times \mathbf{H}(\mathbf{r}, t) = \mathbf{J}(\mathbf{r}, t) + \frac{\partial \mathbf{D}(\mathbf{r}, t)}{\partial t} \quad (\text{Ampere's Law}) \quad (2.4)$$

These four equations, along with the constitutive relations: $\mathbf{B} = \mu\mathbf{H}$ and $\mathbf{D} = \epsilon\mathbf{E}$ are in principle capable of describing all macroscopic electromagnetic phenomena. In practice, given an electromagnetic phenomenon describable as a boundary value problem, it is a formidable task to solve these equations exactly. At present, only

finite element numerical techniques are available to solve a general problem. These numerical calculations are sufficiently resource-hungry in terms of memory and total computation time that in most cases only the simplest geometries and often only the two-dimensional analogs are attempted for a solution.

2.2 Linear Homogenous Isotropic Medium

For the interesting subclass of problems that are related to the scattering of electromagnetic radiation by dielectric and/or magnetic boundaries, the general equations assume a much more symmetrical form. Within this approximation of a linear, time-invariant, homogenous and isotropic medium without any external sources, Maxwell's equations assume the form:

$$\nabla \cdot \mathbf{E}(\mathbf{r}, t) = 0 \quad (2.5)$$

$$\nabla \times \mathbf{E}(\mathbf{r}, t) = -\mu \frac{\partial \mathbf{H}(\mathbf{r}, t)}{\partial t} \quad (2.6)$$

$$\nabla \cdot \mathbf{B}(\mathbf{r}, t) = 0 \quad (2.7)$$

$$\nabla \times \mathbf{H}(\mathbf{r}, t) = \sigma \mathbf{E}(\mathbf{r}, t) + \epsilon \frac{\partial \mathbf{E}(\mathbf{r}, t)}{\partial t} \quad (2.8)$$

Where we have assumed the possibility of an induced current density in the medium equal to $\sigma \mathbf{E}$, where σ is the conductivity of the medium under consideration. Also, for harmonic time-dependence of the external fields, $e^{-i\omega t}$, where ω is the angular frequency, the time derivatives could be factored out, and we obtain the set of coupled partial differential equations in the spatial coordinates alone, with the angular frequency of the excitation as a parameter :

$$\nabla \cdot \mathbf{E}(\mathbf{r}, \omega) = 0 \quad (2.9)$$

$$\nabla \times \mathbf{E}(\mathbf{r}, \omega) = i\omega\mu\mathbf{H}(\mathbf{r}, \omega) \quad (2.10)$$

$$\nabla \cdot \mathbf{B}(\mathbf{r}, \omega) = 0 \quad (2.11)$$

$$\nabla \times \mathbf{H}(\mathbf{r}, \omega) = \sigma \mathbf{E}(\mathbf{r}, \omega) - i\omega\epsilon\mathbf{E}(\mathbf{r}, \omega) \quad (2.12)$$

From now on, we shall use a simplified notation by suppressing the argument list (\mathbf{r}, ω) . Thus Equation 2.12 becomes:

$$\nabla \times \mathbf{H} + i\omega\left(\epsilon + \frac{i\sigma}{\omega}\right)\mathbf{E} = 0 \quad (2.13)$$

And from Equation 2.10 we obtain:

$$\mathbf{H} = \frac{1}{i\omega\mu} \nabla \times \mathbf{E} \quad (2.14)$$

Substituting the expression for \mathbf{H} from Equation 2.14 into Equation 2.13, and introducing the **complex dielectric function** $\hat{\epsilon} = \epsilon + \frac{i\sigma}{\omega}$, we obtain the **Vector Helmholtz Equation** for the electric field vector:

$$\nabla \times \nabla \times \mathbf{E} - \omega^2 \mu \hat{\epsilon} \mathbf{E} = 0 \quad (2.15)$$

Similarly, taking the curl of both sides of Equation 2.13 and substituting for $\nabla \times \mathbf{E}$ from Equation 2.14, we obtain the corresponding Vector Helmholtz Equation for the magnetic field intensity vector:

$$\nabla \times \nabla \times \mathbf{H} - \omega^2 \mu \hat{\epsilon} \mathbf{H} = 0 \quad (2.16)$$

These equations are totally symmetrical in the field variables and they also decouple the electric and magnetic fields. It is the solution to the Vector Helmholtz Equations for specified boundary and radiation conditions that describes the scattering of electromagnetic waves. However, these equations are vector partial differential equations which are sufficiently difficult to solve in general. The most well known non-trivial problem that has been solved exactly, analytically, is that of scattering from a sphere (Mie Scattering, 1908). It is the purpose of this thesis to develop the general technique of vector basis function expansion, for the solution of both the near and far fields in electromagnetic scattering from finite sized objects.

2.3 Solution Space of Vector Helmholtz Equation

The theory of solving the **Scalar Helmholtz Equation**, also known as the Wave Equation, is a very well developed subject [29] [5] [43]. This equation describes the propagation of scalar waves, such as acoustic waves, in a medium.

$$\nabla^2 \psi(\mathbf{r}, t) + k^2 \psi(\mathbf{r}, t) = 0 \quad (2.17)$$

When expressed in certain orthogonal curvilinear coordinate systems, such as the cartesian coordinate system or the spherical polar coordinate system, under assumption of sinusoidal time-dependence, the solution $\psi(\mathbf{r}, t)$ can be obtained by the technique of separation of variables. The separation procedure reduces the partial differential equation to several ordinary differential equations. The separated equations can often be cast in the form of the well known Sturm-Liouville eigenvalue problem for second order ordinary differential equations, so that the solution space is guaranteed to be complete for the scalar Helmholtz equation.

For the moment let us assume that we have obtained a complete set of scalar functions $\{\psi\}$ that are solutions to the scalar wave equation (Eqn 2.17). Let us introduce the **diffraction equation** :

$$\nabla(\nabla \cdot \mathbf{G}) - \nabla \times \nabla \times \mathbf{G} + k^2 \mathbf{G} = 0 \quad (2.18)$$

where $k^2 = \omega^2 \mu \hat{\epsilon}$. The diffraction equation is satisfied by the electric field \mathbf{E} and the magnetic field \mathbf{H} that satisfies the Vector Helmholtz equations since the 'extra' term $\nabla \cdot \mathbf{G}$ will be zero for fields that have zero divergence. So, Equation 2.18 is consistent with Maxwell's equations for electromagnetic waves. Let us define a vector function that is obtained by taking the gradient of the scalar function ψ :

$$\mathbf{L} = \nabla \psi \quad (2.19)$$

\mathbf{L} satisfies the diffraction equation if ψ is a solution to Equation 2.17:

$$\begin{aligned} & \nabla(\nabla \cdot \mathbf{L}) - \nabla \times \nabla \times \mathbf{L} + k^2 \mathbf{L} \\ = & \nabla(\nabla \cdot \nabla \psi) - \nabla \times \nabla \times \nabla \psi + k^2 \nabla \psi \\ = & \nabla(\nabla^2 \psi + k^2 \psi) \quad (\text{Since } \nabla \times \nabla \psi = 0) \\ = & 0 \quad (\text{Since } \nabla^2 \psi + k^2 \psi = 0) \end{aligned} \quad (2.20)$$

$$(2.21)$$

Now let us assume that there exists a vector function \mathbf{M} , with zero divergence, $\nabla \cdot \mathbf{M} = 0$, that is a solution to the diffraction equation (Eqn 2.18). Let us consider the vector $\mathbf{N} = \frac{1}{k} \nabla \times \mathbf{M}$. Assuming k is a constant (homogenous medium), we obtain:

$$\begin{aligned} & \nabla(\nabla \cdot \mathbf{N}) - \nabla \times \nabla \times \mathbf{N} + k^2 \mathbf{N} \\ = & \frac{1}{k} (\nabla(\nabla \cdot \nabla \times \mathbf{M}) - \nabla \times \nabla \times \nabla \times \mathbf{M} + k^2 \nabla \times \mathbf{M}) \end{aligned}$$

$$\begin{aligned}
&= \nabla \times (-\nabla \times (\nabla \times \mathbf{M}) + k^2 \mathbf{M}) \quad (\text{Since } \nabla \cdot (\nabla \times \mathbf{M}) = 0) \\
&= \nabla \times (\nabla(\nabla \cdot \mathbf{M}) - \nabla \times (\nabla \times \mathbf{M}) + k^2 \mathbf{M}) \quad (\text{Since } \nabla \cdot \mathbf{M} = 0) \\
&= 0 \quad (\text{Since } \mathbf{M} \text{ satisfies Eqn 2.18}) \tag{2.22}
\end{aligned}$$

Thus we show that \mathbf{N} , as defined above, also satisfies the diffraction equation. Also $\nabla \cdot \mathbf{N} = 0$, since divergence of curl is zero. So, if we had started with postulating the existence of a vector function \mathbf{N} with zero divergence, we could show that there exists \mathbf{M} with zero divergence. Thus from symmetry arguments alone, we could write $\mathbf{M} = \frac{1}{k} \nabla \times \mathbf{N}$. Specifically, since $\mathbf{N} = \frac{1}{k} \nabla \times \mathbf{M}$, since k is a constant (by assumption of homogeneity of the medium),

$$\nabla \times \mathbf{N} = \frac{1}{k} \nabla \times \nabla \times \mathbf{M} \tag{2.23}$$

$$\nabla \times \mathbf{N} = \frac{1}{k} k^2 \mathbf{M} \quad (\text{Follows from Eqn 2.18}) \tag{2.24}$$

Thus $\mathbf{M} = \frac{1}{k} \nabla \times \mathbf{N}$. Clearly, \mathbf{M} and \mathbf{N} are distinct from \mathbf{L} , since the latter has non-zero divergence in general. So \mathbf{L} must be linearly independent of $\{\mathbf{M}, \mathbf{N}\}$. It is up to us to create a vector function \mathbf{M} (or equivalently \mathbf{N}) from the given scalar function ψ , such that it will have zero divergence and will satisfy the diffraction equation. The point to note is that we could arrive at more than one set of functions $\{\mathbf{M}, \mathbf{N}\}$, and it is the relative algebraic convenience that will dictate the choice of a particular set.

As a concrete example, let us consider $\mathbf{M} = \nabla \times \mathbf{a}\psi$, where ψ is the given scalar solution and \mathbf{a} is an arbitrary constant vector. The divergence condition is satisfied, since divergence of curl is identically zero: $\nabla \cdot \mathbf{M} = \nabla \cdot (\nabla \times \mathbf{a}\psi) = 0$. Using the operator identity (the author has verified this 'identity' for the spherical polar coordinate system and the cylindrical coordinate system in addition to the rectangular coordinate system), $\nabla(\nabla \cdot \mathbf{M}) - \nabla \times \nabla \times \mathbf{M} = \nabla^2 \mathbf{M}$, we can write:

$$\begin{aligned}
&\nabla(\nabla \cdot \mathbf{M}) - \nabla \times \nabla \times \mathbf{M} + k^2 \mathbf{M} \\
&= \nabla^2 \mathbf{M} + k^2 \mathbf{M} \\
&= \nabla^2(\nabla \times \mathbf{a}\psi) + k^2(\nabla \times \mathbf{a}\psi) \\
&= \nabla^2(\nabla\psi \times \mathbf{a} + \psi(\nabla \times \mathbf{a})) + k^2(\nabla\psi \times \mathbf{a} + \psi(\nabla \times \mathbf{a})) \\
&= \nabla^2(\nabla\psi \times \mathbf{a}) + k^2(\nabla\psi \times \mathbf{a}) \quad (\text{Since } \nabla \times \mathbf{a} = 0) \\
&= (\nabla^2(\nabla\psi) + k^2 \nabla\psi) \times \mathbf{a} \quad (\text{Since } \nabla^2 \text{ does not act on } \mathbf{a}) \\
&= (\nabla(\nabla^2\psi + k^2\psi)) \times \mathbf{a} \\
&= 0 \quad (\text{Since } \psi \text{ satisfies Eqn 2.17}) \tag{2.25}
\end{aligned}$$

Also, $\mathbf{M} = \nabla \times \mathbf{a}\psi = \nabla\psi \times \mathbf{a} = \mathbf{L} \times \mathbf{a}$. So, $\mathbf{M} \cdot \mathbf{L} = 0$, i.e. \mathbf{L} and \mathbf{M} are orthogonal. Thus, given a countably infinite set of particular solutions to Eqn 2.17, $\{\psi_n\}$, that are finite, continuous, single-valued and with continuous partial derivatives: associated with each ψ_n one can obtain a triplet of mutually non-coplanar vector solutions $\{\mathbf{L}_n, \mathbf{M}_n, \mathbf{N}_n\}$, satisfying Eqn 2.18. Presumably, any arbitrary solution of the diffraction equation can be expressed as a linear combination of these vector functions. However, the existence of a generalized Fourier series expansion supposes that the set $\{\mathbf{L}_n, \mathbf{M}_n, \mathbf{N}_n\}$ forms a **complete set**.

Proving the completeness of the set $\{\mathbf{L}_n, \mathbf{M}_n, \mathbf{N}_n\}$ is a two step process. First, one has to prove the **existence** of a complete set of functions for the diffraction equation. Next, one has to show that the $\{\mathbf{L}_n, \mathbf{M}_n, \mathbf{N}_n\}$ set can indeed **span** the solution space of the diffraction equation, or equivalently, the vector Helmholtz equations. If the labeling index n is not countable, then an arbitrary solution could be expressed as a generalized Fourier Integral of the basis functions with respect to the labeling parameter.

2.4 Completeness of Vector Eigenfunctions

Our goal is to be able to represent the solution of electromagnetic scattering in a series of vector eigenfunctions of the diffraction operator. The fundamental question we have to address is whether or not such a set is complete (in a strictly mathematical sense). In other words, whether the set of functions under consideration forms a basis. It can be shown that the solution space of the diffraction operator cannot be spanned by any finite set of functions. Assume momentarily that we have obtained only the \mathbf{L}_n functions from the scalar solution, and that we have no knowledge about the existence of the \mathbf{M}_n or \mathbf{N}_n functions. So we have a countably infinite set of functions that satisfy the diffraction operator. But it is easy to prove that such a set does not form a basis. In other words, there are *elements* in the solution space that are *independent* of the \mathbf{L}_n functions. For example, the \mathbf{M}_n functions defined as $\mathbf{L}_n \times \mathbf{a}$ are clearly orthogonal to the \mathbf{L}_n functions. Naturally, the same concerns are valid even with the knowledge of the larger set containing all the three types of functions. We do need to address the question of whether or not the set $\{\mathbf{L}_n, \mathbf{M}_n, \mathbf{N}_n\}$ is a complete set.

It is a well established fact that the set of all plane wave solutions form a complete set in the solution space of the vector Helmholtz operator. Physically this

implies that any scattered wave can be constructed by linear addition/superposition of plane waves. The diffraction operator is somewhat more general than the vector Helmholtz operator in the sense that it is satisfied by 'generalized plane waves' which have non-zero divergence. The vector Helmholtz equation, which follows directly from Maxwell's Equations in a homogenous and isotropic medium is satisfied only by the zero-divergence solutions. Within a non-isotropic medium in which momentum transfer can occur, such as in a crystal, the \mathbf{E} need not be perpendicular to \mathbf{k} , and the zero-divergence solutions cannot describe such a wave. Although we are not directly concerned with non-isotropic media, for the sake of arguments of mathematical completeness, we shall work with the solution space of the more general diffraction equation.

Although the set of all generalized plane waves span the solution space, there is a fundamental difficulty with such a set. It arises from the fact that such a set is uncountable. In other words, the label(s) to identify the individual elements of the set are in this case, continuous variables (being the value of the propagation vector, and its direction cosines, and the direction cosines of the electric field). Such sets are not easily amenable for construction of general scattered wave solutions. It is here that a countable basis comes to our rescue.

To begin, let us identify a few properties of the diffraction operator and its corresponding solution space.

1. The space is linear. That is addition of two solutions and multiplication of a given solution by an arbitrary complex number is also a solution. This follows directly from the linearity of the diffraction operator. In particular, $0 \cdot \mathbf{f} = \mathbf{0}$ for all \mathbf{f} belonging to this space.
2. The space has an inner product and a metric. Mathematically this implies that with any pair of elements \mathbf{a} and \mathbf{b} , we can associate a complex number called the inner product $\langle \mathbf{a} | \mathbf{b} \rangle$ satisfying the following rules:
 - $\langle c\mathbf{a} | \mathbf{b} \rangle = c\langle \mathbf{a} | \mathbf{b} \rangle$ where c is an arbitrary complex number.
 - $\langle \mathbf{d} + \mathbf{a} | \mathbf{b} \rangle = \langle \mathbf{d} | \mathbf{b} \rangle + \langle \mathbf{a} | \mathbf{b} \rangle$ for any \mathbf{d} belonging to the set.
 - $\langle \mathbf{a} | \mathbf{b} \rangle = \langle \mathbf{b} | \mathbf{a} \rangle^*$ where $*$ represents the complex conjugate.
 - $\langle \mathbf{a} | \mathbf{a} \rangle > 0$ for $\mathbf{a} \neq 0$ and $\langle \mathbf{a} | \mathbf{a} \rangle = 0$ only for $\mathbf{a} = 0$.

3. The space is complete since there exists the plane wave set which we know is a complete set. Mathematically it means that every Cauchy sequence is convergent.

With these properties satisfied, the set of all solutions of the diffraction operator form a Hilbert Space. The inner product can be defined as will be seen when considering the solutions in a particular coordinate system, such as the spherical polar coordinate system (Chap 3).

It can be shown that if $\{e_i\}$ is an orthonormal set in a Hilbert Space H , and if x is any vector in H , then the set $S = \{e_i : \langle x|e_i \rangle \neq 0\}$ is either empty or countable [37]. The importance of this theorem is that this guarantees countability of the basis if it exists. It can also be shown that every non-zero Hilbert space contains a complete orthonormal set. This follows from fundamental axioms of set theory embodied in Zorn's Lemma [17]. The important fact to consider at this stage is that the two statements mentioned above concerning Hilbert spaces tell us immediately that there exists a countable basis.

2.4.1 Completeness of the L, M, N set

We have already seen that we can arrive at a set $\{L_n, M_n, N_n\}$, of vector eigenfunctions that are mutually non-coplanar. It is clear that $\nabla\psi_n$ and $\nabla\psi_{n'}$ are different functions in general. Similarly, it can be argued that the set of functions is such that at any given point in space, they are not all pointing in the same direction. In mathematical language, the set is linearly independent. The set also has a countable infinite number of elements in it. The scalar functions $\{\psi_n\}$ are continuous with at least continuous partial derivatives up to second order. This implies that the derived vector functions are continuous as well.

Assume that we are given an arbitrary solution to the diffraction equation, x . By saying that we are given the solution, we mean that its value has been specified at a given set of points, $S = \{x_1, x_2, \dots\}$. For the moment let us assume that this set S is a countable set, as we have indicated by subscripting with natural numbers. For example, if the value has been specified at all coordinates (x, y, z) where $x, y, z \in \{p/q : p, q \in I\}$, then the set can be shown to be countable. Thus the specified set of points can be put in one-to-one correspondence with an index set, such as the natural numbers.

Now if we pick the first specified point where the function is defined, we obtain a vector of a certain magnitude which points along some specified direction. We can immediately pick the triplet of solutions $\{\mathbf{L}_1, \mathbf{M}_1, \mathbf{N}_1\}$, and by virtue of their linear independence, we can choose suitable coefficients so that the sum $a_1\mathbf{L}_1 + b_1\mathbf{M}_1 + c_1\mathbf{N}_1 = \mathbf{x}_1$, where the coefficients a_1, b_1, c_1 are complex numbers. Since the left-hand-side is a linear combination of solutions to the diffraction equation, so we have a valid solution that is equal to the specified solution \mathbf{x} at one point. In general the diffraction operator will propagate the linear combination $a_1\mathbf{L}_1 + b_1\mathbf{M}_1 + c_1\mathbf{N}_1$ so that it will be different from the specified solution at other points (if it does not, then of course we have obtained the desired expansion, and we can stop the process here). So assume that the linear combination just obtained deviates from the solution at point 2, \mathbf{x}_2 . Now we can pick our second triplet $\{\mathbf{L}_2, \mathbf{M}_2, \mathbf{N}_2\}$, and obtain a 'correction' to the original solution so that it matches at both the points. Essentially, we are solving a system of six equations in six unknowns to satisfy the match at the two specified points. Now it is easy to see that we can continue this process to 'match' the specified function in an infinite series of the set of vector eigenfunctions to any arbitrary precision. By virtue of continuity of these functions, their linear combinations are also continuous for any finite number of terms. The difference between the arbitrary solution and the series just obtained can in principle be made as small as we wish. In other words the sequence of approximations will eventually converge to the desired solution (it forms a Cauchy sequence). As a corollary, we immediately note that the set of expansion coefficients so obtained need *not* be unique. It does depend upon the order in which we picked them to satisfy the conditions for a match.

The validity of the statement of convergence of arbitrary Cauchy sequences follow from general considerations of a more restricted space of square-integrable functions, L^2 , with a semimetric. We know that the scattered solutions have to satisfy the radiation conditions. In other words, they have to vanish at infinity in a square-integrable sense. This follows from the finite energy content in any scattered wave from finite objects. The \mathbf{L} , \mathbf{M} and \mathbf{N} functions satisfy such conditions. It can be shown (The Reisz-Fischer Theorem) that every Cauchy sequence in the semimetric space L^2 converges to a function in L^2 , or that it is complete [2].

To conclude this section, we note that the existence theorem concerned itself with an orthonormal set. The set of functions $\{\mathbf{L}_n, \mathbf{M}_n, \mathbf{N}_n\}$ are not entirely orthogonal. However, they are a linearly independent set. This allows us to invoke the process

known as the Gram-Schmidt Orthonormalization procedure to obtain a complete orthonormal set from the given set of linearly independent vectors [37]. In practice, as we shall see later, it is not always required to carry out the process of orthonormalization to begin with.

2.4.2 Zero Divergence Solutions

Consider a solution \mathbf{F} whose divergence is zero. Let us find an expansion of \mathbf{F} in terms of the basis $\{\mathbf{L}_n, \mathbf{M}_n, \mathbf{N}_n\}$, so that

$$\mathbf{F} = \sum_n \{a_n \mathbf{M}_n + b_n \mathbf{N}_n + c_n \mathbf{L}_n\}. \quad (2.26)$$

Taking the divergence of both sides of the above equation, we find

$$\begin{aligned} \nabla \cdot \mathbf{F} &= \sum_n \{a_n \nabla \cdot \mathbf{M}_n + b_n \nabla \cdot \mathbf{N}_n + c_n \nabla \cdot \mathbf{L}_n\} \\ \text{or. } 0 &= \sum_n \{c_n \nabla \cdot \mathbf{L}_n\}. \end{aligned} \quad (2.27)$$

Since this has to hold true at all points, we conclude that all the c_n must be zero. In other words, a zero-divergence solution can be expressed only in terms of the \mathbf{M} and \mathbf{N} functions.

2.5 Boundary Conditions for Time-Varying Fields

Consider an interface between two media 1 and 2, with surface charge density $\sigma(\mathbf{r}, t)$ and a current densities $\mathbf{J}_1(\mathbf{r}, t)$ in medium 1 and $\mathbf{J}_2(\mathbf{r}, t)$ in medium 2. To avoid confusion with notation, conductance will be represented by $g(\mathbf{r})$, since $\sigma(\mathbf{r})$ has been used to represent the surface charge density. Assume the volume charge densities to be $\rho_1(\mathbf{r}, t)$ and $\rho_2(\mathbf{r}, t)$ in the respective media separated by the surface. Let us consider a pillbox as indicated in the Figure 2.1. It has cross-sectional area ΔS and extends δz_1 and δz_2 respectively into medium 1 and 2. The unit normal directed into medium 1 is denoted by $\hat{\mathbf{n}}$. From the continuity equation for charge:

$$\nabla \cdot \mathbf{J}(\mathbf{r}, t) = -\frac{\partial \rho(\mathbf{r}, t)}{\partial t}. \quad (2.28)$$

Integrating both sides of Equation 2.28 over the volume of the pillbox, we obtain:

$$\int \nabla \cdot \mathbf{J}(\mathbf{r}, t) d^3r = -\frac{\partial}{\partial t} \left[\int \rho(\mathbf{r}, t) d^3r \right] = -\frac{\partial \Delta q(t)}{\partial t} \quad (2.29)$$

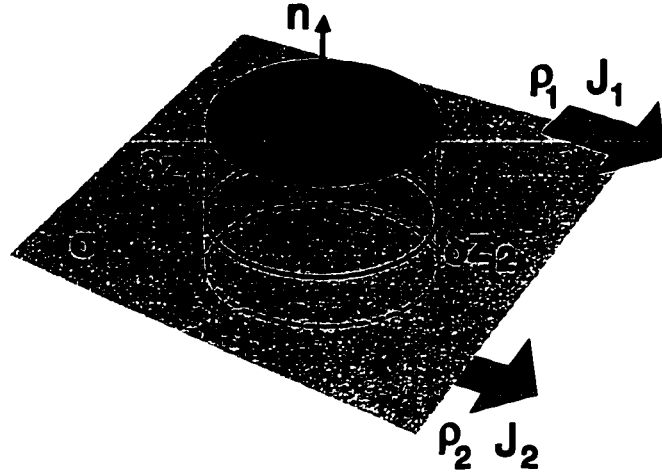


Figure 2.1: Pillbox at an interface between two media. δz_1 and δz_2 are made to approach zero so that the only contribution to the surface integral occurs from the area ΔS only.

where $\Delta q(t)$ is the total charge within the elemental pillbox and is given by :

$$\Delta q(t) = \rho_1(\mathbf{r}, t)\Delta S \delta z_1 + \rho_2(\mathbf{r}, t)\Delta S \delta z_2 + \sigma(\mathbf{r}, t)\Delta S. \quad (2.30)$$

If we let the pillbox thickness shrink, so that δz_1 and δz_2 go to zero in Equation 2.30. and also employ the divergence theorem. we obtain :

$$\oint \mathbf{J} \cdot d\mathbf{S} = -\frac{\partial}{\partial t} \int \sigma(\mathbf{r}, t) dS \quad (2.31)$$

or

$$\int (\mathbf{J}_1(\mathbf{r}, t) \cdot \hat{\mathbf{n}} - \mathbf{J}_2(\mathbf{r}, t) \cdot \hat{\mathbf{n}}) dS = -\frac{\partial}{\partial t} \int \sigma(\mathbf{r}, t) dS \quad (2.32)$$

which, in the limit of dS approaching zero, leads to

$$(\mathbf{J}_1(\mathbf{r}, t) - \mathbf{J}_2(\mathbf{r}, t)) \cdot \hat{\mathbf{n}} = -\frac{\partial \sigma(\mathbf{r}, t)}{\partial t}. \quad (2.33)$$

By similar reasoning, since

$$\nabla \cdot \mathbf{D}(\mathbf{r}, t) = \rho(\mathbf{r}, t) \quad (2.34)$$

we can write the difference in the normal component of \mathbf{D} at an interface

$$(\mathbf{D}_1(\mathbf{r}, t) - \mathbf{D}_2(\mathbf{r}, t)) \cdot \hat{\mathbf{n}} = \sigma(\mathbf{r}, t). \quad (2.35)$$

For sinusoidal time dependence of the excitation field, the surface charge density $\sigma(\mathbf{r}, t) = \sigma_0(\mathbf{r})e^{-i\omega t}$. Also, $\mathbf{J}(\mathbf{r}, t) = g(\mathbf{r}, \omega)\mathbf{E}(\mathbf{r})e^{-i\omega t}$. So from Equation 2.33 we can write

$$g_1(\mathbf{r}, \omega)\mathbf{E}_1(\mathbf{r}, t) \cdot \hat{\mathbf{n}} - g_2(\mathbf{r}, \omega)\mathbf{E}_2(\mathbf{r}, t) \cdot \hat{\mathbf{n}} = i\omega\sigma(\mathbf{r}, t). \quad (2.36)$$

Using Equation 2.35 this becomes

$$g_1(\mathbf{r}, \omega)\mathbf{E}_1(\mathbf{r}, t) \cdot \hat{\mathbf{n}} - g_2(\mathbf{r}, \omega)\mathbf{E}_2(\mathbf{r}, t) \cdot \hat{\mathbf{n}} = i\omega(\mathbf{D}_1(\mathbf{r}, t) \cdot \hat{\mathbf{n}} - \mathbf{D}_2(\mathbf{r}, t) \cdot \hat{\mathbf{n}}) \quad (2.37)$$

Using the constitutive relation $\mathbf{D} = \epsilon\mathbf{E}$ we obtain

$$\left(\epsilon_1 + \frac{ig_1}{\omega}\right)\mathbf{E}_1 \cdot \hat{\mathbf{n}} = \left(\epsilon_2 + \frac{ig_2}{\omega}\right)\mathbf{E}_2 \cdot \hat{\mathbf{n}}. \quad (2.38)$$

So, finally we obtain the time-varying boundary condition, the normal component of (complex) \mathbf{D} is continuous

$$\boxed{\hat{\epsilon}_1\mathbf{E}_1(\mathbf{r}, t) \cdot \hat{\mathbf{n}} = \hat{\epsilon}_2\mathbf{E}_2(\mathbf{r}, t) \cdot \hat{\mathbf{n}}}. \quad (2.39)$$

Here $\hat{\epsilon}$ is the complex dielectric function of the corresponding medium. Thus we find that Equation 2.39 assumes the same form as the equivalent static case by using the **complex dielectric functions**. It is the complex dielectric function that incorporates the losses and phase delays associated with time-varying fields in a medium.

Consider a closed loop across an interface, as indicated in the Figure 2.2. By integrating both sides of the equation

$$\nabla \times \mathbf{E}(\mathbf{r}, t) = -\frac{\partial \mathbf{B}(\mathbf{r}, t)}{\partial t} \quad (2.40)$$

over the surface enclosed by the loop, we obtain

$$\int (\nabla \times \mathbf{E}(\mathbf{r}, t) \cdot d\mathbf{S} = -\int \frac{\partial \mathbf{B}(\mathbf{r}, t)}{\partial t} \cdot d\mathbf{S} \quad (2.41)$$

$$\oint \mathbf{E}(\mathbf{r}, t) \cdot d\mathbf{l} = -\frac{\partial}{\partial t} \int \mathbf{B} \cdot d\mathbf{S} \quad (2.42)$$

$$\oint \mathbf{E}(\mathbf{r}, t) \cdot d\mathbf{l} = 0 \quad (2.43)$$

since the surface integral will vanish in the limit of shrinking the height of the loop. From this it immediately follows that the tangential component of the Electric field (even in the time varying case) must be continuous across an interface between two media. Thus

$$\boxed{\mathbf{E}_1(\mathbf{r}, t) \cdot \hat{\mathbf{t}} = \mathbf{E}_2(\mathbf{r}, t) \cdot \hat{\mathbf{t}}}. \quad (2.44)$$

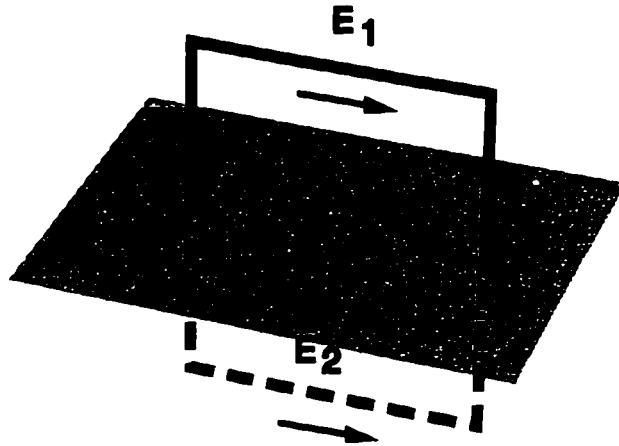


Figure 2.2: When the rectangular loop is made to shrink in height, the contribution to the line-integral will be dominated by only the lengths parallel to the interface.

If we exclude ferromagnetic materials, as well as materials with magnetic hysteresis, then since we do not have magnetic monopoles or the equivalent of an electric current for magnetic fields, the boundary conditions for the magnetic fields will have the same form as the corresponding static boundary conditions. Specifically, the tangential component of \mathbf{H} , the magnetic field, and the normal component of \mathbf{B} , the magnetic induction must be continuous across a magnetic interface:

$$\boxed{\mathbf{H}_1(\mathbf{r}, t) \cdot \hat{\mathbf{t}} = \mathbf{H}_2(\mathbf{r}, t) \cdot \hat{\mathbf{t}}} \quad (2.45)$$

and

$$\boxed{\mu_1 \mathbf{H}_1(\mathbf{r}, t) \cdot \hat{\mathbf{n}} = \mu_2 \mathbf{H}_2(\mathbf{r}, t) \cdot \hat{\mathbf{n}}} \quad (2.46)$$

where μ_1 and μ_2 are the permeabilities of the respective media.

Since there are two independent tangential directions and one normal direction for each point on a surface, these boundary conditions provide us with a total of six equations for each interface between two media. However, these equations may not be all independent of each other. It can be shown [22] that for a plane interface and an arbitrarily polarized plane wave, the equations on continuity of the tangential components of the \mathbf{E} and \mathbf{H} fields are the only independent equations. For non-planar surfaces, that are sufficiently smooth, the same arguments should hold *locally* at any point on the surface where the curvature can be considered negligible and the

arguments for a plane should hold good. Since this holds true for an arbitrary plane wave, it should hold true for any electromagnetic wave such as non-planar or even non-periodic waves. Non-smooth structures such as an edge can be approximated by a surface with finite curvature.

In general, obtaining the solution of vector fields imply that we obtain the solution of three mutually non-coplanar fields. On the boundary surfaces, we can construct three functions from the solution: Two of them representing the tangential components of the fields on the boundary and one representing the normal component on the boundary. The continuity of the three components across the boundary leads to unique determination of a vector field (with three components). For the electromagnetic field, the \mathbf{E} and \mathbf{H} are coupled. So, although we can determine each field independently with three independent equations each on the boundary surfaces, the coupling of the fields tell us at once that not all of them are going to be independent. In summary, one can obtain four independent equations from the boundary conditions for each interface between two media for special geometries. For arbitrarily shaped boundary surfaces we need to consider all the six equations and solve an over-determined system of equations.

Finally, one has to satisfy the radiation conditions which requires the scattered solution to decay inversely as the distance in the far field, and to assume the form of a spherical wave.

Chapter 3

Plane Wave Expansion in Basis Functions

3.1 Introduction

The success of the method of (vector) basis function expansion relies on our ability to express, conveniently, the incident radiation in terms of these basis functions. Although the completeness of this basis set guarantees the existence of unique coefficients for the expansion of an incident plane wave, in practice this involves some non-trivial algebra. It is our goal in this chapter to obtain explicit expansion coefficients for a general plane wave in these basis eigenfunctions. Linearity of Maxwell's equations imply that any excitation, non-planar or even non-periodic, could be solved in principle, from the known solution to plane wave excitations by use of Fourier space analysis. In principle, the set of basis functions obtained in any general orthogonal coordinate system could be considered a valid set of eigenfunctions in which the solution could be expressed. However, strictly algebraic and numerical considerations are in favor of the use of the functions pertaining to the spherical-polar coordinate system, for systems with azimuthal symmetry. The extensive analytical foundation readily available for the spherical Bessel/Hankel functions as well as that for the Associated Legendre functions allow us to obtain the expansion coefficients in closed form expressions.

3.2 The L,M,N basis

The solutions to the scalar Helmholtz equation in spherical polar coordinates are functions of the form (Appendix A):

$$\psi_{mn}(r, \theta, \phi) \sim z_n(kr) P_n^m(\cos \theta) e^{im\phi} \quad (3.1)$$

where $z_n(kr)$ represents either the *spherical Bessel* functions $j_n(kr)$ or the *spherical Hankel functions of the first kind* $h_n^{(1)}(kr)$. The spherical Bessel functions are regular at the origin, whereas the spherical Hankel functions diverge at/near the origin. So

a region including the origin can only feature the spherical bessel functions in its expression for the field. A region not including the origin can have contribution from either of these functions. The labelling indices are $n \in \{0, 1, 2, \dots\}$ and $m \in \{0, \pm 1, \pm 2, \dots, \pm n\}$. The $P_n^m(\cos \theta)$ are the *Associated Legendre Functions*.

We have seen earlier that we can obtain a vector function $\mathbf{L} = \nabla \psi$ which is a solution to the diffraction equation if ψ is a solution to the scalar Helmholtz equation. Thus we can define a set of functions \mathbf{L}_{mn} in the spherical polar coordinate system :

$$\mathbf{L}_{mn} = \mathbf{e}_r \frac{\partial \psi_{mn}}{\partial r} + \mathbf{e}_\theta \frac{1}{r} \frac{\partial \psi_{mn}}{\partial \theta} + \mathbf{e}_\phi \frac{1}{r \sin \theta} \frac{\partial \psi_{mn}}{\partial \phi}. \quad (3.2)$$

Since the solution ψ_{mn} are available in separated form, the partial derivatives reduce to total derivatives since they act on functions of a single variable only. Thus we obtain the \mathbf{L}_{mn} functions as

$$\mathbf{L}_{mn} = \nabla \psi_{mn} = k \left\{ \frac{dz_n(kr)}{d(kr)} P_n^m(\cos \theta) e^{im\phi} \mathbf{e}_r + \frac{z_n(kr)}{kr} \frac{dP_n^m(\cos \theta)}{d\theta} e^{im\phi} \mathbf{e}_\theta + im \frac{z_n(kr)}{kr} \frac{P_n^m(\cos \theta)}{\sin \theta} e^{im\phi} \mathbf{e}_\phi \right\}. \quad (3.3)$$

We have already seen that the \mathbf{M}_{mn} functions can be obtained by defining $\mathbf{M} = \nabla \times \mathbf{a}\psi$, where \mathbf{a} is an arbitrary constant vector. However, for the spherical polar coordinate system, we can obtain a set of \mathbf{M}_{mn} functions by defining

$$\mathbf{M} = \nabla \times (u(r)\psi \mathbf{e}_r). \quad (3.4)$$

where $u(r)$ is an unknown function that is to be determined. Thus we have

$$\begin{aligned} \mathbf{M} &= \frac{1}{r^2 \sin \theta} \begin{vmatrix} \mathbf{e}_r & r\mathbf{e}_\theta & r \sin \theta \mathbf{e}_\phi \\ \frac{\partial}{\partial r} & \frac{\partial}{\partial \theta} & \frac{\partial}{\partial \phi} \\ u\psi & 0 & 0 \end{vmatrix} \\ &= \frac{1}{r \sin \theta} \frac{\partial(u\psi)}{\partial \phi} \mathbf{e}_\theta - \frac{1}{r} \left(\frac{\partial(u\psi)}{\partial \theta} \right) \mathbf{e}_\phi. \end{aligned} \quad (3.5)$$

Now we need to impose the conditions that \mathbf{M} has to satisfy in order to obtain the constraining relations for the function $u(r)$. Assuming continuity of the functions and

their derivatives, we have

$$\begin{aligned}
\nabla \cdot \mathbf{M} &= \frac{1}{r^2 \sin \theta} \left\{ \frac{\partial}{\partial r} (r^2 \sin \theta \cdot 0) + \frac{\partial}{\partial \theta} \left(\frac{\partial(u\psi)}{\partial \phi} \right) \right. \\
&\quad \left. + \frac{\partial}{\partial \phi} \left(-\frac{\partial(u\psi)}{\partial \theta} \right) \right\} \\
&= \frac{1}{r^2 \sin \theta} \left\{ \frac{\partial^2(u\psi)}{\partial \theta \partial \phi} - \frac{\partial^2(u\psi)}{\partial \phi \partial \theta} \right\} = 0.
\end{aligned} \tag{3.6}$$

Thus the divergence is zero for the \mathbf{M} functions chosen according to Equation 3.4. We require the \mathbf{M} functions to satisfy the diffraction equation

$$\nabla(\nabla \cdot \mathbf{M}) - \nabla \times \nabla \times \mathbf{M} + k^2 \mathbf{M} = 0.$$

In order to obtain the necessary conditions to be satisfied, let us evaluate the $\nabla \times \nabla \times \mathbf{M}$ term. We have

$$\begin{aligned}
\nabla \times \mathbf{M} &= \frac{1}{r^2 \sin \theta} \begin{vmatrix} \mathbf{e}_r & r\mathbf{e}_\theta & r \sin \theta \mathbf{e}_\phi \\ \frac{\partial}{\partial r} & \frac{\partial}{\partial \theta} & \frac{\partial}{\partial \phi} \\ 0 & \frac{1}{\sin \theta} \frac{\partial(u\psi)}{\partial \phi} & -\sin \theta \frac{\partial(u\psi)}{\partial \theta} \end{vmatrix} \\
&= \frac{1}{r^2 \sin \theta} \left[\left\{ -\cos \theta \frac{\partial(u\psi)}{\partial \theta} - \sin \theta \frac{\partial^2(u\psi)}{\partial \theta^2} - \frac{1}{\sin \theta} \frac{\partial^2(u\psi)}{\partial \phi^2} \right\} \mathbf{e}_r \right. \\
&\quad \left. + \left\{ r \sin \theta \frac{\partial^2(u\psi)}{\partial r \partial \theta} \right\} \mathbf{e}_\theta + \left\{ r \frac{\partial^2(u\psi)}{\partial r \partial \phi} \right\} \mathbf{e}_\phi \right].
\end{aligned} \tag{3.7}$$

Therefore,

$$\nabla \times \nabla \times \mathbf{M} = \frac{1}{r^2 \sin \theta} \begin{vmatrix} \mathbf{e}_r & r\mathbf{e}_\theta & r \sin \theta \mathbf{e}_\phi \\ \frac{\partial}{\partial r} & \frac{\partial}{\partial \theta} & \frac{\partial}{\partial \phi} \\ \frac{1}{r^2 \sin \theta} \left(-\cos \theta \frac{\partial(u\psi)}{\partial \theta} - \sin \theta \frac{\partial^2(u\psi)}{\partial \theta^2} - \frac{1}{\sin \theta} \frac{\partial^2(u\psi)}{\partial \phi^2} \right) & \frac{\partial^2(u\psi)}{\partial r \partial \theta} & \frac{\partial^2(u\psi)}{\partial r \partial \phi} \end{vmatrix}$$

The \mathbf{e}_r component of $\nabla \times \nabla \times \mathbf{M}$ is

$$(\nabla \times \nabla \times \mathbf{M})_r = \frac{1}{r^2 \sin \theta} \left[\frac{\partial^3(u\psi)}{\partial \theta \partial r \partial \phi} - \frac{\partial^3(u\psi)}{\partial \phi \partial r \partial \theta} \right] = 0.$$

From Equation 3.5 we have the radial component M_r equal to zero. Thus the radial component of the diffraction equation is satisfied by the current choice of \mathbf{M} .

The \mathbf{e}_θ component of $\nabla \times \nabla \times \mathbf{M}$ is given by

$$(\nabla \times \nabla \times \mathbf{M})_\theta = \frac{1}{r \sin \theta} \frac{\partial}{\partial \phi} \left[-\frac{1}{r^2 \sin \theta} \left\{ \frac{\partial}{\partial \theta} \left(\sin \theta \frac{\partial(u\psi)}{\partial \theta} \right) - \frac{1}{r^2 \sin^2 \theta} \frac{\partial^2(u\psi)}{\partial \phi^2} - \frac{\partial^2(u\psi)}{\partial r^2} \right\} \right].$$

So we can write

$$(-\nabla \times \nabla \times \mathbf{M}) \cdot \mathbf{e}_\theta + k^2 \mathbf{M} \cdot \mathbf{e}_\theta = \frac{1}{r \sin \theta} \frac{\partial}{\partial \phi} \left[\frac{\partial^2(u\psi)}{\partial r^2} + \frac{1}{r^2 \sin \theta} \frac{\partial}{\partial \theta} \left(\sin \theta \frac{\partial(u\psi)}{\partial \theta} \right) + \frac{1}{r^2 \sin^2 \theta} \frac{\partial^2(u\psi)}{\partial \phi^2} + k^2 u\psi \right].$$

In order for the diffraction equation to be satisfied, the quantity within the square brackets must be independent of ϕ . By following the same procedure, we obtain

$$(\nabla \times \nabla \times \mathbf{M}) \cdot \mathbf{e}_\phi - k^2 \mathbf{M} \cdot \mathbf{e}_\phi = \frac{1}{r} \frac{\partial}{\partial \theta} \left[\frac{\partial^2(u\psi)}{\partial r^2} + \frac{1}{r^2 \sin \theta} \frac{\partial}{\partial \theta} \left(\sin \theta \frac{\partial(u\psi)}{\partial \theta} \right) + \frac{1}{r^2 \sin^2 \theta} \frac{\partial^2(u\psi)}{\partial \phi^2} + k^2 u\psi \right].$$

As we can see, the expressions within the square brackets for both the θ and ϕ equations above are one and the same. Thus the diffraction equation will be satisfied if the quantity within the square brackets above is some function of r alone, say $f(r)$. In that case the right-hand sides will vanish. In particular, we can choose $f(r) = 0$, so that the condition on $u(r)$ is given by

$$\frac{\partial^2(u\psi)}{\partial r^2} + \frac{1}{r^2 \sin \theta} \frac{\partial}{\partial \theta} \left(\sin \theta \frac{\partial(u\psi)}{\partial \theta} \right) + \frac{1}{r^2 \sin^2 \theta} \frac{\partial^2(u\psi)}{\partial \phi^2} + k^2 u\psi = 0.$$

In addition, if we choose $u(r) = r$, we obtain

$$\frac{\partial^2(r\psi)}{\partial r^2} + \frac{1}{r \sin \theta} \frac{\partial}{\partial \theta} \left(\sin \theta \frac{\partial \psi}{\partial \theta} \right) + \frac{1}{r \sin^2 \theta} \frac{\partial^2 \psi}{\partial \phi^2} + k^2 r\psi = 0.$$

The left-hand side of the above equation is equal to $r \cdot (\nabla^2 \psi + k^2 \psi)$. So for the above choice for $f(r)$ and $u(r)$, we have the diffraction equation satisfied by all the three components of \mathbf{M} , when ψ satisfies the scalar Helmholtz equation. Thus we have :

$$\begin{aligned} \mathbf{M}_{mn} &= \nabla \times (r \mathbf{e}_r \psi_{mn}) \\ &= \psi_{mn} (\nabla \times r \mathbf{e}_r) + \nabla \psi_{mn} \times r \mathbf{e}_r \\ &= \nabla \psi_{mn} \times \mathbf{r} \quad (\text{Since } \nabla \times \mathbf{r} = 0) \\ &= \mathbf{L}_{mn} \times \mathbf{r}. \end{aligned}$$

Therefore, we obtain the desired \mathbf{M}_{mn} functions that have zero divergence :

$$\mathbf{M}_{mn} = imz_n(kr) \frac{P_n^m(\cos \theta)}{\sin \theta} e^{im\phi} \mathbf{e}_\theta - z_n(kr) \frac{dP_n^m(\cos \theta)}{d\theta} e^{im\phi} \mathbf{e}_\phi. \quad (3.8)$$

Having obtained \mathbf{M}_{mn} , we can easily obtain the other set of zero divergence functions, the \mathbf{N}_{mn} , since

$$\mathbf{N}_{mn} = \frac{1}{k} \nabla \times \mathbf{M}_{mn}$$

$$\begin{aligned} &= \frac{1}{kr^2 \sin \theta} \begin{vmatrix} \mathbf{e}_r & r \mathbf{e}_\theta & r \sin \theta \mathbf{e}_\phi \\ \frac{\partial}{\partial r} & \frac{\partial}{\partial \theta} & \frac{\partial}{\partial \phi} \\ 0 & r \left(imz_n(kr) \frac{P_n^m(\cos \theta)}{\sin \theta} e^{im\phi} \right) & r \sin \theta \left(-z_n(kr) \frac{\partial P_n^m(\cos \theta)}{\partial \theta} e^{im\phi} \right) \end{vmatrix} \\ &= \frac{1}{kr^2 \sin \theta} \left[rz_n(kr) \left\{ -\sin \theta \frac{\partial^2 P_n^m(\cos \theta)}{\partial \theta^2} - \cos \theta \frac{\partial P_n^m(\cos \theta)}{\partial \theta} + m^2 \frac{P_n^m(\cos \theta)}{\sin \theta} \right\} \mathbf{e}_r \right. \\ &\quad \left. + \left(r \frac{\partial rz_n(kr)}{\partial r} \right) \sin \theta \frac{\partial P_n^m(\cos \theta)}{\partial \theta} \mathbf{e}_\theta + im \left(r \frac{\partial rz_n(kr)}{\partial r} \right) \frac{P_n^m(\cos \theta)}{\sin \theta} \mathbf{e}_\phi \right] e^{im\phi}. \end{aligned}$$

Since $P_n^m(\cos \theta)$ is the solution to the θ -part of the separated scalar wave equation, therefore

$$\frac{d^2 P_n^m}{d\theta^2} + \frac{\cos \theta}{\sin \theta} \frac{dP_n^m}{d\theta} + \left(n(n+1) - \frac{m^2}{\sin^2 \theta} \right) P_n^m = 0.$$

Equivalently,

$$-\sin \theta \frac{\partial^2 P_n^m(\cos \theta)}{\partial \theta^2} - \cos \theta \frac{\partial P_n^m(\cos \theta)}{\partial \theta} + m^2 \frac{P_n^m(\cos \theta)}{\sin \theta} = n(n+1) P_n^m(\cos \theta) \sin \theta.$$

This simplifies the \mathbf{e}_r term and we obtain, remembering to change the partial derivatives to their corresponding total derivatives :

$$\mathbf{N}_{mn} = n(n+1) \frac{z_n(kr)}{kr} P_n^m(\cos \theta) e^{im\phi} \mathbf{e}_r + \frac{1}{kr} \frac{d(rz_n(kr))}{dr} \frac{dP_n^m(\cos \theta)}{d\theta} e^{im\phi} \mathbf{e}_\theta + im \frac{1}{kr} \frac{d(rz_n(kr))}{dr} \frac{P_n^m(\cos \theta)}{\sin \theta} e^{im\phi} \mathbf{e}_\phi. \quad (3.9)$$

It is of some interest to note that since the expressions for \mathbf{L}_{mn} , \mathbf{M}_{mn} and \mathbf{N}_{mn} have the i and m occurring as a product, we can easily derive the following useful relations:

$$\mathbf{L}_{-mn} = (-1)^m \frac{(n-m)!}{(n+m)!} \mathbf{L}_{mn}^* \quad (3.10)$$

$$\mathbf{M}_{-mn} = (-1)^m \frac{(n-m)!}{(n+m)!} \mathbf{M}_{mn}^* \quad (3.11)$$

$$\mathbf{N}_{-mn} = (-1)^m \frac{(n-m)!}{(n+m)!} \mathbf{N}_{mn}^* \quad (3.12)$$

3.3 Orthogonal Properties of L, M and N Functions

Having obtained explicit expressions for the vector functions \mathbf{L} , \mathbf{M} and \mathbf{N} , it is desirable to examine their orthogonal properties. Denoting the complex conjugate of \mathbf{L}_{mn} as \mathbf{L}_{mn}^* , we have

$$\mathbf{L}_{mn} \cdot \mathbf{L}_{m'n'}^* = k^2 e^{im\phi} e^{-im'\phi} \left[P_n^m(\cos \theta) P_{n'}^{m'}(\cos \theta) \frac{dz_n(kr)}{d(kr)} \frac{dz_{n'}^*(kr)}{d(kr)} + \left(\frac{dP_n^m(\cos \theta)}{d\theta} \frac{dP_{n'}^{m'}(\cos \theta)}{d\theta} + \frac{mm'}{\sin^2 \theta} P_n^m(\cos \theta) P_{n'}^{m'}(\cos \theta) \right) \frac{z_n(kr) z_{n'}^*(kr)}{(kr)^2} \right]. \quad (3.13)$$

On carrying out the ϕ -integration, within the limits of $\phi \in [0, 2\pi]$, since

$$\int_0^{2\pi} d\phi e^{im\phi} e^{-im'\phi} = 2\pi \delta_{mm'}. \quad (3.14)$$

We obtain

$$\int_0^{2\pi} d\phi \mathbf{L}_{mn} \cdot \mathbf{L}_{m'n'}^* = 2\pi k^2 \left[P_n^m(\cos \theta) P_{n'}^{m'}(\cos \theta) \frac{dz_n(kr)}{d(kr)} \frac{dz_{n'}^*(kr)}{d(kr)} + \left(\frac{dP_n^m(\cos \theta)}{d\theta} \frac{dP_{n'}^{m'}(\cos \theta)}{d\theta} + \frac{mm'}{\sin^2 \theta} P_n^m(\cos \theta) P_{n'}^{m'}(\cos \theta) \right) \frac{z_n(kr) z_{n'}^*(kr)}{(kr)^2} \right]. \quad (3.15)$$

$$+ \left(\frac{dP_n^m(\cos \theta)}{d\theta} \frac{dP_{n'}^m(\cos \theta)}{d\theta} + \frac{m^2}{\sin^2 \theta} P_n^m(\cos \theta) P_{n'}^m(\cos \theta) \right) \frac{z_n(kr) z_{n'}^*(kr)}{(kr)^2} \Big].$$

Using the orthogonality relations for the Associated Legendre Functions.

$$\int_{-1}^1 dx P_n^m(x) P_{n'}^m(x) = \frac{2}{2n+1} \frac{(n+m)!}{(n-m)!} \delta_{nn'}. \quad (3.16)$$

and the following relation that we derive in Appendix C.

$$\begin{aligned} \int_0^\pi d\theta \sin \theta \left(\frac{dP_n^m(\cos \theta)}{d\theta} \frac{dP_{n'}^m(\cos \theta)}{d\theta} + \frac{m^2}{\sin^2 \theta} P_n^m(\cos \theta) P_{n'}^m(\cos \theta) \right) \\ = \frac{2n(n+1)}{2n+1} \frac{(n+m)!}{(n-m)!} \delta_{nn'}. \end{aligned} \quad (3.17)$$

we obtain, on carrying out the θ -integration.

$$\begin{aligned} \int_0^{2\pi} d\phi \int_0^\pi d\theta \sin \theta \mathbf{L}_{mn} \cdot \mathbf{L}_{m'n'}^* \\ = 2\pi k^2 \frac{2n(n+1)}{2n+1} \frac{(n+m)!}{(n-m)!} \left\{ \left[\frac{dz_n(kr)}{d(kr)} \right]^2 + \frac{n(n+1)}{(kr)^2} [z_n(kr)]^2 \right\} \delta_{nn'} \delta_{mm'}. \end{aligned} \quad (3.18)$$

where the square denotes the square of the absolute value. Using the recurrence relations on the spherical Bessel/Hankel functions, with $\rho = kr$:

$$\frac{dz_n(\rho)}{d\rho} = \frac{1}{2n+1} \{n z_{n-1}(\rho) - (n+1) z_{n+1}(\rho)\}. \quad (3.19)$$

and

$$\frac{z_n(\rho)}{\rho} = \frac{1}{2n+1} \{z_{n-1}(\rho) + z_{n+1}(\rho)\}. \quad (3.20)$$

we obtain, keeping in mind that the squares of the Bessel/Hankel functions denote the squares of their absolute values in these expressions:

$$\begin{aligned} \int_0^{2\pi} d\phi \int_0^\pi d\theta \sin \theta \mathbf{L}_{mn} \cdot \mathbf{L}_{m'n'}^* \\ = \frac{4\pi k^2}{(2n+1)^2} \frac{(n+m)!}{(n-m)!} [n z_{n-1}^2(kr) + (n+1) z_{n+1}^2(kr)] \delta_{nn'} \delta_{mm'}. \end{aligned} \quad (3.21)$$

Similarly, the orthogonality relation between the \mathbf{M} functions can be obtained:

$$\int_0^{2\pi} d\phi \int_0^\pi d\theta \sin \theta \mathbf{M}_{mn} \cdot \mathbf{M}_{m'n'}^* = \frac{4\pi n(n+1)(n+m)!}{2n+1(n-m)!} z_n^2(kr) \delta_{nn'} \delta_{mm'}. \quad (3.22)$$

Using the following recurrence relation on the spherical Bessel/Hankel functions:

$$\frac{1}{kr} \frac{d}{dr} (r z_n(kr)) = \frac{1}{2n+1} \{ (n+1) z_{n-1}(kr) - n z_{n+1}(kr) \}. \quad (3.23)$$

we obtain the orthogonal relations for the \mathbf{N} functions :

$$\begin{aligned} & \int_0^{2\pi} d\phi \int_0^\pi d\theta \sin \theta \mathbf{N}_{mn} \cdot \mathbf{N}_{m'n'}^* \\ &= \frac{4\pi n(n+1)(n+m)!}{(2n+1)^2(n-m)!} \left[(n+1) z_{n-1}^2(kr) + n z_{n+1}^2(kr) \right] \delta_{nn'} \delta_{mm'}. \end{aligned} \quad (3.24)$$

Now we need to examine the cross terms; orthogonality relations between the \mathbf{L} , \mathbf{M} , \mathbf{N} functions. The obvious ϕ -integrations tell us immediately that functions with different m 's will be orthogonal to each other. So we need to examine the behavior of these cross terms for differing n 's only. We can write

$$\int_0^{2\pi} d\phi \mathbf{L}_{mn} \cdot \mathbf{M}_{m'n'}^* = -2\pi i m k \frac{z_n(kr) z_{n'}^*(kr)}{r} \frac{1}{\sin \theta} \frac{d}{d\theta} (P_n^m(\cos \theta) P_{n'}^m(\cos \theta)). \quad (3.25)$$

For $m = 0$, the expression on the right-hand side vanishes. For $m \neq 0$, the θ -integration vanishes since $P_n^m(x) = (1-x^2)^{d/2} P_n/dx^m$ goes to zero at the limits when $x^2 = \cos^2 \theta = 1$. Thus we have the orthogonality relation (for all n, m):

$$\int_0^{2\pi} d\phi \int_0^\pi d\theta \sin \theta \mathbf{L}_{mn} \cdot \mathbf{M}_{m'n'}^* = 0 \quad (\forall n, m, n', m' \in I) \quad (3.26)$$

By reasoning in exactly the same way we can show that the $\mathbf{M} \cdot \mathbf{N}^*$ term vanishes for all values of n, m :

$$\int_0^{2\pi} d\phi \int_0^\pi d\theta \sin \theta \mathbf{M}_{mn} \cdot \mathbf{N}_{m'n'}^* = 0 \quad (\forall n, m, n', m' \in I) \quad (3.27)$$

Now we examine the cross term $\mathbf{L} \cdot \mathbf{N}$:

$$\begin{aligned}
& \int_0^{2\pi} d\phi \int_0^\pi d\theta \sin \theta \mathbf{L}_{mn} \cdot \mathbf{N}_{m'n'}^* \\
= & 2\pi k \left\{ n'(n'+1) \frac{z_{n'}^*(kr)}{kr} \frac{dz_n(kr)}{d(kr)} \int_0^\pi d\theta \sin \theta P_n^m(\cos \theta) P_{n'}^m(\cos \theta) \right. \\
& + \frac{z_n(kr)}{kr} \frac{1}{kr} \frac{d}{dr} (r z_{n'}^*(kr)) \\
& \left. \int_0^\pi d\theta \sin \theta \left(\frac{dP_n^m(\cos \theta)}{d\theta} \frac{dP_{n'}^m(\cos \theta)}{d\theta} + \frac{m^2}{\sin^2 \theta} P_n^m(\cos \theta) P_{n'}^m(\cos \theta) \right) \right\} \delta_{mm'}
\end{aligned}$$

By virtue of Equation 3.16 and Equation 3.17 we can see that the θ -integrals will vanish for $n \neq n'$. The only isolated case when the integral may not vanish is when $n = n'$, when we can use the recurrence relations on the spherical Bessel/Hankel functions to obtain:

$$\begin{aligned}
& \int_0^{2\pi} d\phi \int_0^\pi d\theta \sin \theta \mathbf{L}_{mn} \cdot \mathbf{N}_{m'n'}^* \\
= & \frac{4\pi kn(n+1)(n+m)!}{(2n+1)^2 (n-m)!} [z_{n-1}^2(kr) - z_{n+1}^2(kr)] \delta_{nn'} \delta_{mm'}. \quad (3.28)
\end{aligned}$$

Since the right-hand side of the above equation is a real number, if we obtain the complex conjugate of either side of the equation, we immediately come to the conclusion that

$$\int_0^{2\pi} d\phi \int_0^\pi d\theta \sin \theta \mathbf{L}_{mn} \cdot \mathbf{N}_{m'n}^* = \int_0^{2\pi} d\phi \int_0^\pi d\theta \sin \theta \mathbf{N}_{m'n} \cdot \mathbf{L}_{mn}^* \quad (3.29)$$

Thus, the $\mathbf{L.M.N}$ basis functions are not completely orthogonal to each other. The *overlap* between the \mathbf{L} and \mathbf{N} functions for the same n requires us to consider both the matrix elements even for cases when we are trying to expand a plane wave that has zero divergence. However, we can easily observe that the $\{\mathbf{L}_{mn}, \mathbf{M}_{mn}, \mathbf{N}_{mn}\}$ functions are *mutually non-coplanar*. Since they also form a complete set of functions in the Hilbert space of all solutions to the diffraction equation, in principle one can use the Gram-Schmidt Orthogonalization procedure to derive an orthonormal set from the given set of functions. However, as we will see shortly, such a theoretical process

is not required for most applications. We can use the **L.M.N** basis functions directly for many types of computations.

3.4 Plane Wave Expansion in L, M, N Basis

The completeness of the set of functions **L**, **M** and **N** assures us of the existence of a valid expansion series for an arbitrary plane electromagnetic wave which satisfies the diffraction equation, in this basis set. Once a valid set of coefficients are obtained, we can offer an *operational* proof of the completeness theorem. If *any* plane wave can be represented in a convergent series of these functions, then it immediately implies that the set must be complete. This follows from the fact that any scattered solution to the vector Helmholtz equation can be constructed from a plane wave basis.

To begin our discussion, let us consider an arbitrary plane wave:

$$\mathbf{F} = \mathbf{E}e^{i\mathbf{k}\cdot\mathbf{r}}. \quad (3.30)$$

Here $\mathbf{E} = E_x\mathbf{e}_x + E_y\mathbf{e}_y + E_z\mathbf{e}_z$ is the (oscillating) electric field of the plane wave. $\mathbf{k} = (k, \alpha, \beta)$ is the propagation vector and $\mathbf{r} = (r, \theta, \phi)$ is the position coordinate. To keep our derivation sufficiently general, we shall allow the orientation of \mathbf{E} and \mathbf{k} to be along arbitrary directions. In reality, for a plane electromagnetic wave in a homogenous and isotropic medium, the \mathbf{E} and \mathbf{k} must be orthogonal, and so the divergence of \mathbf{F} must vanish. However at this stage we do not need to impose such constraints. We shall also allow the E_x, E_y, E_z and k to be complex numbers. This represents any general elliptically polarized wave propagating in a medium that could be attenuating/absorbing or even amplifying.

The completeness of the set of functions validate the following representation:

$$\mathbf{e}_x e^{i\mathbf{k}\cdot\mathbf{r}} = \sum_{mn} \{a_{mn}^x \mathbf{M}_{mn} + b_{mn}^x \mathbf{N}_{mn} + c_{mn}^x \mathbf{L}_{mn}\} \quad (3.31)$$

$$\mathbf{e}_y e^{i\mathbf{k}\cdot\mathbf{r}} = \sum_{mn} \{a_{mn}^y \mathbf{M}_{mn} + b_{mn}^y \mathbf{N}_{mn} + c_{mn}^y \mathbf{L}_{mn}\} \quad (3.32)$$

$$\mathbf{e}_z e^{i\mathbf{k}\cdot\mathbf{r}} = \sum_{mn} \{a_{mn}^z \mathbf{M}_{mn} + b_{mn}^z \mathbf{N}_{mn} + c_{mn}^z \mathbf{L}_{mn}\} \quad (3.33)$$

Therefore, we can write our general plane wave expansion as:

$$\begin{aligned} \mathbf{E}e^{i\mathbf{k}\cdot\mathbf{r}} = & \sum_{mn} \{ (E_x a_{mn}^x + E_y a_{mn}^y + E_z a_{mn}^z) \mathbf{M}_{mn} \\ & + (E_x b_{mn}^x + E_y b_{mn}^y + E_z b_{mn}^z) \mathbf{N}_{mn} \\ & + (E_x c_{mn}^x + E_y c_{mn}^y + E_z c_{mn}^z) \mathbf{L}_{mn} \} \end{aligned} \quad (3.34)$$

If \mathbf{E} is represented by (E, θ_i, ϕ_i) , in the spherical polar coordinate system, then

$$E_x = E \sin \theta_i \cos \phi_i \quad E_y = E \sin \theta_i \sin \phi_i \quad E_z = E \cos \theta_i. \quad (3.35)$$

Therefore, we need to obtain the nine coefficients $\{a_{mn}^x, a_{mn}^y, \dots, c_{mn}^z\}$ which are functions of $\{n, m, \alpha, \beta\}$.

3.4.1 Deriving a_{mn}^z, b_{mn}^z and c_{mn}^z

It can be shown [43] that the exponential part of the expression for a plane wave can be expanded in the following series:

$$e^{i\mathbf{k}\cdot\mathbf{r}} = \sum_{s=0}^{\infty} i^s (2s+1) j_s(kr) \left\{ \sum_{l=0}^s \frac{(s-l)!}{(s+l)!} P_s^l(\cos \alpha) e^{-il\beta} P_s^l(\cos \theta) e^{il\phi} + \sum_{l=1}^s \frac{(s-l)!}{(s+l)!} P_s^l(\cos \alpha) e^{il\beta} P_s^l(\cos \theta) e^{-il\phi} \right\} \quad (3.36)$$

Let us denote $\mathbf{e}_c e^{i\mathbf{k}\cdot\mathbf{r}} \equiv \mathbf{E}_c$, where c denotes x, y or z . Let us introduce the notation:

$$\int_0^{\infty} dr \int_0^{\pi} d\theta \sin \theta \int_0^{2\pi} d\phi \mathbf{E}_c \cdot \mathbf{X}_{mn}^* = \int \mathbf{E}_c \cdot \mathbf{X}_{mn} = \langle \mathbf{E}_c | \mathbf{X}_{mn} \rangle \quad (3.37)$$

where \mathbf{X}_{mn} represents $\mathbf{L}_{mn}, \mathbf{M}_{mn}$ or \mathbf{N}_{mn} . We can view $\langle \mathbf{E}_c | \mathbf{M}_{mn} \rangle$ as the definition of the *inner product* in the Hilbert space of all solutions to the diffraction equation.

From Equation 3.33, we can calculate the coefficients $\{a_{mn}^z, b_{mn}^z, c_{mn}^z\}$ using the orthogonality relations already obtained. Obtaining the inner product of both sides of the equation with respect to $\mathbf{L}_{mn}, \mathbf{M}_{mn}$ and \mathbf{N}_{mn} respectively, we obtain the following relations:

$$\langle \mathbf{E}_z | \mathbf{M}_{mn} \rangle = a_{mn}^z \langle \mathbf{M}_{mn} | \mathbf{M}_{mn} \rangle. \quad (3.38)$$

$$\langle \mathbf{E}_z | \mathbf{L}_{mn} \rangle = b_{mn}^z \langle \mathbf{N}_{mn} | \mathbf{L}_{mn} \rangle + c_{mn}^z \langle \mathbf{L}_{mn} | \mathbf{L}_{mn} \rangle. \quad (3.39)$$

$$\langle \mathbf{E}_z | \mathbf{N}_{mn} \rangle = b_{mn}^z \langle \mathbf{N}_{mn} | \mathbf{N}_{mn} \rangle + c_{mn}^z \langle \mathbf{L}_{mn} | \mathbf{N}_{mn} \rangle. \quad (3.40)$$

which can be readily solved to yield:

$$a_{mn}^z = \frac{\langle \mathbf{E}_z | \mathbf{M}_{mn} \rangle}{\langle \mathbf{M}_{mn} | \mathbf{M}_{mn} \rangle} \quad (3.41)$$

$$b_{mn}^z = \frac{\langle \mathbf{E}_z | \mathbf{L}_{mn} \rangle \langle \mathbf{L}_{mn} | \mathbf{N}_{mn} \rangle - \langle \mathbf{E}_z | \mathbf{N}_{mn} \rangle \langle \mathbf{L}_{mn} | \mathbf{L}_{mn} \rangle}{\langle \mathbf{N}_{mn} | \mathbf{L}_{mn} \rangle \langle \mathbf{L}_{mn} | \mathbf{N}_{mn} \rangle - \langle \mathbf{N}_{mn} | \mathbf{N}_{mn} \rangle \langle \mathbf{L}_{mn} | \mathbf{L}_{mn} \rangle} \quad (3.42)$$

$$c_{mn}^z = \frac{\langle \mathbf{E}_z | \mathbf{N}_{mn} \rangle \langle \mathbf{N}_{mn} | \mathbf{L}_{mn} \rangle - \langle \mathbf{E}_z | \mathbf{L}_{mn} \rangle \langle \mathbf{N}_{mn} | \mathbf{N}_{mn} \rangle}{\langle \mathbf{N}_{mn} | \mathbf{L}_{mn} \rangle \langle \mathbf{L}_{mn} | \mathbf{N}_{mn} \rangle - \langle \mathbf{N}_{mn} | \mathbf{N}_{mn} \rangle \langle \mathbf{L}_{mn} | \mathbf{L}_{mn} \rangle} \quad (3.43)$$

By substituting the label z with x or y in Eqn 3.41, Eqn 3.42 and Eqn 3.43, we immediately obtain the corresponding formula for the remaining coefficients in terms of their inner products with the basis set functions.

The integrals represented by the various inner products in the expressions for the coefficients require a good deal of messy algebra and careful analysis for its evaluation. The integrands involve products of spherical Bessel functions, Associated Legendre functions as well as their derivatives. The non-triviality of these integrations is amplified by the fact that one has to evaluate a double infinite summation (over s and l) to arrive at a closed form expression for these integrals. The inner products between the basis functions are obtained from the corresponding orthogonal relations Equations (3.22, 3.24, 3.21, 3.29). By carrying out the r-integration on both sides of the equation we can show (worked out in the Appendix D):

$$\langle \mathbf{L}_{mn} | \mathbf{L}_{mn} \rangle = \frac{2\pi^2 k (n+m)! (4n^2 + 4n - 1)}{(2n+1)^2 (n-m)! (2n-1)(2n+3)} \quad (3.44)$$

$$\langle \mathbf{M}_{mn} | \mathbf{M}_{mn} \rangle = \frac{2\pi^2 n(n+1) (n+m)!}{k (2n+1)^2 (n-m)!} \quad (3.45)$$

$$\langle \mathbf{N}_{mn} | \mathbf{N}_{mn} \rangle = \frac{2\pi^2 (n+m)! n(n+1)(4n^2 + 4n + 3)}{k(2n+1)^2 (n-m)! (2n-1)(2n+3)} \quad (3.46)$$

$$\langle \mathbf{L}_{mn} | \mathbf{N}_{mn} \rangle = \frac{8\pi^2 (n+m)! n(n+1)}{(2n+1)^2 (n-m)! (2n-1)(2n+3)} \quad (3.47)$$

Since

$$\mathbf{e}_z = \cos \theta \mathbf{e}_r - \sin \theta \mathbf{e}_\theta. \quad (3.48)$$

the integrals involving \mathbf{e}_z will contain only terms of the form $P_{n'}^m$, where n' can be shown to be equal to ± 1 only. The integrals $\langle \mathbf{E}_z | \mathbf{M}_{mn} \rangle$, $\langle \mathbf{E}_z | \mathbf{N}_{mn} \rangle$ and $\langle \mathbf{E}_z | \mathbf{L}_{mn} \rangle$ therefore have the following form for $m \geq 0$:

$$\langle \mathbf{E}_z | \mathbf{M}_{mn} \rangle = \frac{2m\pi^2 i^{n+1}}{k(2n+1)} P_n^m(\cos \alpha) e^{-im\beta} \quad (3.49)$$

$$\langle \mathbf{E}_z | \mathbf{N}_{mn} \rangle = \frac{-2\pi^2 i^{n-1}}{k(2n+1)} \frac{e^{-im\beta}}{(2n-1)(2n+3)} \times \quad (3.50)$$

$$\left[n(n-m+1)(2n-1)P_{n+1}^m(\cos \alpha) - (n+1)(n+m)(2n+3)P_{n-1}^m(\cos \alpha) \right]$$

$$\langle \mathbf{E}_z | \mathbf{L}_{mn} \rangle = \frac{2\pi^2 i^{n-1}}{(2n+1)(2n-1)(2n+3)} \frac{e^{-im\beta}}{\times} \quad (3.51)$$

$$\left[(n+m)(2n+3)P_{n-1}^m(\cos \alpha) + (n-m+1)(2n-1)P_{n+1}^m(\cos \alpha) \right]$$

On substituting the expressions for these integrals back into Equations 3.41, 3.42 and 3.43, we finally obtain the functional form for the coefficients (for $m \geq 0$):

$$a_{mn}^{\pm}(n, m, \alpha, \beta) = i^{n+1} \frac{m(2n+1)(n-m)!}{n(n+1)(n+m)!} P_n^m(\cos \alpha) e^{-im\beta} \quad (m \geq 0) \quad (3.52)$$

$$b_{mn}^{\pm}(n, m, \alpha, \beta) = \frac{i^{n+1}}{n(n+1)(n+m)!} \frac{(n-m)!}{e^{-im\beta}} \left[\begin{array}{c} n(n-m+1)P_{n+1}^m(\cos \alpha) \\ -(n+1)(n+m)P_{n-1}^m(\cos \alpha) \end{array} \right] \quad (m \geq 0) \quad (3.53)$$

$$c_{mn}^{\pm}(n, m, \alpha, \beta) = \frac{i^{n-1}}{k} \frac{(n-m)!}{(n+m)!} (2n+1) e^{-im\beta} \cos \alpha P_n^m(\cos \alpha) \quad (m \geq 0) \quad (3.54)$$

We observe that when $\alpha = \pi/2$, so that \mathbf{E} and \mathbf{k} are perpendicular to each other as in a plane electromagnetic wave, all the c_{mn}^{\pm} coefficients vanish, since the

divergence of such a field is zero. When $\alpha = 0$ or π all the a_{mn}^z coefficients vanish since $P_n^m(\pm 1) = 0$ for $m > 0$, and a_{mn}^z vanish for $m = 0$ because of the factor m in its expression. Similarly, the b_{mn}^z vanish for $\alpha = 0$ or π since $P_n^m(\pm 1) = 0$ for $m > 0$, and for $m = 0$ $P_n^0(\pm 1)(-1)^n$ for $m = 0$ so that the expression within the square brackets become for $m = 0$, $n(n+1) \cdot 1 - (n+1) \cdot n = 0$. So when $\alpha = 0$ or π only the c_{mn}^z coefficients can be non-zero.

When $m < 0$, we can arrive at the corresponding coefficients by examining the changes that occur in the expressions for the individual inner product terms. As shown in the appendix, from considerations of parity of the Associated Legendre functions, we can arrive at the corresponding coefficients when $m < 0$:

$$a_{-mn}^z(n, m, \alpha, \beta) = (-1)^{m+1} e^{2im\beta} \frac{(n+m)!}{(n-m)!} a_{mn}^z(n, m, \alpha, \beta) \quad (m \geq 0) \quad (3.55)$$

$$b_{-mn}^z(n, m, \alpha, \beta) = (-1)^m e^{2im\beta} \frac{(n+m)!}{(n-m)!} b_{mn}^z(n, m, \alpha, \beta) \quad (m \geq 0) \quad (3.56)$$

$$c_{-mn}^z(n, m, \alpha, \beta) = (-1)^m e^{2im\beta} \frac{(n+m)!}{(n-m)!} c_{mn}^z(n, m, \alpha, \beta) \quad (m \geq 0) \quad (3.57)$$

3.4.2 Deriving a_{mn}^x , b_{mn}^x and c_{mn}^x

The process of finding the x-coefficients are similar to that of the z-coefficients that we have just obtained. However, the algebra becomes even more messy, because now we do not have the advantage of having the symmetry about the z-axis. Again, the detailed analysis is shown in Appendix D and we highlight only the key results from such calculations. We have

$$\mathbf{e}_x = \sin \theta \cos \phi \mathbf{e}_r + \cos \theta \cos \phi \mathbf{e}_\theta - \sin \phi \mathbf{e}_\phi \quad (3.58)$$

So now, the integrals of the type $\langle \mathbf{E}_x | \mathbf{L}_{mn} \rangle$, $\langle \mathbf{E}_x | \mathbf{M}_{mn} \rangle$ and $\langle \mathbf{E}_x | \mathbf{N}_{mn} \rangle$ will have terms with $m \pm 1$ because of the extra $\sin \phi$ and $\cos \phi$ terms. The parity of all the parts of

the integrands considered together (the r, θ and ϕ parts) allows only the $l = m \pm 1$ terms to survive. So for $m \geq 0$:

$$\langle \mathbf{E}_x | \mathbf{M}_{mn} \rangle = \frac{\pi^2 i^{n+1}}{k(2n+1)} \left[\begin{array}{l} (n+m)(n-m+1)P_n^{m-1}(\cos \alpha) \epsilon^{-i(m-1)\beta} \\ + P_n^{m+1}(\cos \alpha) \epsilon^{-i(m+1)\beta} \end{array} \right] \quad (3.59)$$

$$\langle \mathbf{E}_x | \mathbf{N}_{mn} \rangle = \frac{\pi^2 i^{n+1}}{k} \frac{1}{(2n+1)(2n-1)(2n+3)} \times \quad (3.60)$$

$$\left[\begin{array}{l} (2n+3)(n+1)(n+m)(n+m-1)P_{n-1}^{m-1}(\cos \alpha) \epsilon^{-i(m-1)\beta} \\ - (2n+3)(n+1)P_{n-1}^{m+1}(\cos \alpha) \epsilon^{-i(m+1)\beta} \\ + (2n-1)n(n-m+2)(n-m+1)P_{n+1}^{m-1}(\cos \alpha) \epsilon^{-i(m-1)\beta} \\ - (2n-1)nP_{n+1}^{m+1}(\cos \alpha) \epsilon^{-i(m+1)\beta} \end{array} \right]$$

$$\langle \mathbf{E}_x | \mathbf{L}_{mn} \rangle = \frac{\pi^2 i^{n+1}}{(2n+1)(2n-1)(2n+3)} \times \quad (3.61)$$

$$\left[\begin{array}{l} (2n+3)(n+m)(n+m-1)P_{n-1}^{m-1}(\cos \alpha) \epsilon^{-i(m-1)\beta} \\ - (2n+3)P_{n-1}^{m+1}(\cos \alpha) \epsilon^{-i(m+1)\beta} \\ - (2n-1)(n-m+2)(n-m+1)P_{n+1}^{m-1}(\cos \alpha) \epsilon^{-i(m-1)\beta} \\ + (2n-1)P_{n+1}^{m+1}(\cos \alpha) \epsilon^{-i(m+1)\beta} \end{array} \right]$$

Using these expressions we obtain:

$$a_{mn}^x(n, m, \alpha, \beta) \quad (m \geq 0) = i^{n+1} \frac{(2n+1)(n-m)!}{2n(n+1)(n+m)!} \times \quad (3.62)$$

$$\left[\begin{array}{l} (n+m)(n-m+1)P_n^{m-1}(\cos \alpha) \epsilon^{-i(m-1)\beta} \\ + P_n^{m+1}(\cos \alpha) \epsilon^{-i(m+1)\beta} \end{array} \right]$$

$$b_{mn}^x(n, m, \alpha, \beta) \quad (m \geq 0) = i^{n+1} \frac{1}{2n(n+1)} \frac{(n-m)!}{(n+m)!} \times \quad (3.63)$$

$$\left[\begin{array}{l} (n+1)(n+m)(n+m-1)P_{n-1}^{m-1}(\cos \alpha) \epsilon^{-i(m-1)\beta} \\ - (n+1)P_{n-1}^{m+1}(\cos \alpha) \epsilon^{-i(m+1)\beta} \\ + n(n-m+2)(n-m+1)P_{n+1}^{m-1}(\cos \alpha) \epsilon^{-i(m-1)\beta} \\ - nP_{n+1}^{m+1}(\cos \alpha) \epsilon^{-i(m+1)\beta} \end{array} \right]$$

$$\begin{aligned}
c_{mn}^x(n, m, \alpha, \beta) &= \frac{i^{n+1} (n-m)!}{2k (n+m)!} \times & (3.64) \\
(m \geq 0) & \left[\begin{aligned} & (n+m)(n+m-1)P_{n-1}^{m-1}(\cos \alpha)e^{-i(m-1)\beta} \\ & - P_{n-1}^{m+1}(\cos \alpha)e^{-i(m+1)\beta} \\ & -(n-m+2)(n-m+1)P_{n+1}^{m-1}(\cos \alpha)e^{-i(m-1)\beta} \\ & + P_{n+1}^{m+1}(\cos \alpha)e^{-i(m+1)\beta} \end{aligned} \right]
\end{aligned}$$

For $m < 0$, the easiest way to obtain the coefficients (explained in Appendix D) are the following recipes:

$$\begin{aligned}
a_{-mn}^x &= (-1)^{m+1} \frac{(n+m)!}{(n-m)!} \left[a_{mn}^x \text{ with } \epsilon^{-i(m\pm 1)\beta} \text{ factors} \right] & (3.65) \\
& \left[\text{changed to } \epsilon^{i(m\pm 1)\beta}. \right] & (3.66) \\
b_{-mn}^x &= (-1)^m \frac{(n+m)!}{(n-m)!} \left[b_{mn}^x \text{ with } \epsilon^{-i(m\pm 1)\beta} \text{ factors} \right] & (3.67) \\
& \left[\text{changed to } \epsilon^{i(m\pm 1)\beta}. \right] & (3.68) \\
c_{-mn}^x &= (-1)^m \frac{(n+m)!}{(n-m)!} \left[c_{mn}^x \text{ with } \epsilon^{-i(m\pm 1)\beta} \text{ factors} \right] & (3.69) \\
& \left[\text{changed to } \epsilon^{i(m\pm 1)\beta}. \right]
\end{aligned}$$

3.4.3 Deriving a_{mn}^y , b_{mn}^y and c_{mn}^y

The y-coefficients are obtained almost identically as compared with the x-coefficients. We realize that the only difference between the two sets arise primarily because of the interchanging of the $\cos \phi$ and the $\sin \phi$ terms due to \mathbf{e}_r being replaced by \mathbf{e}_y . We have

$$\mathbf{e}_y = \sin \theta \sin \phi \mathbf{e}_r + \cos \theta \sin \phi \mathbf{e}_\theta + \cos \phi \mathbf{e}_\phi \quad (3.70)$$

As explained in detail in the appendix(D), the ϕ -integration will cause a change in the sign of the $m+1$ terms while the $m-1$ terms will continue to have the same sign. Also, an extra factor of $-i$ is generated because $\sin \phi = (1/2i)(e^{i\phi} - e^{-i\phi})$. Thus following this general recipe we obtain the y-coefficients:

$$\begin{aligned}
a_{mn}^y(n, m, \alpha, \beta) &= i^n \frac{(2n+1)(n-m)!}{2n(n+1)(n+m)!} \times \\
(m \geq 0) & \left[\begin{aligned} &(n+m)(n-m+1)P_n^{m-1}(\cos \alpha)\epsilon^{-i(m-1)\beta} \\ &-P_n^{m+1}(\cos \alpha)\epsilon^{-i(m+1)\beta} \end{aligned} \right] \quad (3.71)
\end{aligned}$$

$$\begin{aligned}
b_{mn}^y(n, m, \alpha, \beta) &= i^n \frac{1}{2n(n+1)} \frac{(n-m)!}{(n+m)!} \times \\
(m \geq 0) & \left[\begin{aligned} &(n+1)(n+m)(n+m-1)P_{n-1}^{m-1}(\cos \alpha)\epsilon^{-i(m-1)\beta} \\ &+ (n+1)P_{n-1}^{m+1}(\cos \alpha)\epsilon^{-i(m+1)\beta} \\ &+ n(n-m+2)(n-m+1)P_{n+1}^{m-1}(\cos \alpha)\epsilon^{-i(m-1)\beta} \\ &+ nP_{n+1}^{m+1}(\cos \alpha)\epsilon^{-i(m+1)\beta} \end{aligned} \right] \quad (3.72)
\end{aligned}$$

$$\begin{aligned}
c_{mn}^y(n, m, \alpha, \beta) &= \frac{i^n (n-m)!}{2k(n+m)!} \times \\
(m \geq 0) & \left[\begin{aligned} &(n+m)(n+m-1)P_{n-1}^{m-1}(\cos \alpha)\epsilon^{-i(m-1)\beta} \\ &+ P_{n-1}^{m+1}(\cos \alpha)\epsilon^{-i(m+1)\beta} \\ &- (n-m+2)(n-m+1)P_{n+1}^{m-1}(\cos \alpha)\epsilon^{-i(m-1)\beta} \\ &- P_{n+1}^{m+1}(\cos \alpha)\epsilon^{-i(m+1)\beta} \end{aligned} \right] \quad (3.73)
\end{aligned}$$

Transformations similar to what was used for the x-coefficients for $m < 0$ are going to be valid for the y-coefficients as well. Thus the y-coefficients for negative m can be obtained as follows(note the extra (-1) factor as compared to the x-transformations):

$$a_{-mn}^y = (-1)^m \frac{(n+m)!}{(n-m)!} \left[a_{mn}^y \text{ with } e^{-i(m\pm 1)\beta} \text{ factors} \right] \quad (3.74)$$

(3.75)

$$b_{-mn}^y = (-1)^{m+1} \frac{(n+m)!}{(n-m)!} \left[b_{mn}^y \text{ with } e^{-i(m\pm 1)\beta} \text{ factors} \right] \quad (3.76)$$

(3.77)

$$c_{-mn}^y = (-1)^{m+1} \frac{(n+m)!}{(n-m)!} \left[c_{mn}^y \text{ with } e^{-i(m\pm 1)\beta} \text{ factors} \right] \quad (3.78)$$

3.4.4 Numerical Convergence of Basis Function Expansion

It may be pointed out that these coefficients for the expansion of an arbitrary plane wave in terms of the \mathbf{L} , \mathbf{M} , \mathbf{N} basis are *not* necessarily unique. Alternate sets of expansion coefficients can be obtained by, say rearranging of the basis. This follows directly from the general theory of orthonormal basis in Hilbert spaces [37]. Since one can expand *any* plane wave in this basis, as discussed earlier, one can obtain an operational proof of the completeness of this basis. It is also important to realize that simply proving completeness of a set is not the last word in computations. One has to address the question of convergence as well. So numerical verifications are absolutely necessary to validate a certain basis set. To summarize the results, convergence of better than 1% is normally achieved by taking terms up to index n , where $n \sim 1.4|kr|$. This can provide us with the guideline on how many terms to include for a problem in which the geometry can be measured in units of λ , the wavelength of the electromagnetic field in question.

In Figures 3.1 and 3.2 we show the expansion of arbitrary electromagnetic waves in the \mathbf{L} , \mathbf{M} , \mathbf{N} basis. We have specified an arbitrarily directed wave vector \mathbf{k} with direction cosines α and β , with the electric field oriented along some arbitrary direction specified by the angles θ_e and ϕ_e . The values of the exact expression for $\mathbf{E}e^{i\mathbf{k}\cdot\mathbf{r}}$ and the series expansion in the \mathbf{L} , \mathbf{M} , \mathbf{N} basis are compared along some arbitrarily specified line directed along (θ, ϕ) . We observe that the convergence is very good for $|kr| \leq 0.75n$ and this is fairly independent on the choice of the specified directions for \mathbf{E} and \mathbf{k} as well as the path along which the comparison calculations are done. In Figure 3.1 the wave vector is real where as in Figure 3.2 the wave

DEMONSTRATING COMPLETENESS OF BASIS FUNCTIONS

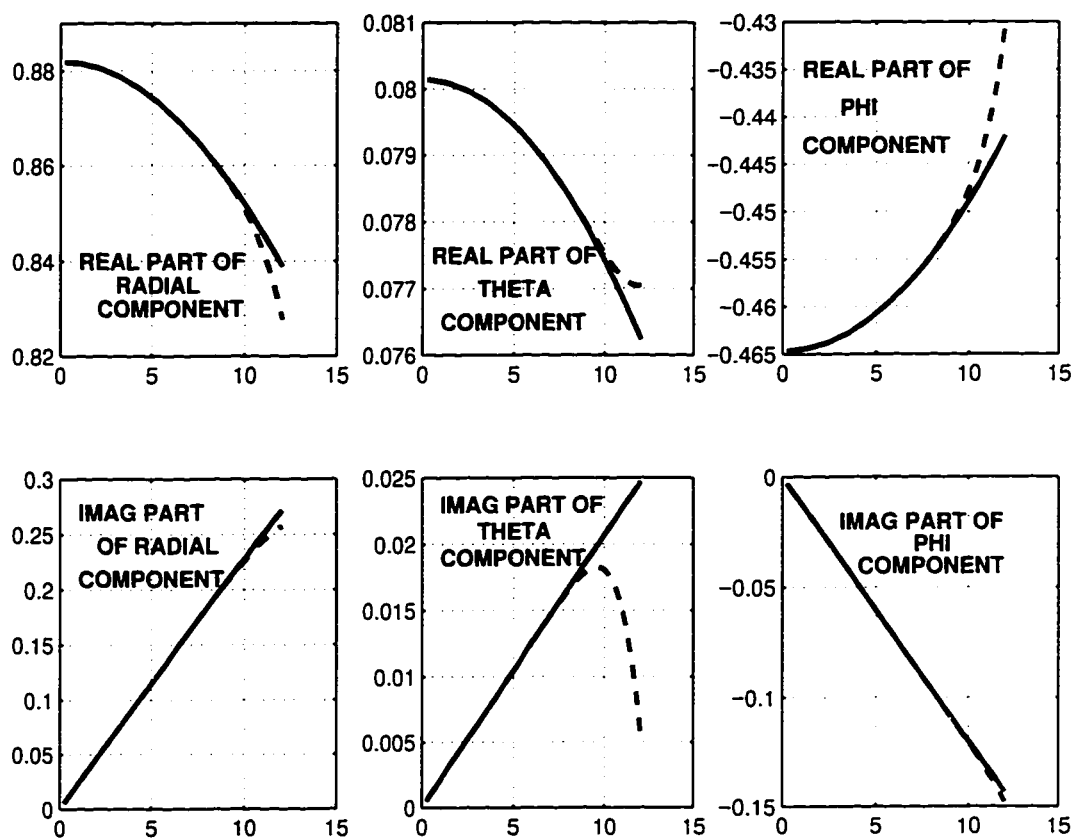


Figure 3.1: Demonstrating completeness of basis function expansion. The expansion of an arbitrarily chosen wave in the L, M and N functions. The solid lines show exact values. The broken lines are computed from a truncated series in the basis functions. The above calculations are done with 15 terms ($n = 15$) for $kr \in [0.12]$, $\theta = 37$ degrees, $\phi = 59$ degrees, $\alpha = 123$ degrees, $\beta = 83$ degrees, $\theta_e = 49$ degrees and $\phi_e = 21$ degrees. Convergence is very good for $|kr| \leq 0.75n$. The horizontal axes are in units of $|kr|$.

vector is complex. Complex wave vectors correspond to an attenuating or amplifying medium. We therefore demonstrate that these functions can be used to expand an electromagnetic field in a general medium. Since the specified \mathbf{E} and \mathbf{k} are not orthogonal in general (as in the above two cases), it is therefore possible to expand waves that are more general than plain electromagnetic waves in a non-attenuating medium. Later we will also examine the possibility to obtain the solution of Maxwell equations in the presence of sources, using the \mathbf{L} , \mathbf{M} , \mathbf{N} basis.

3.5 Numerical Evaluation of \mathbf{L}_{mn} , \mathbf{M}_{mn} and \mathbf{N}_{mn}

Numerical evaluation of \mathbf{L}_{mn} , \mathbf{M}_{mn} and \mathbf{N}_{mn} require us to obtain the values of functions of θ such as $\frac{d}{d\theta} P_n^m(\cos \theta)$, $\frac{P_n^m(\cos \theta)}{\sin \theta}$ and functions of r such as $\frac{1}{kr} \frac{d}{dr}(r z_n(kr))$ and $\frac{z_n(kr)}{kr}$. It is clear that one has to exercise caution in evaluating these functions close to $\theta = 0$ or π and $r = 0$. In this section we indicate numerically stable computational equivalents to these functions.

From Equation C.11, by adding the third and the fourth equations we eliminate the $x P_n^m(x)$ term, and so we obtain:

$$\frac{d}{dx} P_n^m(x) = \frac{1}{2\sqrt{1-x^2}} \left[(n-m+1)(n+m) P_n^{m-1}(x) - P_n^{m+1}(x) \right]. \quad (3.79)$$

and since

$$\frac{d}{d\theta} P_n^m(\cos \theta) = -\sqrt{1-x^2} \frac{d}{dx} P_n^m(x). \quad (3.80)$$

Therefore:

$$\frac{d}{d\theta} P_n^m(\cos \theta) = \frac{1}{2} \left[P_n^{m+1}(x) - (n-m+1)(n+m) P_n^{m-1}(x) \right]. \quad (3.81)$$

From the definition of the Associated Legendre Functions ($m \geq 0$):

$$\begin{aligned} P_n^m(x) &= (-1)^m (1-x^2)^{\frac{m}{2}} \frac{d^m}{dx^m} P_n(x) \\ &= (-1)^{\frac{m}{2}} \sin^m \theta \frac{d^m}{dx^m} P_n(x), \end{aligned} \quad (3.82)$$

where $P_n(x)$ are the Legendre Polynomials and $x = \cos \theta$. we immediately obtain:

$$\frac{P_n^m(\cos \theta)}{\sin \theta} = (-1)^{\frac{m}{2}} \sin^{m-1} \theta \frac{d^m}{dx^m} P_n(\cos \theta). \quad (3.83)$$

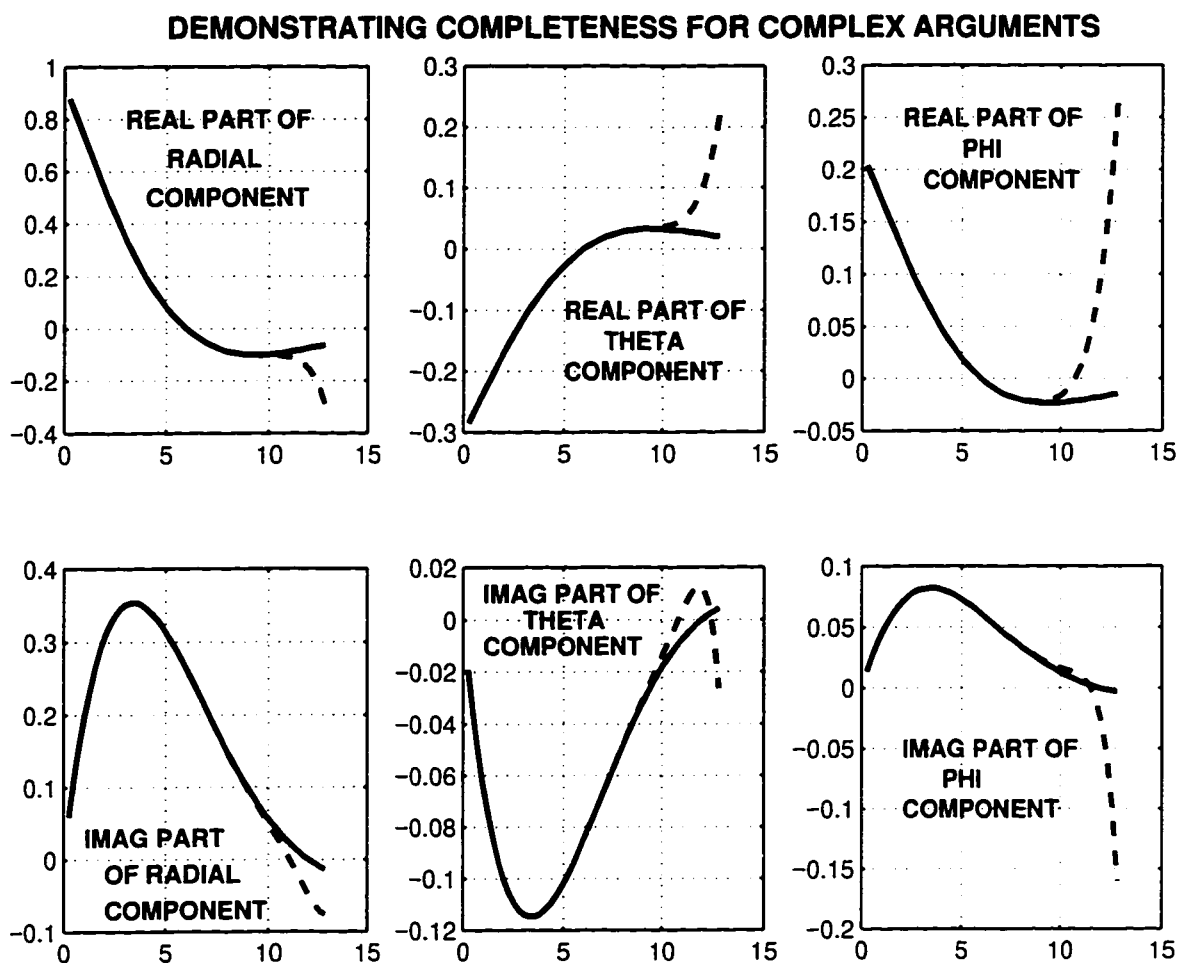


Figure 3.2: Demonstrating completeness of basis function expansion when the specified wave vector is complex. The solid lines show exact values. The broken lines are computed from a truncated series in the basis functions. The above calculations are done with 15 terms ($n = 15$) for $kr_{max} = 10 + 8i$, $\theta = 35$ degrees, $\phi = 42$ degrees, $\alpha = 97$ degrees, $\beta = 82$ degrees, $\theta_e = 21$ degrees and $\phi_e = 79$ degrees. Convergence is very good for $|kr| \leq 0.75n$. The horizontal axes are in units of $|kr|$.

When $m \neq 1$, clearly the right hand side is zero when $\theta = 0$ or π . So, when $m = 1$,

$$\frac{P_n^1(\cos \theta)}{\sin \theta} = -\frac{d}{dx}P_n(x). \quad (3.84)$$

From Legendre's differential equation:

$$(1-x^2)\frac{d^2}{dx^2}P_n(x) - 2x\frac{d}{dx}P_n(x) + n(n+1)P_n(x) = 0, \quad (3.85)$$

we obtain

$$\begin{aligned} \frac{d}{dx}P_n(x) &= \frac{(1-x^2)}{2x}\frac{d^2}{dx^2}P_n(x) + \frac{n(n+1)}{2x}P_n(x) \\ &= \frac{1}{2x}P_n^2(x) + \frac{n(n+1)}{2x}P_n(x) \quad (\text{Using } m=2 \text{ in the defn. of } P_n^m(x)). \end{aligned} \quad (3.86)$$

When $x = \pm 1$, then $P_n^2(x) \rightarrow 0$. Thus :

$$\frac{P_n^m(\cos \theta)}{\sin \theta} = 0 \quad \text{when } m \neq 1 \quad (3.87)$$

$$= -\frac{n(n+1)}{2} \quad \text{when } x = 1, m = 1 \quad (3.88)$$

$$= (-1)^n \frac{n(n+1)}{2} \quad \text{when } x = -1, m = 1 \quad (3.89)$$

$$= \frac{1}{2} \quad \text{when } x = 1, m = -1 \quad (3.90)$$

$$= (-1)^{n+1} \frac{1}{2} \quad \text{when } x = -1, m = -1 \quad (3.91)$$

The functions involving the spherical Bessel and spherical Hankel functions of the first kind for $kr \rightarrow 0$, are best evaluated by using the following recursion relations:

$$\frac{z_n(kr)}{kr} = \frac{1}{(2n+1)} [z_{n-1}(kr) + z_{n+1}(kr)] \quad (3.92)$$

$$\frac{d}{d(kr)} z_n(kr) = \frac{1}{(2n+1)} [nz_{n-1}(kr) - (n+1)z_{n+1}(kr)] \quad (3.93)$$

$$\frac{1}{kr} \frac{d}{dr} (rz_n(kr)) = \frac{1}{(2n+1)} [(n+1)z_{n-1}(kr) - nz_{n+1}(kr)]. \quad (3.94)$$

Here, the $z_n(kr)$ represents either the spherical Bessel or the spherical Hankel functions of the first kind where $n \geq 1$. The argument kr could be complex in general. We do not require to evaluate these terms for $n = 0$ since the **L**, **M** and **N** functions are zero for $n = 0$. The absence of $1/kr$ factors on the right hand side allows straightforward evaluation of these functions as $kr \rightarrow 0$. It is of interest to note that the field on the z-axis will be given only by the $m = 0, \pm 1$ terms, due to the vanishing of the other $\frac{d}{d\theta} P_n^m(\cos\theta)$ and $\frac{P_n^m(\cos\theta)}{\sin\theta}$ functions on the z-axis.

Chapter 4

Shell Problem

4.1 Introduction

As an application of the method of solution by expansion in vector eigenfunctions, we consider a problem of current interest. We shall solve the electromagnetic problem of scattering from concentric spherical shells. There is a lot of interest to understand the electromagnetic response of nanoparticles that have a shell or coating of some other material. We shall solve the problem for a single shell. However, it would be fairly obvious that the method can be generalized to the problem of multiple shells. An underlying assumption of this method is that the macroscopic dielectric function of a particular material continues to be applicable in the nanometer regime as well. For clusters larger than a few hundred atoms and for shell thickness greater than a few monolayers, this is usually a valid approximation.

4.2 The Model

A sphere is centered on the origin, of radius R_1 of a material with dielectric function $\epsilon_1(\omega)$ (Figure 4.1). Surrounding the sphere is a concentric shell of radius R_2 of a material with dielectric function $\epsilon_2(\omega)$. The dielectric functions are complex functions of frequency of the electromagnetic radiation in question. The sphere and shell are embedded in a medium, the dielectric function of which is specified as $\epsilon_3(\omega)$. Without loss of generality, we shall assume that we are dealing with non-magnetic materials, so that the relative permeabilities of the three region are approximately unity.

A plane wave of unit intensity is incident along the z-axis, with its polarization along the x-direction. By symmetry, it doesn't make any physical difference in the choice of the incident direction. However, the expansion coefficients for the plane wave in the $\{M, N\}$ functions assume simple expressions when the wave is incident along the z-axis. In this coordinate system \mathbf{k} is specified as $(k, \alpha = 0, \beta = \pi/2)$. Thus $a_{mn} = a_{mn}^x$ and $b_{mn} = b_{mn}^x$. Since the divergence of a plane wave is zero, we can

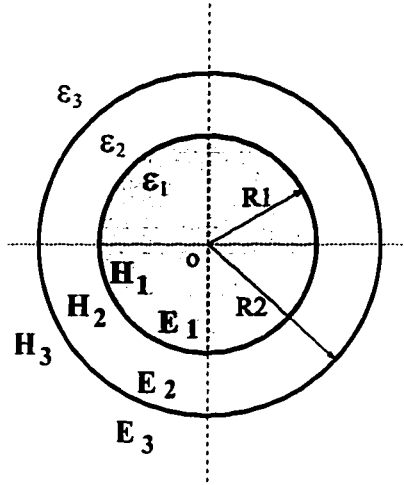


Figure 4.1: Shell-geometry with single shell. There are three spherically concentric regions indicated. The core has dielectric constant ϵ_1 , the shell has dielectric constant ϵ_2 and the exterior has dielectric constant ϵ_3 . In general there can be more number of shells.

expand the incident field in the \mathbf{M} and \mathbf{N} functions alone. The scattered waves are the 'forced' solutions, and they will assume the same form as the incident waves at a given frequency, and so they too can be expanded in the \mathbf{M} and \mathbf{N} functions only:

$$\mathbf{E} = \sum_{mn} \{a_{mn}\mathbf{M}_{mn} + b_{mn}\mathbf{N}_{mn}\}. \quad (4.1)$$

Now for a plane electromagnetic wave $\mathbf{H} = \frac{1}{i\omega\mu}\nabla \times \mathbf{E}$. Therefore:

$$\begin{aligned} \mathbf{H} &= \frac{1}{i\omega\mu} \sum_{mn} \{a_{mn}\nabla \times \mathbf{M}_{mn} + b_{mn}\nabla \times \mathbf{N}_{mn}\} \\ &= \frac{1}{i\omega\mu} \sum_{mn} \{a_{mn}k\mathbf{N}_{mn} + b_{mn}k\mathbf{M}_{mn}\} \\ &= -i\sqrt{\frac{\epsilon}{\mu}} \sum_{mn} \{b_{mn}\mathbf{M}_{mn} + a_{mn}\mathbf{N}_{nm}\}. \end{aligned} \quad (4.2)$$

Using $\alpha = 0$ and $\beta = \pi/2$, only the $n \geq 1$ and $m = \pm 1$ coefficients turn out to be non-zero. We obtain for the expansion coefficients:

$$a_{1n}^x = a_{mn}^x(n, 1, 0, \pi/2) = i^{n+1} \frac{2n+1}{2n(n+1)} \quad (4.3)$$

$$a_{-1n}^x = n(n+1)a_{1n} \quad (4.4)$$

$$b_{1n}^x = b_{mn}^x(n, 1, 0, \pi/2) = i^{n+1} \frac{2n+1}{2n(n+1)} \quad (4.5)$$

$$b_{-1n}^x = -n(n+1)b_{1n} \quad (4.6)$$

Let us represent the core as region 1, the shell as region 2 and the exterior as region 3. Let us assume the following form for the solutions of the scattered \mathbf{E} field in the three regions:

$$\mathbf{E}_1 = \sum_{n=1}^{\infty} \left\{ a_{\pm 1n}^{(1)j} \mathbf{M}_{\pm 1n}^{(1)j} + b_{\pm 1n}^{(1)j} \mathbf{N}_{\pm 1n}^{(1)j} \right\} \quad (4.7)$$

$$\mathbf{E}_2 = \sum_{n=1}^{\infty} \left\{ a_{\pm 1n}^{(2)j} \mathbf{M}_{\pm 1n}^{(2)j} + b_{\pm 1n}^{(2)j} \mathbf{N}_{\pm 1n}^{(2)j} + a_{\pm 1n}^{(2)h} \mathbf{M}_{\pm 1n}^{(2)h} + b_{\pm 1n}^{(2)h} \mathbf{N}_{\pm 1n}^{(2)h} \right\} \quad (4.8)$$

$$\mathbf{E}_3 = \sum_{n=1}^{\infty} \left\{ a_{\pm 1n}^{(3)h} \mathbf{M}_{\pm 1n}^{(3)h} + b_{\pm 1n}^{(3)h} \mathbf{N}_{\pm 1n}^{(3)h} \right\} \quad (4.9)$$

The ± 1 indicates the two choices for the value of m . The superscripts identify the region and the type of function being used. For example, the h superscript in $\mathbf{M}_{1n}^{(2)h}$ represents the \mathbf{M} functions that are derived from the scalar solution that uses spherical Hankel functions of the first kind for their radial part. The j superscript represents functions that have spherical Bessel functions for their radial part. The numeric label identifies the region and so the value of k at the frequency of the incident electromagnetic wave. Specifically, we have (with $m = \pm 1$):

$$\mathbf{M}_{mn}^{(1)j} = imj_n(k_1 r) \frac{P_n^m(\cos\theta)}{\sin\theta} e^{im\phi} \mathbf{e}_\theta - j_n(k_1 r) \frac{dP_n^m(\cos\theta)}{d\theta} e^{im\phi} \mathbf{e}_\phi \quad (4.10)$$

$$\mathbf{M}_{mn}^{(2)j} = imj_n(k_2 r) \frac{P_n^m(\cos\theta)}{\sin\theta} e^{im\phi} \mathbf{e}_\theta - j_n(k_2 r) \frac{dP_n^m(\cos\theta)}{d\theta} e^{im\phi} \mathbf{e}_\phi \quad (4.11)$$

$$\mathbf{M}_{mn}^{(2)h} = imh_n^{(1)}(k_2 r) \frac{P_n^m(\cos\theta)}{\sin\theta} e^{im\phi} \mathbf{e}_\theta - h_n^{(1)}(k_2 r) \frac{dP_n^m(\cos\theta)}{d\theta} e^{im\phi} \mathbf{e}_\phi \quad (4.12)$$

$$\mathbf{M}_{mn}^{(3)j} = imj_n(k_3 r) \frac{P_n^m(\cos\theta)}{\sin\theta} e^{im\phi} \mathbf{e}_\theta - j_n(k_3 r) \frac{dP_n^m(\cos\theta)}{d\theta} e^{im\phi} \mathbf{e}_\phi \quad (4.13)$$

$$\mathbf{M}_{mn}^{(3)h} = imh_n^{(1)}(k_3 r) \frac{P_n^m(\cos\theta)}{\sin\theta} e^{im\phi} \mathbf{e}_\theta - h_n^{(1)}(k_3 r) \frac{dP_n^m(\cos\theta)}{d\theta} e^{im\phi} \mathbf{e}_\phi \quad (4.14)$$

$$\mathbf{N}_{mn}^{(1)j} = n(n+1) \frac{j_n(k_1 r)}{k_1 r} P_n^m(\cos\theta) e^{im\phi} \mathbf{e}_r$$

$$+ \frac{1}{k_1 r} \frac{d(r j_n(k_1 r))}{dr} \left(\frac{dP_n^m(\cos\theta)}{d\theta} e^{im\phi} \mathbf{e}_\theta + im \frac{P_n^m(\cos\theta)}{\sin\theta} e^{im\phi} \mathbf{e}_\phi \right) \quad (4.15)$$

$$\begin{aligned} \mathbf{N}_{mn}^{(2)j} &= n(n+1) \frac{j_n(k_2 r)}{k_2 r} P_n^m(\cos\theta) e^{im\phi} \mathbf{e}_r \\ &+ \frac{1}{k_2 r} \frac{d(r j_n(k_2 r))}{dr} \left(\frac{dP_n^m(\cos\theta)}{d\theta} e^{im\phi} \mathbf{e}_\theta + im \frac{P_n^m(\cos\theta)}{\sin\theta} e^{im\phi} \mathbf{e}_\phi \right) \end{aligned} \quad (4.16)$$

$$\begin{aligned} \mathbf{N}_{mn}^{(2)h} &= n(n+1) \frac{h_n^{(1)}(k_2 r)}{k_2 r} P_n^m(\cos\theta) e^{im\phi} \mathbf{e}_r \\ &+ \frac{1}{k_2 r} \frac{d(r h_n^{(1)}(k_2 r))}{dr} \left(\frac{dP_n^m(\cos\theta)}{d\theta} e^{im\phi} \mathbf{e}_\theta + im \frac{P_n^m(\cos\theta)}{\sin\theta} e^{im\phi} \mathbf{e}_\phi \right) \end{aligned} \quad (4.17)$$

$$\begin{aligned} \mathbf{N}_{mn}^{(3)j} &= n(n+1) \frac{j_n(k_3 r)}{k_3 r} P_n^m(\cos\theta) e^{im\phi} \mathbf{e}_r \\ &+ \frac{1}{k_3 r} \frac{d(r j_n(k_3 r))}{dr} \left(\frac{dP_n^m(\cos\theta)}{d\theta} e^{im\phi} \mathbf{e}_\theta + im \frac{P_n^m(\cos\theta)}{\sin\theta} e^{im\phi} \mathbf{e}_\phi \right) \end{aligned} \quad (4.18)$$

$$\begin{aligned} \mathbf{N}_{mn}^{(3)h} &= n(n+1) \frac{h_n^{(1)}(k_3 r)}{k_3 r} P_n^m(\cos\theta) e^{im\phi} \mathbf{e}_r \\ &+ \frac{1}{k_3 r} \frac{d(r h_n^{(1)}(k_3 r))}{dr} \left(\frac{dP_n^m(\cos\theta)}{d\theta} e^{im\phi} \mathbf{e}_\theta + im \frac{P_n^m(\cos\theta)}{\sin\theta} e^{im\phi} \mathbf{e}_\phi \right) \end{aligned} \quad (4.19)$$

Since region 1 includes the origin, only the spherical Bessel function solutions are allowed. The spherical Hankel function solutions are singular at the origin. In region 2, which does not include the origin, we can therefore have both the spherical Bessel and spherical Hankel function solutions. Region 3 does not include the origin. So we assume an expansion in the spherical Hankel function solutions only. The spherical Bessel function solutions are included in the expansion of the incident field in region 3. Far away from the origin, where the scattered solution must become negligible, we must recover the plane wave field of the incident wave only. Thus this regularity at infinity restricts the scattered solution in region 3 to have only the spherical Hankel function solutions. The incident field itself has to be regular at the origin (since the choice for locating the scattering object at the origin was purely a matter of convenience) and so it is expressible only in terms of the spherical Bessel function solutions:

$$\mathbf{E}_i = \sum_{n=1}^{\infty} \left\{ a_{\pm 1n}^x \mathbf{M}_{\pm 1n}^{(3)j} + b_{\pm 1n}^x \mathbf{N}_{\pm 1n}^{(3)j} \right\} \quad (4.20)$$

The expression for the magnetic field intensity \mathbf{H} in the various regions are:

$$\mathbf{H}_i = -i\sqrt{\frac{\epsilon_3}{\mu_3}} \sum_{n=1}^{\infty} \left\{ a_{\pm 1n}^x \mathbf{N}_{\pm 1n}^{(3)j} + b_{\pm 1n}^x \mathbf{M}_{\pm 1n}^{(3)j} \right\} \quad (4.21)$$

$$\mathbf{H}_1 = -i\sqrt{\frac{\epsilon_1}{\mu_1}} \sum_{n=1}^{\infty} \left\{ a_{\pm 1n}^{(1)j} \mathbf{N}_{\pm 1n}^{(1)j} + b_{\pm 1n}^{(1)j} \mathbf{M}_{\pm 1n}^{(1)j} \right\} \quad (4.22)$$

$$\mathbf{H}_2 = -i\sqrt{\frac{\epsilon_2}{\mu_2}} \sum_{n=1}^{\infty} \left\{ a_{\pm 1n}^{(2)j} \mathbf{N}_{\pm 1n}^{(2)j} + b_{\pm 1n}^{(2)j} \mathbf{M}_{\pm 1n}^{(2)j} + a_{\pm 1n}^{(2)h} \mathbf{N}_{\pm 1n}^{(2)h} + b_{\pm 1n}^{(2)h} \mathbf{M}_{\pm 1n}^{(2)h} \right\} \quad (4.23)$$

$$\mathbf{H}_3 = -i\sqrt{\frac{\epsilon_3}{\mu_3}} \sum_{n=1}^{\infty} \left\{ a_{\pm 1n}^{(3)h} \mathbf{N}_{\pm 1n}^{(3)h} + b_{\pm 1n}^{(3)h} \mathbf{M}_{\pm 1n}^{(3)h} \right\} \quad (4.24)$$

It is easy to generalize to the case of multiple shells. Every additional shell will have its solution expressible in the form given by Equations 4.8 and 4.23. We have a set of four independent equations from the boundary conditions for each interface. A single shell problem with two interfaces has eight independent equations from which we can obtain the sets of eight coefficients $\{a_{1n}^{(1)j}, a_{1n}^{(2)j}, a_{1n}^{(2)h}, a_{1n}^{(3)h}, b_{1n}^{(1)j}, b_{1n}^{(2)j}, b_{1n}^{(2)h}, b_{1n}^{(3)h}\}$. Similarly for a problem with N shells with $N + 1$ interfaces, we have sets of $4N + 4$ unknown coefficients and $4N + 4$ equations from the boundary conditions to solve for them. We shall soon see that the solution for such systems are completely determined.

4.3 Expansion Coefficients of the Scattered Wave

We shall consider the equations of continuity of tangential \mathbf{E} and \mathbf{H} only. The \mathbf{e}_θ and \mathbf{e}_ϕ vectors will serve as the two independent tangential unit vectors. Let us consider the spherical interface at $r = R_1$. The continuity of the tangential components of the fields give us the following equations, valid for all points on the sphere at $r = R_1$:

$$\mathbf{E}_1 \cdot \mathbf{e}_\phi \Big|_{r=R_1} = \mathbf{E}_2 \cdot \mathbf{e}_\phi \Big|_{r=R_1} \quad (4.25)$$

$$\mathbf{E}_1 \cdot \mathbf{e}_\theta \Big|_{r=R_1} = \mathbf{E}_2 \cdot \mathbf{e}_\theta \Big|_{r=R_1} \quad (4.26)$$

$$\mathbf{H}_1 \cdot \mathbf{e}_\phi \Big|_{r=R_1} = \mathbf{H}_2 \cdot \mathbf{e}_\phi \Big|_{r=R_1} \quad (4.27)$$

$$\mathbf{H}_1 \cdot \mathbf{e}_\theta \Big|_{r=R_1} = \mathbf{H}_2 \cdot \mathbf{e}_\theta \Big|_{r=R_1} \quad (4.28)$$

Similarly, the equations from the surface at $r = R_2$ are:

$$\mathbf{E}_2 \cdot \mathbf{e}_\phi \Big|_{r=R_2} = \mathbf{E}_3 \cdot \mathbf{e}_\phi \Big|_{r=R_2} + \mathbf{E}_i \cdot \mathbf{e}_\phi \Big|_{r=R_2} \quad (4.29)$$

$$\mathbf{E}_2 \cdot \mathbf{e}_\theta \Big|_{r=R_2} = \mathbf{E}_3 \cdot \mathbf{e}_\theta \Big|_{r=R_2} + \mathbf{E}_i \cdot \mathbf{e}_\theta \Big|_{r=R_2} \quad (4.30)$$

$$\mathbf{H}_2 \cdot \mathbf{e}_\phi \Big|_{r=R_2} = \mathbf{H}_3 \cdot \mathbf{e}_\phi \Big|_{r=R_2} + \mathbf{H}_i \cdot \mathbf{e}_\phi \Big|_{r=R_2} \quad (4.31)$$

$$\mathbf{H}_2 \cdot \mathbf{e}_\theta \Big|_{r=R_2} = \mathbf{H}_3 \cdot \mathbf{e}_\theta \Big|_{r=R_2} + \mathbf{H}_i \cdot \mathbf{e}_\theta \Big|_{r=R_2} \quad (4.32)$$

The expressions on both sides of the boundary condition equations above are functions of θ and ϕ only. The ϕ -parts are of the form $e^{\pm i\phi}$. Multiplying both sides of these equations by $e^{-i\phi}$ and integrating with respect to ϕ over the interval $\phi \in [0, 2\pi]$ will decouple all the $m = 1$ equations. Similarly all the $m = -1$ equations are decoupled. The expressions on both sides then reduce to being functions of θ alone. Carrying out similar integration of both sides of these equations with respect to θ over the interval $\theta \in [0, \pi]$ could decouple the different n 's, leaving us with linear equations in sets of the desired unknown expansion coefficients of order n .

Let us consider Equation 4.25:

$$\mathbf{E}_1 \cdot \mathbf{e}_\phi = \sum_{n=1}^{\infty} \left\{ a_{\pm 1n}^{(1)j} \mathbf{M}_{\pm 1n}^{(1)j} \cdot \mathbf{e}_\phi + b_{\pm 1n}^{(1)j} \mathbf{N}_{\pm 1n}^{(1)j} \cdot \mathbf{e}_\phi \right\} \quad \text{and} \quad (4.33)$$

$$\mathbf{E}_2 \cdot \mathbf{e}_\phi = \sum_{n=1}^{\infty} \left\{ a_{\pm 1n}^{(2)j} \mathbf{M}_{\pm 1n}^{(2)j} \cdot \mathbf{e}_\phi + b_{\pm 1n}^{(2)j} \mathbf{N}_{\pm 1n}^{(2)j} \cdot \mathbf{e}_\phi + a_{\pm 1n}^{(2)h} \mathbf{M}_{\pm 1n}^{(2)h} \cdot \mathbf{e}_\phi + b_{\pm 1n}^{(2)h} \mathbf{N}_{\pm 1n}^{(2)h} \cdot \mathbf{e}_\phi \right\} \quad (4.34)$$

Now,

$$\mathbf{M}_{m_n}^{(1)j} \cdot \mathbf{e}_\phi \Big|_{r=R_1} = -j_n(k_1 R_1) \frac{d}{d\theta} P_n^m(\cos\theta) e^{im\phi} \quad (4.35)$$

$$\text{And. } \mathbf{N}_{m_n}^{(1)j} \cdot \mathbf{e}_\phi \Big|_{r=R_1} = im \left(\frac{1}{k_1 r} \frac{d}{dr} (r j_n(k_1 r)) \right) \Big|_{r=R_1} \frac{P_n^m(\cos\theta)}{\sin\theta} e^{im\phi} \quad (4.36)$$

Multiplying both sides by $\sin^2\theta P_n^m(\cos\theta) e^{-im\phi}$ and integrating within limits of $\theta \in [0, \pi]$ and $\phi \in [0, 2\pi]$, and observing that

$$\int_0^\pi d\theta \sin^2\theta P_n^m(\cos\theta) \frac{d}{d\theta} P_n^m(\cos\theta) = 0. \quad (4.37)$$

$$\text{and } \int_0^\pi d\theta \sin\theta P_n^m(\cos\theta) P_n^m(\cos\theta) = \frac{2}{2n+1} \frac{(n+m)!}{(n-m)!}. \quad (4.38)$$

the coefficients of all the a_{mn} terms will vanish. On simplifying both sides, we obtain the equation:

$$b_{\pm 1n}^{(1)j} \left(\frac{1}{k_1 r} \frac{d}{dr} (r j_n(k_1 r)) \right)_{r=R_1} - b_{\pm 1n}^{(2)j} \left(\frac{1}{k_2 r} \frac{d}{dr} (r j_n(k_2 r)) \right)_{r=R_1} - b_{\pm 1n}^{(2)h} \left(\frac{1}{k_2 r} \frac{d}{dr} (r h_n^{(1)}(k_2 r)) \right)_{r=R_1} = 0 \quad (4.39)$$

Similarly, when considering Equation 4.26, only the coefficients of the a_{mn} terms will survive. The integration procedure is identical to that used for obtaining Eqn 4.39. Carrying out the procedure, we arrive at:

$$a_{\pm 1n}^{(1)j} (j_n(k_1 R_1)) - a_{\pm 1n}^{(2)j} (j_n(k_2 R_1)) - a_{\pm 1n}^{(2)h} (h_n^{(1)}(k_2 R_1)) = 0 \quad (4.40)$$

To obtain the equations from the continuity of tangential \mathbf{H} , we observe that by virtue of Equation 4.2, we can use the corresponding equations derived for the continuity of tangential \mathbf{E} by interchanging the a_{mn} and b_{mn} coefficients and appending an extra factor of $\sqrt{\frac{\epsilon}{\mu}}$. Thus Equation 4.27 for continuity of tangential \mathbf{H} along \mathbf{e}_ϕ is obtained as:

$$a_{\pm 1n}^{(1)j} \sqrt{\frac{\epsilon_1}{\mu_1}} \left(\frac{1}{k_1 r} \frac{d}{dr} (r j_n(k_1 r)) \right)_{r=R_1} - a_{\pm 1n}^{(2)j} \sqrt{\frac{\epsilon_2}{\mu_2}} \left(\frac{1}{k_2 r} \frac{d}{dr} (r j_n(k_2 r)) \right)_{r=R_1} - a_{\pm 1n}^{(2)h} \sqrt{\frac{\epsilon_2}{\mu_2}} \left(\frac{1}{k_2 r} \frac{d}{dr} (r h_n^{(1)}(k_2 r)) \right)_{r=R_1} = 0. \quad (4.41)$$

and Equation 4.28 gives us the continuity of tangential \mathbf{H} along \mathbf{e}_θ :

$$\begin{aligned}
& b_{\pm 1n}^{(1)j} \sqrt{\frac{\epsilon_1}{\mu_1}} j_n(k_1 R_1) - b_{\pm 1n}^{(2)j} \sqrt{\frac{\epsilon_2}{\mu_2}} j_n(k_2 R_1) \\
& - b_{\pm 1n}^{(2)h} \left(\sqrt{\frac{\epsilon_2}{\mu_2}} h_n^{(1)}(k_2 R_1) \right) = 0.
\end{aligned} \tag{4.42}$$

Similarly the equations for the interface at R_2 are obtained. Continuity of tangential \mathbf{E} along \mathbf{e}_ϕ gives us:

$$\begin{aligned}
& + b_{\pm 1n}^{(2)j} \left(\frac{1}{k_2 r} \frac{d}{dr} (r j_n(k_2 r)) \right)_{r=R_2} + b_{\pm 1n}^{(2)h} \left(\frac{1}{k_2 r} \frac{d}{dr} (r h_n^{(1)}(k_2 r)) \right)_{r=R_2} \\
& - b_{\pm 1n}^{(3)h} \left(\frac{1}{k_3 r} \frac{d}{dr} (r h_n^{(1)}(k_3 r)) \right)_{r=R_2} = b_{\pm 1n}^r \left(\frac{1}{k_3 r} \frac{d}{dr} (r j_n(k_3 r)) \right)_{r=R_2}.
\end{aligned} \tag{4.43}$$

And the continuity of tangential \mathbf{E} along \mathbf{e}_θ at $r = R_2$ gives us:

$$\begin{aligned}
& a_{\pm 1n}^{(2)j} (j_n(k_2 R_2)) + a_{\pm 1n}^{(2)h} (h_n^{(1)}(k_2 R_2)) \\
& - a_{\pm 1n}^{(3)h} (h_n^{(1)}(k_3 R_2)) = a_{\pm 1n}^r (j_n(k_3 R_2)).
\end{aligned} \tag{4.44}$$

The continuity of tangential \mathbf{H} along \mathbf{e}_ϕ at $r = R_2$ gives:

$$\begin{aligned}
& a_{\pm 1n}^{(2)j} \sqrt{\frac{\epsilon_2}{\mu_2}} \left(\frac{1}{k_2 r} \frac{d}{dr} (r j_n(k_2 r)) \right)_{r=R_2} + a_{\pm 1n}^{(2)h} \sqrt{\frac{\epsilon_2}{\mu_2}} \left(\frac{1}{k_2 r} \frac{d}{dr} (r h_n^{(1)}(k_2 r)) \right)_{r=R_2} \\
& - a_{\pm 1n}^{(3)h} \sqrt{\frac{\epsilon_3}{\mu_3}} \left(\frac{1}{k_3 r} \frac{d}{dr} (r h_n^{(1)}(k_3 r)) \right)_{r=R_2} = a_{\pm 1n}^r \sqrt{\frac{\epsilon_3}{\mu_3}} \left(\frac{1}{k_3 r} \frac{d}{dr} (r j_n(k_3 r)) \right)_{r=R_2}.
\end{aligned} \tag{4.45}$$

Finally, the continuity of tangential \mathbf{H} along \mathbf{e}_θ at $r = R_2$ gives:

$$\begin{aligned}
& b_{\pm 1n}^{(2)j} \left(\sqrt{\frac{\epsilon_2}{\mu_2}} j_n(k_2 R_2) \right) + b_{\pm 1n}^{(2)h} \left(\sqrt{\frac{\epsilon_2}{\mu_2}} h_n^{(1)}(k_2 R_2) \right) \\
& - b_{\pm 1n}^{(3)h} \left(\sqrt{\frac{\epsilon_3}{\mu_3}} h_n^{(1)}(k_3 R_2) \right) = b_{\pm 1n}^r \left(\sqrt{\frac{\epsilon_3}{\mu_3}} j_n(k_3 R_2) \right).
\end{aligned} \tag{4.46}$$

Thus, for each n , and $m = \pm 1$, we have a non-homogenous system of eight equations in eight unknowns, and the system is straightforwardly solved. If we set $\epsilon_1 = \epsilon_2$, making the shell and the core the same, then we obtain the solution to Mie scattering. By using the formalism discussed above, a direct solution of Mie scattering could be obtained by solving a simple 4×4 system of equations.

In Figure 4.2 we show the result of our calculation on a glass sphere coated with a thin gold shell. The glass sphere ($\epsilon = 2.5$) and the gold shell have a combined total diameter of 2λ where $\lambda = 620\text{nm}$. The dielectric constant of gold at 2eV (620nm) is $-10.885 + 1.348i$ [24]. The thickness of the shell is reduced from 0.15λ to zero. When the gold shell is sufficiently thick, in excess of several skin depths, the optical field is unable to penetrate the shell. Thus the field inside the sphere will be close to zero. When the shell is made thinner, the optical field ‘leaks’ into the cavity formed by the sphere-shell system. Interestingly, the trapped photons give rise to fields inside the cavity that are stronger than the incident external field. The mode patterns emerge naturally as a result of solving the boundary value problem of the shell-core model. When the gold shell is made sufficiently thin, so that it can be considered a glass sphere only, we observe the familiar effect of lens action, the incident light getting focussed at the opposite end of the sphere. It is evident from these calculations that the screening action of a thin gold shell is remarkably efficient as far as the external field is concerned. The external field itself is not seriously perturbed until the shell thickness is made less than 0.05λ . In other words one could not differentiate a solid sphere of gold from a glass core with a thin gold shell by observation of the external scattered field alone.

4.4 Poynting Vector Calculations

The mean intensity of energy flow at a point in an electromagnetic field with sinusoidal time dependence is given by the real part of what is defined as the complex Poynting

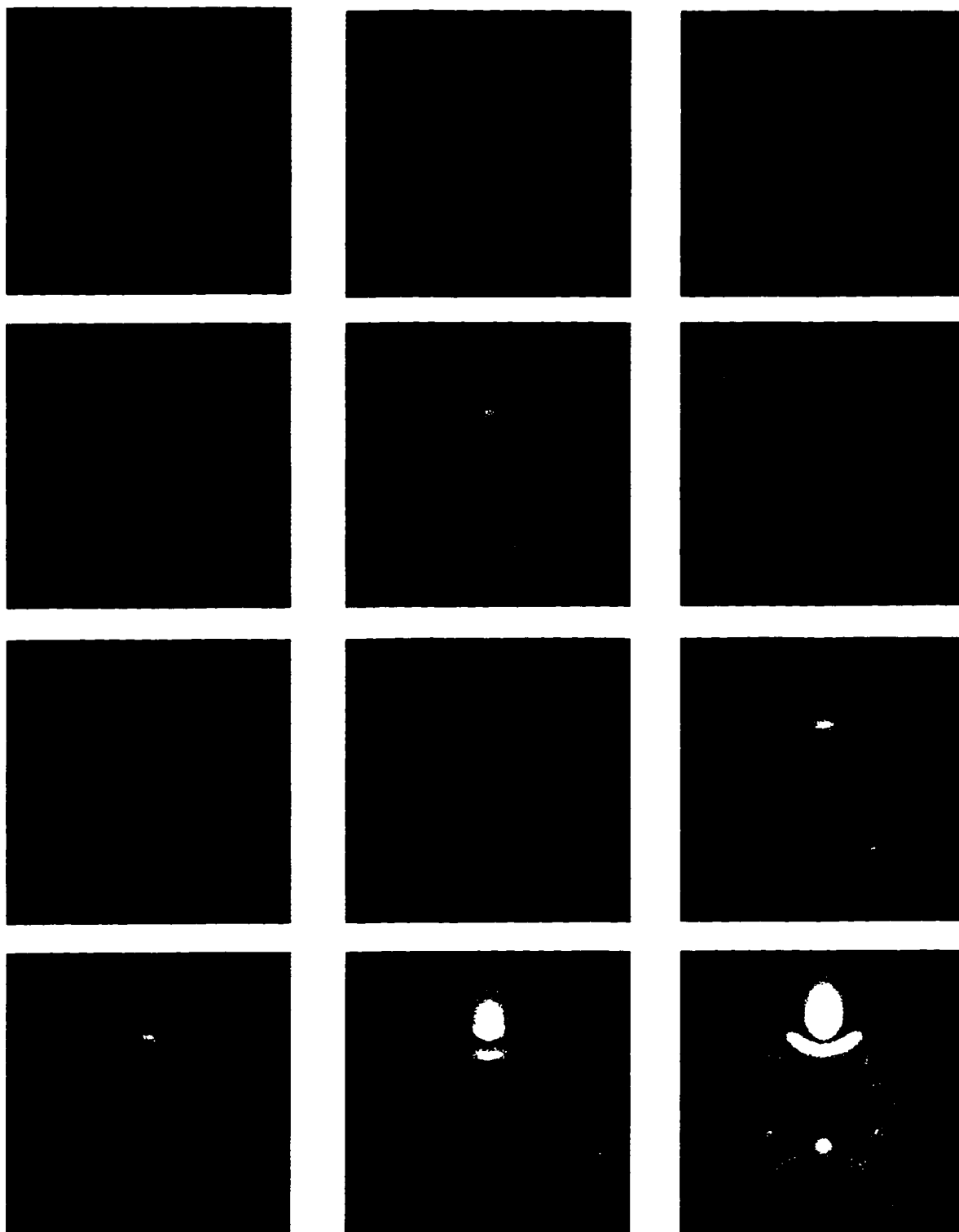


Figure 4.2: Scattering from glass sphere coated with a thin gold shell. The total diameter of the core-shell scatterer is 2λ . The thickness of the gold shell is reduced from 0.15λ (top-left) to zero (bottom-right). Incident light is directed from the bottom of the page with polarization pointing out of the page. White represents larger fields.

vector, \mathbf{S} :

$$\mathbf{S} = \frac{1}{2} \mathbf{E} \times \mathbf{H}^*. \quad (4.47)$$

So, the mean intensity of energy flow is given by

$$\bar{\mathbf{S}} = \frac{1}{2} \text{Re}(\mathbf{E} \times \mathbf{H}^*). \quad (4.48)$$

Although it is only in the far field that this quantity has the simple physical picture of energy flow from a plane wave field, it is still instructive to study the pattern of energy flow in the near field. If we observe the energy flow through a spherical surface, concentric with our scattering object, we can study the relative energy flow from the wave field into the scatterer and vice versa. The knowledge of this near field energy flow and distribution is important for example in the understanding of radiation-induced interactions of adsorbed atoms/molecules on surfaces of nano-particles.

In order to evaluate the energy flow per unit area, using the complex Poynting vector formalism, we need to calculate the total \mathbf{E} and \mathbf{H} and obtain the dot product of \mathbf{S} with \mathbf{e}_r . The radial component of \mathbf{S} is given by

$$\frac{1}{2} [E_\theta H_\phi^* - E_\phi H_\theta^*]. \quad (4.49)$$

Since the \mathbf{E} and \mathbf{H} fields are expressed in terms of the \mathbf{M} and \mathbf{N} functions, both of which are represented by distinct orthogonal components in the spherical polar coordinate system, it is relatively straightforward to obtain the value of the expression above. We show the results of such a calculation for gold clusters of radii, $R = 20\text{nm}$ and $R = 100\text{nm}$, with 2eV (620nm) incident photons in Figure 4.3. The observation point is located on circles with different radii, b , concentric with the cluster. We let b vary from the near field ($b \approx R$) to the far field ($b \gg R$). As explained earlier, by setting both the shell and the core equal to gold, we converge to the equivalent problem of Mie Scattering. It is clear that the energy flow in the near field is fairly non-intuitive. For certain configurations, the near field energy flow is negative, opposite to the normal far field scattering solution which invariably has positive energy flow outward from the scattering object. However, the knowledge of such electromagnetic interactions is vital to our understanding of certain cluster properties. Our results are in excellent agreement with other published works [26] on gold clusters using Mie's theory. This provides us with a simple test against which to check our formalism of basis function expansion for the solution.

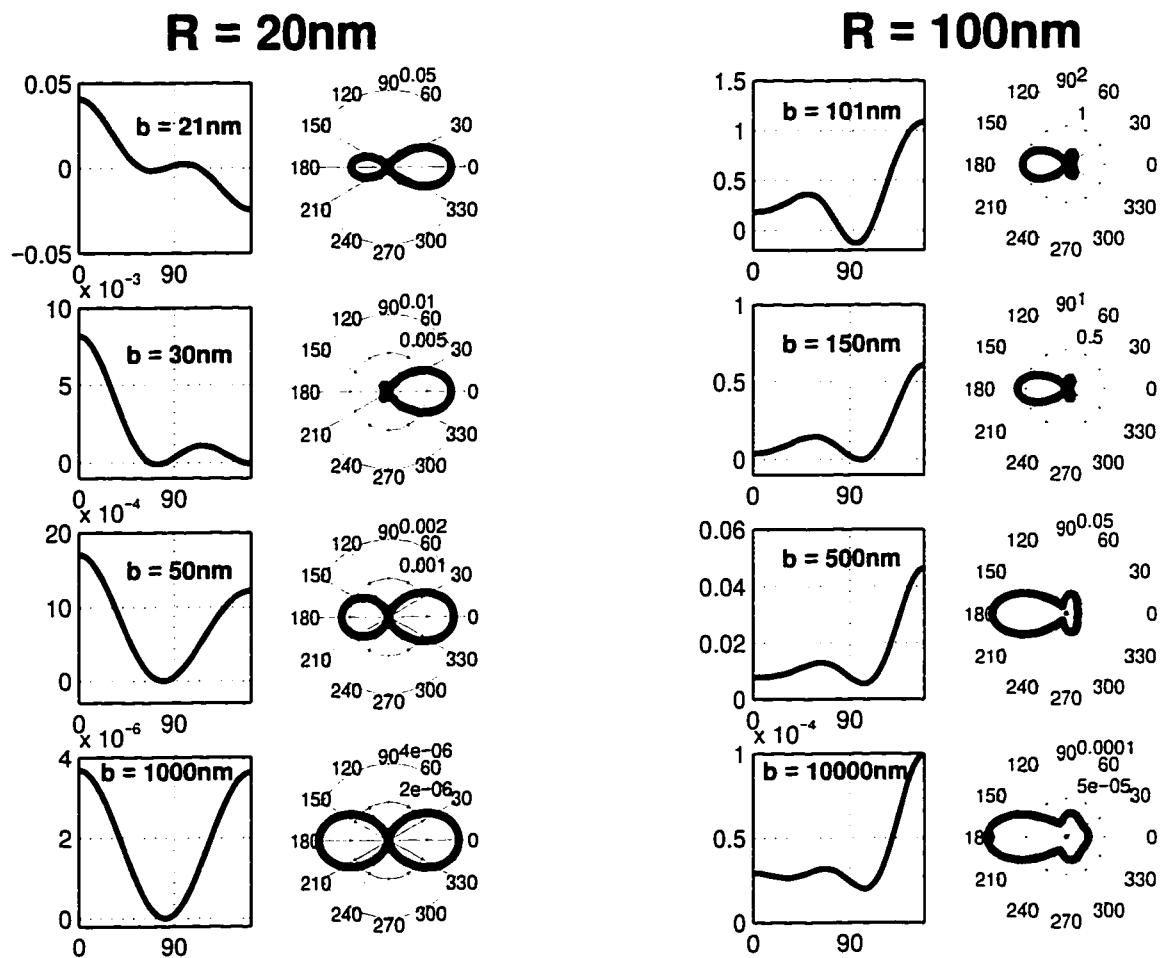


Figure 4.3: Poynting vector calculation for scattering from gold cluster. The incident light at 2.0eV is incident from $\theta = 0^\circ$, with the polarization directed out of the paper. Scattering from two cluster sizes, $R = 20\text{nm}$ and $R = 100\text{nm}$ are shown, where b is the radius of the observation points.

4.5 Numerical Calculations of Total Cross-Section

As shown in the appendix(E, we can obtain the exact expressions for the total cross-section and the scattering cross-section of spherically symmetric particles such as the single shell particle/object we have been considering. The results apply to any multi-shelled particles as well. The expression for the total cross section in terms of the scattering coefficients is :

$$Q_t = -\frac{2\pi}{k_3^2} \text{Re} \sum_{n=1}^{\infty} \frac{4n^2(n+1)^2}{2n+1} \left\{ a_{1n}^x (a_{1n}^{(3)h})^* + b_{1n}^x (b_{1n}^{(3)h})^* \right\}. \quad (4.50)$$

where a_{1n}^x and b_{1n}^x are the usual expansion coefficients of a plane wave incident along the z-axis with its polarization along the x-direction. The symmetry allows us to consider any general plane wave, but the algebra is simpler for the above choice of the incident plane wave. $a_{1n}^{(3)h}$ and $b_{1n}^{(3)h}$ are the scattering coefficients for the exterior region of a single shell scatterer and should be substituted with the relevant coefficients for the exterior region in a given general problem.

The net *extinction* or attenuation of incident energy in an electromagnetic wave propagating through a medium consisting of a random distribution of scatterers is directly proportional to the total cross section of the particles. It is assumed that the distribution is sufficiently dilute and random so that there is no mutual interaction or interference among the scattered waves from the individual particles. For many experimental situations, such as colloids in solution, this is a very reasonable assumption. Thus the theoretical computations on plasmon resonances in such particles can be verified against experimentally observed absorbance/extinction spectra.

As another test for our solution to electromagnetic scattering from coated nanoparticles, we compare the plasmon resonance in gold colloids. Figure 4.4 shows us the experimentally obtained absorbance spectra of gold colloids, of approximately 6nm radius, in an aqueous solution. In the model calculations, we set both the shell and the core as gold. In the same figure we also show the calculated total cross-section of spherical gold particles of 6nm radius surrounded by water ($n = 1.78$). To do the calculations we provided the known dielectric function of gold within the range of 400nm to 1100nm [24]. We assumed the dielectric function of water to be a constant within the same spectral range. There are *no* adjustable parameters in this calculation. The only input is the particle size, which is also experimentally determined [7] by TEM measurements. The resonance at $\sim 520\text{nm}$ is satisfactorily reproduced, including the aspect ratio of the peak to the satellite valley at $\sim 450\text{nm}$. The experimental graph

shows a peak at close to 970nm and that is attributable to water. There are small differences in the peak position as well as the general shape and width of the peak. These differences could result from several factors, including the presence of a shell layer surrounding the particles. Without adequate experimental verification, such differences could be accounted for theoretically by using our general formalism for the shell problem. In the following sections we shall study some of the qualitative aspects of the result of a dielectric shell on a core of a different dielectric. Due to subtle interaction between the three media, the core, the shell and the exterior, both the location of the peak and its shape can undergo dramatic changes.

4.6 Test Dielectric Functions

For calculations of plasmon resonances in single or multi-shelled particles, we need information on the complex dielectric functions of the various materials in question. Although the optical constants are accurately known for a number of materials, it is still not an exhaustive list. There are many materials of current research interest whose optical constants are not known in any great detail. In order to study model systems, we therefore consider the process of obtaining a 'test dielectric function'.

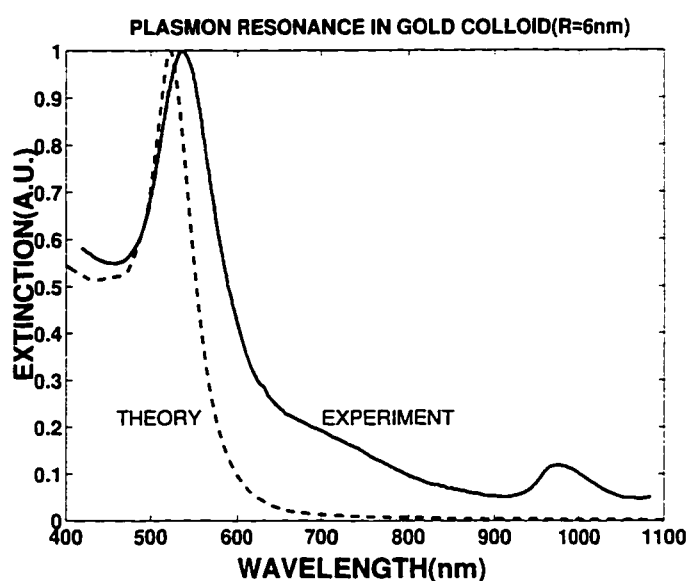


Figure 4.4: Plasmon Resonance in 12nm Gold Colloids in Aqueous Solution

In principle, the known absorbance of a material can provide us with its complex dielectric function by using the Kramers-Kronig relations. In theory this demands the knowledge of the absorbance/extinction function for *all* frequencies. The conversion from an extinction coefficient $k(\nu)$ spectrum to a refractive index spectrum is given by:

$$\begin{aligned}\Delta n(\nu_i) &= n(\nu_i) - n(\infty) \\ &= \frac{2}{\pi} P \int_0^{\infty} d\nu \frac{\nu k(\nu)}{\nu^2 - \nu_i^2}.\end{aligned}\quad (4.51)$$

where P indicates that Cauchy's principle value of the integral on the right-hand side is obtained. To perform a numerical Kramers-Kronig transformation, we assume that $k(\nu)$ is given as a sequence of discrete values k_j , at m frequencies ν_j with equal interval in between each ν_j :

$$\begin{array}{cccccccc} \nu_1 & \nu_2 & \nu_3 & \dots & \nu_j & \dots & \nu_{m-1} & \nu_m \\ k_1 & k_2 & k_3 & \dots & k_j & \dots & k_{m-1} & k_m \end{array}$$

Since $\Delta n(\nu_i)$ has poles at each ν_i , we can evaluate the integral numerically by considering only every other point so that computations at $\nu = \nu_i$ are avoided. Thus when i is an odd number (1, 3, 5, ...), we perform numerical integration by considering ν only at the even numbered frequencies and vice versa. For this method to be of any use, the extinction spectrum $k(\nu)$ must go to zero at both ends of the entire range of ν being considered. Such spectra are difficult to obtain experimentally. However, one could construct a model dielectric function by specifying a suitable extinction spectrum that vanishes outside the interval of interest.

Another approach is based on obtaining an exact analytic formula for a model extinction function that is also specified in a closed form expression. In particular, we consider a double-Lorentzian function for the extinction coefficient $k(\nu)$:

$$k(\nu) = \frac{k_{\max} (\gamma/2)^2}{(\nu - \nu_0)^2 + (\gamma/2)^2} - \frac{k_{\max} (\gamma/2)^2}{(\nu + \nu_0)^2 + (\gamma/2)^2}.\quad (4.52)$$

where k_{\max} is the maximum value of k , at frequency ν_0 and γ is the bandwidth at half height. It can be shown that the corresponding expression for the $\Delta n(\nu)$ spectrum, obtained by taking the Cauchy's principle value of the integral in Kramers-Kronig relations is given by:

$$\Delta n(\nu) = n(\infty) + k_{\max} \left\{ \frac{(\nu + \nu_0)(\gamma/2)}{(\nu + \nu_0)^2 + (\gamma/2)^2} - \frac{(\nu - \nu_0)(\gamma/2)}{(\nu - \nu_0)^2 + (\gamma/2)^2} \right\}.\quad (4.53)$$

Clearly, the addition of the second term in the expression for $k(\nu)$ automatically satisfies the conditions: $k(\nu) = -k(-\nu)$ and $n(\nu) = n(-\nu)$. The real and imaginary parts of the complex dielectric function, $\hat{\epsilon} = \epsilon_r + i\epsilon_i$ are related to the refractive index, n , and the extinction coefficient, k , by the following relations:

$$\epsilon_r = n^2 - k^2 \quad (4.54)$$

$$\epsilon_i = 2nk \quad (4.55)$$

$$n = \left\{ 0.5 \left(\sqrt{\epsilon_r^2 + \epsilon_i^2} + \epsilon_r \right) \right\}^{1/2} \quad (4.56)$$

$$k = \left\{ 0.5 \left(\sqrt{\epsilon_r^2 + \epsilon_i^2} - \epsilon_r \right) \right\}^{1/2} \quad (4.57)$$

In Figure 4.5 we show the results of our calculations of the total cross-section of a gold nanoparticle of 5nm radius with a dielectric overlayer of 1nm thickness. The dielectric function used is obtained from Equations 4.52 and 4.53 with $k_{max} = 1$, $\gamma = 0.5\text{eV}$ and ν_0 is made to vary between 2.2eV and 1.2eV. $n(\infty)$ is set to 1.5, a value typical of many organic and glassy materials that are transparent in the visible range of wavelengths. The important feature that emerges from this calculation is the appearance of a distinct second peak in the total cross-section spectrum of gold nanoparticles. The position and shape of this peak is distinct from that of the corresponding peak in the extinction spectra (k). This illustrates the subtle interaction between the dielectric functions in determining the overall plasmon resonance in a core-shell geometry.

In Figure 4.6 we show the calculations on a gold core of 5nm radius, with a dielectric shell of varying thickness. The test dielectric in this case is specified by $k_{max} = 1$, $\gamma = 0.5\text{eV}$, $n(\infty) = 1.5$ and $\nu_0 = 1.5\text{eV}$. We observe significant relative changes in the two peaks. The plasmon resonance peak at $\sim 500\text{nm}$ shifts towards longer wavelengths. Also the ratio of the peak to the valley at $\sim 450\text{nm}$ increases as the shell thickness increases. The peak at $\sim 750\text{nm}$ shifts towards longer wavelengths as well. This indicates the importance of an 'interfacial' layer in determining the plasmon resonance.

4.6.1 C60 Coated Gold Nanoparticles

In Figure 4.7 we illustrate the subtle interaction between real dielectric media in a core-shell geometry. We simulate a shell of C₆₀ on top of a gold core. The experimentally determined dielectric function for thin films of C₆₀ have been used for this

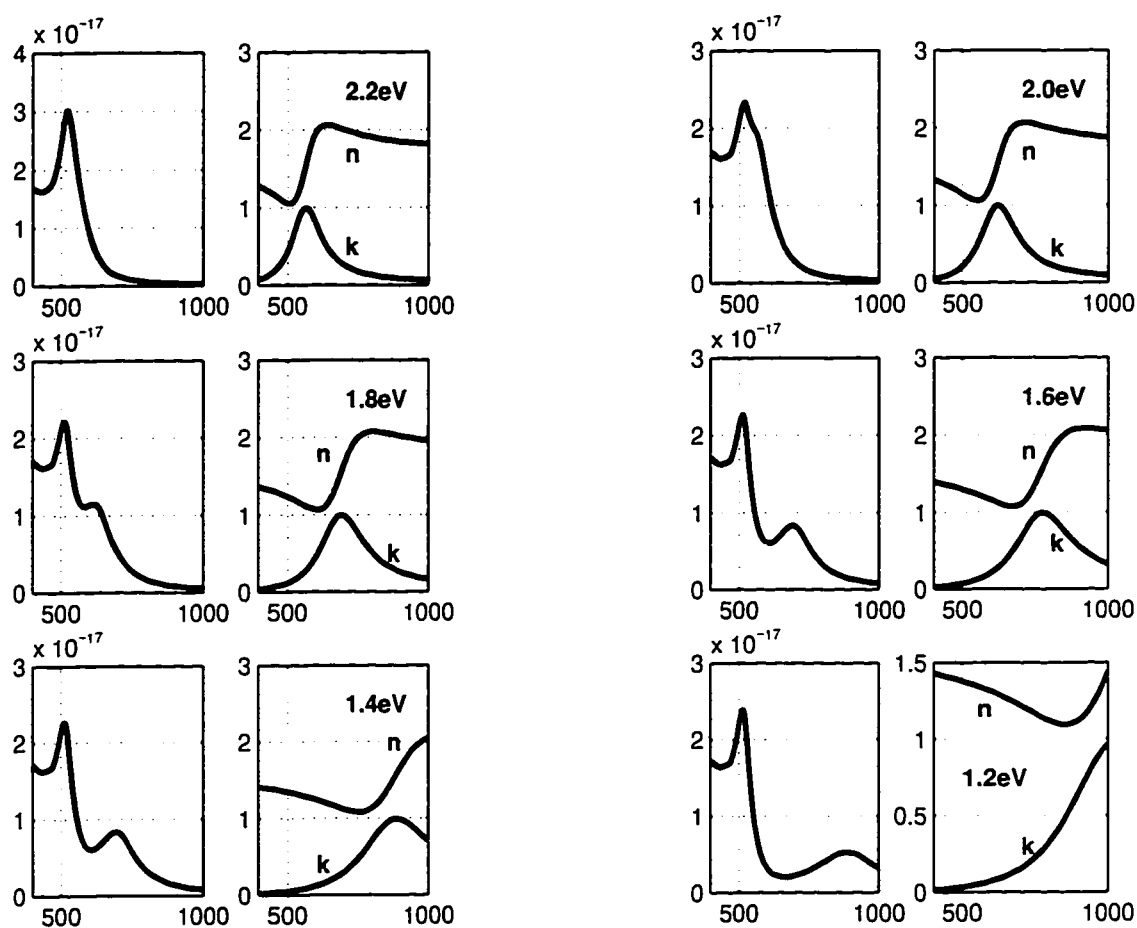


Figure 4.5: Total scattering cross section (in m^2) of gold nanoparticles, of 5nm diameter, coated with a shell of 1nm of a test dielectric whose refractive index, n , and the extinction, k , are also indicated. $k_{max} = 1$, $\gamma = 0.5\text{eV}$ and ν_0 is varied between 2.2eV and 1.2eV.

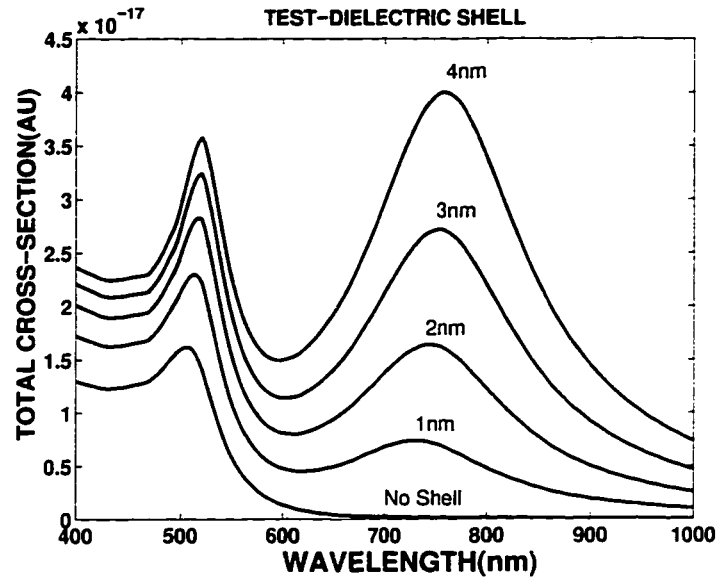


Figure 4.6: Total scattering cross section (in m^2) of gold nanoparticles, of 5nm diameter, coated with a shell of varying thickness of a test dielectric specified by $k_{max} = 1$, $\gamma = 0.5\text{eV}$ and $\nu_0 = 1.5\text{eV}$. The peak positions and shapes change as a function shell thickness.

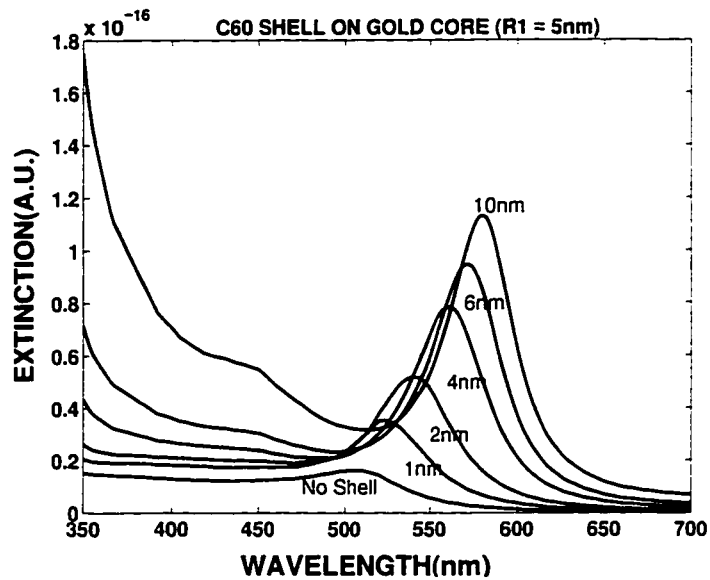


Figure 4.7: Total scattering cross section of gold nanoparticles, of 5nm diameter, coated with a shell of C_{60} . The peak at $\sim 520\text{nm}$ shifts towards longer wavelengths as the thickness of the shell is increased from 1nm to 10nm.

calculation [32]. The striking feature in this simulation is the shift in the plasmon resonance peak at 520nm towards longer wavelengths as the gold core is surrounded by increasingly thicker shells of C_{60} . The gold core is kept constant at 5nm, and the C_{60} shell increases in thickness from 1nm to 10nm. It is also interesting to note that the gold core makes its presence felt even when inside a relatively thick shell of C_{60} . Also, the steepness of the slope and the width of the gold-plasmon peak changes as a function of its environment. This clearly indicates the importance of the role played by the medium surrounding a given nanoparticle in determining its optical response.

4.7 Plasmon Resonance in Gold-Sulfide Systems

There is considerable interest in the scientific community to understand the physics of colloids. In particular, interest in gold-coated nanoparticles has led to experimental observations that are not understood satisfactorily from a theoretical point of view. As we have seen earlier, pure gold colloid (size ~ 10 nm) in an aqueous medium lead to a plasmon resonance peak at approximately 520nm. However, a system of gold-sulfide nanoparticles coated with a layer of gold exhibit remarkable dynamic complexity in its absorption spectra. An absorption peak, distinct from the 520nm resonance, undergoes characteristic non-monotonic shifts.

In Figure 4.8 we show a typical experimental situation [7]. The formation of Au_2S colloids is initiated by mixing together chloroauric acid ($HAuCl_4$) and sodium sulfide (Na_2S). This is indicated as $t = 0$. As the reaction proceeds, absorption spectra are obtained at intervals of a few minutes. Two distinct peaks are seen to evolve. There is the usual peak at 520nm which essentially does not undergo any shift. The other broad peak is at somewhat longer wavelengths and is observed to shift initially towards longer wavelengths but subsequently reverses its direction of shifting towards shorter wavelength. It has been speculated in the literature that such shifts are due to a combination of plasmon resonance in such colloids and resonance due to quantum confinement of electrons in a thin shell (of gold). It has been argued that the initial shift in the second absorption peak towards the red cannot be explained by a plasmon resonance effect.

In Figure 4.9 we show a plasmon resonance calculation of the total cross section of a core-shell particle. The core has a dielectric constant of ~ 5 , which is assumed to model gold-sulfide (Au_2S) within the wavelength range of interest, and the shell is a thin layer of gold. The experimentally determined bulk dielectric function of gold

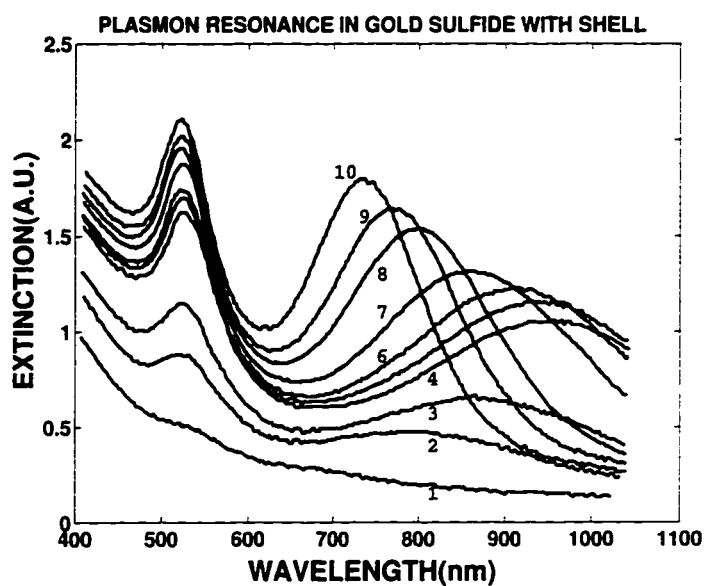


Figure 4.8: Absorbance of gold sulfide colloids coated with a shell of gold. The peak at $\sim 520\text{nm}$ corresponds to gold particles. The peak at longer wavelengths shifts initially towards the red ($1 \rightarrow 4$), but eventually shifts towards shorter wavelengths ($5 \rightarrow 10$).

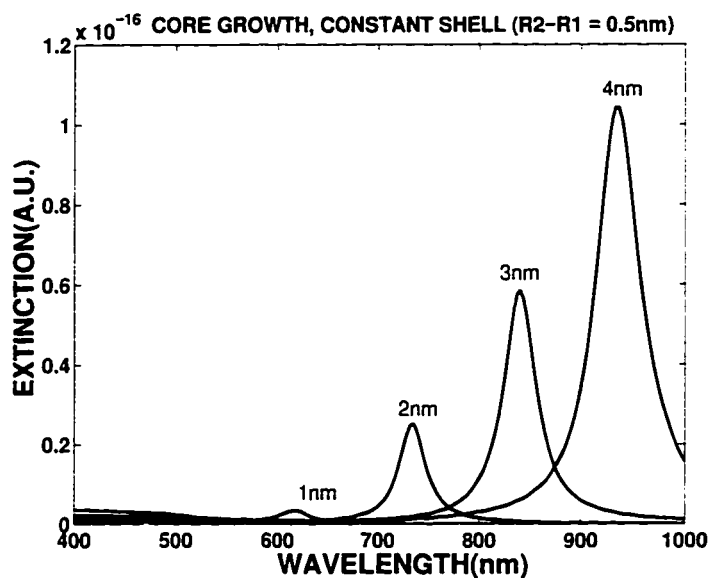


Figure 4.9: Calculated Plasmon Resonance in core-shell model. The shell is of gold. The core is a dielectric with $\epsilon = 5$. The diameter of the core is increased from 1nm to 4nm , but the shell thickness is held constant at 0.5nm . The peak shifts towards the red.

was used for this calculation [24]. The diameter of the core was increased, keeping the shell thickness constant. This is assumed to model the experimental situation where initially the formation of unstable Au_2S causes the particle diameter to increase. However, it is argued that a 'transition' shell of gold is formed as a result of reduction of the Au-S bond on the surface by S^{2-} ions [15] [44]. In this 'core-growth' regime, the calculated plasmon resonance peak shifts towards the red. The peak height increases and this is primarily due to the larger cross sections resulting from increasing particle sizes.

Figure 4.10 and Figure 4.11 are calculations for two different situations that could follow the initial 'core growth' regime. In Figure 4.10 we calculate the cross section when the total diameter of the core-shell composite is held constant, but the diameter of the core itself is made to decrease. This is the 'diffusion mode' which corresponds to the possible physical situation in which the process of Au_2S formation ceases, so the particles cannot grow any bigger, but the process of reduction of Au_2S to Au continues by a diffusive process through the shell, thereby increasing the net shell

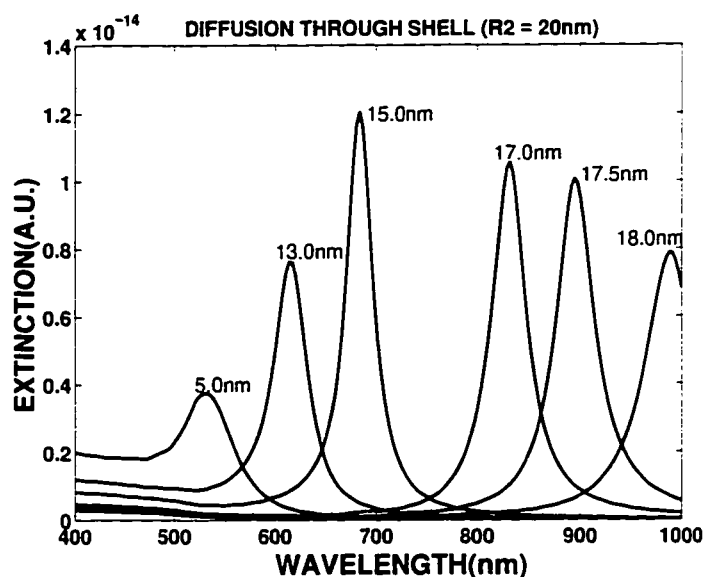


Figure 4.10: Calculated Plasmon Resonance in core-shell model. The shell is gold. The core is a dielectric with $\epsilon = 5$. The total diameter of the core-shell is held constant at 20nm, but the shell increases in thickness from 2nm to 15nm. The peak shifts towards the blue. The absorption becomes more gold-like.

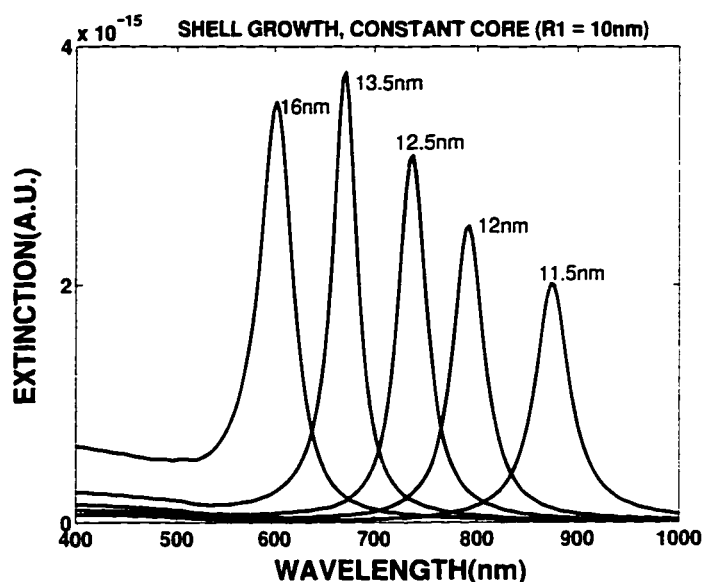


Figure 4.11: Calculated Plasmon Resonance in core-shell model. The shell is of gold. The core is a dielectric with $\epsilon = 5$. The diameter of the core is held constant at 10nm, but the shell increases in thickness from 1.5nm to 6nm. The peak shifts towards the blue.

thickness. An alternative scenario is described by the calculation in Figure 4.11. In this 'constant core' mode, the core of Au_2S is assumed to have stopped growing, but the thickness of the gold shell continues to increase as a result of the formation and deposition of gold on the already existing particles. In either case, the calculated plasmon resonance peak shifts towards the blue. It is of interest to note that the subtle interactions between the core, the shell and the exterior medium result in very non-intuitive shifts, not only in the position of the peak itself, but also on the peak heights and widths. Without further experimental evidence it is not possible at this stage to distinguish between the two possible cases, however, if one considers the slow growth of the Au peak during this blue shift of the Au_2S , it is unlikely that the shell is growing sufficiently in the 'constant-core' model to induce such large shifts. The fact that one can possibly explain the characteristic blue-shifts from such exact calculations of plasmon resonances in the shell-model is worth further attention.

In the above calculations, we did not make any provision for including a statistical distribution of particle sizes. Such distributions will lead to an overall broadening of the peaks. A further source of broadening can occur if the core itself is allowed to be

absorbing. With the availability of accurate dielectric function for Au_2S as well, such a model can be tested theoretically against experimental observations.

Chapter 5

Scattering From Non-Spherical Objects

5.1 Introduction

At present, solving Maxwell equations exactly for the problem of electromagnetic waves scattering from objects with arbitrary shapes can be tackled by finite element numerical methods only. The coupled partial differential equations are solved by finite-element methods for the vector fields \mathbf{E} and \mathbf{H} . Even with such powerful numerical methods there are some serious difficulties. In principle one could enclose the scattering object in question in a sufficiently large box with a linear or non-linear grid defined within it. The computed solution must satisfy the boundary conditions on the surface of the scattering object as well as the bounding box itself. Due to limitations of current computing hardware, one is restricted to a box that may not be made sufficiently large. This leads to an important problem in trying to obtain the boundary conditions on the bounding box itself. If the box is sufficiently large, so that the scattered solution can be assumed to be negligible at the box boundary, one can assume that the total field at the bounding-box boundary is equal to incident (plane wave) field. Since this condition is frequently difficult to satisfy, the computed solution will be in error.

In this chapter, we discuss an 'exact' method of solution for scattering from an object whose boundaries do not conform to the coordinate surfaces in a given coordinate system (the spherical polar coordinate system in this case). We have seen in the previous chapter that the spherical symmetry of the shell-model allows one to decouple the boundary condition equations, so that one has to solve a small matrix (4×4 for Mie scattering and 8×8 for a single-shell problem) to obtain the unknown expansion coefficients of the scattered field. With boundaries of arbitrary shapes one has to solve a larger matrix, since the boundary-condition equations cannot be easily decoupled. We illustrate this method of solution by considering an oblong 'capsule' shaped scatterer. Even for an object that has this relatively simple shape of a 'capsule', one previously had to rely on finite-element numerical methods for the solution.

5.2 The Model

The scattering object is a ‘capsule’, composed of two hemispheres of radius R , separated by a cylinder of radius R and length L . The origin is chosen to coincide with the center of the lower hemisphere as indicated in Figure 5.1. When $L \rightarrow 0$ the capsule degenerates to a sphere of radius R whose scattering solution can be obtained exactly. The axis of symmetry coincides with the z -axis. As we shall see, our choice of azimuthal symmetry makes the different m values decouple. The surface is therefore determined by three piece-wise continuous functions: The upper hemisphere section AB ($\theta \in [0, \theta_h]$), the cylindrical section BC ($\theta \in [\theta_h, \pi/2]$) and the lower hemisphere CD ($\theta \in [\pi/2, \pi]$), where $\tan \theta_h = R/L$:

$$S_{AB} : \left(\frac{r}{R}\right)^2 - 2\left(\frac{r}{R}\right)\left(\frac{L}{R}\right)\cos\theta + \left(\frac{L}{R}\right)^2 - 1 = 0. \quad (5.1)$$

$$S_{BC} : R - r \sin\theta = 0. \quad (5.2)$$

$$S_{CD} : R - r = 0. \quad (5.3)$$

The normal direction at a given point (r, θ) on the surface is obtained by taking the gradient of S : $\mathbf{n} \sim \nabla S$. One of the tangential directions is chosen to be in the \mathbf{e}_ϕ direction, so that the other tangent is given by $\mathbf{n} \times \mathbf{e}_\phi$. Thus the tangents and normals (not normalized to unit length) on the three segments can be shown to be as follows:

$$\begin{aligned} \mathbf{n}^1 &= (r - L \cos\theta) \mathbf{e}_r + L \sin\theta \mathbf{e}_\theta \\ S_{AB} : \mathbf{t}_1^1 &= L \sin\theta \mathbf{e}_r - (r - L \cos\theta) \mathbf{e}_\theta \\ \mathbf{t}_2^1 &= \mathbf{e}_\phi \end{aligned} \quad (5.4)$$

$$\begin{aligned} \mathbf{n}^2 &= \sin\theta \mathbf{e}_r + \cos\theta \mathbf{e}_\theta \\ S_{BC} : \mathbf{t}_1^2 &= \cos\theta \mathbf{e}_r - \sin\theta \mathbf{e}_\theta \\ \mathbf{t}_2^2 &= \mathbf{e}_\phi \end{aligned} \quad (5.5)$$

$$\begin{aligned} \mathbf{n}^3 &= \mathbf{e}_r \\ S_{CD} : \mathbf{t}_1^3 &= \mathbf{e}_\theta \\ \mathbf{t}_2^3 &= \mathbf{e}_\phi \end{aligned} \quad (5.6)$$

The surface is approximated by choosing a set of points on the capsule, labeled as 1,2,3....N. In principle, the more points we specify, the better the approximation to the true surface. By forcing the boundary conditions to be satisfied at the chosen

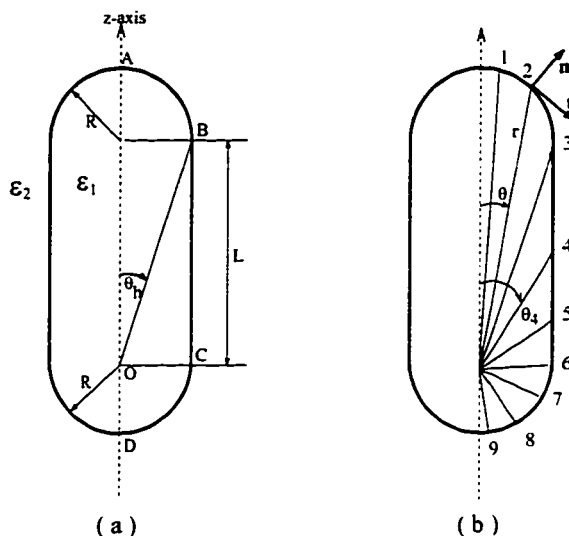


Figure 5.1: (a) Geometry of ‘capsule’ shaped scattering object. Two hemispheres of radius R are attached to the end of a cylinder of length L . Letting $L \rightarrow 0$, the capsule degenerates to a sphere. (b) Approximating the azimuthally symmetrical surface by means of the discrete set of angles θ_i . r as a function of θ is specified by a piece-wise continuous function. \mathbf{n} indicates the normal and \mathbf{t} the tangent orthogonal to \mathbf{e}_ϕ .

points, often in a least-square sense, we can solve for the set of unknown expansion coefficients of the solution in the different regions.

5.2.1 Convergence Consideration

We have seen in Chapter 3 that the number of terms required to obtain convergence (to better than 1%) about the origin, for an arbitrary plane wave expansion in the basis functions is given by $n \sim 1.4|kr|$, where r is the distance from the origin and k is the magnitude of the complex wave-vector in that medium. This provides us a direct way to estimate the number of terms to include in the expansion for the scattered field, given the desired accuracy of the solution and the size of the scattering object. Clearly, the larger the scatterer, the larger the number of terms one needs to include to obtain the scattered solution. Such considerations are equally valid even in the case of the symmetrical scattering objects we encountered in the shell-model. The rationale follows from the following argument: Any scattered field can be expressed as a sum of plane waves, so if the expansion for the plane waves themselves requires a

certain number of terms within a region. so will the expansion of the scattered solution within the same region. For objects that deviate from the spherical geometry. more expansion terms for the scattered fields are required as well.

5.3 Expansion in positive m only

When representing the incident plane wave field. we used a double summation: $n \in [1, 2, 3, \dots]$ and $m \in [0, \pm 1, \pm 2, \dots, \pm n]$ over the \mathbf{M} and \mathbf{N} functions. The ‘forced’ solutions of the scattered fields will have terms corresponding to each source term. By employing certain symmetric relations, we can express the incident field (and so the scattered fields as well) in a series of functions with $m > 0$ only. This will not only reduce the computation by at least 50%. but it will also avoid certain troublesome numerical inaccuracies with computing the $m < 0$ functions. The computation of the Associated Legendre functions for $m < 0$ for large $|m|$ and n involves obtaining ratios of factorials like $(n - m)!/(n + m)!$. and these can lead to severe numerical inaccuracies.

We define a set of functions \mathbf{m}_{emn} , \mathbf{m}_{omn} , \mathbf{n}_{emn} and \mathbf{n}_{omn} where $m \geq 0$ only and the o and e subscripts refer to ‘odd’ and ‘even’ :

$$\mathbf{m}_{emn} = -m z_n(kr) \frac{P_n^m(\cos \theta)}{\sin \theta} \sin m\phi \mathbf{e}_\theta - z_n(kr) \frac{dP_n^m(\cos \theta)}{d\theta} \cos m\phi \mathbf{e}_\phi \quad (5.7)$$

$$\mathbf{m}_{omn} = m z_n(kr) \frac{P_n^m(\cos \theta)}{\sin \theta} \cos m\phi \mathbf{e}_\theta - z_n(kr) \frac{dP_n^m(\cos \theta)}{d\theta} \sin m\phi \mathbf{e}_\phi \quad (5.8)$$

$$\begin{aligned} \mathbf{n}_{emn} = & n(n+1) \frac{z_n(kr)}{kr} P_n^m(\cos \theta) \cos m\phi \mathbf{e}_r + \frac{1}{kr} \frac{d}{dr} (r z_n(kr)) \frac{dP_n^m(\cos \theta)}{d\theta} \cos m\phi \mathbf{e}_\theta \\ & - m \frac{1}{kr} \frac{d}{dr} (r z_n(kr)) \frac{P_n^m(\cos \theta)}{\sin \theta} \sin m\phi \mathbf{e}_\phi \end{aligned} \quad (5.9)$$

$$\begin{aligned} \mathbf{n}_{omn} = & n(n+1) \frac{z_n(kr)}{kr} P_n^m(\cos \theta) \sin m\phi \mathbf{e}_r + \frac{1}{kr} \frac{d}{dr} (r z_n(kr)) \frac{dP_n^m(\cos \theta)}{d\theta} \sin m\phi \mathbf{e}_\theta \\ & + m \frac{1}{kr} \frac{d}{dr} (r z_n(kr)) \frac{P_n^m(\cos \theta)}{\sin \theta} \cos m\phi \mathbf{e}_\phi. \end{aligned} \quad (5.10)$$

where $z_n(kr)$ are either the spherical Bessel or the spherical Hankel functions. It can be verified by straightforward algebra that the following relations hold:

$$\mathbf{M}_{mn} - \mathbf{M}_{mn}^* = 2i \mathbf{m}_{omn} \quad (5.11)$$

$$\mathbf{M}_{mn} + \mathbf{M}_{mn}^* = 2 \mathbf{m}_{emn} \quad (5.12)$$

$$\mathbf{N}_{mn} - \mathbf{N}_{mn}^* = 2i \mathbf{n}_{omn} \quad (5.13)$$

$$\mathbf{N}_{mn} + \mathbf{N}_{mn}^* = 2 \mathbf{n}_{emn}. \quad (5.14)$$

Now we have already seen that:

$$\mathbf{M}_{-mn} = (-1)^m \frac{(n-m)!}{(n+m)!} \mathbf{M}_{mn}^* \quad (5.15)$$

$$\mathbf{N}_{-mn} = (-1)^m \frac{(n-m)!}{(n+m)!} \mathbf{N}_{mn}^*. \quad (5.16)$$

Since the \mathbf{M}^* and \mathbf{N}^* functions can be expressed as scalar multiples of the \mathbf{M} and \mathbf{N} functions, therefore they satisfy the diffraction equation as well. Also, since the \mathbf{m} and \mathbf{n} functions defined above are linear combinations of the \mathbf{M} and \mathbf{N} and their complex conjugates, they too are solutions of the diffraction equation.

Consider an expansion for a p-polarized incident wave as shown in Figure 5.2. Both \mathbf{E} and \mathbf{k} are confined in the XZ plane, so that $\beta = 0$ (β is the azimuthal angle of \mathbf{k}). Since the incident electric field, $\mathbf{E} = (E_x, 0, E_z)$, do not have any component in

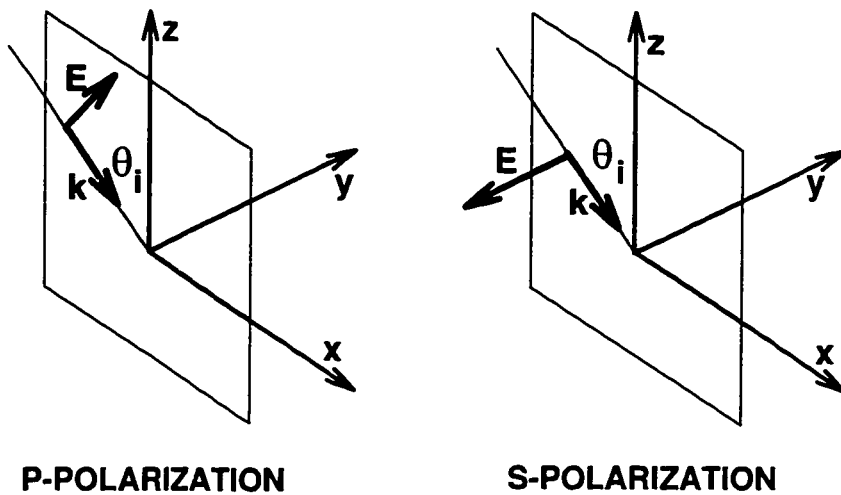


Figure 5.2: Defining the relative orientation of \mathbf{E} and \mathbf{k} for s and p polarization geometries. The definition assumes the presence of an interface at the xy -plane.

the y -direction, we can write (since the $n = 0$ terms, \mathbf{M} and \mathbf{N} are identically zero):

$$\begin{aligned}
\mathbf{E}e^{i\mathbf{k}\cdot\mathbf{r}} &= \sum_{n=1}^{\infty} \sum_{m=-n}^n \{(E_x a_{mn}^x + E_z a_{mn}^z) \mathbf{M}_{mn} + (E_x b_{mn}^x + E_z b_{mn}^z) \mathbf{N}_{mn}\} \quad (5.17) \\
&= \sum_{n=1}^{\infty} \sum_{m=0}^n \{(E_x a_{mn}^x + E_z a_{mn}^z) \mathbf{M}_{mn} + (E_x b_{mn}^x + E_z b_{mn}^z) \mathbf{N}_{mn} \\
&\quad + (E_x a_{-mn}^x + E_z a_{-mn}^z) \mathbf{M}_{-mn} + (E_x b_{-mn}^x + E_z b_{-mn}^z) \mathbf{N}_{-mn}\} \\
&= \sum_{n=1}^{\infty} \sum_{m=0}^n \left\{ E_x (a_{mn}^x \mathbf{M}_{mn} + a_{-mn}^x \mathbf{M}_{-mn}) + E_x (b_{mn}^x \mathbf{N}_{mn} + b_{-mn}^x \mathbf{N}_{-mn}) \right. \\
&\quad \left. + E_z (a_{mn}^z \mathbf{M}_{mn} + a_{-mn}^z \mathbf{M}_{-mn}) + E_z (b_{mn}^z \mathbf{N}_{mn} + b_{-mn}^z \mathbf{N}_{-mn}) \right\}
\end{aligned}$$

where in the last two steps we remember to count the $m = 0$ term only once. Now, since $\beta = 0$ in the chosen geometry, we have

$$a_{-mn}^x = (-1)^{m+1} \frac{(n+m)!}{(n-m)!} a_{mn}^x \quad \text{and} \quad a_{-mn}^z = (-1)^{m+1} \frac{(n+m)!}{(n-m)!} a_{mn}^z.$$

Similarly,

$$b_{-mn}^x = (-1)^m \frac{(n+m)!}{(n-m)!} b_{mn}^x \quad \text{and} \quad b_{-mn}^z = (-1)^m \frac{(n+m)!}{(n-m)!} b_{mn}^z.$$

So we have:

$$\begin{aligned}
a_{mn}^x \mathbf{M}_{mn} + a_{-mn}^x \mathbf{M}_{-mn} &= a_{mn}^x (\mathbf{M}_{mn} + (-1)^{m+1} (-1)^m \mathbf{M}_{mn}^*) \\
&= a_{mn}^x (\mathbf{M}_{mn} - \mathbf{M}_{mn}^*) \\
&= 2ia_{mn}^x \mathbf{m}_{omn} \quad (5.18)
\end{aligned}$$

$$\begin{aligned}
a_{mn}^z \mathbf{M}_{mn} + a_{-mn}^z \mathbf{M}_{-mn} &= a_{mn}^z (\mathbf{M}_{mn} + (-1)^{m+1} (-1)^m \mathbf{M}_{mn}^*) \\
&= a_{mn}^z (\mathbf{M}_{mn} - \mathbf{M}_{mn}^*) \\
&= 2ia_{mn}^z \mathbf{m}_{omn} \quad (5.19)
\end{aligned}$$

$$\begin{aligned}
b_{mn}^x \mathbf{N}_{mn} + b_{-mn}^x \mathbf{N}_{-mn} &= b_{mn}^x (\mathbf{N}_{mn} + (-1)^m (-1)^m \mathbf{N}_{mn}^*) \\
&= b_{mn}^x (\mathbf{N}_{mn} + \mathbf{N}_{mn}^*) \\
&= 2b_{mn}^x \mathbf{n}_{emn} \quad (5.20)
\end{aligned}$$

$$\begin{aligned}
b_{mn}^z \mathbf{N}_{mn} + b_{-mn}^z \mathbf{N}_{-mn} &= b_{mn}^z (\mathbf{N}_{mn} + (-1)^m (-1)^m \mathbf{N}_{mn}^*) \\
&= b_{mn}^z (\mathbf{N}_{mn} + \mathbf{N}_{mn}^*) \\
&= 2b_{mn}^z \mathbf{n}_{emn}.
\end{aligned} \tag{5.21}$$

Substituting these relations back into the expression for the incident field, we finally obtain an expansion in $m \geq 0$ only. Here $E_x = E_0 \sin \theta_i$ and $E_z = E_0 \cos \theta_i$, and the wave vector is $\mathbf{k} = (k, \alpha = \pi - \theta_i, \beta = 0)$.

$$\begin{aligned}
\mathbf{E} e^{i\mathbf{k}\cdot\mathbf{r}} &= \sum_{n=1}^{\infty} \sum_{m=0}^n \left\{ 2i (E_x a_{mn}^x + E_z a_{mn}^z) \mathbf{m}_{omn} \right. \\
&\quad \left. + 2 (E_x b_{mn}^x + E_z b_{mn}^z) \mathbf{n}_{emn} \right\}
\end{aligned} \tag{5.22}$$

(p-polarization)

Similarly, for s-polarization, with $\mathbf{E} = E_0 \mathbf{e}_y$ and $\mathbf{k} = (k, \alpha = \pi - \theta_i, \beta = 0)$, we obtain:

$$\mathbf{E} e^{i\mathbf{k}\cdot\mathbf{r}} = E_0 \sum_{n=1}^{\infty} \sum_{m=0}^n \left\{ (a_{mn}^y \mathbf{M}_{mn} + a_{-mn}^y \mathbf{M}_{-mn}) + (b_{mn}^y \mathbf{N}_{mn} + b_{-mn}^y \mathbf{N}_{-mn}) \right\}.$$

Using the properties of sign changes in the a_{mn}^y and the b_{mn}^y coefficients, we obtain

$$\begin{aligned}
\mathbf{E} e^{i\mathbf{k}\cdot\mathbf{r}} &= E_0 \sum_{n=1}^{\infty} \sum_{m=0}^n \left\{ 2 a_{mn}^y \mathbf{m}_{emn} + 2i b_{mn}^y \mathbf{n}_{omn} \right\}
\end{aligned} \tag{5.23}$$

(s-polarization)

Now that the expansion for the s and p-polarized incident fields are known, one could obtain the expansion for any elliptically polarized wave from linear combinations of the s and p polarized wave expansions. When $\beta \neq 0$, we can always solve for the fields in a coordinate system for which $\beta = 0$, and once the field coefficients are determined, transform the azimuthal angle $\phi \rightarrow \phi - \beta$ to obtain the solution in the coordinate system of interest. This amounts to simply multiplying the solutions by $e^{\pm im\beta}$.

5.4 Boundary Condition Equations

For the problem of scattering from a capsule, we have two regions: inside the capsule surface where the dielectric function is ϵ_1 , and outside the surface where the dielectric function is ϵ_2 . As in the case of scattering from spherical shells, we assume ϵ_2 to be a real function of the incident wave frequency. This validates the expansion of the incident electric field in the spherical bessel function solutions. Since the origin is enclosed within the surface, the solution in region 1 will have the spherical bessel function solutions only.

Consider an s-polarized incident wave of unit strength ($|\mathbf{E}_i| = 1$) with the polarization oriented along the y-axis and \mathbf{k} confined to the xz-plane ($\beta = 0$):

$$\mathbf{E}_i = \sum_{n=1}^{\infty} \sum_{m=0}^n \left\{ a_{mn} \mathbf{m}_{emn}^{2j} + b_{mn} \mathbf{n}_{omn}^{2j} \right\} \quad (5.24)$$

$$\mathbf{H}_i = -i \sqrt{\frac{\epsilon_2}{\mu_2}} \sum_{n=1}^{\infty} \sum_{m=0}^n \left\{ b_{mn} \mathbf{m}_{omn}^{2j} + a_{mn} \mathbf{n}_{emn}^{2j} \right\} \quad (5.25)$$

where $a_{mn} = 2a_{mn}^y$ and $b_{mn} = 2ib_{mn}^y$, and the superscript 2 for the \mathbf{m} and \mathbf{n} functions refer to medium 2. We assume the scattered electromagnetic fields in the two regions to have the following forms (expanding in the $m \geq 0$ terms only) :

$$\mathbf{E}_1 = \sum_{n=1}^{\infty} \sum_{m=0}^n \left\{ a_{mn}^{1j} \mathbf{m}_{emn}^{1j} + b_{mn}^{1j} \mathbf{n}_{omn}^{1j} \right\} \quad (5.26)$$

$$\mathbf{H}_1 = -i \sqrt{\frac{\epsilon_1}{\mu_1}} \sum_{n=1}^{\infty} \sum_{m=0}^n \left\{ b_{mn}^{1j} \mathbf{m}_{omn}^{1j} + a_{mn}^{1j} \mathbf{n}_{emn}^{1j} \right\} \quad (5.27)$$

$$\mathbf{E}_2 = \sum_{n=1}^{\infty} \sum_{m=0}^n \left\{ a_{mn}^{2h} \mathbf{m}_{emn}^{2h} + b_{mn}^{2h} \mathbf{n}_{omn}^{2h} \right\} \quad (5.28)$$

$$\mathbf{H}_2 = -i \sqrt{\frac{\epsilon_2}{\mu_2}} \sum_{n=1}^{\infty} \sum_{m=0}^n \left\{ b_{mn}^{2h} \mathbf{m}_{omn}^{2h} + a_{mn}^{2h} \mathbf{n}_{emn}^{2h} \right\} \quad (5.29)$$

For each point on the surface, we can write down six equations corresponding to the boundary conditions. As discussed before, not all of them are linearly independent. In fact when $L = 0$, corresponding to a sphere, the equations of continuity of the tangential fields of \mathbf{E} and \mathbf{H} alone will yield a linearly independent set:

$$\mathbf{E}_1 \cdot \mathbf{t}_1 = \mathbf{E}_2 \cdot \mathbf{t}_1 + \mathbf{E}_i \cdot \mathbf{t}_1 \quad (5.30)$$

$$\mathbf{E}_1 \cdot \mathbf{t}_2 = \mathbf{E}_2 \cdot \mathbf{t}_2 + \mathbf{E}_i \cdot \mathbf{t}_2 \quad (5.31)$$

$$\mathbf{H}_1 \cdot \mathbf{t}_1 = \mathbf{H}_2 \cdot \mathbf{t}_1 + \mathbf{H}_i \cdot \mathbf{t}_1 \quad (5.32)$$

$$\mathbf{H}_1 \cdot \mathbf{t}_2 = \mathbf{H}_2 \cdot \mathbf{t}_2 + \mathbf{H}_i \cdot \mathbf{t}_2. \quad (5.33)$$

In general, we have the remaining two equations arising from the continuity of the normal components of $\mathbf{D} = \epsilon\mathbf{E}$ and $\mathbf{B} = \mu\mathbf{H}$. Here \mathbf{n} (without the subscripts) refer to the normal vector and not one of the field-functions :

$$\epsilon_1 \mathbf{E}_1 \cdot \mathbf{n} = \epsilon_2 \mathbf{E}_2 \cdot \mathbf{n} + \epsilon_2 \mathbf{E}_i \cdot \mathbf{n} \quad (5.34)$$

$$\mu_1 \mathbf{H}_1 \cdot \mathbf{n} = \mu_2 \mathbf{H}_2 \cdot \mathbf{n} + \mu_2 \mathbf{H}_i \cdot \mathbf{n}. \quad (5.35)$$

Each of the terms above of the form $\mathbf{E} \cdot \mathbf{t}$ is expressible as an infinite series when we substitute the expression for the appropriate field expansion. Thus for example:

$$\mathbf{E}_1 \cdot \mathbf{t}_1 = \sum_{n=1}^{\infty} \sum_{m=0}^n \left\{ a_{mn}^{1j} (\mathbf{m}_{emn}^{1j} \cdot \mathbf{t}_1) + b_{mn}^{1j} (\mathbf{n}_{omn}^{1j} \cdot \mathbf{t}_1) \right\}. \quad (5.36)$$

In order to obtain these coefficients we approximate the field expansions by truncating the series to a finite number of terms. The number of terms to include is decided finally by the overall error in the total solution. The ϕ -dependence in each of the terms of the boundary condition equations are of the form $\sin m\phi$ or $\cos m\phi$. On multiplying both sides of a boundary condition equation, say Equation 5.30, by $\epsilon^{im'\phi}$ and integrating with respect to ϕ between the limits $\phi \in [0, 2\pi]$, only the $m = m'$ terms survive. It can be easily verified that in fact both sides of these equations have the same ϕ -dependence. For example, since $\mathbf{t}_1 \sim t_{1r}\mathbf{e}_r + t_{1\theta}\mathbf{e}_\theta$, and $\mathbf{m}_{emn} \cdot \mathbf{e}_r = 0$, $\mathbf{m}_{emn} \cdot \mathbf{e}_\theta \sim \sin m\phi$, $\mathbf{n}_{omn} \cdot \mathbf{e}_r \sim \sin m\phi$ and $\mathbf{n}_{omn} \cdot \mathbf{e}_\theta \sim \cos m\phi$, both the left and right hand side expressions of Equation 5.30 will contain only $\sin m\phi$ factors. Thus we have all the boundary condition equations above decouple for the same m . This is a direct consequence of the assumptions on azimuthal symmetry on the shape of the scattering object. For a chosen m , only $n \geq m$ terms will survive due to the factors containing the Associated Legendre functions. So the boundary condition equations (after 'm'-decoupling) will assume the form, for Equation 5.30 say:

$$\sum_{n=m}^{m+N-1} \left\{ a_{mn}^{1j} (\mathbf{m}_{emn}^{1j} \cdot \mathbf{t}_1) - a_{mn}^{2h} (\mathbf{m}_{emn}^{2h} \cdot \mathbf{t}_1) + b_{mn}^{1j} (\mathbf{n}_{omn}^{1j} \cdot \mathbf{t}_1) - b_{mn}^{2h} (\mathbf{n}_{omn}^{2h} \cdot \mathbf{t}_1) \right\}$$

$$= \sum_{n=m}^{m+N-1} \left\{ a_{mn} (\mathbf{m}_{emn}^{2j} \cdot \mathbf{t}_1) + b_{mn} (\mathbf{n}_{omn}^{2j} \cdot \mathbf{t}_1) \right\} \quad (5.37)$$

where the right hand side of the equation contains the 'source'-terms only. Similarly, we can write Equation 5.31 as:

$$\begin{aligned} & \sum_{n=m}^{m+N-1} \left\{ a_{mn}^{1j} (\mathbf{m}_{emn}^{1j} \cdot \mathbf{t}_2) - a_{mn}^{2h} (\mathbf{m}_{emn}^{2h} \cdot \mathbf{t}_2) + b_{mn}^{1j} (\mathbf{n}_{omn}^{1j} \cdot \mathbf{t}_2) - b_{mn}^{2h} (\mathbf{n}_{omn}^{2h} \cdot \mathbf{t}_2) \right\} \\ &= \sum_{n=m}^{m+N-1} \left\{ a_{mn} (\mathbf{m}_{emn}^{2j} \cdot \mathbf{t}_2) + b_{mn} (\mathbf{n}_{omn}^{2j} \cdot \mathbf{t}_2) \right\}. \end{aligned} \quad (5.38)$$

Equation 5.32 becomes, cancelling the common factor $-i$ from the expressions for \mathbf{H} in the different regions :

$$\begin{aligned} & \sum_{n=m}^{m+N-1} \left\{ a_{mn}^{1j} \left(\sqrt{\frac{\epsilon_1}{\mu_1}} \mathbf{n}_{emn}^{1j} \cdot \mathbf{t}_1 \right) - a_{mn}^{2h} \left(\sqrt{\frac{\epsilon_2}{\mu_2}} \mathbf{n}_{emn}^{2h} \cdot \mathbf{t}_1 \right) \right. \\ & \quad \left. + b_{mn}^{1j} \left(\sqrt{\frac{\epsilon_1}{\mu_1}} \mathbf{m}_{omn}^{1j} \cdot \mathbf{t}_1 \right) - b_{mn}^{2h} \left(\sqrt{\frac{\epsilon_2}{\mu_2}} \mathbf{m}_{omn}^{2h} \cdot \mathbf{t}_1 \right) \right\} \\ &= \sum_{n=m}^{m+N-1} \left\{ a_{mn} \left(\sqrt{\frac{\epsilon_2}{\mu_2}} \mathbf{n}_{emn}^{2j} \cdot \mathbf{t}_1 \right) + b_{mn} \left(\sqrt{\frac{\epsilon_2}{\mu_2}} \mathbf{m}_{omn}^{2j} \cdot \mathbf{t}_1 \right) \right\}. \end{aligned} \quad (5.39)$$

and Equation 5.33 becomes:

$$\begin{aligned} & \sum_{n=m}^{m+N-1} \left\{ a_{mn}^{1j} \left(\sqrt{\frac{\epsilon_1}{\mu_1}} \mathbf{n}_{emn}^{1j} \cdot \mathbf{t}_2 \right) - a_{mn}^{2h} \left(\sqrt{\frac{\epsilon_2}{\mu_2}} \mathbf{n}_{emn}^{2h} \cdot \mathbf{t}_2 \right) \right. \\ & \quad \left. + b_{mn}^{1j} \left(\sqrt{\frac{\epsilon_1}{\mu_1}} \mathbf{m}_{omn}^{1j} \cdot \mathbf{t}_2 \right) - b_{mn}^{2h} \left(\sqrt{\frac{\epsilon_2}{\mu_2}} \mathbf{m}_{omn}^{2h} \cdot \mathbf{t}_2 \right) \right\} \\ &= \sum_{n=m}^{m+N-1} \left\{ a_{mn} \left(\sqrt{\frac{\epsilon_2}{\mu_2}} \mathbf{n}_{emn}^{2j} \cdot \mathbf{t}_2 \right) + b_{mn} \left(\sqrt{\frac{\epsilon_2}{\mu_2}} \mathbf{m}_{omn}^{2j} \cdot \mathbf{t}_2 \right) \right\}. \end{aligned} \quad (5.40)$$

Finally the boundary condition equation from the continuity of the normal component of \mathbf{D} assumes the form:

$$\begin{aligned} & \sum_{n=m}^{m+N-1} \left\{ a_{mn}^{1j} (\epsilon_1 \mathbf{m}_{emn}^{1j} \cdot \mathbf{n}) - a_{mn}^{2h} (\epsilon_2 \mathbf{m}_{emn}^{2h} \cdot \mathbf{n}) \right. \\ & \quad \left. + b_{mn}^{1j} (\epsilon_1 \mathbf{n}_{omn}^{1j} \cdot \mathbf{n}) - b_{mn}^{2h} (\epsilon_2 \mathbf{n}_{omn}^{2h} \cdot \mathbf{n}) \right\} \\ &= \sum_{n=m}^{m+N-1} \left\{ a_{mn} (\epsilon_2 \mathbf{m}_{emn}^{2j} \cdot \mathbf{n}) + b_{mn} (\epsilon_2 \mathbf{n}_{omn}^{2j} \cdot \mathbf{n}) \right\}. \end{aligned} \quad (5.41)$$

and the continuity of the normal component of \mathbf{B} gives us the equation:

$$\begin{aligned} & \sum_{n=m}^{m+N-1} \left\{ a_{mn}^{1j} \left(\mu_1 \sqrt{\frac{\epsilon_1}{\mu_1}} \mathbf{n}_{emn}^{1j} \cdot \mathbf{n} \right) - a_{mn}^{2h} \left(\mu_2 \sqrt{\frac{\epsilon_2}{\mu_2}} \mathbf{n}_{emn}^{2h} \cdot \mathbf{n} \right) \right. \\ & \quad \left. + b_{mn}^{1j} \left(\mu_1 \sqrt{\frac{\epsilon_1}{\mu_1}} \mathbf{m}_{omn}^{1j} \cdot \mathbf{n} \right) - b_{mn}^{2h} \left(\mu_2 \sqrt{\frac{\epsilon_2}{\mu_2}} \mathbf{m}_{omn}^{2h} \cdot \mathbf{n} \right) \right\} \\ & = \sum_{n=m}^{m+N-1} \left\{ a_{mn} \left(\mu_2 \sqrt{\frac{\epsilon_2}{\mu_2}} \mathbf{n}_{emn}^{2j} \cdot \mathbf{n} \right) + b_{mn} \left(\mu_2 \sqrt{\frac{\epsilon_2}{\mu_2}} \mathbf{m}_{omn}^{2j} \cdot \mathbf{n} \right) \right\}. \quad (5.42) \end{aligned}$$

In these *truncated* boundary-condition equations, the right hand sides are completely known, and they constitute the source terms. The left hand sides are linear expressions in the unknowns a_{mn}^{1j} , b_{mn}^{1j} , a_{mn}^{2h} and b_{mn}^{2h} (with $n \in m, m+1, \dots, m+N-1$). Thus each of the equations above can be considered a linear equation in $4N$ unknowns, where N is the specified maximum number of terms to use for a specified m . The coefficients in these equations are functions of r and θ (the ϕ part cancels out in the process of decoupling the equations for the same m). So for each specified point on the boundary, we obtain six equations in $4N$ unknowns. By specifying more points on the boundary, we can obtain more equations. The structure of the resulting system of equations can be written in matrix notation which has the form shown in Figure 5.3.

The ‘coefficient matrix’ contains blocks of 6×4 elements and all the blocks corresponding to a given θ_i are obtained from the boundary condition equations for the point θ_i . Specifying more points on the boundary or including more terms in the truncated expansion for the scattered fields would tend to give us increasingly better approximations to the exact solution but at the expense of increasing the size of the boundary-condition matrix.

5.5 Solving the Boundary Condition Equations

The procedure outlined in the previous section allows us to reduce the problem of electromagnetic waves scattering from an azimuthally symmetrical object, to solving an overdetermined set of boundary-condition equations, $\mathbf{Ax} = \mathbf{b}$. By the nature of the basis functions \mathbf{M} and \mathbf{N} (or the equivalent \mathbf{m} and \mathbf{n} functions), the radiation conditions, i.e., the boundary conditions at infinity, are automatically satisfied. This is of non-trivial significance since we can essentially eliminate the source of error from having to consider ‘approximate’ boundary conditions at the enclosing box boundary, which is often approximated to be at infinity.

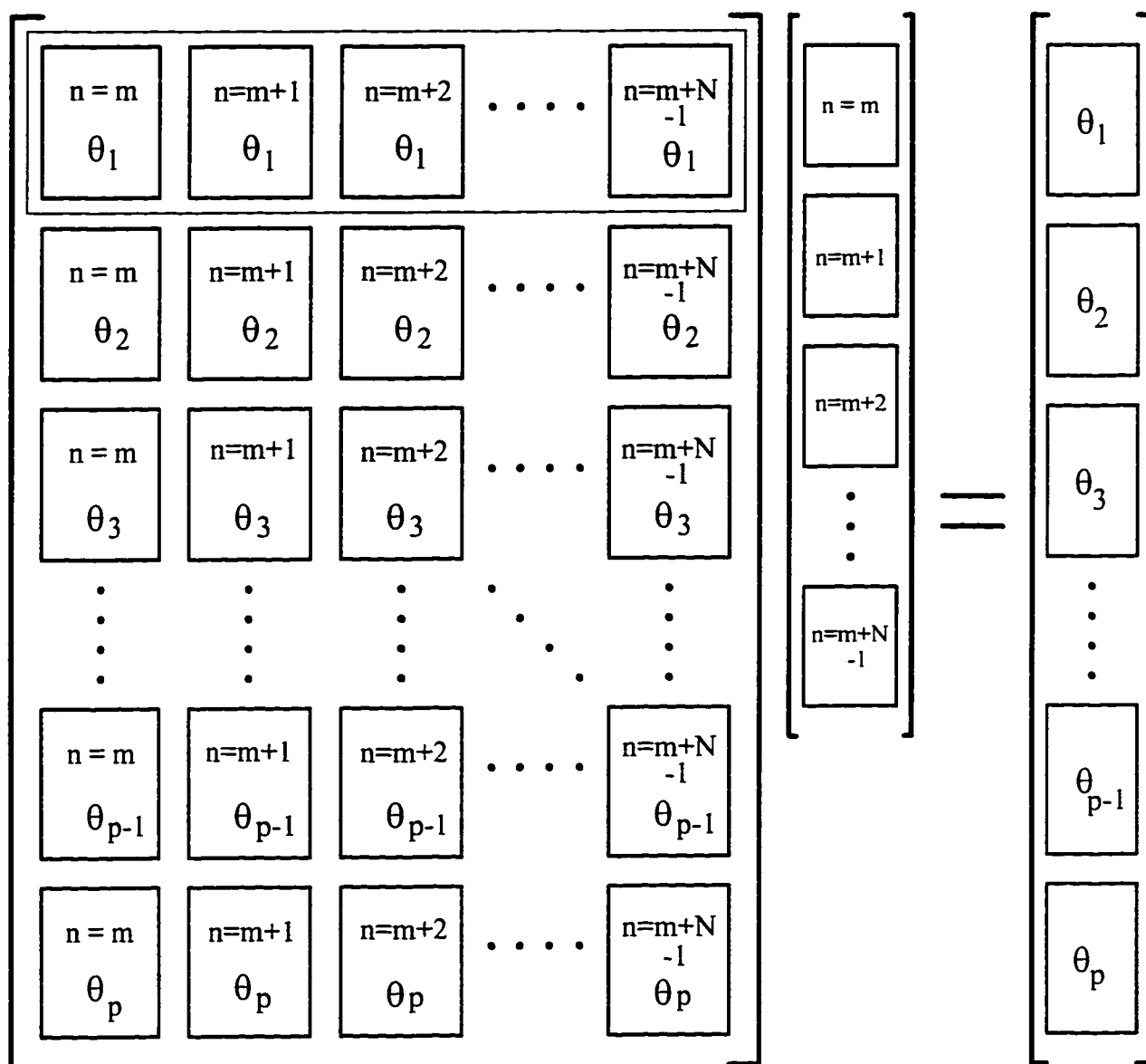


Figure 5.3: Structure of the matrix derived from the boundary condition equations for a specified m . We obtain $6p$ equations from specifying p points on the boundary to solve for the $4N$ unknown expansion coefficients. All the blocks corresponding to say θ_1 , represent the six boundary condition equations for point θ_1 . The unknown expansion coefficients of the scattered fields are obtained from the over determined system of equations by a linear least-square method (we require $6p \geq 6N$).

The system is deliberately allowed to be an over determined system (number of rows, $M >$ number of columns, N) since we are considering scattering objects with arbitrary shapes. We can solve the system in a least-square sense. It can be shown [31] that this essentially involves obtaining the solution of the corresponding system of the *normal equations* $\mathbf{A}\mathbf{A}^T = \mathbf{A}^T\mathbf{b}$. However, the matrix $\mathbf{A}\mathbf{A}^T$ will typically have a larger condition number (indicating greater numerical instability) as compared to matrix \mathbf{A} . Instead, the preferred method of solving the linear least-square problem is to obtain the singular value decomposition of the boundary condition matrix, \mathbf{A} , and eliminate the troublesome singular values before attempting to solve the system.

In order to verify that this method of solution is valid, we compare the computations of the least-square solution with the exact solution in the special case of scattering from a sphere for which the exact solution can be obtained easily by the method described in the shell-problem. In Figure 5.4 we show the result of such a comparison. The calculations are done on a glass sphere ($\epsilon = 2.5$) of radius $R = 1\lambda$. The optical field is focussed by ‘lens-action’ and the maximum field strength is approximately 7 times the incident field strength. We have calculated the field in the following two cases:

- (a) The incident wave propagates along the z-axis ($\theta_i = 0$). Only $m = 1$ terms are allowed in this case.
- (b) The angle of incidence is 45 degrees with respect to the z-axis. The incident wave has been expanded in a series with all allowed m . The calculation shown is done with $m \leq 5$ only.

The fields are calculated using $N = 12$, where $m + N - 1$ is the maximum value of n for a given m . For the least-square solution we specified 30 points on the surface of the sphere. For both cases (a) and (b), the solutions computed using the method of linear least-square are almost identical to the exact solutions as testified by the field calculations, validating the accuracy of this method. Although the calculation in case (b) involves a different set of coefficients and a larger number of terms, physically we expect both the solutions to be identical, with redefinition of the z-axis to coincide with the direction of incidence. The computations show us that indeed this is almost the case, the fields in case (b) are just rotated (by 45 degrees) version of the fields shown in case (a). The minor difference in the field patterns in the rotated case as compared to the non-rotated case are probably due to round-off errors involved in

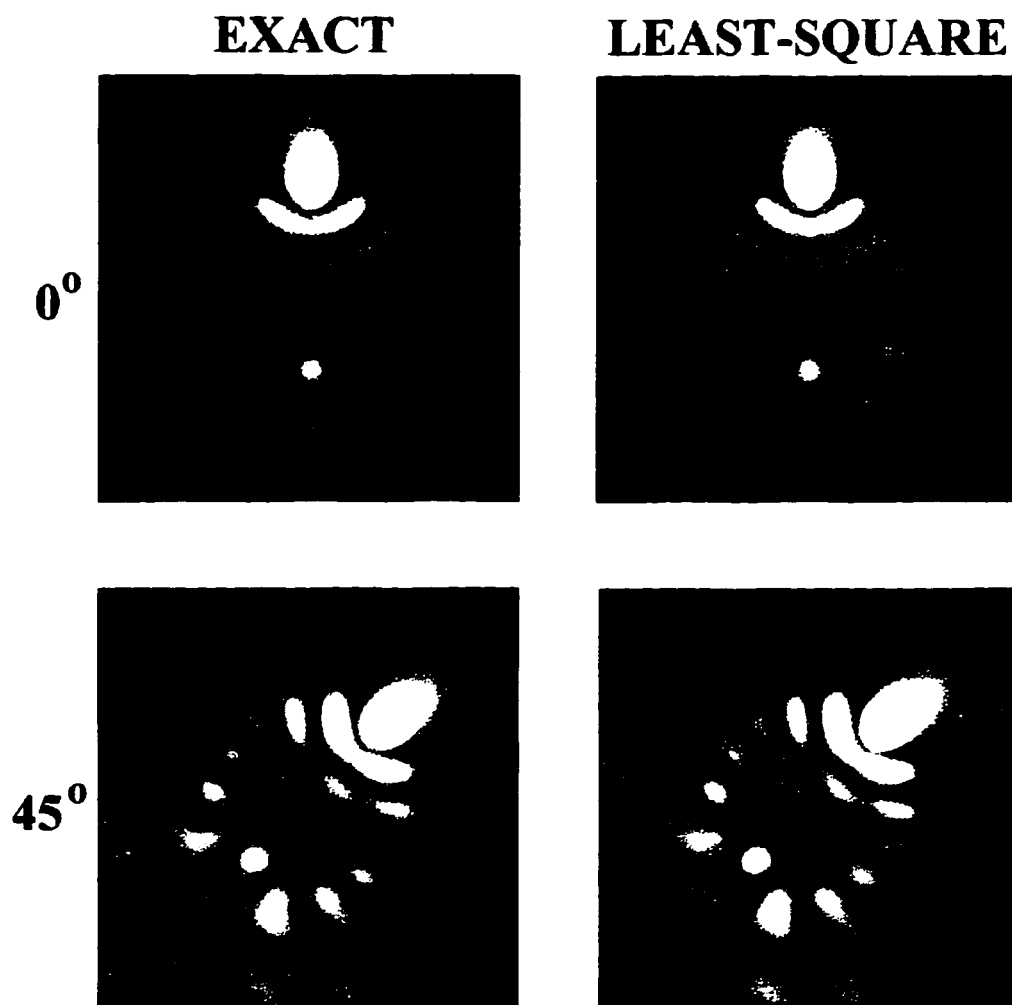


Figure 5.4: Comparing the method of linear least-square solution of the boundary-condition equations with the 'exact' solution for scattering from a glass sphere ($\epsilon = 2.5$) of radius $R = 1\lambda$. The optical field is focussed to ≥ 7 times the incident field by 'lens-action'. The incident field is polarized normal to the plane of the figure. (a) $\theta_i = 0^\circ$ (top row) , (b) $\theta_i = 45^\circ$ (bottom row). Physically, the 45 degree incidence case should have been identical to the 0 degree incidence except for an overall rotation by 45 degrees. The differences are due to round-off errors in evaluation of the basis functions.

the calculations. Since the field patterns for the ‘exact’ computation and the least-square computations are almost identical for both the incidence angles, the errors are probably not contributed from the least-square fitting procedure, but rather by inaccuracies (due to round-off errors) introduced by the function evaluation of the spherical Bessel/Hankel functions (of complex arguments) or the Associated Legendre functions.

In Figure 5.5 we show a sequence of calculations by adding the contribution from the next higher order term in m . The $m = 0$ figure is the field calculation with only the $m = 0$ term included. The $m = 1$ label indicates that both $m = 0$ and $m = 1$ terms are included. The field pattern becomes increasingly accurate with higher orders of m included in the calculations.

In Figure 5.6 we show the contribution from each order of m separately. It is evident that the major contribution of the field magnitude will result from $m \leq 4$ within the region shown in these figures.

Having demonstrated the validity of the numerical techniques involved in these calculations, we now show in Figure 5.7 a sequence of calculated fields for scatterers that are made increasingly more oblong. The incident light in this case is made to approach along the z-axis. The object is elongated from a sphere by 60% (L ranges from 0 to 0.3λ and $R = 0.5\lambda$). The continuity of the fields across the boundaries as L is increased affords visual testimony to the accuracy of the computed fields.

In Figure 5.8 we show the calculation done on a capsule shaped scatterer with the incident wave approaching from an arbitrary direction. As discussed before, the scattering object has azimuthal symmetry about the z-axis. However the arbitrary incidence direction of the incident plane wave breaks the symmetry. Calculations are shown for a sequence of incidence angles ranging from 0° to 180° . Physically we expect the field patterns to vary continuously as θ_i , the incidence angle, changes. For example, when θ_i is equal to 90° , the field pattern ought to be symmetrical about the center of the capsule, even though the origin for defining the basis functions is located non-symmetrically with respect to the center of the scattering object. The same situation applies when $\theta = 180^\circ$.

5.6 The Sphere-Plane Model

Considerable interest exists in the problem of solving for near-field scattering of electromagnetic waves incident on a geometric structure often called the sphere-plane

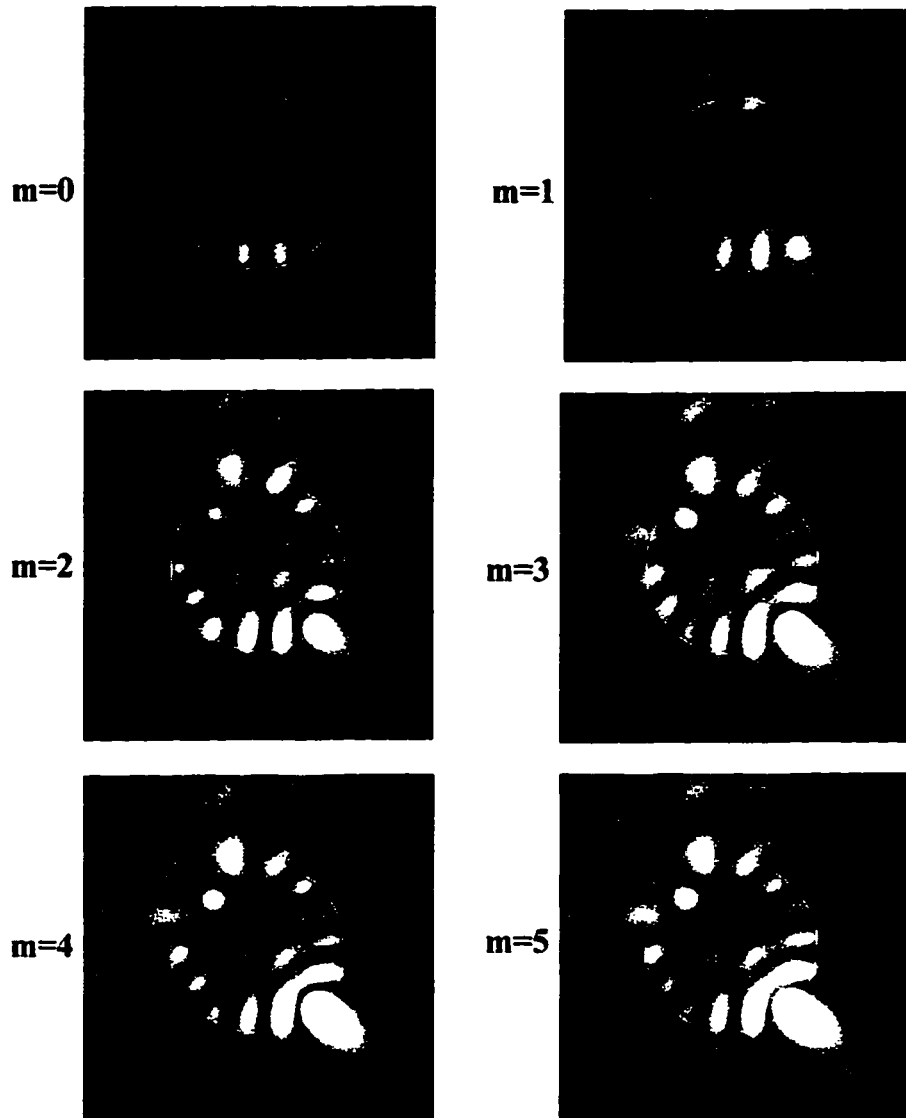


Figure 5.5: Field calculations by including higher orders of m , from $m = 0$ up to $m = 5$. Glass sphere ($\epsilon = 2.5$) of radius $R = 1\lambda$ and $\theta_i = 45^\circ$. Although $m = 1$ appears to be the ‘dominant’ term in this sequence, serving to establish the overall field distribution, the higher orders are necessary to obtain more accurate calculation of the field intensities.

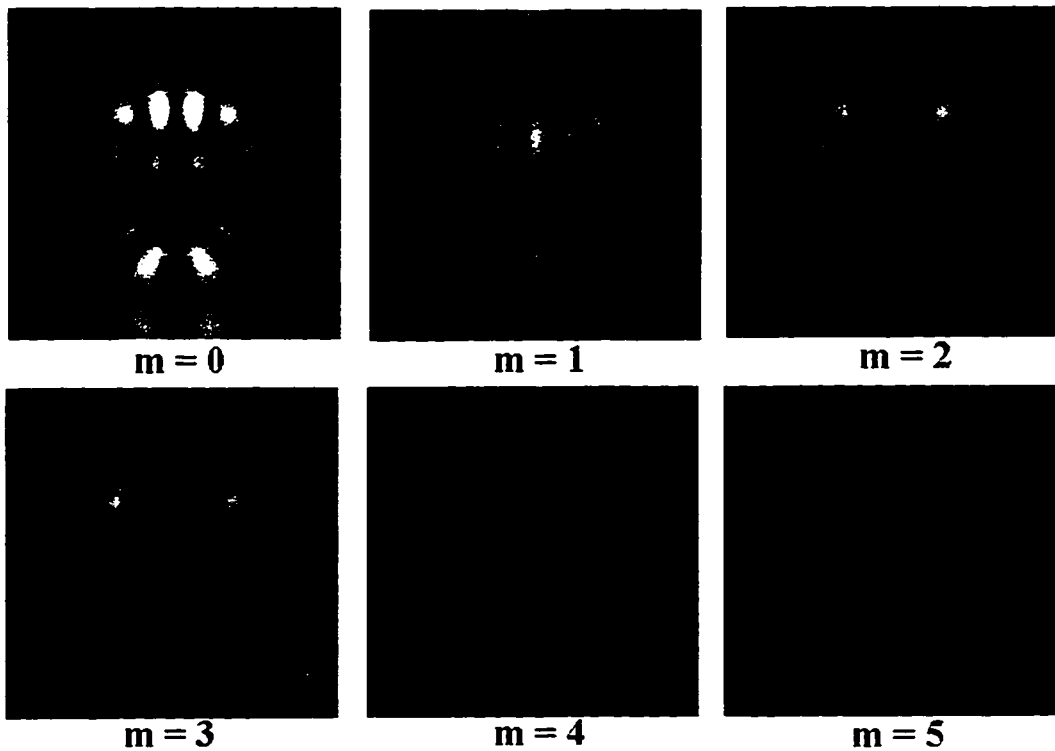


Figure 5.6: Field calculations for different orders of m , from $m = 0$ up to $m = 5$. Glass sphere ($\epsilon = 2.5$) of radius $R = 1\lambda$ and $\theta_i = 45^\circ$. The $m = 1$ contribution appears to be the most 'dominant' term in this sequence. The contributions from $m = 4$ and $m = 5$ terms are going to be small.

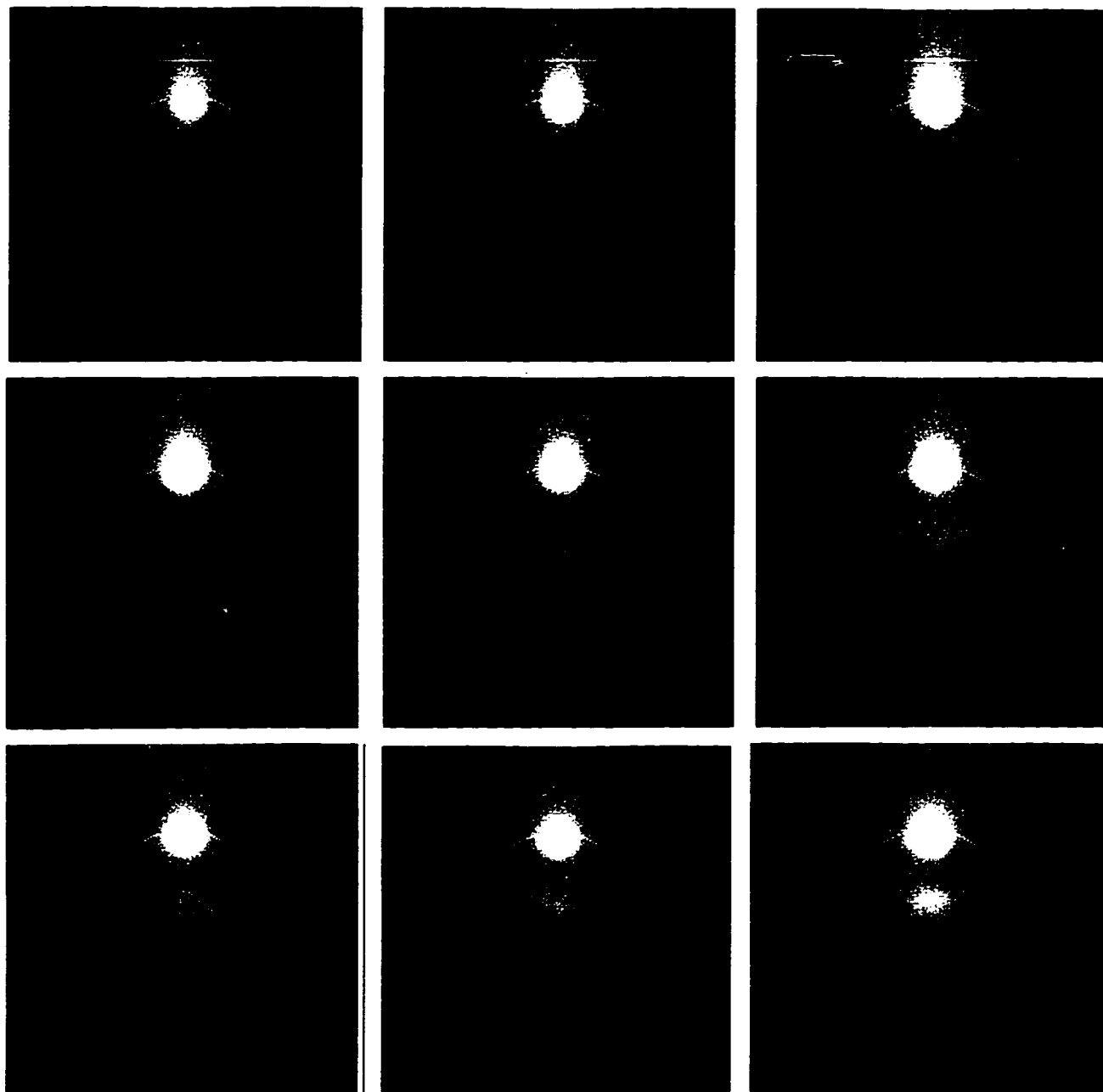


Figure 5.7: Electromagnetic scattering from a 'capsule' scatterer. $R = 0.5\lambda$ and L is increased from zero (sphere) to 0.3λ . The dielectric constant of the scatterer is taken as 2.5 in these calculations. Light is incident from the bottom of the figure with the polarization directed out of the paper.

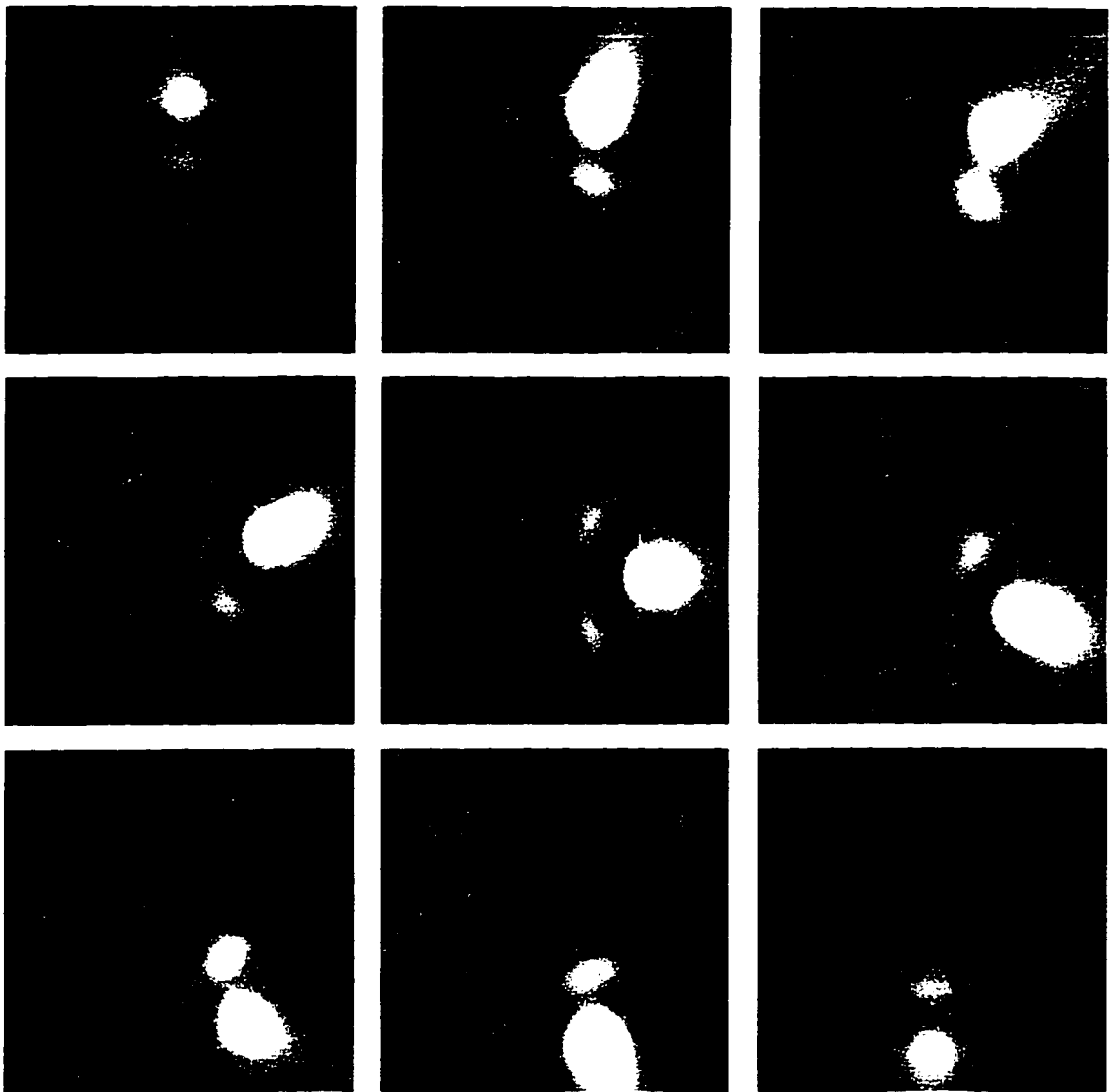


Figure 5.8: Electromagnetic scattering from a 'capsule' scatterer. The incident light approaches from different directions. From top-left to bottom-right the images are shown with θ_i changing by 22.5° between the images. Although the 0° and the 180° situations are computationally different (due to lack of symmetry about the origin), the fields evaluate identically, which is expected physically. The 'focused' spot achieves higher intensity for 22.5° incidence angle.

model. This geometry has been used to do theoretical study of field-enhancements that could be responsible for the phenomena such as SERS (Surface Enhance Raman Spectroscopy) [3] [33] [39]. A sphere of radius R , made of a material whose dielectric function is ϵ_1 , is separated by distance d from a plane (Figure 5.9). The half-space containing the sphere is composed of a material with dielectric function ϵ_2 . The half-space not containing the sphere is composed of a dielectric with dielectric function ϵ_3 . The incident wave propagates in region 2 and is reflected and scattered at the planar interface as well as the sphere boundary. Region 2 is assumed to have a non-lossy dielectric function, so that the plane wave expansions are strictly valid.

The sphere plane problem has been attempted for solution by many researchers for nearly two decades now. The usual approach has been to obtain a solution in the quasistatic approximation, i.e., to solve Laplace's equation [3] [33] [34]. However, as discussed before, the introduction of complex dielectric functions in the quasi-static approximation is artificial. Under static field configurations there cannot be any losses or phase delays which result from a complex dielectric function. In fact such equations do not satisfy Maxwell's equations since the principle of conservation of energy is violated. Furthermore, such an approximation is valid only when $R \ll \lambda$.

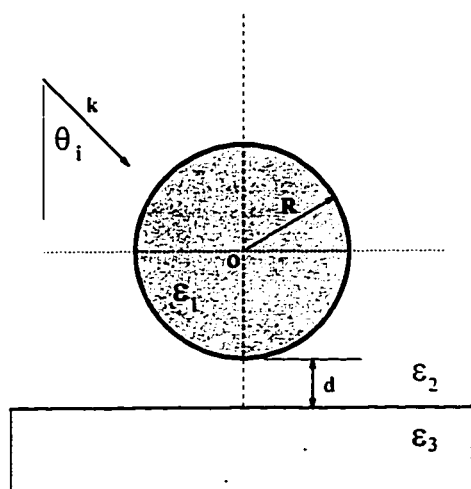


Figure 5.9: The Sphere-Plane model. The dielectric function of the sphere is ϵ_1 and that of the plane is ϵ_3 . The medium surrounding the sphere has non-dissipative dielectric function ϵ_2 . k is the propagation vector of the incident radiation. Such a model is often used to do theoretical studies of plasmon resonances on roughened surfaces.

even for real dielectric functions. An ‘exact’ approach for solving the sphere-plane model that takes exact account of retardation effects is based on solving the vector Helmholtz equation with the aid of a tensor Green’s function [39]. The incident electromagnetic wave scatters off the spherical surface as well as the planar surface. These scattered waves in turn scatter back and forth between the two surfaces. The final field is obtained by summing over the total contribution from each pass. This method is also computationally intensive.

In our approach to solving the sphere-plane model we use our basis functions to represent the field in the three regions. Analogous to the case of the elongated-scatterer problem, the electromagnetic scattering problem is reduced to solving a system of linear equations obtained from the boundary conditions on *both* the surfaces. The boundary condition equations are easily decoupled on the sphere surface (since we are working in the spherical polar coordinate system) and the only task that remains is that of satisfying the boundary conditions on the plane boundary. However, unlike the problem of the elongated scatterer whose boundary can be enclosed in a finite volume, there is a problem in the sphere-plane problem related to the fact that the plane extends to infinity. The plane wave approximation implies that the fields are non-vanishing at infinity. So, in order to satisfy the boundary conditions on the plane, far away from the origin, we require an infinite number of terms in the expansion of the fields.

We overcome the problem by using our knowledge of Fresnel’s formulae for reflection/refraction of a plane wave at a planar boundary. We write the electromagnetic field solutions for regions 2 and 3 as the sum of two parts each. In region 2 the total field is that due to the incident field, \mathbf{E}_i , the reflected field (off the substrate), \mathbf{E}_r (assuming the sphere is absent), and the scattered field in region 2 due to the presence of the sphere. Similarly, in region 3 the total field solution can be thought of as the sum of the transmitted field, \mathbf{E}_t (again assuming the sphere is absent) and the scattered field in region 3 (due to the sphere in region 2) required to satisfy the boundary conditions on the substrate.

Fresnel’s formulae are obtained by satisfying the boundary conditions on a plane boundary for an incident plane wave [22] [12]. The problem is reformulated as follows: If the sphere was absent then the solution for the field in the two regions separated by the plane is given by Fresnel’s formulae. The incident wave gives rise to a reflected wave as well as a transmitted wave. In region 2 the incident and the reflected fields would add together to determine the total field in region 2. In region 3 only the

transmitted wave contributes to the field. Since all three fields are plane wave fields, we can express them in a series of the basis functions. However, since we already know the solution, such a process is not necessary. In fact we do not gain anything by doing this. Now we imagine bringing the sphere from infinity along the z-axis. It is going to be subjected to two plane-wave fields: the incident wave field and the reflected wave field. We know how to solve the sphere-only problem for arbitrary incidence angles. Therefore the two fields in region 2 can be added together to provide a single 'excitation' field to which the sphere is subjected. The sphere will scatter and the boundary conditions on the sphere surface will determine the relation between the coefficients of the scattered fields in regions 1 and 2. The scattered fields in region 2 will give rise to scattered fields in region 3 as well. Since the incident, reflected and refracted fields of the plane wave excitation are already made to satisfy the boundary conditions on the plane (Fresnel's formulae), so now it is only the scattered fields in regions 2 and 3 that have to satisfy the boundary conditions on the plane. Since the scattered fields decay as $\sim 1/r$, we need to consider points on the plane-boundary only far enough for the scattered fields to decrease to a small fraction of the incident and reflected fields added together. The remaining procedure is going to be identical to that followed for the elongated-scatterer problem. We set up the boundary conditions matrix and solve for the (six) unknown coefficients in the three regions. The scattered solutions in regions 2 and 3 will again be represented by the spherical Hankel function solutions alone, since the transmitted field due to the incident plane wave will be represented by the spherical Bessel function solutions and they will determine the asymptotic behavior of the total solution.

5.6.1 Fresnel's Formulae

Consider a plane wave (polarization not specified at the moment) incident on a planar interface as shown in Figure 5.10. The incidence angle is θ_i and the incident wavevector is represented as \mathbf{k}_i . θ_r and θ_t correspond to the reflected and refracted angles and \mathbf{k}_r and \mathbf{k}_t represent the reflected and transmitted wavevectors. If the wavevector is complex in a passive medium then of course the wave will be attenuated. Thus the incident, reflected and refracted (plane wave) fields in the two media takes the following forms:

$$\mathbf{E}_i = E_0^i e^{i(\mathbf{k}_i \cdot \mathbf{r} - \omega t)} \quad \mathbf{H}_i = \frac{1}{i\omega\mu_2} \nabla \times \mathbf{E}_i \quad (5.43)$$

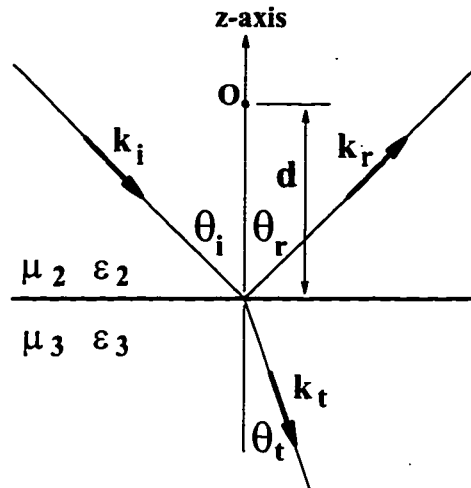


Figure 5.10: Plane wave incident at a planar interface. Reflection and refraction occurs. The plane is located at $z = d$. The phase must satisfy spatial invariance on the plane.

$$\mathbf{E}_r = E_0^r e^{i(\mathbf{k}_r \cdot \mathbf{r} - \omega t + \delta_r)} \quad \mathbf{H}_r = \frac{1}{i\omega\mu_2} \nabla \times \mathbf{E}_r \quad (5.44)$$

$$\mathbf{E}_t = E_0^t e^{i(\mathbf{k}_t \cdot \mathbf{r} - \omega t + \delta_t)} \quad \mathbf{H}_t = \frac{1}{i\omega\mu_3} \nabla \times \mathbf{E}_t \quad (5.45)$$

The fields have to satisfy definite boundary conditions at the interface. Spatial invariance on the plane (by symmetry, the same relation must hold for every point on the plane) requires that at all times the phase factors $\mathbf{k}_i \cdot \mathbf{r}$, $\mathbf{k}_r \cdot \mathbf{r} + \delta_r$ and $\mathbf{k}_t \cdot \mathbf{r} + \delta_t$ are equal. Otherwise the field relations would depend on the position on the plane, which is physically disallowed. Since all points are equally valid on the plane, we consider the point of intersection of the z -axis with the planar boundary. We can immediately write (for this chosen point):

$$\mathbf{k}_i \cdot \mathbf{r} = \mathbf{k}_i \cdot (-d \mathbf{e}_z) = k_i d \cos \theta_i \quad (5.46)$$

$$\mathbf{k}_r \cdot \mathbf{r} = \mathbf{k}_r \cdot (-d \mathbf{e}_z) = -k_r d \cos \theta_r \quad (5.47)$$

$$\mathbf{k}_t \cdot \mathbf{r} = \mathbf{k}_t \cdot (-d \mathbf{e}_z) = k_t d \cos \theta_t. \quad (5.48)$$

Using the equality of the phases, we immediately arrive at the expression for δ_r :

$$\delta_r = 2 k_i d \cos \theta_i \quad (5.49)$$

Using Snell's Law:

$$\sin \theta_t = \frac{k_i}{k_t} \sin \theta_i. \quad \text{Or} \quad (5.50)$$

$$\cos \theta_t = \sqrt{1 - \sin^2 \theta_t}. \quad (5.51)$$

If k_i/k_t is a complex number then we obtain a complex number for $\cos \theta_t$ from the equation above. This in turn will yield a complex number for the phase in region 3. So, we can write the expression for δ_t as:

$$\delta_t = k_i d \cos \theta_i - k_t d \cos \theta_t. \quad (5.52)$$

Having determined the phases, we can compute the field in the two regions (2 and 3) that satisfy the boundary conditions. The relation between the amplitudes E_0^i , E_0^r and E_0^t is given by the Fresnel's relations [22]. For s-polarization (\mathbf{E} directed out of the paper in Figure 5.10) with $n = \sqrt{\epsilon\mu}$:

$$\frac{E_0^t}{E_0^i} = \frac{2n_2 \cos \theta_i}{n_2 \cos \theta_i + \frac{\mu_2}{\mu_3} \sqrt{n_3^2 - n_2^2 \sin^2 \theta_i}} \quad (5.53)$$

$$\frac{E_0^r}{E_0^i} = \frac{n_2 \cos \theta_i - \frac{\mu_2}{\mu_3} \sqrt{n_3^2 - n_2^2 \sin^2 \theta_i}}{n_2 \cos \theta_i + \frac{\mu_2}{\mu_3} \sqrt{n_3^2 - n_2^2 \sin^2 \theta_i}}. \quad (5.54)$$

The corresponding expressions for p-polarization (\mathbf{H} directed out of the plane of the figure) are :

$$\frac{E_0^t}{E_0^i} = \frac{2n_2 n_3 \cos \theta_i}{\frac{\mu_2}{\mu_3} n_3^2 \cos \theta_i + n_2 \sqrt{n_3^2 - n_2^2 \sin^2 \theta_i}} \quad (5.55)$$

$$\frac{E_0^r}{E_0^i} = \frac{\frac{\mu_2}{\mu_3} n_3^2 \cos \theta_i - n_2 \sqrt{n_3^2 - n_2^2 \sin^2 \theta_i}}{\frac{\mu_2}{\mu_3} n_3^2 \cos \theta_i + n_2 \sqrt{n_3^2 - n_2^2 \sin^2 \theta_i}}. \quad (5.56)$$

With the knowledge of the plane wave fields satisfying the boundary conditions on the substrate, we can readily handle the case of satisfying the boundary conditions for the scattered fields due to the sphere.

5.6.2 The Boundary Condition Matrix

In Figure 5.11 we show the schematic of the matrix derived from the boundary condition equations. As a variation in the numerical techniques for solving this problem.

we shall try to obtain the solution by solving a square matrix derived from the boundary condition equations. This is suitable when the lengths involved (R and d) are much smaller than the wavelength of the incident radiation. When these lengths become comparable to the wavelength, higher precision floating point calculations are necessary for preventing excessive round-off errors. We try to obtain the solution in a truncated expansion with the maximum value of $n = m + N - 1$. Thus the matrix we are required to solve will have dimension $6N \times 6N$. Since we require that $6N = 4N + 6N_{sub}$ (a square matrix), where N_{sub} is the number of specified points on the substrate, N must be divisible by 3.

The first $4N$ equations correspond to the boundary conditions on the sphere surface. As in the case of a simple isolated spherical scatterer, these equations decouple with respect to different n 's and so the first $4N$ rows consists of 'diagonal' blocks of 4×6 . The remaining elements in this upper section of the matrix are zero. In other words, we are combining all the individual 4×4 equations for a sphere and then attempting to solve them all at once. Within these blocks only the entries corresponding to the coefficients in regions 1 and 2 will be non-zero. We require $6N_{sub}$ equations for the substrate corresponding to the N_{sub} specified points. For the substrate equations, the elements corresponding to the coefficients of region 1 will be zero. Convergence of the solution can be checked by either increasing the number of points on the substrate or changing the location of the points themselves. Either way, the solution may not be perturbed by more than the error limits defined for the problem at hand.

5.6.3 Field on the z-axis

On the z -axis, i.e. when $\theta = 0$ or π , evaluation of the total electric field is made simpler because many of the terms in the expression for the total electric field vanishes. When \mathbf{k} lies entirely in the xz -plane, for s -polarization (\mathbf{E} directed along the y -axis), \mathbf{E} can be written as a linear combination of \mathbf{m}_{emn} and \mathbf{n}_{omn} functions. Now,

$$\mathbf{m}_{emn} = -m z_n(kr) \frac{P_n^m(\cos \theta)}{\sin \theta} \sin m\phi \mathbf{e}_\theta - z_n(kr) \frac{dP_n^m(\cos \theta)}{d\theta} \cos m\phi \mathbf{e}_\phi. \quad (5.57)$$

Clearly, the first term is going to be zero on the z -axis, for any $m \neq \pm 1$. For $m \geq 0$ the $P_n^m(x = \pm 1) = 0$, and for $m = 0$, the factor m ensures that the first term is always zero on the z -axis. As we have seen before, on the z -axis, the second term containing the derivative of the Associated Legendre function will be zero for $m \neq 1$.

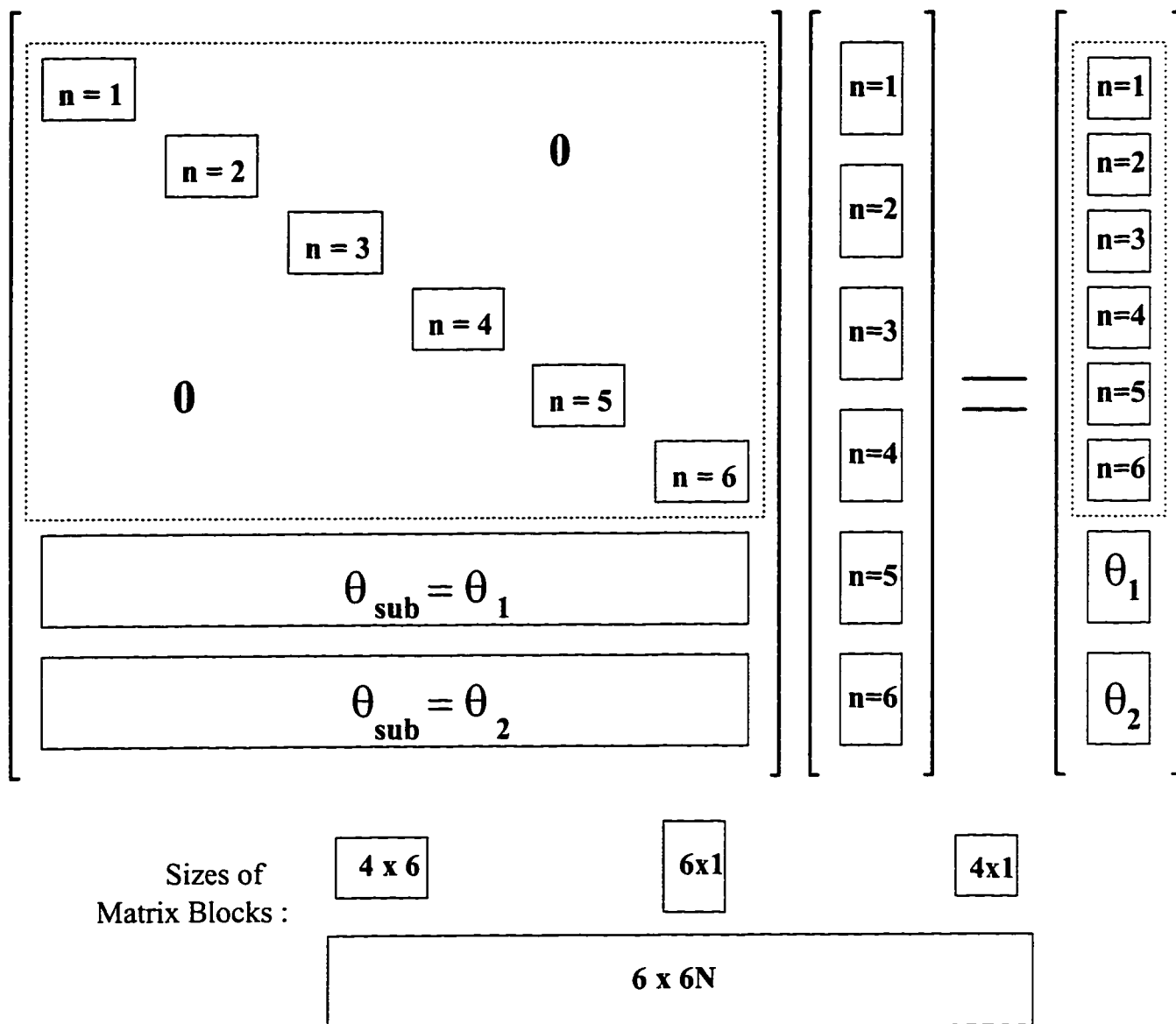


Figure 5.11: Structure of the matrix derived for the sphere-plane model from the boundary condition equations for a specified m . We obtain $6N$ equations in $6N$ unknowns by specifying $N/3$ points on the substrate. The equations for the sphere boundary (indicated by the dotted box) are exact. The matrix above is shown for $n = 6$ and so the number of points specified on the substrate, $N_{sub} = 2$.

Similarly, by examining

$$\begin{aligned} \mathbf{n}_{omn} = & n(n+1) \frac{z_n(kr)}{kr} P_n^m(\cos \theta) \sin m\phi \mathbf{e}_r + \frac{1}{kr} \frac{d}{dr} (rz_n(kr)) \frac{dP_n^m(\cos \theta)}{d\theta} \sin m\phi \mathbf{e}_\theta \\ & + m \frac{1}{kr} \frac{d}{dr} (rz_n(kr)) \frac{P_n^m(\cos \theta)}{\sin \theta} \cos m\phi \mathbf{e}_\phi. \end{aligned} \quad (5.58)$$

we notice that the first term is going to be zero for any m because of the product $P_n^m(\pm 1) \sin m\phi$. The second and third terms are going to be non-zero on the z-axis only for $m = 1$. Thus, for the s-polarization case the total electric field on the axis will not have any radial component. This is physically reasonable since the incident electric field does not have any radial component on the z-axis either. The total electric field on the axis can therefore be obtained by solving the $m = 1$ matrix only.

In the case of p-polarization, the scattered electric fields are expressed in terms of the \mathbf{m}_{omn} and \mathbf{n}_{emn} functions. Now,

$$\mathbf{m}_{omn} = mz_n(kr) \frac{P_n^m(\cos \theta)}{\sin \theta} \cos m\phi \mathbf{e}_\theta - z_n(kr) \frac{dP_n^m(\cos \theta)}{d\theta} \sin m\phi \mathbf{e}_\phi. \quad (5.59)$$

and,

$$\begin{aligned} \mathbf{n}_{emn} = & n(n+1) \frac{z_n(kr)}{kr} P_n^m(\cos \theta) \cos m\phi \mathbf{e}_r + \frac{1}{kr} \frac{d}{dr} (rz_n(kr)) \frac{dP_n^m(\cos \theta)}{d\theta} \cos m\phi \mathbf{e}_\theta \\ & - m \frac{1}{kr} \frac{d}{dr} (rz_n(kr)) \frac{P_n^m(\cos \theta)}{\sin \theta} \sin m\phi \mathbf{e}_\phi. \end{aligned} \quad (5.60)$$

As for the \mathbf{m}_{omn} functions, only the $m = 1$ terms are non-zero on the z-axis. For the \mathbf{n}_{emn} functions, the first term is going to be non-zero for $\theta = 0, \pi$ for $m = 0$ only. The \mathbf{e}_θ and \mathbf{e}_ϕ components are going to be non-zero only for the $m = 1$ case. Thus, in the case of p-polarization, the total radial electric field will be contributed by only the $m = 0$ solution, and the total electric field in the direction orthogonal to \mathbf{e}_r will be contributed by the $m = 1$ solution only.

This turns out to be a great simplification in the computation of plasmon resonances in a sphere-plane geometry. Since the electric field at various points in the same medium are linearly related to each other, evaluation of the field on the axis to determine plasmon resonances in a given geometrical configuration is a sound choice from the point of view of numerical efficiency.

5.6.4 Plasmon Resonances in The Sphere-Plane Model

We calculate the plasmon resonances in the sphere-plane model for three systems: (a) Silver sphere on silver substrate, (b) Gold sphere on gold substrate and (c) Copper

sphere on copper substrate. We use the experimentally determined bulk dielectric functions for gold, silver and copper [24]. The incident light is s-polarized and the incidence angle is 45° . Calculations are done with a sphere of radius $R = 30\text{nm}$, the sphere-plane separation $d = 5\text{nm}$ and the ‘observation’ location is at the intersection point of the substrate and the z-axis. We have used $n = 12$, and tests with higher number of basis functions do not alter the results, confirming that the solution had converged. We choose points on the surface at fixed angular intervals. The boundary conditions are made to satisfy exactly at these points. If convergence is reached then the final solution should not depend on the particular choice of these chosen boundary points.

We compare the results of our computations with the experimental data of Berndt et.al. [10]. The experimental data shows the spectrum of light emission from a tip-substrate geometry in the ‘field-emission’ regime (the tip-substrate voltage difference is approximately $\geq 100\text{Volts}$). Presumably, the field-emitted electrons would excite the plasmon resonances in the tip-substrate geometry. The theoretically obtained data on the plasmon resonances is weighted by the detector sensitivity graph of Berndt et.al. [10].

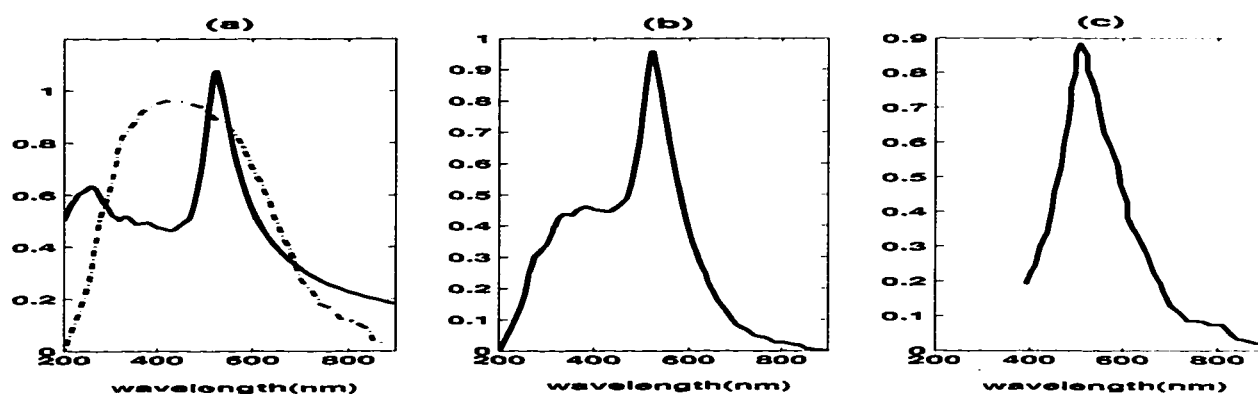


Figure 5.12: Plasmon resonance in sphere-plane model. A Gold sphere of radius 30nm located 5nm from a gold substrate. the sphere are gold. (a) Theoretical calculation of plasmon resonance based on experimentally obtained bulk dielectric function for gold; the broken line shows the assumed detector response in the photoemission experiment in (c). (b) Multiplying the calculated spectrum in (a) by the detector response. (c) Experimentally obtained spectrum of photon emission from a tip-substrate geometry in the ‘field-emission’ regime.

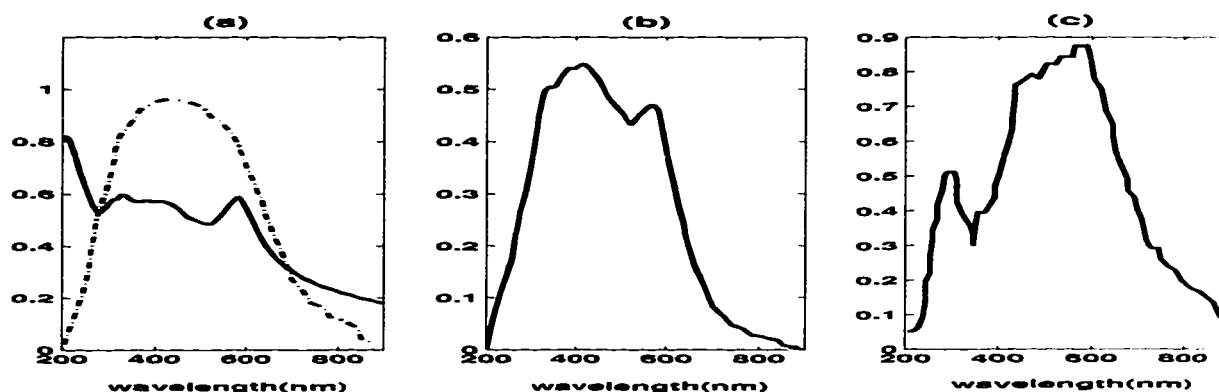


Figure 5.13: Plasmon resonance in sphere-plane model. A Copper sphere of radius 30nm located 5nm from a copper substrate. the sphere are copper. (a) Theoretical calculation of plasmon resonance based on experimentally obtained bulk dielectric function for copper; the broken line shows the assumed detector response in the photoemission experiment in (c). (b) Multiplying the calculated spectrum in (a) by the detector response. (c) Experimentally obtained spectrum of photon emission from a tip-substrate geometry in the ‘field-emission’ regime.

The peaks in the computed plasmon resonance spectra correspond very closely to the peaks in the photon emission spectra in the field-emission experiments. The differences observed could be due to several reasons, including contributions from other processes, inaccuracy in the assumed detector response function, artifacts of the detection system (such as observing higher order diffraction peaks) and round-off errors in the computation itself. However, the strong correlation suggests that the light emission process in the ‘field-emission’ regime is due to a plasmon-resonance effect.

The plasmon-resonance peak in the case of a silver sphere over a silver substrate exhibit large field enhancements. In the case of this calculation with s-polarized excitation, the enhancement is by a factor of ~ 10 . This implies that the effective intensity of the optical field is enhanced by a factor of ~ 100 . This is in agreement with the quasi-static calculations done by Arvind and Metiu [3]. Processes such as surface enhanced Raman scattering of molecules that depend on the square of the field intensity can therefore exhibit considerable enhancements ($\geq 10^4$) due to nanometric irregularities on substrate surfaces.

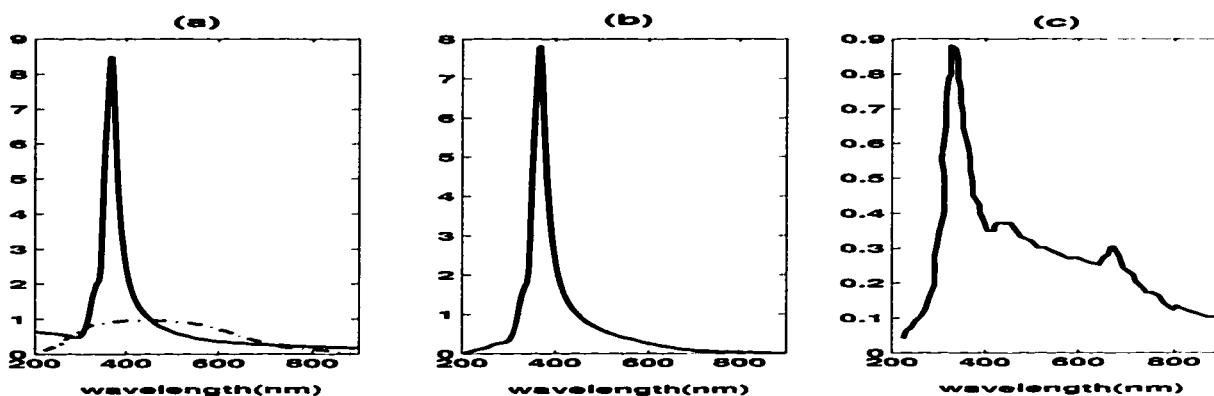


Figure 5.14: Plasmon resonance in sphere-plane model. A silver sphere of radius 30nm located 5nm from a silver substrate. The sphere is silver. (a) Theoretical calculation of plasmon resonance based on experimentally obtained bulk dielectric function for silver; the broken line shows the assumed detector response in the photoemission experiment in (c). (b) Multiplying the calculated spectrum in (a) by the detector response. (c) Experimentally obtained spectrum of photon emission from a tip-substrate geometry in the 'field-emission' regime. Notice the field enhancement at resonance (by a factor of ~ 10).

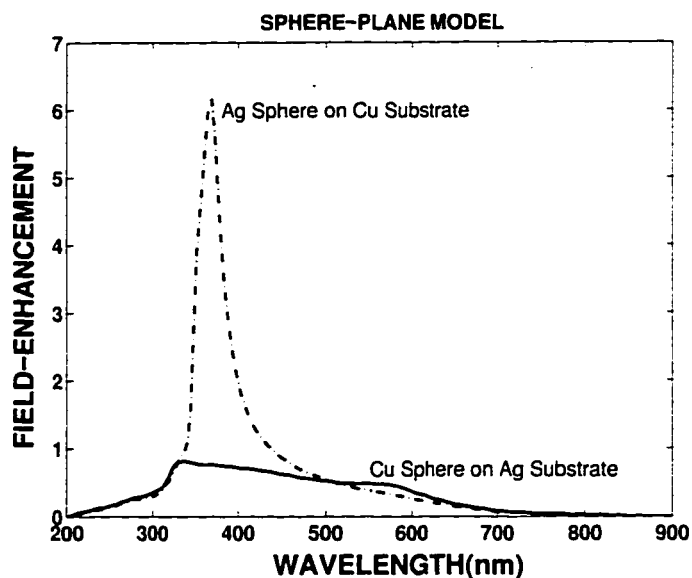


Figure 5.15: Comparison of field enhancements with a silver sphere on a copper substrate and a copper sphere on a silver substrate. In this case, it is clear that the enhancements are contributed more by the nature of the sphere as compared to the substrate.

The large field enhancements in the case of a silver sphere over a silver substrate leads to the following question: Which of the two, the sphere or the plane, is more important in this enhancement process. It has been customary to assume in the existing literature to attribute such field enhancements to the substrate. It has been argued that the role of the particle (the sphere or a tip) has been merely to break the symmetry (translational invariance) of the plane, so that the surface plasmons can couple to the radiation field by allowing conservation of momentum to take place. To answer such a question we compare the results of our calculation in a sphere-plane geometry in (a) a copper sphere on a silver substrate, and (b) a silver sphere on a copper substrate. The results are shown in Figure 5.15. The incident radiation is again s-polarized and the incidence angle is 45° . The sphere diameter is 30nm and the sphere-plane separation is 5nm and the field observation point is at the point of intersection of the z-axis and the substrate. It is clear from this calculation that in this case at least, it is the particle (the plasmon resonance of the particle) that is more important than the substrate. However it is a truly coupled phenomena. For example, the enhancement in the case of a silver sphere on a copper substrate, although large (~ 6), is still smaller than the the enhancements with a silver sphere on a silver substrate.

Chapter 6

Conclusion

In this thesis we have been developing the technique of vector basis function solution of Maxwell's equations. In all the different 'example' cases in which this approach has been applied, such as electromagnetic scattering from concentric shells or the calculation of plasmon resonance in a sphere-plane geometry, the incident electromagnetic field has been assumed to be *plane waves*. The increasing sophistication of experimental techniques has brought the domain of ultrashort (sub-picosecond) optical excitations into many different contemporary experiments. The plane wave approximation may not be valid in these situations for several reasons. The dielectric relaxation times (which indirectly determine the dielectric functions) are often much longer than the duration of the optical excitation itself. We are speaking of a truly transient response in the sub-picosecond time scales. Furthermore, the extent of the optical 'wave-train' may often be shorter than the dimension of the scattering objects themselves. Also, we have not considered the problem of solving the Maxwell equations in the presence of *sources*, namely charges and current densities. Although such general problems are certainly not of mere academic interest, the mathematical and computational tools available to solve these problems effectively are still far from being satisfactory at the present.

6.1 Transient Excitation

The basic problem of transient response can in principle be handled by the method of Fourier decomposition of the source terms. Typically an experimental situation consists of a stream of ultrashort pulses, whose Fourier decomposition is determinable. One could in principle solve the problem for each of these component excitations up to some limiting order and obtain the final sum. In principle this can be readily accomplished for a linear medium. In nonlinear media the summation process will not be straightforward.

It is the author's belief that a more elegant approach of solving the transient problem is possible by further research to find a suitable 'Laplace-like' transform (Generalized Fourier Transform) to represent the pulsed excitation. Since the 'basis' functions form a complete set, therefore the basis set satisfies the property of 'convergence in the mean' (this is in fact a weaker property than completeness). This however validates the process of interchanging the order of an infinite summation and an integration to obtain the generalized Fourier/Laplace transforms [21]. So the transform of an infinite sum is equal to the infinite sum of the transforms of each term. The method should be similar to that of solving for transients in electrical networks consisting of linear, lumped and time-invariant elements.

The importance of the transient problem lies in its potential to elucidate experimentally, the dynamical properties of nanometric systems (such as the scaling of dielectric functions with particle sizes in the nanometer regime, for example) by comparison with theoretical calculations. With our increasing dependence on the scanning probe techniques to understand basic physical phenomena on surfaces, the importance of the transient problem is clearly established.

6.2 Related Problems

In this thesis we have developed the method of basis function solution in the spherical polar coordinate system. We have demonstrated the feasibility of using this basis set for solving boundary value problems in which the boundaries may not conform to the coordinate surfaces of the spherical polar coordinate system (the problem of scattering from the 'capsule'-shaped scatterer or the sphere-plane model for example).

In principle, we could solve the problem of plasmon resonances in what is called the tip-substrate geometry using the same techniques. Such a geometrical configuration is of importance in the modeling and understanding of electromagnetic interactions at the tunneling junction of a scanning tunneling microscope. Such an understanding is important in many of the other scanning probe microscopies as well, such as AFM or SNOM etc., when light is coupled into the tip-substrate junction.

If we could allow the sphere in the sphere-plane model to assume the shape of an elongated scatterer that is sufficiently long, in principle we could model the tip-substrate problem. However, such an approach might require more sophisticated numerical techniques to solve the boundary condition equations than those employed in this thesis. The elements in the boundary condition matrix contains products of

spherical Bessel or spherical Hankel functions of the first kind and the Associated Legendre functions. The columns in these matrices contain these functions with the index n increasing from left to right. Now these functions scale as a function of n and z as follows:

$$j_n(z) \sim \frac{z^n}{1 \cdot 3 \cdot 5 \cdots (2n + 1)} \quad (6.1)$$

$$n_n(x) \sim \frac{1 \cdot 3 \cdot 5 \cdots (2n - 1)}{z^{n+1}} \quad (6.2)$$

$$h_n(z) = j_n(z) + i n_n(z). \quad (6.3)$$

This kind of dependence makes the matrix highly ill-conditioned. The problem is similar (if not worse) to that which is encountered when trying to invert matrices of the type known as Vandermonde matrices [31]. These arise in connection with problems of polynomial fitting. When we need to include more terms (to achieve a better approximation), the matrix could become unduly lopsided from left to right. This will invariably lead to numerical instabilities in the solution when the ratio of the largest to the smallest elements exceeds the available machine precision. For scattering geometries that deviate significantly from the spherical coordinate surfaces, one would need to include more terms. This will lead to a more ill-conditioned matrix.

One way to overcome such a problem may be to use higher precision floating point computations. Software libraries exist in Netlib and elsewhere to allow one to perform quadruple precision floating point calculations or even arbitrary precision calculations. Trade-off will have to be made with respect to the desired accuracy of the solution and the increased computation loads resulting from the higher precision data types. Probably it is only necessary to perform the process of solving the matrix in higher precision, since it is the most critical step in determining the overall round-off errors.

Another alternative could be to use a coordinate system whose coordinate surfaces are closer to the boundaries of the problem in question. The 'recipe' for obtaining the basis set without any reference to a particular coordinate system has been outlined in Chapter 2. That such a set will be complete has also been proved without reference to a particular coordinate system. For example, in the tip-substrate geometry one could use the prolate spheroidal coordinate system. The main handicap at present is the lack of adequate analytical treatments of the eigenfunctions of the scalar Helmholtz equation in the prolate spheroidal coordinate system. This has been the primary

justification in this thesis to develop the subject in the spherical polar coordinate system. The eigenfunctions in the spherical polar coordinate system are composed of functions like the spherical Bessel and Hankel functions and the Associated Legendre functions. The supporting literature for these functions is very satisfactory. However, there are a few isolated works that have a fairly comprehensive account on the subject of spheroidal functions and these will provide the necessary groundwork on which to build the subject of basis function expansion in the prolate or oblate spheroidal coordinate systems [16] [6].

Other related problems that are of interest are the solution of electromagnetic scattering from roughened surfaces (the substrate has a hemispherical bump), the problem of electromagnetic interaction among clusters in nanometer proximity to each other (many coherent scatterers). There is also the class of problems related to magnetic shielding. The present apparatus of vector basis functions can allow exact solutions to a shielding problems, be it electric or magnetic shielding [27].

6.3 Antenna Problem

We now address the important problem of solving the Maxwell equations in the presence of sources. In the process of developing the general formalism for scattering-like problems (homogenous problem), we created a complete basis consisting of the \mathbf{L} , \mathbf{M} and \mathbf{N} functions. However, with zero-divergence plane waves and in the absence of sources, the \mathbf{L} functions did not seem to play any role other than its contribution to make the total set attain the property of mathematical completeness. All our scattering solutions were based on the \mathbf{M} and \mathbf{N} functions only. As it turns out it is the \mathbf{L} functions that provide the missing link to solving the inhomogenous Maxwell's equations.

Maxwell equations in a linear, homogenous, isotropic and time-invariant medium (that is ϵ and μ are not functions of \mathbf{r} or t), are of the form:

$$\nabla \cdot \mathbf{E}(\mathbf{r}, t) = \frac{\rho(\mathbf{r}, t)}{\epsilon} \quad (6.4)$$

$$\nabla \cdot \mathbf{H}(\mathbf{r}, t) = 0 \quad (6.5)$$

$$\nabla \times \mathbf{E}(\mathbf{r}, t) = -\mu \frac{\partial \mathbf{H}(\mathbf{r}, t)}{\partial t} \quad (6.6)$$

$$\nabla \times \mathbf{H}(\mathbf{r}, t) = \mathbf{J}(\mathbf{r}, t) + \epsilon \frac{\partial \mathbf{E}(\mathbf{r}, t)}{\partial t}. \quad (6.7)$$

Taking divergence of both sides of Equation 6.7, since divergence of curl is zero, we obtain the continuity equation for electric charges:

$$\nabla \cdot \mathbf{J} + \epsilon \frac{\partial}{\partial t}(\nabla \cdot \mathbf{E}) = \nabla \cdot (\nabla \times \mathbf{H}) = 0 \quad (6.8)$$

$$\text{Or,} \quad \nabla \cdot \mathbf{J} + \frac{\partial \rho}{\partial t} = 0 \quad (6.9)$$

Taking curl of both sides of Equation 6.6 and Equation 6.7, we obtain:

$$\nabla \times \nabla \times \mathbf{E} = -\mu \frac{\partial \mathbf{J}}{\partial t} - \mu \epsilon \frac{\partial^2 \mathbf{E}}{\partial t^2} \quad (6.10)$$

$$\nabla \times \nabla \times \mathbf{H} = \nabla \times \mathbf{J} - \mu \epsilon \frac{\partial^2 \mathbf{H}}{\partial t^2}. \quad (6.11)$$

Or, assuming sinusoidal time dependence $e^{-i\omega t}$, so that $\frac{\partial}{\partial t} \equiv -i\omega$, and $\frac{\partial^2}{\partial t^2} \equiv -\omega^2$, we obtain:

$$(i\omega\mu\mathbf{J}) - \nabla \times \nabla \times \mathbf{E} + k^2\mathbf{E} = 0 \quad (6.12)$$

$$(\nabla \times \mathbf{J}) - \nabla \times \nabla \times \mathbf{H} + k^2\mathbf{H} = 0 \quad (6.13)$$

where $k^2 = \omega^2\mu\epsilon$. Now, Equation 6.12 would resemble the form of the diffraction equation (Eqn 2.18), if

$$\begin{aligned} \nabla(\nabla \cdot \mathbf{E}) &= \frac{\nabla\rho}{\epsilon} = i\omega\mu\mathbf{J} \\ \text{Or,} \quad \nabla\rho &= i\omega\mu\epsilon\mathbf{J} \\ \text{Or,} \quad \nabla^2\rho &= i\omega\mu\epsilon\nabla \cdot \mathbf{J} \\ \text{Or,} \quad \nabla^2\rho &= i\omega\mu\epsilon(i\omega\rho) \quad (\text{From Eqn 6.9}) \\ \text{Or,} \quad \nabla^2\rho + k^2\rho &= 0. \end{aligned} \quad (6.14)$$

Similarly, Equation 6.13 would resemble the form of the diffraction equation (Eqn 2.18), if

$$\nabla \times \mathbf{J} = \nabla(\nabla \cdot \mathbf{H}) = 0 \quad (\text{Since } \nabla \cdot \mathbf{H} = 0). \quad (6.15)$$

From $\nabla\rho = i\omega\mu\epsilon\mathbf{J}$, obtaining curl of both sides of the equation and noting that the curl of gradient is zero, we have $\nabla \times \mathbf{J} = 0$. So, if $\rho(\mathbf{r}, \omega)$ satisfies the scalar Helmholtz

equation, then both \mathbf{E} and \mathbf{H} will satisfy the diffraction equation. In other words, both \mathbf{E} and \mathbf{H} can be expressed in a series of the $\{\mathbf{L}_n, \mathbf{M}_n, \mathbf{N}_n\}$ functions and ρ can be expressed in a series of the scalar solutions $\{\psi_n\}$. Thus:

$$\rho(\mathbf{r}, \omega) = \sum_n d_n \psi_n \quad (6.16)$$

$$\mathbf{J}(\mathbf{r}, \omega) = \frac{1}{i\omega\mu\epsilon} \sum_n d_n \nabla\psi_n = \sum_n f_n \mathbf{L}_n \quad (6.17)$$

$$\mathbf{E}(\mathbf{r}, \omega) = \sum_n \{c_n^e \mathbf{L}_n + a_n^e \mathbf{M}_n + b_n^e \mathbf{N}_n\} \quad (6.18)$$

$$\mathbf{H}(\mathbf{r}, \omega) = \sum_n \{c_n^h \mathbf{L}_n + a_n^h \mathbf{M}_n + b_n^h \mathbf{N}_n\}. \quad (6.19)$$

where the coefficients of the expansion can be determined by matching the boundary conditions. This is the solution to the famous **antenna problem**. We have the additional boundary condition stating the conservation of charge. *Normal component of \mathbf{J} is continuous at a boundary:*

$$\mathbf{J}_1 \cdot \hat{\mathbf{n}} = \mathbf{J}_2 \cdot \hat{\mathbf{n}}. \quad (6.20)$$

Thus, given a certain antenna geometry, the charge density can be obtained by solving the scalar boundary value problem for ρ . This in turn will give the solution for the current densities on the boundary of the antenna. Alternatively, the boundary conditions on \mathbf{J} can be invoked. The tangential component of \mathbf{J} enter the boundary conditions on \mathbf{E} and \mathbf{H} . The \mathbf{E} and \mathbf{H} fields can therefore be obtained by matching the boundary conditions between the assumed solutions across the boundary. As it turns out, $\rho = 0$ does indeed satisfy the conditions of this problem, and this subset is what we were concerned with, for solution to the scattering problems. Thus our original nomenclature of calling Equation 2.18 as the 'diffraction equation' is actually a misnomer as the class of electromagnetic problems it represents is more general than that required to study diffraction and scattering only.

The vector basis function solution to the inhomogenous Maxwell's equations will open up the path to handling complicated radiation problems and their near field behavior. Such problems are extremely difficult to handle with existing techniques to solve the problem. To the best of our knowledge, this is the first time the antenna problem has been shown to be solvable as a boundary value problem using a complete set of basis functions.

6.4 Final Remarks

We have developed the technique of basis function expansion in the spherical polar coordinate system and solved a few representative problems. The problem of plasmon resonance in colloids, diffraction from an elongated scatterer and the sphere-plane model have been solved using one and the same technique. Even the inhomogeneous Maxwell equations are solved (in principle) using the same techniques. Although the method of expanding solutions in ingeniously created functions has been around for some time, this thesis establishes the aspect of applicability of this method to very general problems.

Bibliography

- [1] Arthur L. Aden and Milton Kerker. Scattering of electromagnetic waves from two concentric spheres. *Journal of Applied Physics*, 22(10):1242–1246, 1951.
- [2] Tom M. Apostol. *Mathematical analysis: a modern approach to advanced calculus*. Addison-Wesley, Reading, Mass, 1957.
- [3] P. K. Aravind and Horia Metiu. The effects of the interaction between resonances in the electromagnetic response of a sphere-plane structure: applications to surface enhanced spectroscopy. *Surface Science*, 124:506–528, 1983.
- [4] P. K. Aravind, R. W. Rendell, and Horia Metiu. A new geometry for field enhancement in surface-enhanced spectroscopy. *Chemical Physics Letters*, 85(4):396–403, 1982.
- [5] G. Arfken. *Mathematical methods for Physicists, 2nd Ed.* Academic, New York, 1970.
- [6] Shoji Asano and Giichi Yamamoto. Light scattering by a spheroidal particle. *Applied Optics*, 14(1):29–49, 1975.
- [7] R. Averitt, D. Sarkar, and N. J. Halas. Studies on Au₂S and Au colloids. Manuscript in preparation.
- [8] R. Berndt, R. Gaisch, W. D. Schneider, J. K. Gimzewski, B. Reihl, R. R. Schlittler, and M. Tschudy. Atomic resolution in photon emission induced by a scanning tunneling microscope. *Physical Review Letters*, 74(1):102–105, 1992.
- [9] R. Berndt, J. K. Gimzewski, and P. Johansson. Electromagnetic interactions of metallic objects in nanometer proximity. *Physical Review Letters*, 71(21):3493–3496, 1993.
- [10] Richard Berndt, James K. Gimzewski, and Peter Johansson. Inelastic tunneling excitation of tip-induced plasmon modes on noble-metal surfaces. *Physical Review Letters*, 67(27):3796–3799, 1991.

- [11] Craig F. Bohren and Donald R. Huffman. *Absorption and Scattering of Light by Small Particles*. John Wiley & Sons. New York. 1983.
- [12] Max Born and Emil Wolf. *Principles of Optics : Electromagnetic Theory of Propagation, Interference and Diffraction of Light*. Pergamon Press. Oxford. UK. 1980.
- [13] J. J. Bowman, T. B. A. Senior, and P. L. E. Uslenghi. *Electromagnetic and Acoustic Scattering by Simple Shapes*. Hemisphere Publishing Company. New York. 1987.
- [14] Winfried Denk and Dieter W. Pohl. Near-field optics: Microscopy with nanometer-size fields. *J. Vac. Sci. Technol.*, B9(2):510–513. 1991.
- [15] Mikio Eto and Kiyoshi Kawamura. Quantum size effect on optical absorption in a small spherical shell. *Physical Review B*, 51(15):10119–10126. 1995.
- [16] Carson Flammer. *Spheroidal Wave Functions*. Stanford University Press. Stanford, CA. USA. 1957.
- [17] Paul R. Halmos. *Naive Set Theory*. D. Van Nostrand Company, Inc. New York. 1960.
- [18] W. W. Hansen. A new type of expansion in radiation problems. *Physical Review*, 47:139–143. 1935.
- [19] W. W. Hansen. Directional characteristics of any antenna over a plane earth. *Physics*, 7:460–465, 1936.
- [20] W. W. Hansen. Transformations useful in certain antenna calculations. *Journal of Applied Physics*, 8:282–286. 1937.
- [21] Mayer Humi and William Miller. *Second Course in Ordinary Differential Equations for Scientists and Engineers*. Springer-Verlag. New York. 1988.
- [22] J. D. Jackson. *Classical Electrodynamics*. John Wiley & Sons, Inc. New York. 1975.
- [23] Peter Johansson, R. Monreal, and Peter Apell. Theory of light emission from a scanning tunneling microscope. *Physical Review B*, 42(14):9210–9213. 1990.

- [24] P. B. Johnson and R. W. Christy. Optical constants of noble metals. *Physical Review B*, 6(12):4370–4379, 1972.
- [25] D. S. Jones. *Methods in Electromagnetic Wave Propagation, 2nd Ed.* Clarendon Press, Oxford, UK, 1994.
- [26] Uwe Kreibig and Michael Vollmer. *Optical Properties of Metal Clusters.* Springer-Verlag, Berlin Heidelberg, Germany, 1995.
- [27] H. N. Kritikos and D. L. Jaggard. *Recent Advances in Electromagnetic Theory.* Springer-Verlag, New York, 1990.
- [28] A. Madrazo, M. Nieto-Vesperinas, and N. Garcia. Exact calculation of Maxwell equations for a tip-metallic interface configuration: Application to atomic resolution by photon emission. *Physical Review B*, 53(7):3654–3657, 1996.
- [29] P. M. Morse and H. Feshbach. *Methods of Theoretical Physics (Vol 1 and 2).* McGraw-Hill, New York, 1953.
- [30] Claus Muller. *Foundations of the Mathematical Theory of Electromagnetic Waves.* Springer-Verlag, Berlin, Germany, 1969.
- [31] William H. Press, Saul A. Teukolsky, William T. Vetterling, and Brian P. Flannery. *Numerical Recipes in C: The Art of Scientific Computing, Second Edition.* Cambridge University Press, New York, 1992.
- [32] S. L. Ren, Y. Wang, A. M. Rao, E. McRae, J. M. Holden, T. Hager, KaiAn Wang, Wen-Tse Lee, H. F. Hi, J. Selegue, and P. C. Eklund. Ellipsometric determination of the optical constants of C_{60} . *Applied Physics Letters*, 59(21):2678–2680, 1991.
- [33] R. Ruppin. Surface modes and optical absorption of a small sphere above a substrate. *Surface Science*, 127:108–118, 1983.
- [34] R. Ruppin. Optical absorption by a small sphere above a substrate with inclusion of nonlocal effects. *Physical Review B*, 45(19):11209, 1992.
- [35] C. E. Schensted. Electromagnetic and acoustical scattering by a semi-infinite body of revolution. *Journal of Applied Physics*, 26(3):306–308, 1955.

- [36] K. M. Siegel, J. W. Crispin, and C. E. Schensted. Electromagnetic and acoustical scattering from a semi-infinite cone. *Journal of Applied Physics*. 26(3):309–313. 1955.
- [37] G. F. Simmons. *Introduction to Topology and Modern Analysis*. McGraw-Hill Kogakusha, Tokyo, 1963.
- [38] Julius Adams Stratton. *Electromagnetic Theory*. McGraw-Hill. New York. 1941.
- [39] Tadashi Takemori, Masahiro Inoue, and Kazuo Ohtaka. Optical response of a sphere coupled to a metal substrate. *Journal of the Physical Society of Japan*. 56(4):1587–1602, 1987.
- [40] H. C. van de Hulst. *Light Scattering by Small Particles*. Dover. New York. 1981.
- [41] James R. Wait. Scattering of a plane wave from a circular dielectric cylinder at oblique incidence. *Canadian Journal of Physics*. 33:189–195. 19XX.
- [42] G. N. Watson. *Theory of Bessel Functions*. 2nd Ed. Cambridge University Press. New York. 1952.
- [43] H. W. Wylde. *Mathematical Methods for Physics*. W. A. Benjamin, Inc. Ontario. 1976.
- [44] H. S. Zhou, I. Honma, H. Komiyama, and J. W. Haus. Controlled synthesis and quantum-size effect in gold-coated nanoparticles. *Physical Review B*. 50(16):12052–12056, 1994.

Appendix A

Helmholtz Equation in Spherical Polar Coordinates

In spherical polar coordinate system, the scalar wave equation is readily solved by the method of separation of variables. Thus, given the wave equation

$$\nabla^2 u(\mathbf{r}) + k^2 u(\mathbf{r}) = 0, \quad (\text{A.1})$$

we assume the existence of solutions of the form $u(r, \theta, \phi) = R(r)P(\theta)\Phi(\phi)$. In spherical polar coordinates, the Laplacian operator has the form:

$$\nabla^2 \equiv \frac{1}{r^2 \sin \theta} \left[\frac{\partial}{\partial r} \left(r^2 \sin \theta \frac{\partial}{\partial r} \right) + \frac{\partial}{\partial \theta} \left(\sin \theta \frac{\partial}{\partial \theta} \right) + \frac{\partial}{\partial \phi} \left(\frac{1}{\sin \theta} \frac{\partial}{\partial \phi} \right) \right]. \quad (\text{A.2})$$

On substitution of $u = RP\Phi$ into Equation A.1. and dividing by $RP\Phi$, we obtain:

$$\frac{1}{Rr} \frac{d^2}{dr^2}(rR) + \frac{1}{P\Phi r^2 \sin \theta} \left[\frac{\partial}{\partial \theta} \left(\sin \theta \frac{\partial(P\Phi)}{\partial \theta} \right) + \frac{1}{\sin \theta} \frac{\partial^2(P\Phi)}{\partial \phi^2} \right] + k^2 = 0. \quad (\text{A.3})$$

A.1 Radial Equation

Introducing the separation constant λ

$$\frac{1}{P\Phi} \frac{1}{\sin \theta} \left[\frac{\partial}{\partial \theta} \left(\sin \theta \frac{\partial(P\Phi)}{\partial \theta} \right) + \frac{1}{\sin \theta} \frac{\partial^2(P\Phi)}{\partial \phi^2} \right] = -\lambda, \quad (\text{A.4})$$

we obtain the separated radial equation:

$$\frac{1}{Rr} \frac{d^2}{dr^2}(rR) + k^2 - \frac{\lambda}{r^2} = 0. \quad (\text{A.5})$$

If $k^2 \neq 0$, we let $r = \rho/k$ and the equation becomes

$$\frac{d^2 R}{d\rho^2} + \frac{2}{\rho} \frac{dR}{d\rho} + \left(1 - \frac{\lambda}{\rho^2} \right) R = 0. \quad (\text{A.6})$$

If we let $R = S/\sqrt{\rho}$, then the radial equation can finally be written in the form:

$$\frac{d^2 S}{d\rho^2} + \frac{1}{\rho} \frac{dS}{d\rho} + \left(1 - \frac{\beta^2}{\rho^2}\right) S = 0. \quad (\text{A.7})$$

where $\beta = \sqrt{\lambda + \frac{1}{4}}$. This is Bessel's Equation and the solutions are the well known Bessel and Hankel functions $S(\rho) = AJ_\beta(\rho) + BH_\beta^{(1,2)}(\rho)$. Equivalently,

$$R(r) = A \frac{1}{\sqrt{kr}} J_\beta(kr) + B \frac{1}{\sqrt{kr}} H_\beta^{(1,2)}(kr) \quad (\text{A.8})$$

where A and B are arbitrary constants and the 1 and 2 in $H_\beta^{(1,2)}$ indicate the Hankel functions of the first and second kind respectively. When $k^2 = 0$, corresponding to dc or quasistatic conditions, we obtain Laplace's equation and the radial equation becomes much simpler:

$$\frac{1}{r} \frac{d^2}{dr^2}(rR) - \frac{\lambda}{r^2} R = 0. \quad (\text{A.9})$$

Assuming solution of the form $R = r^\alpha$, we obtain a quadratic equation for the roots of α , so that $\alpha_\pm = \frac{1}{2}(-1 \pm \sqrt{1 + 4\lambda})$. So the general solution to the radial equation for $k = 0$ will be of the form:

$$R(r) = Ar^{\alpha_+} + Br^{\alpha_-}. \quad (\text{A.10})$$

A.2 Angular Equations

From Equation A.4 we immediately obtain:

$$\frac{1}{P \sin \theta} \frac{d}{d\theta} \left(\sin \theta \frac{dP}{d\theta} \right) + \frac{1}{\sin^2 \theta} \frac{1}{\Phi} \frac{d^2 \Phi}{d\phi^2} + \lambda = 0. \quad (\text{A.11})$$

The ϕ -equation separates if we let

$$\frac{1}{\Phi} \frac{d^2 \Phi}{d\phi^2} = -m^2. \quad (\text{A.12})$$

so that

$$\Phi(\phi) = C e^{im\phi} + D e^{-im\phi}. \quad (\text{A.13})$$

If the full range of $\phi \in [0, 2\pi]$ is allowed in a given problem, then the requirement of single-valued solutions imply that m can only assume integer values $m \in \{0, \pm 1, \pm 2, \pm 3, \dots\}$.

The corresponding θ -equation becomes

$$\frac{d^2 P}{d\theta^2} + \frac{\cos \theta}{\sin \theta} \frac{dP}{d\theta} + \left(\lambda - \frac{m^2}{\sin^2 \theta} \right) P = 0. \quad (\text{A.14})$$

On changing variables to $x = \cos \theta$, the θ -equation transforms immediately to Legendre's equation:

$$\frac{d^2 P}{dx^2} - \frac{2x}{1-x^2} \frac{dP}{dx} + \frac{1}{1-x^2} \left(\lambda - \frac{m^2}{1-x^2} \right) P = 0. \quad (\text{A.15})$$

with solutions of the form $P(x) = EP_n^m(x) + FQ_n^m(x)$, where $\lambda = n(n+1)$. The solutions are the well known Legendre (and Associated Legendre) functions $P_n^m(x)$. The second independent solution to Legendre's equation are the $Q_n^m(x)$ which are singular on the z-axis. A problem in which the z-axis is not included must have these solutions included in the expression for the general solution.

A.3 Eigenfunctions of the Helmholtz Equation

We substitute $\lambda = n(n+1)$ in the expression for the solution to the radial equations. Since $\beta^2 = \lambda + \frac{1}{4}$, we obtain $\beta = n + \frac{1}{2}$, and the solution to the radial equations assume the form:

$$\begin{aligned} R(r) &= A \frac{1}{\sqrt{kr}} J_{n+\frac{1}{2}}(kr) + B \frac{1}{\sqrt{kr}} H_{n+\frac{1}{2}}^{(1,2)}(kr) \\ &= A' j_n(kr) + B' h_n^{(1,2)}(kr) \end{aligned} \quad (\text{A.16})$$

where

$$j_n(\rho) = \sqrt{\frac{\pi}{2\rho}} J_{n+\frac{1}{2}}(\rho) \quad (\text{A.17})$$

are the spherical Bessel functions, and

$$h_n^{(1,2)}(\rho) = \sqrt{\frac{\pi}{2\rho}} H_{n+\frac{1}{2}}^{(1,2)}(\rho) \quad (\text{A.18})$$

are the spherical Hankel functions of the first and second kind. Therefore, in a region that includes the origin and so the z-axis as well, and where ϕ can range over the full azimuthal range $[0, 2\pi]$, the eigenfunctions to the scalar Helmholtz equation assume the following form:

$$u(r, \theta, \phi) \sim j_n(kr) P_n^m(\cos \theta) e^{im\phi}. \quad (\text{A.19})$$

with $n \in \{0, 1, 2, \dots\}$ and $m \in \{0, \pm 1, \pm 2, \dots, \pm n\}$. For a region that excludes the origin, but not the z-axis, the spherical Hankel functions are to be used instead of the spherical Bessel functions.

Appendix B

Spherical Bessel Functions

It has been shown that the radial part of the solution to the scalar Helmholtz equation consists of the spherical Bessel and spherical Hankel functions:

$$j_n(x) = \sqrt{\frac{\pi}{2x}} J_{n+\frac{1}{2}}(x) \quad (\text{B.1})$$

$$h_n^{(1,2)}(x) = j_n(x) \pm i n_n(x) \quad (\text{B.2})$$

$$= \sqrt{\frac{\pi}{2x}} J_{n+\frac{1}{2}}(x) \pm i \sqrt{\frac{\pi}{2x}} N_{n+\frac{1}{2}}(x). \quad (\text{B.3})$$

Here $n_n(x)$ are the spherical Neumann functions, derived from the Neuman functions, $N_l(x)$, as indicated above. The argument x can be complex in general. In the definition of the spherical Hankel functions, the first and second kinds correspond to the positive and negative signs respectively. Explicitly,

$$j_n(x) = 2^n x^n \sum_{m=0}^{\infty} \frac{(-1)^m (n+m)!}{m! (2n+2m+1)!} x^{2m} \quad \text{and} \quad (\text{B.4})$$

$$n_n(x) = -\frac{1}{2^n x^{n+1}} \sum_{m=0}^{\infty} \frac{(2n-2m)!}{m! (n-m)!} x^{2m}. \quad (\text{B.5})$$

Clearly, when $x \rightarrow 0$, $j_n(x) \sim x^n \rightarrow 0$ for $n \neq 0$. So only $j_0(x)$ is non-zero as $x \rightarrow 0$. The spherical Neumann functions, $n_n(x) \sim 1/x^{n+1} \rightarrow \infty$ as $x \rightarrow 0$. The convergence is slow for large arguments, and it is computationally desirable to expand in a series of inverse powers of x . This can in fact be done and the resulting series is actually expressible in a *finite* number of terms [42]. Thus we have ($|x| > 0$):

$$j_n(x) = \frac{1}{2x} \left[e^{ix} \sum_{k=0}^n \frac{i^{-(n-k+1)} (n+k)!}{k! (n-k)! (2x)^k} + e^{-ix} \sum_{k=0}^n \frac{(-i)^{-(n-k+1)} (n+k)!}{k! (n-k)! (2x)^k} \right]. \quad (\text{B.6})$$

$$h_n^{(1)}(x) = \frac{1}{i^{n+1} x} e^{ix} \sum_{k=0}^n \frac{(-1)^k (n+k)!}{k! (n-k)! (2ix)^k} \quad \text{and} \quad (\text{B.7})$$

$$h_n^{(2)}(x) = \frac{i^{n+1}}{x} e^{-ix} \sum_{k=0}^n \frac{(n+k)!}{k! (n-k)! (2ix)^k} \quad (\text{B.8})$$

Thus, unlike the normal Bessel and Hankel functions, the spherical counterparts are amenable for exact numerical computations that does not involve truncation errors resulting from limiting the number of terms used in the computation of the series expansion for these functions. As $x \rightarrow \infty$, we have the following asymptotic behavior:

$$h_n^{(1)}(x) \sim \frac{1}{x} (-i)^{n+1} e^{ix} \quad (\text{B.9})$$

$$h_n^{(2)}(x) \sim \frac{1}{x} i^{n+1} e^{-ix} \quad (\text{B.10})$$

$$j_n(x) \sim \frac{1}{x} \cos\left(x - \frac{n+1}{2}\pi\right) \quad (\text{B.11})$$

$$n_n(x) \sim \frac{1}{x} \sin\left(x - \frac{n+1}{2}\pi\right). \quad (\text{B.12})$$

A function $f(kx - \omega t)$ represents a wave travelling in the direction of increasing x . In other words, as t increases, the constant-phase points correspond to increasing x values. Similarly $f(kx + \omega t)$ represents a wave travelling in the direction of decreasing x . Now with the *convention* of allowing the time dependence of the excitation to be of the form $e^{-i\omega t}$ (as opposed to $e^{i\omega t}$), a wave $\sim e^{ikr} e^{-i\omega t} = e^{i(kr - \omega t)}$ represents an outgoing (increasing r) spherical wave. Thus with the convention of time-dependence $\sim e^{-i\omega t}$, we immediately recognize that the functions that describe the correct asymptotic behavior are the spherical Hankel functions of the first kind. The spherical Hankel functions of the second kind represent incoming waves and are not appropriate for expressing solutions to scattering problems. The spherical Bessel and spherical Hankel functions of the first kind are two independent sets of functions in which our scattering solutions can be expressed.

B.1 Recurrence Relations

The recurrence relations of the spherical Bessel and spherical Hankel functions follow directly from the corresponding recurrence relations of the normal Bessel and Hankel functions. If $Z_n(x)$ represent either the Bessel function or the Hankel functions, and $z_n(x)$ represent the corresponding spherical counterparts, then, we have:

$$Z_{p-1}(x) + Z_{p+1}(x) = \frac{2p}{x} Z_p(x). \quad (\text{B.13})$$

Multiplying both sides by $\sqrt{\pi/(2x)}$ and letting $p = n + \frac{1}{2}$, we obtain :

$$\sqrt{\frac{\pi}{2x}} Z_{n-\frac{1}{2}}(x) + \sqrt{\frac{\pi}{2x}} Z_{n+\frac{3}{2}}(x) = \frac{2n+1}{x} \sqrt{\frac{\pi}{2x}} Z_{n+\frac{1}{2}}(x). \quad (\text{B.14})$$

Or,

$$z_{n-1}(x) + z_{n+1}(x) = \frac{2n+1}{x} z_n(x) \quad (\text{B.15})$$

Similarly, by using the recurrence relation:

$$\frac{dZ_p(x)}{dx} = \frac{1}{2} [Z_{p-1}(x) - Z_{p+1}(x)]. \quad (\text{B.16})$$

we obtain

$$\frac{dz_n(x)}{dx} = \frac{1}{2n+1} [n z_{n-1}(x) - (n+1) z_{n+1}(x)] \quad (\text{B.17})$$

In addition we have the following recurrence relations:

$$\frac{d}{dx} [x^{n+1} z_n(x)] = x^{n+1} z_{n-1}(x) \quad (\text{B.18})$$

$$\frac{d}{dx} [x^{-n} z_n(x)] = -x^{-n} z_{n+1}(x) \quad (\text{B.19})$$

Now,

$$\begin{aligned} \frac{1}{r} \frac{d}{dr} (r z_n(kr)) &= \frac{d}{dr} z_n(kr) + \frac{z_n(kr)}{r} \\ &= \frac{k}{2n+1} (n z_{n-1}(kr) - (n+1) z_{n+1}(kr)) \end{aligned} \quad (\text{B.20})$$

$$+ \frac{k}{2n+1} (z_{n-1}(kr) + z_{n+1}(kr)). \quad (\text{B.21})$$

Thus,

$$\frac{1}{r} \frac{d}{dr} (r z_n(kr)) = \frac{k}{2n+1} ((n+1) z_{n-1}(kr) - n z_{n+1}(kr)) \quad (\text{B.22})$$

B.2 Special Integrals of Spherical Bessel Functions

A fundamental integral involved in obtaining the expansion coefficients of an incident plane wave in the **L, M, N** basis, is the following:

$$\int_0^{\infty} J_{\mu}(at) J_{\nu}(at) \frac{dt}{t} = \frac{2 \sin\left((\nu - \mu)\frac{\pi}{2}\right)}{\pi (\nu^2 - \mu^2)}. \quad (\text{B.23})$$

Substituting the expression for the spherical Bessel functions (Equation B.1) into the left hand side of the integral above, we immediately obtain:

$$\int_0^{\infty} j_{\mu}(at) j_{\nu}(at) dt = \frac{1}{a} \frac{\sin\left((\nu - \mu)\frac{\pi}{2}\right)}{(\nu + \mu + 1)(\nu - \mu)}. \quad (\text{B.24})$$

When $\nu \rightarrow \mu$, the right hand side has the factor of the form :

$$\lim_{\nu \rightarrow \mu} \frac{\sin\left((\nu - \mu)\frac{\pi}{2}\right) \pi}{(\nu - \mu)\frac{\pi}{2}} = \frac{\pi}{2}. \quad (\text{B.25})$$

So we have the following important results :

$$\begin{aligned} \int_0^{\infty} j_{\mu}(at) j_{\nu}(at) dt &= \frac{\pi}{2a(2n+1)} \quad (\nu = \mu) \\ &= 0 \quad (\nu - \mu) \text{ is even} \\ &\neq 0 \quad (\nu - \mu) \text{ is odd.} \end{aligned} \quad (\text{B.26})$$

Using the recurrence relations in the previous section, we can deduce some important integrals. Clearly:

$$\int_0^{\infty} j_n(kr) j_n(kr) dr = \frac{\pi}{2k(2n+1)} \quad (\text{B.27})$$

$$\int_0^{\infty} j_{n-1}(kr) j_{n-1}(kr) dr = \frac{\pi}{2k(2n-1)} \quad (\text{B.28})$$

$$\int_0^{\infty} j_{n+1}(kr) j_{n+1}(kr) dr = \frac{\pi}{2k(2n+3)} \quad (\text{B.29})$$

Since

$$\frac{j_n(kr)}{kr} = \frac{1}{2n+1} (j_{n-1}(kr) + j_{n+1}(kr)). \quad (\text{B.30})$$

therefore.

$$\int_0^\infty \frac{j_n(kr)}{kr} j_{n-1}(kr) = \int_0^\infty \frac{1}{2n+1} (j_{n-1}(kr) + j_{n+1}(kr)) j_{n-1}(kr). \quad (\text{B.31})$$

Only the $j_{n-1}(kr)j_{n-1}(kr)$ product term will evaluate to a non-zero integral. The other term, $j_{n-1}(kr)j_{n+1}(kr)$ will yeild a vanishing integral because $n-1-(n+1)$ is an even number. Thus:

$$\int_0^\infty dr \frac{j_n(kr)}{kr} j_{n-1}(kr) = \frac{\pi}{2k(2n-1)(2n+1)} \quad (\text{B.32})$$

Similarly.

$$\int_0^\infty dr \frac{j_n(kr)}{kr} j_{n+1}(kr) = \frac{\pi}{2k(2n+1)(2n+3)} \quad (\text{B.33})$$

Using the recurrence relation

$$\frac{1}{kr} \frac{d}{dr} (rj_n(kr)) = \frac{1}{2n+1} ((n+1)j_{n-1}(kr) - nj_{n+1}(kr)). \quad (\text{B.34})$$

we obtain the important integrals:

$$\int_0^\infty dr j_{n-1}(kr) \cdot \frac{1}{kr} \frac{d}{dr} (rj_n(kr)) = \frac{\pi(n+1)}{2k(2n-1)(2n+1)} \quad (\text{B.35})$$

and.

$$\int_0^\infty dr j_{n+1}(kr) \cdot \frac{1}{kr} \frac{d}{dr} (rj_n(kr)) = -\frac{\pi n}{2k(2n+1)(2n+3)} \quad (\text{B.36})$$

Finally, using the recurrence relation

$$\frac{d}{d(kr)} (j_n(kr)) = \frac{1}{2n+1} (nj_{n-1}(kr) - (n+1)j_{n+1}(kr)). \quad (\text{B.37})$$

we deduce the following integrals:

$$\int_0^\infty dr j_{n-1}(kr) \cdot \frac{d}{d(kr)} (j_n(kr)) = \frac{\pi n}{2k(2n-1)(2n+1)} \quad (\text{B.38})$$

and

$$\int_0^\infty dr j_{n+1}(kr) \cdot \frac{d}{d(kr)} (j_n(kr)) = -\frac{\pi(n+1)}{2k(2n+1)(2n+3)} \quad (\text{B.39})$$

Appendix C

Associated Legendre Functions

C.1 Legendre and Associated Legendre Functions

The θ -part of the separated scalar Helmholtz equation has been shown to reduce to the following differential equation, known as **Legendre's Equation**:

$$\frac{d^2 P}{dx^2} - \frac{2x}{1-x^2} \frac{dP}{dx} + \frac{1}{1-x^2} \left(n(n+1) - \frac{m^2}{1-x^2} \right) P = 0 \quad (\text{C.1})$$

The general solution to Legendre's equation is given as:

$$P(\cos\theta) = C_{mn} P_n^m(\cos\theta) + D_{mn} Q_n^m(\cos\theta) \quad (\text{C.2})$$

Here $n \in \{0, 1, 2, \dots\}$ and $m \in \{0, \pm 1, \pm 2, \dots, \pm n\}$. The functions $Q_n^m(x)$ have logarithmic singularity at $x = \pm 1$ i.e., on the z-axis. We will not be concerned with these functions since the points on the z-axis, at $x = \pm 1$, are going to be included in the problems.

There is a certain degree of variation in the definition for the Associated Legendre Functions. It is mostly in the definition of the phase that different authors have chosen to follow different conventions. In this work, we have throughout followed the convention of Magnus and Oberhettinger [22]. This is the same phase convention followed by Jackson [22] and the reference handbook by Gradshteyn and Ryzhik. We choose to follow the following definition for the Associated Legendre Functions:

$$\begin{aligned} P_n^m(x) &= (-1)^m (1-x^2)^{m/2} \frac{d^m}{dx^m} P_n(x), \\ &= \frac{(-1)^m}{2^n (n!)} (1-x^2)^{m/2} \frac{d^{n+m}}{dx^{n+m}} (x^2-1)^n \end{aligned} \quad (\text{C.3})$$

where $x = \cos\theta$ and $P_n(x)$ are the Legendre polynomials, which are solutions to Legendre's equation with $m=0$.

The Associated Legendre Functions follow these basic properties:

$$P_n^{-m}(x) = (-1)^m \frac{(n-m)!}{(n+m)!} P_n^m(x) \quad (\text{C.4})$$

$$P_n^m(-x) = (-1)^{n+m} P_n^m(x) \quad (\text{C.5})$$

$$P_n^m(\pm 1) = 0, \quad (\text{C.6})$$

and the orthogonality relation:

$$\int_{-1}^1 dx P_n^m(x) P_{n'}^m(x) = \frac{2}{2n+1} \frac{(n+m)!}{(n-m)!} \delta_{nn'} \quad (\text{C.7})$$

C.2 Recursion Relations of Associated Legendre Functions

We enumerate a few recursion relations that will be used for solving some of the integrals in the next section. Here $x = \cos\theta$ where $\theta \in [0, \pi]$:

$$P_{n-1}^m(x) - P_{n+1}^m(x) = (2n+1)\sqrt{1-x^2} P_n^{m-1}(x) \quad (\text{C.8})$$

$$P_{n-1}^m(x) - x P_n^m(x) = (n-m+1)\sqrt{1-x^2} P_n^{m-1}(x) \quad (\text{C.9})$$

$$x P_n^m(x) - P_{n+1}^m(x) = (n+m)\sqrt{1-x^2} P_n^{m-1}(x) \quad (\text{C.10})$$

$$(1-x^2) \frac{d}{dx} P_n^m(x) = (n+1)x P_n^m(x) - (n-m+1) P_{n+1}^m(x) \quad (\text{C.11})$$

$$= -nx P_n^m(x) + (n+m) P_{n-1}^m(x) \quad (\text{C.12})$$

$$= -\sqrt{1-x^2} P_n^{m+1}(x) - mx P_n^m(x) \quad (\text{C.13})$$

$$(1-x^2) \frac{d}{dx} P_n^m(x) = (n-m+1)(n+m)\sqrt{1-x^2} P_n^{m-1}(x) + mx P_n^m(x) \quad (\text{C.14})$$

$$(2n+1)x P_n^m(x) = (n-m+1) P_{n+1}^m(x) + (n+m) P_{n-1}^m(x) \quad (\text{C.15})$$

$$P_{-n-1}^m(x) = P_n^m(x) \quad (\text{C.16})$$

Equation C.8 can be rewritten by letting $n \rightarrow n-1$:

$$\frac{P_n^m(x)}{\sqrt{1-x^2}} = -(2n-1) P_{n-1}^{m-1}(x) + \frac{P_{n-2}^m(x)}{\sqrt{1-x^2}} \quad (\text{C.17})$$

Similarly, we can write:

$$\frac{P_{n+1}^m(x)}{\sqrt{1-x^2}} = -(2n+1)P_n^{m-1}(x) + \frac{P_{n-1}^m(x)}{\sqrt{1-x^2}} \quad (\text{C.18})$$

$$\frac{P_n^m(x)}{\sqrt{1-x^2}} = -(2n-1)P_{n-1}^{m-1}(x) + \frac{P_{n-2}^m(x)}{\sqrt{1-x^2}} \quad (\text{C.19})$$

$$\frac{P_n^{m+1}(x)}{\sqrt{1-x^2}} = -(2n-1)P_{n-1}^m(x) + \frac{P_{n-2}^{m+1}(x)}{\sqrt{1-x^2}} \quad (\text{C.20})$$

$$\frac{P_{n-1}^m(x)}{\sqrt{1-x^2}} = -(2n-3)P_{n-2}^{m-1}(x) + \frac{P_{n-3}^m(x)}{\sqrt{1-x^2}} \quad (\text{C.21})$$

$$\frac{P_{n+1}^{m+1}(x)}{\sqrt{1-x^2}} = -(2n+1)P_n^m(x) + \frac{P_{n-1}^{m+1}(x)}{\sqrt{1-x^2}} \quad (\text{C.22})$$

$$\frac{P_{n-1}^{m+1}(x)}{\sqrt{1-x^2}} = -(2n-3)P_{n-2}^m(x) + \frac{P_{n-3}^{m+1}(x)}{\sqrt{1-x^2}} \quad (\text{C.23})$$

$$\frac{P_n^{m-1}(x)}{\sqrt{1-x^2}} = -(2n-1)P_{n-1}^{m-2}(x) + \frac{P_{n-2}^{m-1}(x)}{\sqrt{1-x^2}} \quad (\text{C.24})$$

$$\frac{P_{n-1}^{m-1}(x)}{\sqrt{1-x^2}} = -(2n-3)P_{n-2}^{m-2}(x) + \frac{P_{n-3}^{m-1}(x)}{\sqrt{1-x^2}} \quad (\text{C.25})$$

$$\frac{P_{n+1}^{m-1}(x)}{\sqrt{1-x^2}} = -(2n+1)P_n^{m-2}(x) + \frac{P_{n-1}^{m-1}(x)}{\sqrt{1-x^2}} \quad (\text{C.26})$$

$$(\text{C.27})$$

We can also write:

$$\sqrt{1-x^2}P_n^{m-1}(x) = \frac{1}{(2n+1)}[P_{n-1}^m(x) - P_{n+1}^m(x)] \quad (\text{C.28})$$

$$\sqrt{1-x^2}P_{n-1}^{m-1}(x) = \frac{1}{(2n-1)}[P_{n-2}^m(x) - P_n^m(x)] \quad (\text{C.29})$$

$$\sqrt{1-x^2}P_n^m(x) = \frac{1}{(2n+1)}[P_{n-1}^{m+1}(x) - P_{n+1}^{m+1}(x)] \quad (\text{C.30})$$

$$\sqrt{1-x^2}P_{n+1}^{m+1}(x) = \frac{1}{(2n+1)}[P_{n-1}^{m+2}(x) - P_{n+1}^{m+2}(x)] \quad (\text{C.31})$$

$$\sqrt{1-x^2} P_{n+1}^{m+1}(x) = \frac{1}{(2n+3)} [P_n^{m+2}(x) - P_{n+2}^{m+2}(x)] \quad (\text{C.32})$$

$$\sqrt{1-x^2} P_{n-1}^{m+1}(x) = \frac{1}{(2n-1)} [P_{n-2}^{m+2}(x) - P_n^{m+2}(x)] \quad (\text{C.33})$$

$$\sqrt{1-x^2} P_{n+1}^{m-1}(x) = \frac{1}{(2n+3)} [P_n^m(x) - P_{n+2}^m(x)]. \quad (\text{C.34})$$

Using Equation C.15 we can immediately write the following equations as well:

$$x P_n^m(x) = \frac{1}{(2n+1)} [(n-m+1)P_{n+1}^m(x) + (n+m)P_{n-1}^m(x)] \quad (\text{C.35})$$

$$x P_n^{m-1}(x) = \frac{1}{(2n+1)} [(n-m+2)P_{n+1}^{m-1}(x) + (n+m-1)P_{n-1}^{m-1}(x)] \quad (\text{C.36})$$

$$x P_n^{m+1}(x) = \frac{1}{(2n+1)} [(n-m)P_{n+1}^{m+1}(x) + (n+m+1)P_{n-1}^{m+1}(x)] \quad (\text{C.37})$$

$$x P_{n+1}^{m+1}(x) = \frac{1}{(2n+3)} [(n-m+1)P_{n+2}^{m+1}(x) + (n+m+2)P_n^{m+1}(x)] \quad (\text{C.38})$$

$$x P_{n-1}^{m+1}(x) = \frac{1}{(2n-1)} [(n-m-1)P_n^{m+1}(x) + (n+m)P_{n-2}^{m+1}(x)] \quad (\text{C.39})$$

$$x P_{n-1}^{m-1}(x) = \frac{1}{(2n-1)} [(n-m+1)P_n^{m-1}(x) + (n+m-2)P_{n-2}^{m-1}(x)] \quad (\text{C.40})$$

$$x P_{n+1}^{m-1}(x) = \frac{1}{(2n+3)} [(n-m+3)P_{n+2}^{m-1}(x) + (n+m)P_n^{m-1}(x)] \quad (\text{C.41})$$

$$x P_{n-1}^m(x) = \frac{1}{(2n-1)} [(n-m)P_n^m(x) + (n+m-1)P_{n-2}^m(x)] \quad (\text{C.42})$$

$$x P_{n+1}^m(x) = \frac{1}{(2n+3)} [(n-m+2)P_{n+2}^m(x) + (n+m+1)P_n^m(x)] \quad (\text{C.43})$$

C.3 Useful Integrals of Associated Legendre Functions

Now we shall evaluate a number of integrals that use the recursion relations listed above and the orthogonality relations of the Associated Legendre functions. These integrals are useful for evaluating the scalar products involving **L**, **M** and **N** functions.

Let us consider integrals of the form:

$$\int_0^\pi d\theta \sin\theta P_{n\pm 1}^{m\pm 1}(\cos\theta) P_n^m(\cos\theta) = \int_{-1}^1 dx \sqrt{1-x^2} P_{n\pm 1}^{m\pm 1}(x) P_n^m(x).$$

Thus:

$$\begin{aligned} \int_{-1}^1 dx \sqrt{1-x^2} P_{n-1}^{m-1}(x) P_n^m(x) &= \frac{1}{(2n-1)} \int_{-1}^1 dx [P_{n-2}^m(x) - P_n^m(x)] P_n^m(x) \\ &= -\frac{1}{(2n-1)} \int_{-1}^1 dx P_n^m(x) P_n^m(x) \\ &= -\frac{2}{(2n-1)(2n+1)} \frac{(n+m)!}{(n-m)!} \end{aligned}$$

$$\int_{-1}^1 dx \sqrt{1-x^2} P_{n-1}^{m-1}(x) P_n^m(x) = \frac{(-2)}{(2n-1)(2n+1)} \frac{(n+m)!}{(n-m)!} \quad (m \geq 0) \quad (\text{C.44})$$

$$\begin{aligned} \int_{-1}^1 dx \sqrt{1-x^2} P_{n+1}^{m-1}(x) P_n^m(x) &= \frac{1}{(2n+3)} \int_{-1}^1 dx [P_n^m(x) - P_{n+2}^m(x)] P_n^m(x) \\ &= \frac{1}{(2n+3)} \int_{-1}^1 dx P_n^m(x) P_n^m(x) \end{aligned}$$

$$\int_{-1}^1 dx \sqrt{1-x^2} P_{n+1}^{m-1}(x) P_n^m(x) = \frac{2}{(2n+1)(2n+3)} \frac{(n+m)!}{(n-m)!} \quad (m \geq 0) \quad (\text{C.45})$$

$$\begin{aligned} \int_{-1}^1 dx \sqrt{1-x^2} P_{n-1}^{m+1}(x) P_n^m(x) &= \frac{1}{(2n+1)} \int_{-1}^1 dx P_{n-1}^{m+1} [P_{n-1}^{m+1}(x) - P_{n+1}^{m+1}(x)] P_n^m(x) \\ &= \frac{1}{(2n+1)} \int_{-1}^1 dx P_{n-1}^{m+1}(x) P_{n-1}^{m+1}(x) \end{aligned}$$

$$\int_{-1}^1 dx \sqrt{1-x^2} P_{n-1}^{m+1}(x) P_n^m(x) = \frac{2}{(2n+1)(2n-1)} \frac{(n+m)!}{(n-m-2)!} \quad (m \geq 0) \quad (\text{C.46})$$

$$\begin{aligned} \int_{-1}^1 dx \sqrt{1-x^2} P_{n+1}^{m+1}(x) P_n^m(x) &= \frac{1}{(2n+1)} \int_{-1}^1 dx P_{n+1}^{m+1} [P_{n-1}^{m+1}(x) - P_{n+1}^{m+1}(x)] P_n^m(x) \\ &= -\frac{1}{(2n+1)} \int_{-1}^1 dx P_{n+1}^{m+1}(x) P_{n+1}^{m+1}(x) \end{aligned}$$

$$\int_{-1}^1 dx \sqrt{1-x^2} P_{n+1}^{m+1}(x) P_n^m(x) = \frac{(-2)}{(2n+1)(2n+3)} \frac{(n+m+2)!}{(n-m)!} \quad (m \geq 0) \quad (C.47)$$

Integrals of the type:

$$\int_0^\pi d\theta \cos\theta P_{n\pm 1}^{m\pm 1}(\cos\theta) P_{n-1}^m(\cos\theta) = \int_{-1}^1 dx \frac{x}{\sqrt{1-x^2}} P_{n\pm 1}^{m\pm 1}(x) P_{n-1}^m(x).$$

We have

$$x P_{n-1}^m(x) = \frac{1}{(2n-1)} [(n-m)P_n^m(x) + (n+m-1)P_{n-2}^m(x)].$$

Now since

$$\frac{P_{n-1}^{m+1}(x)}{\sqrt{1-x^2}} = -(2n-3)P_{n-2}^m(x) + \frac{P_{n-3}^{m+1}(x)}{\sqrt{1-x^2}}.$$

we can continue the recursion on the second term on the right hand side. For every recursion the second term on the right hand side will have the 'n' index reduced by 2 where as the 'm' index remains the same. Thus eventually we will have the m index exceeding the n index and the recursive series will stop at that point. All the terms of the right hand side generated by carrying out the recursion will contain factors of the type P_{n-i}^m only. Thus in the product of terms generated by expanding the integrands, we have only one term that will be non-zero due to the orthogonality relations of the Associated Legendre Functions.

$$\begin{aligned} &\int_{-1}^1 dx \frac{x}{\sqrt{1-x^2}} P_{n-1}^m(x) P_{n-1}^{m+1}(x) \\ &= \frac{1}{(2n-1)} \int_{-1}^1 dx [(n-m)P_n^m(x) + (n+m-1)P_{n-2}^m(x)] \times \\ &\quad [- (2n-3)P_{n-2}^m(x) - (2n-7)P_{n-4}^m(x) - \dots] \\ &= -\frac{(2n-3)(n+m-1)}{(2n-1)} \int_{-1}^1 dx P_{n-2}^m(x) P_{n-2}^m(x) \end{aligned}$$

$$\int_{-1}^1 dx \frac{x}{\sqrt{1-x^2}} P_{n-1}^m(x) P_{n-1}^{m+1}(x) = \frac{(-2)(n+m-1)(n+m-2)!}{(2n-1)(n-m-2)!} \quad (m \geq 0) \quad (\text{C.48})$$

$$\begin{aligned} & \int_{-1}^1 dx \frac{x}{\sqrt{1-x^2}} P_{n-1}^m(x) P_{n-1}^{m-1}(x) \\ &= \frac{1}{(2n-1)} \int_{-1}^1 dx \left[(n-m+1) P_n^{m-1}(x) + (n+m-2) P_{n-2}^{m-1}(x) \right] \times \\ & \quad \left[-(2n-3) P_{n-2}^{m-1}(x) - (2n-7) P_{n-4}^{m-1} - \dots \right] \\ &= -\frac{(2n-3)(n+m-2)}{(2n-1)} \int_{-1}^1 dx P_{n-2}^{m-1}(x) P_{n-2}^{m-1}(x) \end{aligned}$$

$$\int_{-1}^1 dx \frac{x}{\sqrt{1-x^2}} P_{n-1}^m(x) P_{n-1}^{m-1}(x) = \frac{(-2)(n+m-2)!}{(2n-1)(n-m-1)!} \quad (m \geq 0) \quad (\text{C.49})$$

$$\begin{aligned} & \int_{-1}^1 dx \frac{x}{\sqrt{1-x^2}} P_{n-1}^m(x) P_{n+1}^{m+1}(x) \\ &= \frac{1}{(2n-1)} \int_{-1}^1 dx \left[(n-m) P_n^m(x) + (n+m-1) P_{n-2}^m(x) \right] \times \\ & \quad \left[-(2n+1) P_n^m(x) - (2n-3) P_{n-2}^m - \dots \right] \\ &= -\frac{1}{(2n-1)} \left[(n-m)(2n+1) \int_{-1}^1 dx P_n^m(x) P_n^m(x) \right. \\ & \quad \left. + (n+m-1)(2n-3) \int_{-1}^1 dx P_{n-2}^m(x) P_{n-2}^m(x) \right] \\ &= \frac{(-2)}{(2n-1)} \left[\frac{(n+m)!}{(n-m-1)!} + \frac{(n+m-1)!}{(n-m-2)!} \right] \end{aligned}$$

$$\int_{-1}^1 dx \frac{x}{\sqrt{1-x^2}} P_{n-1}^m(x) P_{n+1}^{m+1}(x) = (-2) \frac{(n+m-1)!}{(n-m-1)!} \quad (m \geq 0) \quad (\text{C.50})$$

$$\begin{aligned}
& \int_{-1}^1 dx \frac{x}{\sqrt{1-x^2}} P_{n-1}^m(x) P_{n+1}^{m-1}(x) \\
&= \frac{1}{(2n+3)} \int_{-1}^1 dx \left[(n-m+3) P_{n+2}^{m-1}(x) + (n+m) P_n^{m-1}(x) \right] \times \\
& \quad \left[-(2n-3) P_{n-2}^{m-1}(x) - (2n-7) P_{n-4}^{m-1} - \dots \right]
\end{aligned}$$

So there is no overlap, and the integral should vanish:

$$\int_{-1}^1 dx \frac{x}{\sqrt{1-x^2}} P_{n-1}^m(x) P_{n+1}^{m-1}(x) = 0 \quad (m \geq 0) \quad (\text{C.51})$$

$$\begin{aligned}
& \int_{-1}^1 dx \frac{1}{\sqrt{1-x^2}} P_n^m(x) P_{n+1}^{m+1}(x) \\
&= \int_{-1}^1 dx P_n^m(x) \left[-(2n+1) P_n^m(x) - (2n-3) P_{n-2}^m - \dots \right] \\
&= -(2n+1) \int_{-1}^1 P_n^m(x) P_n^m(x)
\end{aligned}$$

$$\int_{-1}^1 dx \frac{1}{\sqrt{1-x^2}} P_n^m(x) P_{n+1}^{m+1}(x) = (-2) \frac{(n+m)!}{(n-m)!} \quad (m \geq 0) \quad (\text{C.52})$$

$$\begin{aligned}
& \int_{-1}^1 dx \frac{1}{\sqrt{1-x^2}} P_n^m(x) P_{n-1}^{m+1}(x) \\
&= \int_{-1}^1 dx P_n^m(x) \left[-(2n+1) P_{n-2}^m(x) - (2n-3) P_{n-4}^m - \dots \right]
\end{aligned}$$

$$\int_{-1}^1 dx \frac{1}{\sqrt{1-x^2}} P_n^m(x) P_{n-1}^{m+1}(x) = 0 \quad (m \geq 0) \quad (\text{C.53})$$

$$\begin{aligned}
& \int_{-1}^1 dx \frac{1}{\sqrt{1-x^2}} P_n^m(x) P_{n-1}^{m-1}(x) \\
&= \int_{-1}^1 dx P_{n-1}^{m-1}(x) \left[-(2n-1) P_{n-1}^{m-1}(x) - (2n-5) P_{n-3}^{m-1} - \dots \right] \\
&= -(2n-1) \int_{-1}^1 P_{n-1}^{m-1}(x) P_{n-1}^{m-1}(x)
\end{aligned}$$

$$\int_{-1}^1 dx \frac{1}{\sqrt{1-x^2}} P_n^m(x) P_{n-1}^{m-1}(x) = (-2) \frac{(n+m-2)!}{(n-m)!} \quad (m \geq 0) \quad (\text{C.54})$$

$$\begin{aligned}
& \int_{-1}^1 dx \frac{1}{\sqrt{1-x^2}} P_n^m(x) P_{n+1}^{m-1}(x) \\
&= \int_{-1}^1 dx P_n^m(x) \left[-(2n-1) P_{n-1}^{m-1}(x) - (2n-5) P_{n-3}^{m-1} - \dots \right]
\end{aligned}$$

$$\int_{-1}^1 dx \frac{1}{\sqrt{1-x^2}} P_n^m(x) P_{n+1}^{m-1}(x) = 0 \quad (m \geq 0) \quad (\text{C.55})$$

$$\begin{aligned}
& \int_{-1}^1 dx \frac{x^2}{\sqrt{1-x^2}} P_n^m(x) P_{n+1}^{m+1}(x) \\
&= \int_{-1}^1 dx \frac{1}{\sqrt{1-x^2}} P_n^m(x) P_{n+1}^{m+1}(x) - \int_{-1}^1 dx \sqrt{1-x^2} P_n^m(x) P_{n+1}^{m+1}(x) \\
&= (-2) \frac{(n+m)!}{(n-m)!} + \frac{2}{(2n+1)(2n+3)} \frac{(n+m+2)!}{(n-m)!}
\end{aligned}$$

$$\int_{-1}^1 dx \frac{x^2}{\sqrt{1-x^2}} P_n^m(x) P_{n+1}^{m+1}(x) = 2 \frac{(n+m)!}{(n-m)!} \left[\frac{(n+m+2)(n+m+1)}{(2n+1)(2n+3)} - 1 \right] \quad (\text{C.56})$$

$$\int_{-1}^1 dx \frac{x^2}{\sqrt{1-x^2}} P_n^m(x) P_{n-1}^{m+1}(x)$$

$$\begin{aligned}
&= \int_{-1}^1 dx \frac{1}{\sqrt{1-x^2}} P_n^m(x) P_{n-1}^{m+1}(x) - \int_{-1}^1 dx \sqrt{1-x^2} P_n^m(x) P_{n-1}^{m+1}(x) \\
&= 0 - \frac{2}{(2n+1)(2n-1)} \frac{(n+m)!}{(n-m-2)!}
\end{aligned}$$

$$\int_{-1}^1 dx \frac{x^2}{\sqrt{1-x^2}} P_n^m(x) P_{n-1}^{m+1}(x) = \frac{(-2)}{(2n+1)(2n-1)} \frac{(n+m)!}{(n-m-2)!} \quad (\text{C.57})$$

$$\begin{aligned}
&\int_{-1}^1 dx \frac{x^2}{\sqrt{1-x^2}} P_n^m(x) P_{n-1}^{m-1}(x) \\
&= \int_{-1}^1 dx \frac{1}{\sqrt{1-x^2}} P_n^m(x) P_{n-1}^{m-1}(x) - \int_{-1}^1 dx \sqrt{1-x^2} P_n^m(x) P_{n-1}^{m-1}(x) \\
&= (-2) \frac{(n+m-2)!}{(n-m)!} + \frac{2}{(2n+1)(2n-1)} \frac{(n+m)!}{(n-m)!}
\end{aligned}$$

$$\int_{-1}^1 dx \frac{x^2}{\sqrt{1-x^2}} P_n^m(x) P_{n-1}^{m-1}(x) = 2 \frac{(n+m-2)!}{(n-m)!} \left[\frac{(n+m)(n+m-1)}{(2n+1)(2n-1)} - 1 \right] \quad (\text{C.58})$$

$$\begin{aligned}
&\int_{-1}^1 dx \frac{x^2}{\sqrt{1-x^2}} P_n^m(x) P_{n+1}^{m-1}(x) \\
&= \int_{-1}^1 dx \frac{1}{\sqrt{1-x^2}} P_n^m(x) P_{n+1}^{m-1}(x) - \int_{-1}^1 dx \sqrt{1-x^2} P_n^m(x) P_{n+1}^{m-1}(x) \\
&= 0 - \frac{2}{(2n+1)(2n+3)} \frac{(n+m)!}{(n-m)!}
\end{aligned}$$

$$\int_{-1}^1 dx \frac{x^2}{\sqrt{1-x^2}} P_n^m(x) P_{n+1}^{m-1}(x) = \frac{(-2)}{(2n+1)(2n+3)} \frac{(n+m)!}{(n-m)!} \quad (\text{C.59})$$

Now we have seen that

$$\frac{d}{d\theta} P_n^m(x) = \frac{1}{\sqrt{1-x^2}} \left[nx P_n^m(x) - (n+m) P_{n-1}^m(x) \right]$$

and therefore

$$\begin{aligned}
& \int_0^\pi d\theta \sin \theta \cos \theta \left(\frac{d}{d\theta} P_n^m(\cos \theta) \right) P_{n+1}^{m+1}(\cos \theta) \\
&= n \int_{-1}^1 dx \frac{x^2}{\sqrt{1-x^2}} P_n^m(x) P_{n+1}^{m+1}(x) - (n+m) \int_{-1}^1 dx \frac{x}{\sqrt{1-x^2}} P_{n-1}^m(x) P_{n+1}^{m+1}(x) \\
&= n 2 \frac{(n+m)!}{(n-m)!} \left[\frac{(n+m+2)(n+m+1)}{(2n+1)(2n+3)} - 1 \right] - (n+m)(-2) \frac{(n+m-1)!}{(n-m-1)!}
\end{aligned}$$

$$\begin{aligned}
& \int_0^\pi d\theta \sin \theta \cos \theta \left(\frac{d}{d\theta} P_n^m(\cos \theta) \right) P_{n+1}^{m+1}(\cos \theta) \quad (C.60) \\
&= 2 \frac{(n+m)!}{(n-m)!} \left[\frac{n(n+m+2)(n+m+1)}{(2n+1)(2n+3)} - m \right]
\end{aligned}$$

$$\begin{aligned}
& \int_0^\pi d\theta \sin \theta \cos \theta \left(\frac{d}{d\theta} P_n^m(\cos \theta) \right) P_{n-1}^{m+1}(\cos \theta) \\
&= n \int_{-1}^1 dx \frac{x^2}{\sqrt{1-x^2}} P_n^m(x) P_{n-1}^{m+1}(x) - (n+m) \int_{-1}^1 dx \frac{x}{\sqrt{1-x^2}} P_{n-1}^m(x) P_{n-1}^{m+1}(x) \\
&= n \frac{(-2)}{(2n+1)(2n-1)} \frac{(n+m)!}{(n-m-2)!} - (n+m) \frac{(-2)(n+m-1)}{(2n-1)} \frac{(n+m-2)!}{(n-m-2)!}
\end{aligned}$$

$$\begin{aligned}
& \int_0^\pi d\theta \sin \theta \cos \theta \left(\frac{d}{d\theta} P_n^m(\cos \theta) \right) P_{n-1}^{m+1}(\cos \theta) \quad (C.61) \\
&= \frac{2(n+1)}{(2n-1)(2n+1)} \frac{(n+m)!}{(n-m-2)!}
\end{aligned}$$

$$\begin{aligned}
& \int_0^\pi d\theta \sin \theta \cos \theta \left(\frac{d}{d\theta} P_n^m(\cos \theta) \right) P_{n+1}^{m-1}(\cos \theta) \\
&= n \int_{-1}^1 dx \frac{x^2}{\sqrt{1-x^2}} P_n^m(x) P_{n+1}^{m-1}(x) - (n+m) \int_{-1}^1 dx \frac{x}{\sqrt{1-x^2}} P_{n-1}^m(x) P_{n+1}^{m-1}(x) \\
&= n \frac{(-2)}{(2n+1)(2n+3)} \frac{(n+m)!}{(n-m)!} - 0
\end{aligned}$$

$$\int_0^\pi d\theta \sin \theta \cos \theta \left(\frac{d}{d\theta} P_n^m(\cos \theta) \right) P_{n+1}^{m-1}(\cos \theta) \quad (C.62)$$

$$= \frac{(-2)n}{(2n+3)(2n+1)} \frac{(n+m)!}{(n-m)!}$$

$$\int_0^\pi d\theta \sin \theta \cos \theta \left(\frac{d}{d\theta} P_n^m(\cos \theta) \right) P_{n-1}^{m-1}(\cos \theta)$$

$$= n \int_{-1}^1 dx \frac{x^2}{\sqrt{1-x^2}} P_n^m(x) P_{n-1}^{m-1}(x) - (n+m) \int_{-1}^1 dx \frac{x}{\sqrt{1-x^2}} P_{n-1}^m(x) P_{n-1}^{m-1}(x)$$

$$= n 2 \frac{(n+m-2)!}{(n-m)!} \left[\frac{(n+m)(n+m-1)}{(2n-1)(2n+1)} - 1 \right] - (n+m) \frac{(-2)}{(2n-1)} \frac{(n+m-2)!}{(n-m-1)!}$$

$$\int_0^\pi d\theta \sin \theta \cos \theta \left(\frac{d}{d\theta} P_n^m(\cos \theta) \right) P_{n-1}^{m-1}(\cos \theta) \quad (C.63)$$

$$= \frac{2(n+m)}{(2n-1)} \frac{(n+m-2)!}{(n-m)!} \left[(n-m) + n \left(\frac{(n+m-1)}{(2n+1)} - \frac{(2n-1)}{(n+m)} \right) \right]$$

$$\int_{-1}^1 dx \frac{1}{\sqrt{1-x^2}} P_n^m(x) P_{n+1}^{m+1}(x) = \int_{-1}^1 dx P_n^m(x) \left[-(2n+1)P_n^m(x) - (2n-3)P_{n-2}^m - \dots \right]$$

$$\int_{-1}^1 dx \frac{1}{\sqrt{1-x^2}} P_n^m(x) P_{n+1}^{m+1}(x) = (-2) \frac{(n+m)!}{(n-m)!} \quad (C.64)$$

$$\int_{-1}^1 dx \frac{1}{\sqrt{1-x^2}} P_n^m(x) P_{n+1}^{m-1}(x)$$

$$= \int_{-1}^1 dx P_{n+1}^{m-1}(x) \left[-(2n-1)P_{n-1}^{m-1}(x) - (2n-5)P_{n-3}^{m-1} - \dots \right]$$

$$\int_{-1}^1 dx \frac{1}{\sqrt{1-x^2}} P_n^m(x) P_{n+1}^{m-1}(x) = 0 \quad (C.65)$$

$$\begin{aligned} & \int_{-1}^1 dx \frac{1}{\sqrt{1-x^2}} P_n^m(x) P_{n-1}^{m+1}(x) \\ &= \int_{-1}^1 dx P_n^m(x) \left[-(2n-3)P_{n-2}^m(x) - (2n-7)P_{n-4}^m - \dots \right] \end{aligned}$$

$$\int_{-1}^1 dx \frac{1}{\sqrt{1-x^2}} P_n^m(x) P_{n-1}^{m+1}(x) = 0 \quad (\text{C.66})$$

$$\begin{aligned} & \int_{-1}^1 dx \frac{1}{\sqrt{1-x^2}} P_n^m(x) P_{n-1}^{m-1}(x) \\ &= \int_{-1}^1 dx P_{n-1}^{m-1}(x) \left[-(2n-1)P_{n-1}^{m-1}(x) - (2n-5)P_{n-3}^{m-1} - \dots \right] \\ &= -(2n-1) \int_{-1}^1 dx P_{n-1}^{m-1}(x) P_{n-1}^{m-1}(x) \end{aligned}$$

$$\int_{-1}^1 dx \frac{1}{\sqrt{1-x^2}} P_n^m(x) P_{n-1}^{m-1}(x) = (-2) \frac{(n+m-2)!}{(n-m)!} \quad (\text{C.67})$$

Making the substitution $n' = n + 1$ we obtain

$$\begin{aligned} & \int_{-1}^1 dx \frac{x}{\sqrt{1-x^2}} P_n^m(x) P_n^{m+1}(x) \\ & \xrightarrow{n \rightarrow n'-1} \int_{-1}^1 dx \frac{x}{\sqrt{1-x^2}} P_{n'-1}^m(x) P_{n'-1}^{m+1}(x). \end{aligned}$$

We have already evaluated such integrals (Equation C.48). Thus we obtain the answer by simple substitution $n \rightarrow n - 1$ in the previously found result:

$$\int_{-1}^1 dx \frac{x}{\sqrt{1-x^2}} P_n^m(x) P_n^{m+1}(x) = \frac{(-2)}{(2n+1)} \frac{(n+m)!}{(n-m-1)!} \quad (\text{C.68})$$

Similarly,

$$\begin{aligned} & \int_{-1}^1 dx \frac{x}{\sqrt{1-x^2}} P_n^m(x) P_n^{m-1}(x) \\ & \xrightarrow{n \rightarrow n'-1} \int_{-1}^1 dx \frac{x}{\sqrt{1-x^2}} P_{n'-1}^m(x) P_{n'-1}^{m-1}(x). \end{aligned}$$

Using the result already obtained (Equation C.49) we obtain:

$$\int_{-1}^1 dx \frac{x}{\sqrt{1-x^2}} P_n^m(x) P_n^{m-1}(x) = \frac{(-2)}{(2n+1)} \frac{(n+m-1)!}{(n-m)!} \quad (\text{C.69})$$

$$\begin{aligned} & \int_0^\pi d\theta \sin \theta \left(\frac{d}{d\theta} P_n^m(\cos \theta) \right) P_n^{m+1}(\cos \theta) \\ &= n \int_{-1}^1 dx \frac{x}{\sqrt{1-x^2}} P_n^m(x) P_n^{m+1}(x) - (n+m) \int_{-1}^1 dx \frac{1}{\sqrt{1-x^2}} P_{n-1}^m(x) P_n^{m+1}(x). \end{aligned}$$

The second integral with the substitution $n \rightarrow n+1$ is immediately transformed to an integral of type given by Equation C.52. The first integral is of the type just obtained in Equation C.68. Thus we obtain on substitution:

$$\int_0^\pi d\theta \sin \theta \left(\frac{d}{d\theta} P_n^m(\cos \theta) \right) P_n^{m+1}(\cos \theta) = \frac{2(n+1)}{(2n+1)} \frac{(n+m)!}{(n-m-1)!} \quad (\text{C.70})$$

$$\begin{aligned} & \int_0^\pi d\theta \sin \theta \left(\frac{d}{d\theta} P_n^m(\cos \theta) \right) P_n^{m-1}(\cos \theta) \\ &= n \int_{-1}^1 dx \frac{x}{\sqrt{1-x^2}} P_n^m(x) P_n^{m-1}(x) - (n+m) \int_{-1}^1 dx \frac{1}{\sqrt{1-x^2}} P_{n-1}^m(x) P_n^{m-1}(x). \end{aligned}$$

Now the second integral with the substitution $n \rightarrow n+1$ is immediately transformed to an integral of type given by Equation C.55 and therefore vanishes. The first integral is of the type obtained in Equation C.69. Thus we obtain on substitution:

$$\int_0^\pi d\theta \sin \theta \left(\frac{d}{d\theta} P_n^m(\cos \theta) \right) P_n^{m-1}(\cos \theta) = \frac{(-2)n}{(2n+1)} \frac{(n+m-1)!}{(n-m)!} \quad (\text{C.71})$$

$$\begin{aligned} & \int_{-1}^1 dx x P_n^m(x) P_{n-1}^m(x) \\ &= \frac{1}{(2n+1)} \int_{-1}^1 dx P_{n-1}^m(x) \left[(n-m+1) P_{n+1}^m(x) + (n+m) P_{n-1}^m(x) \right] \\ &= \frac{(n+m)}{(2n+1)} \int_{-1}^1 dx P_{n-1}^m(x) P_{n-1}^m(x) \end{aligned}$$

$$\int_{-1}^1 dx x P_n^m(x) P_{n-1}^m(x) = \frac{2}{(2n-1)(2n+1)} \frac{(n+m)!}{(n-m-1)!} \quad (\text{C.72})$$

$$\begin{aligned} & \int_{-1}^1 dx x P_n^m(x) P_{n+1}^m(x) \\ &= \frac{1}{(2n+1)} \int_{-1}^1 dx P_{n+1}^m(x) \left[(n-m+1) P_{n+1}^m(x) + (n+m) P_{n-1}^m(x) \right] \\ &= \frac{(n-m+1)}{(2n+1)} \int_{-1}^1 dx P_{n+1}^m(x) P_{n+1}^m(x) \end{aligned}$$

$$\int_{-1}^1 dx x P_n^m(x) P_{n+1}^m(x) = \frac{2}{(2n+3)(2n+1)} \frac{(n+m+1)!}{(n-m)!} \quad (\text{C.73})$$

$$\begin{aligned} & \int_0^\pi d\theta \sin^2 \theta \left(\frac{d}{d\theta} P_n^m(\cos \theta) \right) P_{n+1}^m(\cos \theta) \\ &= n \int_{-1}^1 dx x P_n^m(x) P_{n+1}^m(x) - (n+m) \int_{-1}^1 dx P_{n-1}^m(x) P_{n+1}^m(x). \end{aligned}$$

The second integral vanishes immediately due to the orthogonality of the $P_n^m(x)$ functions. The first integral is obtained from Equation C.73. Thus on simplification we obtain:

$$\int_0^\pi d\theta \sin^2 \theta \left(\frac{d}{d\theta} P_n^m(\cos \theta) \right) P_{n+1}^m(\cos \theta) = \frac{2n}{(2n+1)(2n+3)} \frac{(n+m+1)!}{(n-m)!} \quad (\text{C.74})$$

$$\begin{aligned} & \int_0^\pi d\theta \sin^2 \theta \left(\frac{d}{d\theta} P_n^m(\cos \theta) \right) P_{n-1}^m(\cos \theta) \\ &= n \int_{-1}^1 dx x P_n^m(x) P_{n-1}^m(x) - (n+m) \int_{-1}^1 dx P_{n-1}^m(x) P_{n-1}^m(x) \\ &= n \frac{2}{(2n-1)(2n+1)} \frac{(n+m)!}{(n-m)!} - (n+m) \frac{2}{(2n-1)} \frac{(n+m-1)!}{(n-m-1)!} \end{aligned}$$

$$\int_0^\pi d\theta \sin^2 \theta \left(\frac{d}{d\theta} P_n^m(\cos \theta) \right) P_{n-1}^m(\cos \theta) = \frac{(-2)(n+1)}{(2n+1)(2n-1)} \frac{(n+m)!}{(n-m-1)!} \quad (\text{C.75})$$

C.4 Additional Integrals

The (Associated) Legendre's differential equation can be written in the following form:

$$\frac{d}{dx} \left[(1-x^2) \frac{dP_n^m}{dx} \right] + \left[n(n+1) - \frac{m^2}{1-x^2} \right] P_n^m = 0. \quad (\text{C.76})$$

where P_n^m are the usual Associated Legendre functions. We can write

$$\frac{d}{dx} \left[(1-x^2) \frac{dP_n^m}{dx} \right] = (1-x^2) \frac{d^2 P_n^m}{dx^2} - 2x \frac{dP_n^m}{dx}.$$

and

$$\frac{d}{dx} \left[(1-x^2) P_{n'}^m \frac{dP_n^m}{dx} \right] = P_{n'}^m \frac{d}{dx} \left[(1-x^2) \frac{dP_n^m}{dx} \right] + (1-x^2) \frac{dP_n^m}{dx} \frac{dP_{n'}^m}{dx}$$

So

$$P_{n'}^m \frac{d}{dx} \left[(1-x^2) \frac{dP_n^m}{dx} \right] = \frac{d}{dx} \left[(1-x^2) P_{n'}^m \frac{dP_n^m}{dx} \right] - (1-x^2) \frac{dP_n^m}{dx} \frac{dP_{n'}^m}{dx}. \quad (\text{C.77})$$

Multiplying both sides of Equation C.76 by $P_{n'}^m$ and P_n^m respectively, we obtain:

$$\begin{aligned} P_{n'}^m \frac{d}{dx} \left[(1-x^2) \frac{dP_n^m}{dx} \right] + \left[n(n+1) - \frac{m^2}{1-x^2} \right] P_{n'}^m P_n^m &= 0 \\ P_n^m \frac{d}{dx} \left[(1-x^2) \frac{dP_{n'}^m}{dx} \right] + \left[n'(n'+1) - \frac{m^2}{1-x^2} \right] P_n^m P_{n'}^m &= 0 \end{aligned}$$

Or,

$$\frac{d}{dx} \left[(1-x^2) P_{n'}^m \frac{dP_n^m}{dx} \right] - (1-x^2) \frac{dP_n^m}{dx} \frac{dP_{n'}^m}{dx} + \left[n(n+1) - \frac{m^2}{1-x^2} \right] P_{n'}^m P_n^m = 0 \quad (\text{C.78})$$

$$\frac{d}{dx} \left[(1-x^2) P_n^m \frac{dP_{n'}^m}{dx} \right] - (1-x^2) \frac{dP_{n'}^m}{dx} \frac{dP_n^m}{dx} + \left[n'(n'+1) - \frac{m^2}{1-x^2} \right] P_n^m P_{n'}^m = 0 \quad (\text{C.79})$$

Subtracting Equation C.79 from Equation C.78 we obtain

$$\frac{d}{dx} \left[(1-x^2) \left\{ P_{n'}^m \frac{dP_n^m}{dx} - P_n^m \frac{dP_{n'}^m}{dx} \right\} \right] + [n(n+1) - n'(n'+1)] P_n^m P_{n'}^m = 0.$$

Integrating both sides with respect to x , between -1 and 1 , we obtain

$$(1-x^2) \left\{ P_{n'}^m \frac{dP_n^m}{dx} - P_n^m \frac{dP_{n'}^m}{dx} \right\} \Big|_{-1}^1 + [n(n+1) - n'(n'+1)] \int_{-1}^1 dx P_n^m P_{n'}^m = 0.$$

The first term vanishes at $x = \pm 1$ since the factor $(1-x^2)$ vanishes. The second term must therefore be zero. So, if $n \neq n'$ then we arrive at our usual orthogonal relation:

$$\int_{-1}^1 dx P_n^m(x) P_{n'}^m(x) = 0 \quad (n \neq n') \quad (\text{C.80})$$

Adding Equation C.79 and Equation C.78 we obtain

$$\begin{aligned} \frac{d}{dx} \left[(1-x^2) \left\{ P_{n'}^m \frac{dP_n^m}{dx} + P_n^m \frac{dP_{n'}^m}{dx} \right\} \right] + [n(n+1) + n'(n'+1)] P_n^m P_{n'}^m \\ = 2(1-x^2) \frac{dP_n^m}{dx} \frac{dP_{n'}^m}{dx} + \frac{2m^2}{1-x^2} P_n^m P_{n'}^m. \end{aligned}$$

Integrating both sides with respect to x , between -1 and 1 , the first term on the left hand side will vanish again because of the $(1-x^2)$ factor. Therefore we immediately arrive at the following relation:

$$\frac{n(n+1) + n'(n'+1)}{2} \int_{-1}^1 dx P_n^m P_{n'}^m = \int_{-1}^1 dx \left\{ (1-x^2) \frac{dP_n^m}{dx} \frac{dP_{n'}^m}{dx} + \frac{m^2}{1-x^2} P_n^m P_{n'}^m \right\}.$$

Changing the variables to θ , so that

$$\begin{aligned} \frac{d}{dx} P_n^m(x) &= -\frac{1}{\sin \theta} \frac{d}{d\theta} P_n^m(\cos \theta) \quad \text{and,} \\ (1-x^2) \frac{d}{dx} P_n^m(x) \frac{d}{dx} P_{n'}^m(x) &= \frac{d}{d\theta} P_n^m(\cos \theta) \frac{d}{d\theta} P_{n'}^m(\cos \theta). \end{aligned}$$

we arrive at the important integral

$$\begin{aligned} \int_0^\pi d\theta \sin \theta \left(\frac{d}{d\theta} P_n^m(\cos \theta) \frac{d}{d\theta} P_{n'}^m(\cos \theta) + \frac{m^2}{\sin^2 \theta} P_n^m(\cos \theta) P_{n'}^m(\cos \theta) \right) \\ \frac{n(n+1) + n'(n'+1)}{2} \int_{-1}^1 dx P_n^m(x) P_{n'}^m(x) \end{aligned}$$

Using the orthogonality of the P_n^m , this immediately implies:

$$\int_0^\pi d\theta \sin \theta \left(\frac{d}{d\theta} P_n^m \frac{d}{d\theta} P_{n'}^m + \frac{m^2}{\sin^2 \theta} P_n^m P_{n'}^m \right) = \frac{2n(n+1)(n+m)!}{2n+1(n-m)!} \delta_{nn'} \quad (\text{C.81})$$

Appendix D

Evaluating Inner Product Integrals

D.1 Introduction

In this appendix we show the details of carrying out various integrations, required to obtain the inner products in the determination of the expansion coefficients of a plane wave. We will employ various results summarized in some of the other appendices, in particular the appendices on spherical Bessel functions and the Associated Legendre functions will be used frequently. We have:

$$e^{i\mathbf{k}\cdot\mathbf{r}} = \sum_{s=0}^{\infty} i^s (2s+1) j_s(kr) \left\{ \sum_{l=0}^s \frac{(s-l)!}{(s+l)!} P_s^l(\cos\alpha) \epsilon^{-il\beta} P_s^l(\cos\theta) \epsilon^{il\phi} + \sum_{l=1}^s \frac{(s-l)!}{(s+l)!} P_s^l(\cos\alpha) \epsilon^{il\beta} P_s^l(\cos\theta) \epsilon^{-il\phi} \right\}. \quad (\text{D.1})$$

where α , β specify the direction cosines of \mathbf{k} , and θ , ϕ give the direction cosines of \mathbf{r} . Also $|\mathbf{k}| = k$ and $|\mathbf{r}| = r$ in the above expression. The unit vectors of the cartesian coordinate system assume the following form in spherical polar coordinates:

$$\mathbf{e}_x = \sin\theta \cos\phi \mathbf{e}_r + \cos\theta \cos\phi \mathbf{e}_\theta - \sin\phi \mathbf{e}_\phi \quad (\text{D.2})$$

$$\mathbf{e}_y = \sin\theta \sin\phi \mathbf{e}_r + \cos\theta \sin\phi \mathbf{e}_\theta + \cos\phi \mathbf{e}_\phi \quad (\text{D.3})$$

$$\mathbf{e}_z = \cos\theta \mathbf{e}_r - \sin\theta \mathbf{e}_\theta. \quad (\text{D.4})$$

The $e^{i\mathbf{k}\cdot\mathbf{r}}$ term involves a double infinite summation in the indices s and l . As we shall soon find out, the various orthogonal properties of the functions involved in these integrations of the inner products will eventually allow only a few surviving terms. This will allow us to carry out these integrations analytically, giving us closed form expressions for the final results.

D.2 Evaluation of $\langle \mathbf{E}_z | \mathbf{M}_{mn} \rangle$

These inner products are necessary to evaluate the a_{mn}^z coefficients. We recall the definition for the inner product:

$$\langle \mathbf{E}_z | \mathbf{M}_{mn} \rangle = \int_0^\infty dr \int_0^\pi d\theta \sin \theta \int_0^{2\pi} d\phi \mathbf{e}_z \cdot \mathbf{M}_{mn}^* e^{i\mathbf{k}\cdot\mathbf{r}} = \int_{r\theta\phi} \mathbf{e}_z \cdot \mathbf{M}_{mn}^* e^{i\mathbf{k}\cdot\mathbf{r}}. \quad (\text{D.5})$$

where the $r\theta\phi$ below the last integral sign is a short-hand notation indicating that the integration is to be performed with respect to all three variables r , θ and ϕ . Similarly if we had only $r\theta$ below the integral sign, it would indicate that the ϕ -integration has already been carried out. Now,

$$\mathbf{M}_{mn}^* = -imj_n(kr) \frac{P_n^m(\cos \theta)}{\sin \theta} e^{-im\phi} \mathbf{e}_\theta - j_n(kr) \frac{dP_n^m(\cos \theta)}{d\theta} e^{-im\phi} \mathbf{e}_\phi. \quad (\text{D.6})$$

The \mathbf{M}_{mn}^* does not have any \mathbf{e}_r component, therefore we obtain

$$\begin{aligned} \langle \mathbf{E}_z | \mathbf{M}_{mn} \rangle &= \int_{r\theta\phi} (-\sin \theta \mathbf{e}_\theta) \cdot (-imj_n(kr) \frac{P_n^m(\cos \theta)}{\sin \theta} e^{-im\phi} \mathbf{e}_\theta) e^{i\mathbf{k}\cdot\mathbf{r}} \\ &= im \int_{r\theta\phi} e^{i\mathbf{k}\cdot\mathbf{r}} j_n(kr) P_n^m(\cos \theta) e^{-im\phi}. \end{aligned} \quad (\text{D.7})$$

This clearly vanishes when $m = 0 \Rightarrow a_{0n}^z = 0$. The $e^{i\mathbf{k}\cdot\mathbf{r}}$ factor has ϕ -dependence of the form $e^{\pm i l \phi}$. Therefore, the ϕ -integrations involved in this case are:

$$\int_0^{2\pi} d\phi e^{i l \phi} e^{-im\phi} = 2\pi \delta_{l,m} \quad \text{and} \quad (\text{D.8})$$

$$\int_0^{2\pi} d\phi e^{-i l \phi} e^{-im\phi} = 2\pi \delta_{l,-m}. \quad (\text{D.9})$$

Thus among all the terms in the l -summations, only $l = \pm m$ terms survive as a result of the orthogonality properties of the complex exponential functions. Since $l \geq 0$ in the summations for $e^{i\mathbf{k}\cdot\mathbf{r}}$, when $m > 0$, only the terms corresponding $l = m$ will contribute, that is those terms containing the factor $e^{-im\phi}$. On the other hand, when $m < 0$, only the $e^{im\phi}$ terms can be non-zero. The θ -integrations involved are of the form :

$$\int_0^\pi d\theta \sin \theta P_s^l(\cos \theta) P_n^m(\cos \theta) \quad (l = \pm m) \quad (\text{D.10})$$

Until we know the constraints imposed on the values of s , we still have another potentially infinite summation to deal with. Let us consider the r -integration for the moment:

$$\int_0^\infty dr j_s(kr) j_n(kr) = 0 \quad (s - n \text{ is even, } s \neq n) \quad (\text{D.11})$$

Let us consider the parity of the θ -integral. Since $P_n^m(-x) = (-1)^{m+n} P_n^m(x)$, we immediately see that the parity of the integrand in the theta integration is:

$$\int_{-1}^1 dx P_s^l(x) P_n^m(x) \quad \text{has parity} \sim (-1)^{s+l+n+m}.$$

Since $l = \pm m$ the θ -integral will be non-zero only for $s + n$ equal to an even number, i.e. $s + n = 2k$, where k is an integer. Equivalently stated, the θ -integral may not vanish only when s and n differ by an even number, including zero. On the other hand, the r -integral vanishes when s and n differ by an even number, except zero. Thus the only possible term that survive from considering the parity of both the θ and the r integrations is the $n = s$ term. Thus, from the double infinite summation we have only one surviving term that can contribute to the integral for the inner product. Thus with $l = m$ and $s = n$, the θ -integral is evaluated in the following way:

$$\int_0^\pi d\theta \sin \theta P_n^m(\cos \theta) P_n^m(\cos \theta) = \int_{-1}^1 dx P_n^m(x) P_n^m(x) = \frac{2}{2n+1} \frac{(n+m)!}{(n-m)!} \quad (\text{D.12})$$

and the r -integral becomes:

$$\int_0^\infty dr j_n(kr) j_n(kr) = \frac{\pi}{2k(2n+1)}$$

Thus, for $m \geq 0$, we have:

$$\begin{aligned} \langle \mathbf{E}_z | \mathbf{M}_{mn} \rangle &= im \int_{r\theta\phi} e^{i\mathbf{k}\cdot\mathbf{r}} j_n(kr) P_n^m(\cos \theta) e^{-im\phi} \\ &= im \int_0^\infty dr \int_0^\pi d\theta \sin \theta \int_0^{2\pi} d\phi \sum_{s=0}^\infty i^s (2s+1) j_s(kr) \times \\ &\quad \left\{ \sum_{l=0}^s \frac{(s-l)!}{(s+l)!} P_s^l(\cos \alpha) e^{-il\beta} P_s^l(\cos \theta) e^{il\phi} \right. \\ &\quad \left. + \sum_{l=1}^s \frac{(s-l)!}{(s+l)!} P_s^l(\cos \alpha) e^{il\beta} P_s^l(\cos \theta) e^{-il\phi} \right\} j_n(kr) P_n^m(\cos \theta) e^{-im\phi} \\ &= 2\pi im \sum_{s=0}^\infty i^s (2s+1) \left(\int_0^\infty dr j_s(kr) j_n(kr) \right) \times \\ &\quad \left(\frac{(s-m)!}{(s+m)!} P_s^m(\cos \alpha) e^{-im\beta} \int_0^\pi d\theta \sin \theta P_s^m(\cos \theta) P_n^m(\cos \theta) \right) \\ &= 2\pi im i^n (2n+1) \frac{\pi}{2k(2n+1)} \times \quad (\text{Since only } s = n \text{ allowed}) \\ &\quad \frac{(n-m)!}{(n+m)!} P_n^m(\cos \alpha) e^{-im\beta} \frac{2}{(2n+1)} \frac{(n+m)!}{(n-m)!}. \end{aligned}$$

Thus the expression for the inner product becomes:

$$\langle \mathbf{E}_z | \mathbf{M}_{mn} \rangle = i^{n+1} \frac{\pi^2}{k} \frac{2m}{(2n+1)} P_n^m(\cos \alpha) e^{-im\beta} \quad (\text{D.13})$$

D.3 Evaluation of $\langle \mathbf{E}_z | \mathbf{N}_{mn} \rangle$

The $\langle \mathbf{E}_z | \mathbf{N}_{mn} \rangle$ integrals are used to evaluate the b_{mn}^* coefficients. We have:

$$\langle \mathbf{E}_z | \mathbf{N}_{mn} \rangle = \int_0^\infty dr \int_0^\pi d\theta \sin \theta \int_0^{2\pi} d\phi \mathbf{e}_z \cdot \mathbf{N}_{mn}^* e^{i\mathbf{k} \cdot \mathbf{r}} = \int_{r\theta\phi} \mathbf{e}_z \cdot \mathbf{N}_{mn}^* e^{i\mathbf{k} \cdot \mathbf{r}}. \quad (\text{D.14})$$

Now,

$$\begin{aligned} \mathbf{N}_{mn}^* = & n(n+1) \frac{j_n(kr)}{kr} P_n^m(\cos \theta) e^{-im\phi} \mathbf{e}_r + \frac{1}{kr} \frac{d(rj_n(kr))}{dr} \frac{dP_n^m(\cos \theta)}{d\theta} e^{-im\phi} \mathbf{e}_\theta \\ & - im \frac{1}{kr} \frac{d(rj_n(kr))}{dr} \frac{P_n^m(\cos \theta)}{\sin \theta} e^{-im\phi} \mathbf{e}_\phi. \end{aligned} \quad (\text{D.15})$$

Therefore,

$$\begin{aligned} \mathbf{e}_z \cdot \mathbf{N}_{mn}^* = & n(n+1) \frac{j_n(kr)}{kr} \cos \theta P_n^m(\cos \theta) e^{-im\phi} \\ & - \frac{1}{kr} \frac{d(rj_n(kr))}{dr} \sin \theta \frac{dP_n^m(\cos \theta)}{d\theta} e^{-im\phi}. \end{aligned} \quad (\text{D.16})$$

As in the previous case, the ϕ -integrals will be non-vanishing for $l = \pm m$ only. However, the r -integrals are now of the form:

$$\int_0^\infty dr j_s(kr) \frac{j_n(kr)}{kr} \quad \text{and} \quad \int_0^\infty dr j_s(kr) \frac{1}{kr} \frac{d(rj_n(kr))}{dr}.$$

As derived in the appendix on the spherical Bessel functions, such integrals are non-vanishing when $s = n \pm 1$ or when $s - n$ is an even number. Let us now consider the parity of the θ -integrals:

$$\begin{aligned} \int_0^\pi d\theta \sin \theta \cos \theta P_n^m(\cos \theta) P_s^m(\cos \theta) & \sim (-1)^{1+m+n+m+s} \sim (-1)^{s+n+1} \\ \int_0^\pi d\theta \sin \theta \sin \theta \left(\frac{d}{d\theta} P_n^m(\cos \theta) \right) P_s^m(\cos \theta) & \sim (-1)^{m+n+1+m+s} \sim (-1)^{s+n-1}. \end{aligned}$$

where the $\sin \theta$ does not change sign (since $\sin \theta = \sin(\pi - \theta)$) and the parity of the derivative of Associated Legendre functions will be one greater than the corresponding Associated Legendre function (see eqn C.11). Thus in either case above, the θ -integrals will vanish when $s + n$ is an even number (or equivalently, $s - n$ is an even number). The θ -integrals may be non-vanishing when $s = n \pm 1$. Thus, by considering the mutual parity of the r and θ integrals we conclude that *only* the $s = n \pm 1$ and $l = \pm m$ terms can contribute to the expression for $\langle \mathbf{E}_z | \mathbf{N}_{mn} \rangle$.

For $m \geq 0$ we have the $s = n + 1$ terms:

$$2\pi i^{n+1} (2n+3) e^{-im\beta} P_{n+1}^m(\cos \alpha) \frac{(n+1-m)!}{(n+1+m)!} \times \\ \left[\left(n(n+1) \int_0^\infty dr j_{n+1}(kr) \frac{j_n(kr)}{kr} \right) \cdot \left(\int_0^\pi d\theta \sin \theta \cos \theta P_n^m(\cos \theta) P_{n+1}^m(\cos \theta) \right) \right. \\ \left. - \left(\int_0^\infty dr j_{n+1}(kr) \frac{1}{kr} \frac{d(rj_n(kr))}{dr} \right) \cdot \left(\int_0^\pi d\theta \sin^2 \theta \frac{d}{d\theta} P_n^m(\cos \theta) P_{n+1}^m(\cos \theta) \right) \right].$$

The θ -integrals are readily obtained from Equations C.73 and C.74. The r -integrals are obtained from Equations B.33 and B.36. Thus we obtain the $s = n + 1$ term :

$$2\pi i^{n+1} (2n+3) e^{-im\beta} P_{n+1}^m(\cos \alpha) \frac{(n+1-m)!}{(n+1+m)!} \times \\ \left[\left(n(n+1) \frac{\pi}{2k(2n+1)(2n+3)} \right) \cdot \left(\frac{2}{(2n+1)(2n+3)} \frac{(n+m+1)!}{(n-m)!} \right) \right. \\ \left. - \left(-\frac{\pi n}{2k(2n+1)(2n+3)} \right) \cdot \left(\frac{2n}{(2n+1)(2n+3)} \frac{(n+m+1)!}{(n-m)!} \right) \right] \\ = i^{n+1} \frac{\pi^2}{k} \frac{2n(n-m+1)}{(2n+1)(2n+3)} e^{-im\beta} P_{n+1}^m(\cos \alpha). \quad (\text{D.17})$$

Similarly, the $s = n - 1$ terms are given by:

$$2\pi i^{n-1} (2n-1) e^{-im\beta} P_{n-1}^m(\cos \alpha) \frac{(n-1-m)!}{(n-1+m)!} \times \\ \left[\left(n(n+1) \int_0^\infty dr j_{n-1}(kr) \frac{j_n(kr)}{kr} \right) \cdot \left(\int_0^\pi d\theta \sin \theta \cos \theta P_n^m(\cos \theta) P_{n-1}^m(\cos \theta) \right) \right. \\ \left. - \left(\int_0^\infty dr j_{n-1}(kr) \frac{1}{kr} \frac{d(rj_n(kr))}{dr} \right) \cdot \left(\int_0^\pi d\theta \sin^2 \theta \frac{d}{d\theta} P_n^m(\cos \theta) P_{n-1}^m(\cos \theta) \right) \right].$$

Now the θ -integrals are given by Equations C.72 and C.75. The r -integrals are obtained from Equations B.32 and B.35. Therefore we obtain for the $s = n - 1$ term

:

$$\begin{aligned}
& 2\pi i^{n-1} (2n-1) e^{-im\beta} P_{n-1}^m(\cos \alpha) \frac{(n-1-m)!}{(n-1+m)!} \times \\
& \left[\left(n(n+1) \frac{\pi}{2k(2n-1)(2n+1)} \right) \cdot \left(\frac{2}{(2n-1)(2n+1)} \frac{(n+m)!}{(n-m-1)!} \right) \right. \\
& \quad \left. - \left(\frac{\pi(n+1)}{2k(2n-1)(2n+1)} \right) \cdot \left(-\frac{2(n+1)}{(2n-1)(2n+1)} \frac{(n+m)!}{(n-m-1)!} \right) \right] \\
& = i^{n-1} \frac{\pi^2 2(n+1)(n+m)}{k(2n-1)(2n+1)} e^{-im\beta} P_{n-1}^m(\cos \alpha). \tag{D.18}
\end{aligned}$$

The sum of the $s = n + 1$ and $s = n - 1$ terms give us the desired expression for the inner product $\langle \mathbf{E}_z | \mathbf{N}_{mn} \rangle$:

$$\begin{aligned}
\langle \mathbf{E}_z | \mathbf{N}_{mn} \rangle = & i^{n+1} \frac{2\pi^2}{k} \frac{e^{-im\beta}}{(2n+1)} \left[\frac{n(n-m+1)}{2n+3} P_{n+1}^m(\cos \alpha) \right. \\
& \left. - \frac{(n+1)(n+m)}{2n-1} P_{n-1}^m(\cos \alpha) \right] \tag{D.19}
\end{aligned}$$

D.4 Evaluation of $\langle \mathbf{E}_z | \mathbf{L}_{mn} \rangle$

The $\langle \mathbf{E}_z | \mathbf{L}_{mn} \rangle$ integrals are used to evaluate the c_{mn}^z coefficients. These can be evaluated in a way very similar to the process of obtaining the $\langle \mathbf{E}_z | \mathbf{N}_{mn} \rangle$ integral. Now.

$$\mathbf{L}_{mn}^* \cdot \mathbf{e}_z = k \left[\frac{dj_n(kr)}{d(kr)} \cos \theta P_n^m(\cos \theta) e^{-im\phi} - \frac{j_n(kr)}{kr} \sin \theta \frac{dP_n^m(\cos \theta)}{d\theta} e^{-im\phi} \right] \tag{D.20}$$

Again, by similar considerations on the parity of the ϕ , θ and r integrals, it is easy to see that only the $l = \pm m$ and $s = n \pm 1$ terms can be non-zero. For $m \geq 0$ we have the $s = n + 1$ terms:

$$\begin{aligned}
& k 2\pi i^{n+1} (2n+3) e^{-im\beta} P_{n+1}^m(\cos \alpha) \frac{(n+1-m)!}{(n+1+m)!} \times \\
& \left[\left(\int_0^\infty dr j_{n+1}(kr) \frac{d}{d(kr)} j_n(kr) \right) \cdot \left(\int_0^\pi d\theta \sin \theta \cos \theta P_n^m(\cos \theta) P_{n+1}^m(\cos \theta) \right) \right. \\
& \quad \left. - \left(\int_0^\infty dr j_{n+1}(kr) \frac{j_n(kr)}{kr} \right) \cdot \left(\int_0^\pi d\theta \sin^2 \theta \frac{d}{d\theta} P_n^m(\cos \theta) P_{n+1}^m(\cos \theta) \right) \right].
\end{aligned}$$

The θ -integrals are readily obtained from Equations C.73 and C.74. The r -integrals are obtained from Equations B.33 and B.39. Thus we obtain the $s = n + 1$ term :

$$\begin{aligned}
& k 2\pi i^{n+1} (2n+3) e^{-im\beta} P_{n+1}^m(\cos \alpha) \frac{(n+1-m)!}{(n+1+m)!} \times \\
& \left[\left(-\frac{\pi(n+1)}{2k(2n+1)(2n+3)} \right) \cdot \left(\frac{2}{(2n+1)(2n+3)} \frac{(n+m+1)!}{(n-m)!} \right) \right. \\
& \quad \left. - \left(\frac{\pi}{2k(2n+1)(2n+3)} \right) \cdot \left(\frac{2n}{(2n+1)(2n+3)} \frac{(n+m+1)!}{(n-m)!} \right) \right] \\
& = -2\pi^2 i^{n+1} \frac{(n-m+1)}{(2n+1)(2n+3)} e^{-im\beta} P_{n+1}^m(\cos \alpha). \tag{D.21}
\end{aligned}$$

Similarly, the $s = n - 1$ terms are given by:

$$\begin{aligned}
& k 2\pi i^{n-1} (2n-1) e^{-im\beta} P_{n-1}^m(\cos \alpha) \frac{(n-1-m)!}{(n-1+m)!} \times \\
& \left[\left(\int_0^\infty dr j_{n-1}(kr) \frac{d}{d(kr)} j_n(kr) \right) \cdot \left(\int_0^\pi d\theta \sin \theta \cos \theta P_n^m(\cos \theta) P_{n-1}^m(\cos \theta) \right) \right. \\
& \quad \left. - \left(\int_0^\infty dr j_{n-1}(kr) \frac{j_n(kr)}{kr} \right) \cdot \left(\int_0^\pi d\theta \sin^2 \theta \frac{d}{d\theta} P_n^m(\cos \theta) P_{n-1}^m(\cos \theta) \right) \right].
\end{aligned}$$

The θ -integrals are given by Equations C.72 and C.75. The r -integrals are obtained from Equations B.32 and B.38. Thus we obtain the $s = n - 1$ term :

$$\begin{aligned}
& k 2\pi i^{n-1} (2n-1) e^{-im\beta} P_{n-1}^m(\cos \alpha) \frac{(n-1-m)!}{(n-1+m)!} \times \\
& \left[\left(\frac{\pi n}{2k(2n-1)(2n+1)} \right) \cdot \left(\frac{2}{(2n-1)(2n+1)} \frac{(n+m)!}{(n-m-1)!} \right) \right. \\
& \quad \left. - \left(\frac{\pi}{2k(2n-1)(2n+1)} \right) \cdot \left(-\frac{2(n+1)}{(2n-1)(2n+1)} \frac{(n+m)!}{(n-m-1)!} \right) \right] \\
& = 2\pi^2 i^{n-1} \frac{(n-m)}{(2n-1)(2n+1)} e^{-im\beta} P_{n-1}^m(\cos \alpha). \tag{D.22}
\end{aligned}$$

The sum of the $s = n + 1$ and $s = n - 1$ terms give us the desired expression for the inner product $\langle \mathbf{E}_z | \mathbf{L}_{mn} \rangle$:

$$\langle \mathbf{E}_z | \mathbf{L}_{mn} \rangle = 2\pi^2 i^{n-1} \frac{e^{-im\beta}}{(2n+1)} \left[\frac{(n+m)}{2n-1} P_{n-1}^m(\cos \alpha) + \frac{(n-m+1)}{2n+3} P_{n+1}^m(\cos \alpha) \right] \quad (\text{D.23})$$

D.5 Evaluating $\langle \mathbf{E}_x | \mathbf{N}_{mn} \rangle$

We write \mathbf{e}_x in the following form:

$$\mathbf{e}_x = \frac{1}{2} \left[\sin \theta (e^{i\phi} + e^{-i\phi}) \mathbf{e}_r + \cos \theta (e^{i\phi} + e^{-i\phi}) \mathbf{e}_\theta + i (e^{i\phi} - e^{-i\phi}) \mathbf{e}_\phi \right]. \quad (\text{D.24})$$

Thus we have:

$$\begin{aligned} \mathbf{N}_{mn}^* \cdot \mathbf{e}_x &= \frac{1}{2} \left[n(n+1) \frac{j_n(kr)}{kr} \sin \theta P_n^m(\cos \theta) (e^{i\phi} + e^{-i\phi}) e^{-im\phi} \right. \\ &\quad + \frac{1}{kr} \frac{d(rj_n(kr))}{dr} \cos \theta \frac{dP_n^m(\cos \theta)}{d\theta} (e^{i\phi} + e^{-i\phi}) e^{-im\phi} \\ &\quad \left. + m \frac{1}{kr} \frac{d(rj_n(kr))}{dr} \frac{P_n^m(\cos \theta)}{\sin \theta} (e^{i\phi} - e^{-i\phi}) e^{-im\phi} \right]. \quad (\text{D.25}) \end{aligned}$$

The ϕ -integrals assume the following form now:

$$\int_0^{2\pi} d\phi (e^{i\phi} \pm e^{-i\phi}) e^{-im\phi} e^{i\phi} = 2\pi (\delta_{l,m-1} \pm \delta_{l,m+1}) \quad (\text{D.26})$$

$$\int_0^{2\pi} d\phi (e^{i\phi} \pm e^{-i\phi}) e^{-im\phi} e^{-i\phi} = 2\pi (\delta_{l,-m+1} \pm \delta_{l,-m-1}). \quad (\text{D.27})$$

Thus only $l = m \pm 1$ terms are allowed from the l -summation in $\epsilon^{i\mathbf{k}\cdot\mathbf{r}}$. The θ -integrals and their respective parities are as follows:

$$\begin{aligned} \int_0^\pi d\theta \sin \theta P_n^m(\cos \theta) \sin \theta P_s^{m\pm 1}(\cos \theta) &\sim (-1)^{m+n+m\pm 1+s} \sim (-1)^{n+s\pm 1} \\ \int_0^\pi d\theta \sin \theta \cos \theta \frac{dP_n^m(\cos \theta)}{d\theta} P_s^{m\pm 1}(\cos \theta) &\sim (-1)^{m+n+1+l+m\pm 1+s} \sim (-1)^{n+s\pm 1} \\ \int_0^\pi d\theta \sin \theta \frac{P_n^m(\cos \theta)}{\sin \theta} P_s^{m\pm 1}(\cos \theta) &\sim (-1)^{m+n+m\pm 1+s} \sim (-1)^{n+s\pm 1}. \end{aligned}$$

Thus only when $n + s \pm 1$ is even can these θ -integrals assume non-zero values. The r -integrals are of the form:

$$\int_0^\infty dr j_s(kr) \frac{j_n(kr)}{kr} \quad \text{and} \quad \int_0^\infty dr j_s(kr) \frac{1}{kr} \frac{d(rj_n(kr))}{dr}.$$

Again, these r -integrals can be non-zero only when $s - n$ is even or when $s = n \pm 1$. In the former case, the corresponding θ -integrals will be zero. Thus the only allowed values in the double infinite summation are terms corresponding to $l = m \pm 1$ and $s = n \pm 1$. a

Now the $s = n + 1$ contribution is given by:

$$\begin{aligned}
& 2\pi i^{n+1}(2n+3)\frac{1}{2}\left[n(n+1)\left(\int_0^\infty dr j_{n+1}(kr)\frac{j_n(kr)}{kr}\right) \times \right. \\
& \left. \left\{ \frac{(n+1-m+1)!}{(n+1+m-1)!} e^{-i(m-1)\beta} P_{n+1}^{m-1}(\cos\alpha) \int_0^\pi d\theta \sin\theta P_n^m(\cos\theta) \sin\theta P_{n+1}^{m-1}(\cos\theta) \right. \right. \\
& \left. \left. + \frac{(n+1-m-1)!}{(n+1+m+1)!} e^{-i(m+1)\beta} P_{n+1}^{m+1}(\cos\alpha) \int_0^\pi d\theta \sin\theta P_n^m(\cos\theta) \sin\theta P_{n+1}^{m+1}(\cos\theta) \right\} \right. \\
& \left. + \left(\int_0^\infty dr j_{n+1}(kr)\frac{1}{kr}\frac{d(rj_n(kr))}{dr}\right) \times \right. \\
& \left. \left\{ \frac{(n+1-m+1)!}{(n+1+m-1)!} e^{-i(m-1)\beta} P_{n+1}^{m-1}(\cos\alpha) \int_0^\pi d\theta \sin\theta \frac{dP_n^m(\cos\theta)}{d\theta} \cos\theta P_{n+1}^{m-1}(\cos\theta) \right. \right. \\
& \left. \left. + \frac{(n+1-m-1)!}{(n+1+m+1)!} e^{-i(m+1)\beta} P_{n+1}^{m+1}(\cos\alpha) \int_0^\pi d\theta \sin\theta \frac{dP_n^m(\cos\theta)}{d\theta} \cos\theta P_{n+1}^{m+1}(\cos\theta) \right\} \right. \\
& \left. + m \left(\int_0^\infty dr j_{n+1}(kr)\frac{1}{kr}\frac{d(rj_n(kr))}{dr}\right) \times \right. \\
& \left. \left\{ \frac{(n+1-m+1)!}{(n+1+m-1)!} e^{-i(m-1)\beta} P_{n+1}^{m-1}(\cos\alpha) \int_0^\pi d\theta \sin\theta \frac{P_n^m(\cos\theta)}{\sin\theta} P_{n+1}^{m-1}(\cos\theta) \right. \right. \\
& \left. \left. - \frac{(n+1-m-1)!}{(n+1+m+1)!} e^{-i(m+1)\beta} P_{n+1}^{m+1}(\cos\alpha) \int_0^\pi d\theta \sin\theta \frac{P_n^m(\cos\theta)}{\sin\theta} P_{n+1}^{m+1}(\cos\theta) \right\} \right].
\end{aligned}$$

Using Equations C.45, C.47, C.60, C.62, C.64, C.65 for the θ -integrals and Equations B.33, B.36 for the r -integrals, we can evaluate the $s = n + 1$ term :

$$\begin{aligned}
& \pi i^{n+1}(2n+3)\left[n(n+1)\left(\frac{\pi}{2k(2n+1)(2n+3)}\right) \times \right. \\
& \left. \left\{ \frac{(n-m+2)!}{(n+m)!} e^{-i(m-1)\beta} P_{n+1}^{m-1}(\cos\alpha) \left(\frac{2}{(2n+1)(2n+3)}\frac{(n+m)!}{(n-m)!}\right) \right. \right. \\
& \left. \left. + \frac{(n-m)!}{(n+m+2)!} e^{-i(m+1)\beta} P_{n+1}^{m+1}(\cos\alpha) \left(-\frac{2}{(2n+1)(2n+3)}\frac{(n+m+2)!}{(n-m)!}\right) \right\} \right. \\
& \left. + \left(-\frac{\pi n}{2k(2n+1)(2n+3)}\right) \times \right.
\end{aligned}$$

$$\begin{aligned}
& \left\{ \frac{(n-m+2)!}{(n+m)!} e^{-i(m-1)\beta} P_{n+1}^{m-1}(\cos \alpha) \left(-\frac{2n}{(2n+1)(2n+3)} \frac{(n+m)!}{(n-m)!} \right) \right. \\
& + \frac{(n-m)!}{(n+m+2)!} e^{-i(m+1)\beta} P_{n+1}^{m+1}(\cos \alpha) \times \\
& \quad \left. \left(\frac{2(n+m)!}{(n-m)!} \left(\frac{n(n+m+2)(n+m+1)}{(2n+1)(2n+3)} - m \right) \right) \right\} \\
& + \left(-\frac{\pi mn}{2k(2n+1)(2n+3)} \right) \times \\
& \left\{ \frac{(n-m+2)!}{(n+m)!} e^{-i(m-1)\beta} P_{n+1}^{m-1}(\cos \alpha) \times (0) \right. \\
& \quad \left. - \frac{(n-m)!}{(n+m+2)!} e^{-i(m+1)\beta} P_{n+1}^{m+1}(\cos \alpha) \left(-\frac{2(n+m)!}{(n-m)!} \right) \right\}.
\end{aligned}$$

On simplification, this gives us for the $s = n + 1$ term:

$$i^{n+1} \frac{\pi^2}{k} \frac{n}{(2n+1)(2n+3)} \left[(n-m+2)(n-m+1) P_{n+1}^{m-1}(\cos \alpha) e^{-i(m-1)\beta} \right. \\
\left. - P_{n+1}^{m+1}(\cos \alpha) e^{-i(m+1)\beta} \right]$$

Similarly, the $s = n - 1$ term is:

$$\begin{aligned}
& 2\pi i^{n-1} (2n-1) \frac{1}{2} \left[n(n+1) \left(\int_0^\infty dr j_{n-1}(kr) \frac{j_n(kr)}{kr} \right) \times \right. \\
& \left\{ \frac{(n-1-m+1)!}{(n-1+m-1)!} e^{-i(m-1)\beta} P_{n-1}^{m-1}(\cos \alpha) \int_0^\pi d\theta \sin \theta P_n^m(\cos \theta) \sin \theta P_{n-1}^{m-1}(\cos \theta) \right. \\
& \left. + \frac{(n-1-m-1)!}{(n-1+m+1)!} e^{-i(m+1)\beta} P_{n-1}^{m+1}(\cos \alpha) \int_0^\pi d\theta \sin \theta P_n^m(\cos \theta) \sin \theta P_{n-1}^{m+1}(\cos \theta) \right\} \\
& + \left(\int_0^\infty dr j_{n-1}(kr) \frac{1}{kr} \frac{d(rj_n(kr))}{dr} \right) \times \\
& \left\{ \frac{(n-1-m+1)!}{(n-1+m-1)!} e^{-i(m-1)\beta} P_{n-1}^{m-1}(\cos \alpha) \int_0^\pi d\theta \sin \theta \frac{dP_n^m(\cos \theta)}{d\theta} \cos \theta P_{n-1}^{m-1}(\cos \theta) \right. \\
& \left. + \frac{(n-1-m-1)!}{(n-1+m+1)!} e^{-i(m+1)\beta} P_{n-1}^{m+1}(\cos \alpha) \int_0^\pi d\theta \sin \theta \frac{dP_n^m(\cos \theta)}{d\theta} \cos \theta P_{n-1}^{m+1}(\cos \theta) \right\} \\
& + m \left(\int_0^\infty dr j_{n-1}(kr) \frac{1}{kr} \frac{d(rj_n(kr))}{dr} \right) \times \\
& \left\{ \frac{(n-1-m+1)!}{(n-1+m-1)!} e^{-i(m-1)\beta} P_{n-1}^{m-1}(\cos \alpha) \int_0^\pi d\theta \sin \theta \frac{P_n^m(\cos \theta)}{\sin \theta} P_{n-1}^{m-1}(\cos \theta) \right.
\end{aligned}$$

$$\left. - \frac{(n-1-m-1)!}{(n-1+m+1)!} e^{-i(m+1)\beta} P_{n-1}^{m+1}(\cos \alpha) \int_0^\pi d\theta \sin \theta \frac{P_n^m(\cos \theta)}{\sin \theta} P_{n-1}^{m+1}(\cos \theta) \right\} \Bigg].$$

Using Equations C.44, C.46, C.61, C.63, C.66, C.67 for the θ -integrals and Equations B.32, B.35 for the r -integrals, we can evaluate the $s = n - 1$ term :

$$\begin{aligned} & \pi i^{n-1} (2n-1) \left[n(n+1) \left(\frac{\pi}{2k(2n-1)(2n+1)} \right) \times \right. \\ & \left\{ \frac{(n-m)!}{(n+m-2)!} e^{-i(m-1)\beta} P_{n-1}^{m-1}(\cos \alpha) \left(-\frac{2}{(2n-1)(2n+1)} \frac{(n+m)!}{(n-m)!} \right) \right. \\ & \left. + \frac{(n-m-2)!}{(n+m)!} e^{-i(m+1)\beta} P_{n-1}^{m+1}(\cos \alpha) \left(\frac{2}{(2n-1)(2n+1)} \frac{(n+m)!}{(n-m-2)!} \right) \right\} \\ & + \left(\frac{\pi(n+1)}{2k(2n-1)(2n+1)} \right) \times \\ & \left\{ \frac{(n-m)!}{(n+m-2)!} e^{-i(m-1)\beta} P_{n-1}^{m-1}(\cos \alpha) \times \right. \\ & \quad \left(\frac{2(n+m)(n+m-2)!}{(2n-1)(n-m)!} \left(n-m+n \left(\frac{n+m-1}{2n+1} - \frac{2n-1}{n+m} \right) \right) \right) \\ & \left. + \frac{(n-m-2)!}{(n+m)!} e^{-i(m+1)\beta} P_{n-1}^{m+1}(\cos \alpha) \left(\frac{2(n+1)}{(2n-1)(2n+1)} \frac{(n+m)!}{(n-m-2)!} \right) \right\} \\ & + \left(\frac{\pi m(n+1)}{2k(2n-1)(2n+1)} \right) \times \\ & \left\{ \frac{(n-m)!}{(n+m-2)!} e^{-i(m-1)\beta} P_{n-1}^{m-1}(\cos \alpha) \times \left(-\frac{2(n+m-2)!}{(n-m)!} \right) \right. \\ & \left. - \frac{(n-m-2)!}{(n+m)!} e^{-i(m+1)\beta} P_{n-1}^{m+1}(\cos \alpha) (0) \right\} \Bigg]. \end{aligned}$$

On simplification, this gives us for the $s = n - 1$ term:

$$i^{n+1} \frac{\pi^2}{k} \frac{(n+1)}{(2n-1)(2n+1)} \left[(n+m)(n+m-1) P_{n-1}^{m-1}(\cos \alpha) e^{-i(m-1)\beta} \right. \\ \left. - P_{n-1}^{m+1}(\cos \alpha) e^{-i(m+1)\beta} \right]$$

Finally, adding the $s = n - 1$ and $s = n + 1$ contributions we obtain:

$$\begin{aligned}
\langle \mathbf{E}_x | \mathbf{N}_{mn} \rangle &= \frac{i^{n+1} \pi^2}{(2n+1) k} \times \\
&\left[\frac{n(n-m+2)(n-m+1)}{(2n+3)} P_{n+1}^{m-1}(\cos \alpha) e^{-i(m-1)\beta} \right. \\
&- \frac{n}{(2n+3)} P_{n+1}^{m+1}(\cos \alpha) e^{-i(m+1)\beta} \\
&+ \frac{(n+1)(n+m)(n+m-1)}{(2n-1)} P_{n-1}^{m-1}(\cos \alpha) e^{-i(m-1)\beta} \\
&\left. - \frac{(n+1)}{(2n-1)} P_{n-1}^{m+1}(\cos \alpha) e^{-i(m+1)\beta} \right]
\end{aligned} \tag{D.28}$$

D.6 Evaluating $\langle \mathbf{E}_x | \mathbf{M}_{mn} \rangle$

We have

$$\begin{aligned}
\mathbf{M}_{mn}^* \cdot \mathbf{e}_x &= \frac{1}{2} \left[-im j_n(kr) \cos \theta \frac{P_n^m(\cos \theta)}{\sin \theta} (\epsilon^{i\phi} + \epsilon^{-i\phi}) \epsilon^{-im\phi} \right. \\
&\quad \left. - i j_n(kr) \frac{dP_n^m(\cos \theta)}{d\theta} (\epsilon^{i\phi} - \epsilon^{-i\phi}) \epsilon^{-im\phi} \right]. \tag{D.29}
\end{aligned}$$

As in the previous case, the ϕ -integration allows only the $l = m \pm 1$ terms to be non-zero. The θ -integrals in this case are of the following forms, indicated along with their parities:

$$\begin{aligned}
\int_0^\pi d\theta \sin \theta \frac{P_n^m(\cos \theta)}{\sin \theta} \cos \theta P_s^{m\pm 1}(\cos \theta) &\sim (-1)^{m+n+1+m\pm 1+s} \sim (-1)^{n+s} \\
\int_0^\pi d\theta \sin \theta \frac{dP_n^m(\cos \theta)}{d\theta} P_s^{m\pm 1}(\cos \theta) &\sim (-1)^{m+n+1+m\pm 1+s} \sim (-1)^{n+s}.
\end{aligned}$$

So, only the $s = n$ and $s + n = \text{even}$ terms are allowed by the θ -integration. The r -integration in this case is the straightforward integral:

$$\int_0^\infty dr j_s(kr) j_n(kr),$$

which is non-zero only for $s = n$ or $s + n = \text{odd}$. Thus, the only allowed term from the s -summation when both r and θ -integrations are considered together is the $s = n$ term. So for $m \geq 0$ we have $\langle \mathbf{E}_x | \mathbf{M}_{mn} \rangle$ equal to:

$$\begin{aligned}
& 2\pi i^{n+1}(2n+1)\frac{1}{2}\left(\int_0^\infty dr j_n(kr) j_n(kr)\right) \times \\
& \left[-m \frac{(n-m+1)!}{(n+m-1)!} e^{-i(m-1)\beta} P_n^{m-1}(\cos \alpha) \int_0^\pi d\theta \sin \theta \frac{P_n^m(\cos \theta)}{\sin \theta} \cos \theta P_n^{m-1}(\cos \theta) \right. \\
& -m \frac{(n-m-1)!}{(n+m+1)!} e^{-i(m+1)\beta} P_n^{m+1}(\cos \alpha) \int_0^\pi d\theta \sin \theta \frac{P_n^m(\cos \theta)}{\sin \theta} \cos \theta P_n^{m+1}(\cos \theta) \\
& -\frac{(n-m+1)!}{(n+m-1)!} e^{-i(m-1)\beta} P_n^{m-1}(\cos \alpha) \int_0^\pi d\theta \sin \theta \frac{dP_n^m(\cos \theta)}{d\theta} P_n^{m-1}(\cos \theta) \\
& \left. +\frac{(n-m-1)!}{(n+m+1)!} e^{-i(m+1)\beta} P_n^{m+1}(\cos \alpha) \int_0^\pi d\theta \sin \theta \frac{dP_n^m(\cos \theta)}{d\theta} P_n^{m+1}(\cos \theta) \right].
\end{aligned}$$

Using Equations C.68. C.69. C.70. C.71, for the θ -integrals and Equation B.27 for the r -integral, we obtain :

$$\begin{aligned}
\langle \mathbf{E}_x | \mathbf{M}_{mn} \rangle &= \pi i^{n+1}(2n+1) \left(\frac{\pi}{2k(2n+1)} \right) \times \\
& \left[-m \frac{(n-m+1)!}{(n+m-1)!} e^{-i(m-1)\beta} P_n^{m-1}(\cos \alpha) \left(-\frac{2(n+m-1)(n+m-2)!}{(2n+1)(n-m)!} \right) \right. \\
& -m \frac{(n-m-1)!}{(n+m+1)!} e^{-i(m+1)\beta} P_n^{m+1}(\cos \alpha) \left(-\frac{2(n+m)(n+m-1)!}{(2n+1)(n-m-1)!} \right) \\
& -\frac{(n-m+1)!}{(n+m-1)!} e^{-i(m-1)\beta} P_n^{m-1}(\cos \alpha) \left(-\frac{2n}{(2n+1)} \frac{(n+m-1)!}{(n-m)!} \right) \\
& \left. +\frac{(n-m-1)!}{(n+m+1)!} e^{-i(m+1)\beta} P_n^{m+1}(\cos \alpha) \left(-\frac{2(n+1)}{(2n+1)} \frac{(n+m)!}{(n-m-1)!} \right) \right].
\end{aligned}$$

On simplification, we finally obtain:

$$\boxed{
\begin{aligned}
\langle \mathbf{E}_x | \mathbf{M}_{mn} \rangle &= \frac{i^{n+1}}{(2n+1)} \frac{\pi^2}{k} \left[P_n^{m+1}(\cos \alpha) e^{-i(m+1)\beta} \right. \\
& \left. + (n+m)(n-m+1) P_n^{m-1}(\cos \alpha) e^{-i(m-1)\beta} \right]
\end{aligned}
} \quad (D.30)$$

D.7 Evaluating $\langle \mathbf{E}_x | \mathbf{L}_{mn} \rangle$

We have

$$\begin{aligned} \mathbf{L}_{mn}^* \cdot \mathbf{e}_x = & k \frac{1}{2} \left[\left(\frac{d}{d(kr)} j_n(kr) \right) \sin \theta P_n^m(\cos \theta) (e^{i\phi} + e^{-i\phi}) e^{-im\phi} \right. \\ & + \frac{j_n(kr)}{kr} \cos \theta \frac{dP_n^m(\cos \theta)}{d\theta} (e^{i\phi} + e^{-i\phi}) e^{-im\phi} \\ & \left. + m \frac{j_n(kr)}{kr} \frac{P_n^m(\cos \theta)}{\sin \theta} (e^{i\phi} - e^{-i\phi}) e^{-im\phi} \right]. \quad (\text{D.31}) \end{aligned}$$

As in the case of $\langle \mathbf{E}_x | \mathbf{N}_{mn} \rangle$, the ϕ -integration allows only the $l = m \pm 1$ terms to be non-zero. The θ -integrals in this case have the same form as their counterparts in the evaluation of $\langle \mathbf{E}_x | \mathbf{N}_{mn} \rangle$, so that only when $n + s \pm 1$ is even can these terms be non-zero. The r -integrals are of the form:

$$\int_0^\infty dr j_s(kr) \frac{j_n(kr)}{kr} \quad \text{and} \quad \int_0^\infty dr j_s(kr) \frac{d}{d(kr)} j_n(kr).$$

and these integrals are non-zero for $s = n \pm 1$ or $s + n \pm 1$ is an odd number. So in this case too, the combined action of the θ and r integrations allow only the $l = m \pm 1$ and $s = n \pm 1$ terms to survive.

Now the $s = n + 1$ contribution is given by:

$$\begin{aligned} & 2\pi i^{n+1} (2n+3) \frac{k}{2} \left[\left(\int_0^\infty dr j_{n+1}(kr) \frac{d}{d(kr)} j_n(kr) \right) \times \right. \\ & \left\{ \frac{(n+1-m+1)!}{(n+1+m-1)!} e^{-i(m-1)\beta} P_{n+1}^{m-1}(\cos \alpha) \int_0^\pi d\theta \sin \theta P_n^m(\cos \theta) \sin \theta P_{n+1}^{m-1}(\cos \theta) \right. \\ & \left. + \frac{(n+1-m-1)!}{(n+1+m+1)!} e^{-i(m+1)\beta} P_{n+1}^{m+1}(\cos \alpha) \int_0^\pi d\theta \sin \theta P_n^m(\cos \theta) \sin \theta P_{n+1}^{m+1}(\cos \theta) \right\} \\ & + \left(\int_0^\infty dr j_{n+1}(kr) \frac{j_n(kr)}{kr} \right) \times \\ & \left\{ \frac{(n+1-m+1)!}{(n+1+m-1)!} e^{-i(m-1)\beta} P_{n+1}^{m-1}(\cos \alpha) \int_0^\pi d\theta \sin \theta \frac{dP_n^m(\cos \theta)}{d\theta} \cos \theta P_{n+1}^{m-1}(\cos \theta) \right. \\ & \left. + \frac{(n+1-m-1)!}{(n+1+m+1)!} e^{-i(m+1)\beta} P_{n+1}^{m+1}(\cos \alpha) \int_0^\pi d\theta \sin \theta \frac{dP_n^m(\cos \theta)}{d\theta} \cos \theta P_{n+1}^{m+1}(\cos \theta) \right\} \\ & + m \left(\int_0^\infty dr j_{n+1}(kr) \frac{j_n(kr)}{kr} \right) \times \end{aligned}$$

$$\left\{ \frac{(n+1-m+1)!}{(n+1+m-1)!} e^{-i(m-1)\beta} P_{n+1}^{m-1}(\cos \alpha) \int_0^\pi d\theta \sin \theta \frac{P_n^m(\cos \theta)}{\sin \theta} P_{n+1}^{m-1}(\cos \theta) \right. \\ \left. - \frac{(n+1-m-1)!}{(n+1+m+1)!} e^{-i(m+1)\beta} P_{n+1}^{m+1}(\cos \alpha) \int_0^\pi d\theta \sin \theta \frac{P_n^m(\cos \theta)}{\sin \theta} P_{n+1}^{m+1}(\cos \theta) \right\}.$$

Using Equations C.45, C.47, C.60, C.62, C.64, C.65 for the θ -integrals and Equations B.33, B.39 for the r -integrals, we can evaluate the $s = n + 1$ term :

$$k\pi i^{n+1}(2n+3) \left[\left(-\frac{\pi(n+1)}{2k(2n+1)(2n+3)} \right) \times \right. \\ \left. \left\{ \frac{(n-m+2)!}{(n+m)!} e^{-i(m-1)\beta} P_{n+1}^{m-1}(\cos \alpha) \left(\frac{2}{(2n+1)(2n+3)} \frac{(n+m)!}{(n-m)!} \right) \right. \right. \\ \left. \left. + \frac{(n-m)!}{(n+m+2)!} e^{-i(m+1)\beta} P_{n+1}^{m+1}(\cos \alpha) \left(-\frac{2}{(2n+1)(2n+3)} \frac{(n+m+2)!}{(n-m)!} \right) \right\} \right. \\ \left. + \left(\frac{\pi}{2k(2n+1)(2n+3)} \right) \times \right. \\ \left. \left\{ \frac{(n-m+2)!}{(n+m)!} e^{-i(m-1)\beta} P_{n+1}^{m-1}(\cos \alpha) \left(-\frac{2n}{(2n+1)(2n+3)} \frac{(n+m)!}{(n-m)!} \right) \right. \right. \\ \left. \left. + \frac{(n-m)!}{(n+m+2)!} e^{-i(m+1)\beta} P_{n+1}^{m+1}(\cos \alpha) \times \right. \right. \\ \left. \left. \left(\frac{2(n+m)!}{(n-m)!} \left(\frac{n(n+m+2)(n+m+1)}{(2n+1)(2n+3)} - m \right) \right) \right\} \right. \\ \left. + \left(\frac{\pi m}{2k(2n+1)(2n+3)} \right) \times \right. \\ \left. \left\{ \frac{(n-m+2)!}{(n+m)!} e^{-i(m-1)\beta} P_{n+1}^{m-1}(\cos \alpha) \times (0) \right. \right. \\ \left. \left. - \frac{(n-m)!}{(n+m+2)!} e^{-i(m+1)\beta} P_{n+1}^{m+1}(\cos \alpha) \left(-\frac{2(n+m)!}{(n-m)!} \right) \right\} \right].$$

On simplification, this gives us for the $s = n + 1$ term:

$$i^{n+1} \frac{\pi^2}{(2n+1)(2n+3)} \left[P_{n+1}^{m+1}(\cos \alpha) e^{-i(m+1)\beta} \right. \\ \left. - (n-m+2)(n-m+1) P_{n+1}^{m-1}(\cos \alpha) e^{-i(m-1)\beta} \right].$$

Similarly, the $s = n - 1$ term is:

$$2\pi i^{n-1}(2n-1) \frac{k}{2} \left[\left(\int_0^\infty dr j_{n-1}(kr) \frac{d}{d(kr)} j_n(kr) \right) \times \right.$$

$$\begin{aligned}
& \left\{ \frac{(n-1-m+1)!}{(n-1+m-1)!} e^{-i(m-1)\beta} P_{n-1}^{m-1}(\cos \alpha) \int_0^\pi d\theta \sin \theta P_n^m(\cos \theta) \sin \theta P_{n-1}^{m-1}(\cos \theta) \right. \\
& \left. + \frac{(n-1-m-1)!}{(n-1+m+1)!} e^{-i(m+1)\beta} P_{n-1}^{m+1}(\cos \alpha) \int_0^\pi d\theta \sin \theta P_n^m(\cos \theta) \sin \theta P_{n-1}^{m+1}(\cos \theta) \right\} \\
& + \left(\int_0^\infty dr j_{n-1}(kr) \frac{j_n(kr)}{kr} \right) \times \\
& \left\{ \frac{(n-1-m+1)!}{(n-1+m-1)!} e^{-i(m-1)\beta} P_{n-1}^{m-1}(\cos \alpha) \int_0^\pi d\theta \sin \theta \frac{dP_n^m(\cos \theta)}{d\theta} \cos \theta P_{n-1}^{m-1}(\cos \theta) \right. \\
& \left. + \frac{(n-1-m-1)!}{(n-1+m+1)!} e^{-i(m+1)\beta} P_{n-1}^{m+1}(\cos \alpha) \int_0^\pi d\theta \sin \theta \frac{dP_n^m(\cos \theta)}{d\theta} \cos \theta P_{n-1}^{m+1}(\cos \theta) \right\} \\
& + m \left(\int_0^\infty dr j_{n-1}(kr) \frac{j_n(kr)}{kr} \right) \times \\
& \left\{ \frac{(n-1-m+1)!}{(n-1+m-1)!} e^{-i(m-1)\beta} P_{n-1}^{m-1}(\cos \alpha) \int_0^\pi d\theta \sin \theta \frac{P_n^m(\cos \theta)}{\sin \theta} P_{n-1}^{m-1}(\cos \theta) \right. \\
& \left. - \frac{(n-1-m-1)!}{(n-1+m+1)!} e^{-i(m+1)\beta} P_{n-1}^{m+1}(\cos \alpha) \int_0^\pi d\theta \sin \theta \frac{P_n^m(\cos \theta)}{\sin \theta} P_{n-1}^{m+1}(\cos \theta) \right\} \Bigg].
\end{aligned}$$

Using Equations C.44, C.46, C.61, C.63, C.66, C.67 for the θ -integrals and Equations B.32, B.38 for the r -integrals, we can evaluate the $s = n - 1$ term :

$$\begin{aligned}
& \pi i^{n-1} (2n-1) \left[\left(\frac{\pi n}{2k(2n-1)(2n+1)} \right) \times \right. \\
& \left\{ \frac{(n-m)!}{(n+m-2)!} e^{-i(m-1)\beta} P_{n-1}^{m-1}(\cos \alpha) \left(-\frac{2}{(2n-1)(2n+1)} \frac{(n+m)!}{(n-m)!} \right) \right. \\
& \left. + \frac{(n-m-2)!}{(n+m)!} e^{-i(m+1)\beta} P_{n-1}^{m+1}(\cos \alpha) \left(\frac{2}{(2n-1)(2n+1)} \frac{(n+m)!}{(n-m-2)!} \right) \right\} \\
& + \left(\frac{\pi}{2k(2n-1)(2n+1)} \right) \times \\
& \left\{ \frac{(n-m)!}{(n+m-2)!} e^{-i(m-1)\beta} P_{n-1}^{m-1}(\cos \alpha) \times \right. \\
& \quad \left(\frac{2(n+m)(n+m-2)!}{(2n-1)(n-m)!} \left(n-m+n \left(\frac{n+m-1}{2n+1} - \frac{2n-1}{n+m} \right) \right) \right) \\
& \left. + \frac{(n-m-2)!}{(n+m)!} e^{-i(m+1)\beta} P_{n-1}^{m+1}(\cos \alpha) \left(\frac{2(n+1)}{(2n-1)(2n+1)} \frac{(n+m)!}{(n-m-2)!} \right) \right\}
\end{aligned}$$

$$+ \left(\frac{\pi m}{2k(2n-1)(2n+1)} \right) \times \left\{ \frac{(n-m)!}{(n+m-2)!} e^{-i(m-1)\beta} P_{n-1}^{m-1}(\cos \alpha) \times \left(-\frac{2(n+m-2)!}{(n-m)!} \right) - \frac{(n-m-2)!}{(n+m)!} e^{-i(m+1)\beta} P_{n-1}^{m+1}(\cos \alpha) (0) \right\}.$$

On simplification, this gives us for the $s = n - 1$ term:

$$i^{n+1} \frac{\pi^2}{(2n-1)(2n+1)} \left[-P_{n-1}^{m+1}(\cos \alpha) \epsilon^{-i(m+1)\beta} + (n+m)(n+m-1) P_{n-1}^{m-1}(\cos \alpha) \epsilon^{-i(m-1)\beta} \right]$$

Finally, adding the $s = n - 1$ and $s = n + 1$ contributions we obtain:

$$\langle \mathbf{E}_x | \mathbf{L}_{mn} \rangle = \frac{i^{n+1} \pi^2}{(2n-1)(2n+1)(2n+3)} \times \left[-(2n-1)(n-m+2)(n-m+1) P_{n+1}^{m-1}(\cos \alpha) \epsilon^{-i(m-1)\beta} + (2n-1) P_{n+1}^{m+1}(\cos \alpha) \epsilon^{-i(m+1)\beta} + (2n+3)(n+m)(n+m-1) P_{n-1}^{m-1}(\cos \alpha) \epsilon^{-i(m-1)\beta} - (2n+3) P_{n-1}^{m+1}(\cos \alpha) \epsilon^{-i(m+1)\beta} \right] \quad (\text{D.32})$$

D.8 Evaluating $\langle \mathbf{E}_y | \mathbf{N}_{mn} \rangle$, $\langle \mathbf{E}_y | \mathbf{M}_{mn} \rangle$ and $\langle \mathbf{E}_y | \mathbf{L}_{mn} \rangle$

We write \mathbf{e}_y in the following form:

$$\begin{aligned} \mathbf{e}_y &= \sin \theta \sin \phi \mathbf{e}_r + \cos \theta \sin \phi \mathbf{e}_\theta + \cos \phi \mathbf{e}_\phi \quad (\text{D.33}) \\ &= \frac{-i}{2} \left[\sin \theta (\epsilon^{i\phi} - \epsilon^{-i\phi}) \mathbf{e}_r + \cos \theta (\epsilon^{i\phi} - \epsilon^{-i\phi}) \mathbf{e}_\theta + i (\epsilon^{i\phi} + \epsilon^{-i\phi}) \mathbf{e}_\phi \right] \end{aligned}$$

When compared with \mathbf{e}_x which has the form

$$\mathbf{e}_x = \frac{1}{2} \left[\sin \theta (\epsilon^{i\phi} + \epsilon^{-i\phi}) \mathbf{e}_r + \cos \theta (\epsilon^{i\phi} + \epsilon^{-i\phi}) \mathbf{e}_\theta + i (\epsilon^{i\phi} - \epsilon^{-i\phi}) \mathbf{e}_\phi \right]. \quad (\text{D.34})$$

we can immediately notice that the only difference between the expressions for \mathbf{e}_y and \mathbf{e}_x is that the former can be obtained from latter by changing the sign of the $\epsilon^{-i\phi}$ terms and finally multiplying the entire expression with an additional factor of $-i$.

When we observe the ϕ -integrals:

$$\int_0^{2\pi} d\phi (e^{i\phi} \pm e^{-i\phi}) e^{-im\phi} e^{il\phi} = 2\pi (\delta_{l,m-1} \pm \delta_{l,m+1}) \quad (D.35)$$

$$\int_0^{2\pi} d\phi (e^{i\phi} \pm e^{-i\phi}) e^{-im\phi} e^{-il\phi} = 2\pi (\delta_{l,-m+1} \pm \delta_{l,-m-1}). \quad (D.36)$$

it is clear that the above transformation will lead to a change in the sign of the $m+1$ term, while the $m-1$ terms will not change their sign. The only difference between the \mathbf{E}_x and \mathbf{E}_y terms arise from this source, since the other factors in the integrands of $\langle \mathbf{E}_y | \mathbf{N}_{mn} \rangle$, $\langle \mathbf{E}_y | \mathbf{M}_{mn} \rangle$ and $\langle \mathbf{E}_y | \mathbf{L}_{mn} \rangle$ are the same as the corresponding \mathbf{E}_x integrals. Thus we can obtain the \mathbf{E}_y integrals from the corresponding \mathbf{E}_x integrals by changing the signs of the ' $m+1$ ' terms and finally adding an extra factor of $-i$. Thus we obtain the following expression:

$$\begin{aligned} \langle \mathbf{E}_y | \mathbf{N}_{mn} \rangle = & \frac{i^n \pi^2}{(2n+1)k} \times \\ & \left[\frac{n(n-m+2)(n-m+1)}{(2n+3)} P_{n+1}^{m-1}(\cos \alpha) e^{-i(m-1)\beta} \right. \\ & + \frac{n}{(2n+3)} P_{n+1}^{m+1}(\cos \alpha) e^{-i(m+1)\beta} \\ & + \frac{(n+1)(n+m)(n+m-1)}{(2n-1)} P_{n-1}^{m-1}(\cos \alpha) e^{-i(m-1)\beta} \\ & \left. + \frac{(n+1)}{(2n-1)} P_{n-1}^{m+1}(\cos \alpha) e^{-i(m+1)\beta} \right] \end{aligned} \quad (D.37)$$

$$\begin{aligned} \langle \mathbf{E}_x | \mathbf{L}_{mn} \rangle = & \frac{i^n \pi^2}{(2n-1)(2n+1)(2n+3)} \times \\ & \left[-(2n-1)(n-m+2)(n-m+1) P_{n+1}^{m-1}(\cos \alpha) e^{-i(m-1)\beta} \right. \\ & - (2n-1) P_{n+1}^{m+1}(\cos \alpha) e^{-i(m+1)\beta} \\ & + (2n+3)(n+m)(n+m-1) P_{n-1}^{m-1}(\cos \alpha) e^{-i(m-1)\beta} \\ & \left. + (2n+3) P_{n-1}^{m+1}(\cos \alpha) e^{-i(m+1)\beta} \right] \end{aligned} \quad (D.38)$$

$$\langle \mathbf{E}_y | \mathbf{M}_{mn} \rangle = \frac{i^n}{(2n+1)} \frac{\pi^2}{k} \left[-P_n^{m+1}(\cos \alpha) \epsilon^{-i(m+1)\beta} + (n+m)(n-m+1) P_n^{m-1}(\cos \alpha) \epsilon^{-i(m-1)\beta} \right] \quad (\text{D.39})$$

D.9 Evaluating $\langle \mathbf{M}_{mn} | \mathbf{M}_{mn} \rangle$, $\langle \mathbf{N}_{mn} | \mathbf{N}_{mn} \rangle$ and $\langle \mathbf{L}_{mn} | \mathbf{L}_{mn} \rangle$

These integrals are easy to evaluate by using the expressions already derived in Chapter 3. Since we are interested in a plane wave expansion that is regular at the origin, i.e. an expansion in terms of the spherical Bessel functions alone, $z_n(kr)$ represents $j_n(kr)$. The θ and ϕ integrations are already performed, and the r -integrations can be easily performed using the integrals derived in Appendix B. Since we know from the orthogonality relation between the \mathbf{M} functions (Equation 3.22) that

$$\int_0^{2\pi} d\phi \int_0^\pi d\theta \sin \theta \mathbf{M}_{mn} \cdot \mathbf{M}_{m'n'}^* = \frac{4\pi n(n+1)}{2n+1} \frac{(n+m)!}{(n-m)!} j_n^2(kr) \delta_{nn'} \delta_{mm'}. \quad (\text{D.40})$$

therefore using Equation B.27 we can integrate both sides of this equation giving us (with $n = n'$ and $m = m'$):

$$\langle \mathbf{M}_{mn} | \mathbf{M}_{mn} \rangle = \frac{2\pi^2}{k} \frac{n(n+1)}{(2n+1)^2} \frac{(n+m)!}{(n-m)!} \quad (\text{D.41})$$

Similarly, using the orthogonality relation between the \mathbf{N} functions, (Equation 3.24) where now $n = n'$ and $m = m'$:

$$\begin{aligned} & \int_0^{2\pi} d\phi \int_0^\pi d\theta \sin \theta \mathbf{N}_{mn} \cdot \mathbf{N}_{m'n'}^* \\ &= \frac{4\pi n(n+1)}{(2n+1)^2} \frac{(n+m)!}{(n-m)!} \left[(n+1)j_{n-1}^2(kr) + nj_{n+1}^2(kr) \right] \delta_{nn'} \delta_{mm'}. \end{aligned} \quad (\text{D.42})$$

and the integrals in Equation B.28 and Equation B.29, we immediately obtain the expression for the inner product:

$$\langle \mathbf{N}_{mn} | \mathbf{N}_{mn} \rangle = \frac{2\pi^2}{k(2n+1)^2} \frac{(n+m)! n(n+1)(4n^2+4n+3)}{(n-m)! (2n-1)(2n+3)}. \quad (\text{D.43})$$

Finally, using the orthogonality of the \mathbf{L} functions (Equation 3.21) :

$$\begin{aligned} & \int_0^{2\pi} d\phi \int_0^\pi d\theta \sin\theta \mathbf{L}_{mn} \cdot \mathbf{L}_{m'n'}^* \\ &= \frac{4\pi k^2}{(2n+1)^2} \frac{(n+m)!}{(n-m)!} \left[n j_{n-1}^2(kr) + (n+1) j_{n+1}^2(kr) \right] \delta_{nn'} \delta_{mm'}. \end{aligned} \quad (\text{D.44})$$

and the integrals given by Equation B.28 and Equation B.29 the expression for the inner product between the \mathbf{L} functions assume the form:

$$\langle \mathbf{L}_{mn} | \mathbf{L}_{mn} \rangle = \frac{2\pi^2 k}{(2n+1)^2} \frac{(n+m)! (4n^2+4n-1)}{(n-m)! (2n-1)(2n+3)}. \quad (\text{D.45})$$

When we consider the inner products for $m < 0$, by virtue of Equations 3.10, 3.11 and 3.12, the inner product for the (negative) $-m$'s will be equal to the inner products for the corresponding (positive) m times a non-negative factor. Thus:

$$\begin{aligned} \langle \mathbf{L}_{-mn} | \mathbf{L}_{-mn} \rangle &= \left(\frac{(n-m)!}{(n+m)!} \right)^2 \langle \mathbf{L}_{mn} | \mathbf{L}_{mn} \rangle \\ \langle \mathbf{M}_{-mn} | \mathbf{M}_{-mn} \rangle &= \left(\frac{(n-m)!}{(n+m)!} \right)^2 \langle \mathbf{M}_{mn} | \mathbf{M}_{mn} \rangle \\ \langle \mathbf{N}_{-mn} | \mathbf{N}_{-mn} \rangle &= \left(\frac{(n-m)!}{(n+m)!} \right)^2 \langle \mathbf{N}_{mn} | \mathbf{N}_{mn} \rangle \end{aligned} \quad (\text{D.46})$$

D.10 Evaluating Inner Products when $m < 0$

When $m < 0$ we can evaluate the inner products from the known results for $m > 0$. The $m = 0$ case can be evaluated using either sets of formula. We will address this

issue with a specific example. By virtue of Equation 3.11 we can write:

$$\langle \mathbf{E}_x | \mathbf{M}_{-mn} \rangle = \int_{r\theta\phi} \mathbf{e}_x \cdot \mathbf{M}_{-mn}^* e^{i\mathbf{k}\cdot\mathbf{r}} = (-1)^m \frac{(n-m)!}{(n+m)!} \int_{r\theta\phi} \mathbf{e}_x \cdot \mathbf{M}_{mn} e^{i\mathbf{k}\cdot\mathbf{r}}. \quad (\text{D.47})$$

Now it can be easily verified that the following identities hold true:

$$\int_0^{2\pi} d\phi e^{im\phi} (e^{i\phi} + e^{-i\phi}) e^{-il\phi} = \int_0^{2\pi} d\phi e^{-im\phi} (e^{i\phi} + e^{-i\phi}) e^{il\phi} \quad (\text{D.48})$$

$$\int_0^{2\pi} d\phi e^{im\phi} (e^{i\phi} - e^{-i\phi}) e^{-il\phi} = - \int_0^{2\pi} d\phi e^{-im\phi} (e^{i\phi} - e^{-i\phi}) e^{il\phi} \quad (\text{D.49})$$

$$\int_0^{2\pi} d\phi e^{im\phi} (e^{i\phi} + e^{-i\phi}) e^{il\phi} = + \int_0^{2\pi} d\phi e^{-im\phi} (e^{i\phi} + e^{-i\phi}) e^{-il\phi} \quad (\text{D.50})$$

$$\int_0^{2\pi} d\phi e^{im\phi} (e^{i\phi} - e^{-i\phi}) e^{il\phi} = - \int_0^{2\pi} d\phi e^{-im\phi} (e^{i\phi} - e^{-i\phi}) e^{-il\phi} \quad (\text{D.51})$$

We have

$$\begin{aligned} \mathbf{M}_{mn} \cdot \mathbf{e}_x = \frac{1}{2} \left[im j_n(kr) \cos \theta \frac{P_n^m(\cos \theta)}{\sin \theta} (e^{i\phi} + e^{-i\phi}) e^{im\phi} \right. \\ \left. - i j_n(kr) \frac{dP_n^m(\cos \theta)}{d\theta} (e^{i\phi} - e^{-i\phi}) e^{im\phi} \right]. \quad (\text{D.52}) \end{aligned}$$

and

$$\begin{aligned} \mathbf{M}_{mn}^* \cdot \mathbf{e}_x = \frac{1}{2} \left[-im j_n(kr) \cos \theta \frac{P_n^m(\cos \theta)}{\sin \theta} (e^{i\phi} + e^{-i\phi}) e^{-im\phi} \right. \\ \left. - i j_n(kr) \frac{dP_n^m(\cos \theta)}{d\theta} (e^{i\phi} - e^{-i\phi}) e^{-im\phi} \right]. \quad (\text{D.53}) \end{aligned}$$

On multiplying both sides of the above two equations by $e^{i\mathbf{k}\cdot\mathbf{r}}$ and carrying out the ϕ -integration only, the $(e^{i\phi} + e^{-i\phi})$ term in $\mathbf{M}_{mn} \cdot \mathbf{e}_x$ will have the same sign as the corresponding $(e^{i\phi} + e^{-i\phi})$ term in $\mathbf{M}_{mn}^* \cdot \mathbf{e}_x$, but the $(e^{i\phi} - e^{-i\phi})$ term in $\mathbf{M}_{mn} \cdot \mathbf{e}_x$ will have opposite sign as compared to the $(e^{i\phi} - e^{-i\phi})$ term in $\mathbf{M}_{mn}^* \cdot \mathbf{e}_x$. Thus, overall the $\mathbf{M}_{mn} \cdot \mathbf{e}_x$ integral will acquire an extra negative sign as compared to the $\mathbf{M}_{mn}^* \cdot \mathbf{e}_x$ integral after the ϕ -integration is carried out. The remaining θ and r integrations will yield identical values in the two cases, except that the $e^{-il\beta}$ factors are replaced by $e^{il\beta}$. The second l -series of $e^{i\mathbf{k}\cdot\mathbf{r}}$ is used when the integral is carried out with $e^{im\phi}$ instead of $e^{-im\phi}$, l being always greater than zero. However, the $\mathbf{M}_{mn}^* \cdot \mathbf{e}_x$

integral above is precisely the one used in the evaluation of $\langle \mathbf{E}_x | \mathbf{M}_{mn} \rangle$. So we can readily obtain the inner product for negative m 's in this case by following the recipe:

$$\langle \mathbf{E}_x | \mathbf{M}_{-mn} \rangle = (-1)^{m+1} \frac{(n-m)!}{(n+m)!} \times \left[\langle \mathbf{E}_x | \mathbf{M}_{mn} \rangle \text{ with } \epsilon^{-i(m\pm 1)\beta} \right. \\ \left. \text{factors changed to } \epsilon^{i(m\pm 1)\beta} \right] \quad (\text{D.54})$$

Similarly, since:

$$\mathbf{N}_{mn}^* \cdot \mathbf{e}_x = \frac{1}{2} \left[n(n+1) \frac{j_n(kr)}{kr} \sin \theta P_n^m(\cos \theta) (\epsilon^{i\phi} + \epsilon^{-i\phi}) \epsilon^{-im\phi} \right. \\ \left. + \frac{1}{kr} \frac{d(rj_n(kr))}{dr} \cos \theta \frac{dP_n^m(\cos \theta)}{d\theta} (\epsilon^{i\phi} + \epsilon^{-i\phi}) \epsilon^{-im\phi} \right. \\ \left. + m \frac{1}{kr} \frac{d(rj_n(kr))}{dr} \frac{P_n^m(\cos \theta)}{\sin \theta} (\epsilon^{i\phi} - \epsilon^{-i\phi}) \epsilon^{-im\phi} \right] \quad (\text{D.55})$$

and

$$\mathbf{N}_{mn} \cdot \mathbf{e}_x = \frac{1}{2} \left[n(n+1) \frac{j_n(kr)}{kr} \sin \theta P_n^m(\cos \theta) (\epsilon^{i\phi} + \epsilon^{-i\phi}) \epsilon^{im\phi} \right. \\ \left. + \frac{1}{kr} \frac{d(rj_n(kr))}{dr} \cos \theta \frac{dP_n^m(\cos \theta)}{d\theta} (\epsilon^{i\phi} + \epsilon^{-i\phi}) \epsilon^{im\phi} \right. \\ \left. - m \frac{1}{kr} \frac{d(rj_n(kr))}{dr} \frac{P_n^m(\cos \theta)}{\sin \theta} (\epsilon^{i\phi} - \epsilon^{-i\phi}) \epsilon^{im\phi} \right] \quad (\text{D.56})$$

now the ϕ integration will cause a change in the sign in the third term, but no change of sign for the first and second terms. In effect there will be no extra negative sign as that obtained in the previous case. Thus we can immediately write down the short-cut to obtaining the negative m inner products in this case:

$$\langle \mathbf{E}_x | \mathbf{N}_{-mn} \rangle = (-1)^m \frac{(n-m)!}{(n+m)!} \times \left[\langle \mathbf{E}_x | \mathbf{N}_{mn} \rangle \text{ with } \epsilon^{-i(m\pm 1)\beta} \right. \\ \left. \text{factors changed to } \epsilon^{i(m\pm 1)\beta} \right] \quad (\text{D.57})$$

Exactly the same considerations are valid for evaluating $\langle \mathbf{E}_x | \mathbf{L}_{-mn} \rangle$ since the ϕ parts in the integrands are identical to that used in evaluating $\langle \mathbf{E}_x | \mathbf{N}_{-mn} \rangle$. So we have the following expression:

$$\langle \mathbf{E}_x | \mathbf{L}_{-mn} \rangle = (-1)^m \frac{(n-m)!}{(n+m)!} \times \left[\langle \mathbf{E}_x | \mathbf{L}_{mn} \rangle \text{ with } e^{-i(m\pm 1)\beta} \text{ factors changed to } e^{i(m\pm 1)\beta} \right] \quad (\text{D.58})$$

Now we consider the \mathbf{e}_y terms. We have:

$$\mathbf{M}_{mn} \cdot \mathbf{e}_y = \frac{1}{2} \left[m j_n(kr) \cos \theta \frac{P_n^m(\cos \theta)}{\sin \theta} (e^{i\phi} - e^{-i\phi}) e^{im\phi} - j_n(kr) \frac{dP_n^m(\cos \theta)}{d\theta} (e^{i\phi} + e^{-i\phi}) e^{im\phi} \right]. \quad (\text{D.59})$$

and

$$\mathbf{M}_{mn}^* \cdot \mathbf{e}_y = \frac{1}{2} \left[-m j_n(kr) \cos \theta \frac{P_n^m(\cos \theta)}{\sin \theta} (e^{i\phi} - e^{-i\phi}) e^{-im\phi} - j_n(kr) \frac{dP_n^m(\cos \theta)}{d\theta} (e^{i\phi} + e^{-i\phi}) e^{-im\phi} \right]. \quad (\text{D.60})$$

So now the ϕ -integration will change the sign of the first term and not change the sign of the second term, so that there will be no relative sign difference in the above two terms. Thus:

$$\langle \mathbf{E}_y | \mathbf{M}_{-mn} \rangle = (-1)^m \frac{(n-m)!}{(n+m)!} \times \left[\langle \mathbf{E}_y | \mathbf{M}_{mn} \rangle \text{ with } e^{-i(m\pm 1)\beta} \text{ factors changed to } e^{i(m\pm 1)\beta} \right] \quad (\text{D.61})$$

Similarly, since we have:

$$\mathbf{N}_{mn}^* \cdot \mathbf{e}_y = \frac{1}{2} \left[-in(n+1) \frac{j_n(kr)}{kr} \sin \theta P_n^m(\cos \theta) (e^{i\phi} - e^{-i\phi}) e^{-im\phi} - i \frac{1}{kr} \frac{d(rj_n(kr))}{dr} \cos \theta \frac{dP_n^m(\cos \theta)}{d\theta} (e^{i\phi} - e^{-i\phi}) e^{-im\phi} - im \frac{1}{kr} \frac{d(rj_n(kr))}{dr} \frac{P_n^m(\cos \theta)}{\sin \theta} (e^{i\phi} + e^{-i\phi}) e^{-im\phi} \right]. \quad (\text{D.62})$$

and

$$\mathbf{N}_{mn} \cdot \mathbf{e}_y = \frac{1}{2} \left[-in(n+1) \frac{j_n(kr)}{kr} \sin \theta P_n^m(\cos \theta) (e^{i\phi} - e^{-i\phi}) e^{im\phi} - i \frac{1}{kr} \frac{d(rj_n(kr))}{dr} \cos \theta \frac{dP_n^m(\cos \theta)}{d\theta} (e^{i\phi} - e^{-i\phi}) e^{im\phi} + im \frac{1}{kr} \frac{d(rj_n(kr))}{dr} \frac{P_n^m(\cos \theta)}{\sin \theta} (e^{i\phi} + e^{-i\phi}) e^{im\phi} \right] \quad (\text{D.63})$$

So in this case, the ϕ -integration will change the sign of the first two terms and not change the sign of the third term. The result is an overall factor of -1. Thus:

$$\langle \mathbf{E}_y | \mathbf{N}_{-mn} \rangle = (-1)^{m+1} \frac{(n-m)!}{(n+m)!} \times \left[\langle \mathbf{E}_y | \mathbf{N}_{mn} \rangle \text{ with } e^{-i(m\pm 1)\beta} \text{ factors changed to } e^{i(m\pm 1)\beta} \right] \quad (\text{D.64})$$

Also, as discussed before, the $\langle \mathbf{E}_y | \mathbf{L}_{-mn} \rangle$ integral will have the same sign inversions as the $\langle \mathbf{E}_y | \mathbf{L}_{mn} \rangle$ integral and so,

$$\langle \mathbf{E}_y | \mathbf{L}_{-mn} \rangle = (-1)^{m+1} \frac{(n-m)!}{(n+m)!} \times \left[\langle \mathbf{E}_y | \mathbf{L}_{mn} \rangle \text{ with } e^{-i(m\pm 1)\beta} \text{ factors changed to } e^{i(m\pm 1)\beta} \right] \quad (\text{D.65})$$

Finally, we take a look at the \mathbf{e}_z integrals for negative m 's. We have:

$$\mathbf{e}_z \cdot \mathbf{M}_{mn}^* = (-\sin \theta) \left(-im j_n(kr) \frac{P_n^m(\cos \theta)}{\sin \theta} e^{-im\phi} \right) \quad (\text{D.66})$$

$$\mathbf{e}_z \cdot \mathbf{M}_{mn} = (-\sin \theta) \left(im j_n(kr) \frac{P_n^m(\cos \theta)}{\sin \theta} e^{im\phi} \right). \quad (\text{D.67})$$

It is easily seen that the two expressions differ in sign. So, we can immediately write down the transformation rule for the inner product in this case (also, since $l = \pm m$ are the allowed terms, the exponential factors are $e^{\pm im\beta}$):

$$\langle \mathbf{E}_z | \mathbf{M}_{-mn} \rangle = (-1)^{m+1} \frac{(n-m)!}{(n+m)!} \times \left[\langle \mathbf{E}_z | \mathbf{M}_{mn} \rangle \text{ with } e^{-im\beta} \text{ factors changed to } e^{im\beta} \right] \quad (\text{D.68})$$

Both, the \mathbf{L} and \mathbf{N} functions have their im factor in the ϕ components only. Since \mathbf{e}_z does not have any \mathbf{e}_ϕ component, therefore there is not extra phase change in the case of \mathbf{L} and \mathbf{N} functions, and therefore:

$$\langle \mathbf{E}_z | \mathbf{N}_{-mn} \rangle = (-1)^m \frac{(n-m)!}{(n+m)!} \times \left[\langle \mathbf{E}_z | \mathbf{N}_{mn} \rangle \text{ with } e^{-im\beta} \text{ factors changed to } e^{im\beta} \right] \quad (\text{D.69})$$

$$\langle \mathbf{E}_z | \mathbf{L}_{-mn} \rangle = (-1)^m \frac{(n-m)!}{(n+m)!} \times \left[\langle \mathbf{E}_y | \mathbf{L}_{mn} \rangle \text{ with } e^{-im\beta} \text{ factors} \right. \\ \left. \text{changed to } e^{im\beta}. \right] \quad (\text{D.70})$$

Appendix E

Scattering Cross-Section and Total Cross-Section

In this appendix we derive the formula for the scattering cross-section and the total cross-section of a spherically symmetric particle, subjected to plane electromagnetic waves. The total field outside the particle is the sum of the incident and the scattered fields:

$$\mathbf{E} = \mathbf{E}_i + \mathbf{E}_s \quad (\text{E.1})$$

$$\mathbf{H} = \mathbf{H}_i + \mathbf{H}_s \quad (\text{E.2})$$

where the subscripts i and s denote incident and scattered respectively.

We begin with the definition of the complex Poynting vector

$$\mathbf{S}^* = \frac{1}{2} \mathbf{E} \times \mathbf{H}^* \quad (\text{asterix '*' indicate complex conjugate}). \quad (\text{E.3})$$

Now, since

$$E_\theta = E_{i\theta} + E_{s\theta}; \quad E_\phi = E_{i\phi} + E_{s\phi}; \quad H_\theta = H_{i\theta} + H_{s\theta}; \quad H_\phi = H_{i\phi} + H_{s\phi}.$$

So the radial component of the total complex flow vector is:

$$\begin{aligned} S_r^* &= \frac{1}{2} [E_\theta H_\phi^* - E_\phi H_\theta^*] \\ &= \frac{1}{2} [(E_{i\theta} + E_{s\theta})(H_{i\phi}^* + H_{s\phi}^*) - (E_{i\phi} + E_{s\phi})(H_{i\theta}^* + H_{s\theta}^*)] \\ &= \frac{1}{2} (E_{i\theta} H_{i\phi}^* - E_{i\phi} H_{i\theta}^*) + \frac{1}{2} (E_{s\theta} H_{s\phi}^* - E_{s\phi} H_{s\theta}^*) \\ &\quad + \frac{1}{2} (E_{i\theta} H_{s\phi}^* + E_{s\theta} H_{i\phi}^* - E_{i\phi} H_{s\theta}^* - E_{s\phi} H_{i\theta}^*) \end{aligned} \quad (\text{E.4})$$

Assume a spherical surface of radius R , concentric with the scatterer and enclosing it. The real part of S_r^* integrated over this sphere is equal to the net flow of energy across its surface. Total energy absorbed by the sphere is given by

$$W_a = -Re \int_0^\pi d\theta \sin \theta \int_0^{2\pi} d\phi r^2 S_r^* \quad (\text{E.5})$$

The first term in the right hand side of Equation E.4 measures the flow of energy in the incident wave. When integrated over a closed surface, this gives zero, as long as $\sigma_2 = 0$ (i.e. surrounding medium is non-absorbing). The second term measures the outward flow of the energy scattered from the particle, and so the total scattered energy is

$$W_s = \frac{1}{2} Re \int_0^\pi d\theta \sin \theta \int_0^{2\pi} d\phi r^2 (E_{s\theta} H_{s\phi}^* - E_{s\phi} H_{s\theta}^*) \quad (E.6)$$

Since the total energy must be conserved, therefore the third term in Equation E.4 must equal in magnitude to the sum of the absorbed and scattered energies. So the total energy derived from the primary wave and dissipated as heat and scattered radiation is given by

$$\begin{aligned} W_t &= W_a + W_s \\ &= -\frac{1}{2} Re \int_0^\pi d\theta \sin \theta \int_0^{2\pi} d\phi r^2 (E_{i\theta} H_{s\phi}^* + E_{s\theta} H_{i\phi}^* - E_{i\phi} H_{s\theta}^* - E_{s\phi} H_{i\theta}^*) \end{aligned} \quad (E.7)$$

Since we are considering a spherically symmetric scatterer, therefore we can choose the incident wave to be directed along any arbitrary direction. We choose the direction of approach to the z-axis, so that we can write the incident fields in the following form:

$$\mathbf{E}_i = \sum_{n=1}^{\infty} \frac{i^n (2n+1)}{n(n+1)} \{ a_n^i \mathbf{m}_{o1n}^{(2)j} + i b_n^i \mathbf{n}_{e1n}^{(2)j} \} \quad (E.8)$$

and since $\nabla \times \mathbf{m} = k\mathbf{n}$ and $\nabla \times \mathbf{n} = k\mathbf{m}$, therefore,

$$\begin{aligned} \mathbf{H}_i &= \frac{1}{i\omega\mu_2} \nabla \times \mathbf{E}_i \\ &= \frac{k_2}{i\omega\mu_2} \sum_{n=1}^{\infty} \frac{i^n (2n+1)}{n(n+1)} \{ i b_n^i \mathbf{m}_{e1n}^{(2)j} + a_n^i \mathbf{n}_{o1n}^{(2)j} \} \\ &= \frac{k_2}{\omega\mu_2} \sum_{n=1}^{\infty} \frac{i^n (2n+1)}{n(n+1)} \{ i b_n^i \mathbf{m}_{e1n}^{(2)j} - i a_n^i \mathbf{n}_{o1n}^{(2)j} \}. \end{aligned} \quad (E.9)$$

Similarly, the scattered fields can be written as:

$$\mathbf{E}_s = \sum_{n=1}^{\infty} \frac{i^n (2n+1)}{n(n+1)} \{ a_n^{sh} \mathbf{m}_{o1n}^{(2)h} + i b_n^{sh} \mathbf{n}_{e1n}^{(2)h} \} \quad (E.10)$$

$$\mathbf{H}_s = \frac{k_2}{\omega\mu_2} \sum_{n=1}^{\infty} \frac{i^n (2n+1)}{n(n+1)} \{ i b_n^{sh} \mathbf{m}_{e1n}^{(2)h} - i a_n^{sh} \mathbf{n}_{o1n}^{(2)h} \}. \quad (E.11)$$

So we have:

$$\begin{aligned}
E_{s\theta} &= \sum_{n=1}^{\infty} \frac{i^n(2n+1)}{n(n+1)} \left\{ a_n^{sh} \mathbf{m}_{o1n}^{(2)h} \cdot \mathbf{e}_\theta + i b_n^{sh} \mathbf{n}_{e1n}^{(2)h} \cdot \mathbf{e}_\theta \right\} \\
&= \sum_{n=1}^{\infty} \frac{i^n(2n+1)}{n(n+1)} \left\{ a_n^{sh} h_n^{(1)}(kr) \cdot \frac{P_n^1(\cos \theta)}{\sin \theta} \cdot \cos \phi \right. \\
&\quad \left. + i b_n^{sh} \frac{1}{kr} \frac{d}{dr} (r h_n^{(1)}(kr)) \cdot \frac{d}{d\theta} P_n^1(\cos \theta) \cos \phi \right\} \quad (\text{E.12})
\end{aligned}$$

Similarly:

$$\begin{aligned}
E_{s\phi} &= \sum_{n=1}^{\infty} \frac{i^n(2n+1)}{n(n+1)} \left\{ a_n^{sh} \cdot (-h_n^{(1)}(kr)) \cdot \frac{d}{d\theta} P_n^1(\cos \theta) \cdot \sin \phi \right. \\
&\quad \left. + i b_n^{sh} \left(-\frac{1}{kr} \frac{d}{dr} (r h_n^{(1)}(kr)) \right) \cdot \frac{P_n^1(\cos \theta)}{\sin \theta} \cdot \sin \phi \right\}. \quad (\text{E.13})
\end{aligned}$$

$$\begin{aligned}
H_{s\theta} &= \frac{k_2}{\omega \mu_2} \sum_{n=1}^{\infty} \frac{i^n(2n+1)}{n(n+1)} \left\{ b_n^{sh} \mathbf{m}_{e1n}^{(2)h} \cdot \mathbf{e}_\theta - i a_n^{sh} \mathbf{n}_{o1n}^{(2)h} \cdot \mathbf{e}_\theta \right\} \\
&= \frac{k_2}{\omega \mu_2} \sum_{n=1}^{\infty} \frac{i^n(2n+1)}{n(n+1)} \left\{ b_n^{sh} (-h_n^{(1)}(kr)) \cdot \frac{P_n^1(\cos \theta)}{\sin \theta} \cdot \sin \phi \right. \\
&\quad \left. - i a_n^{sh} \left(\frac{1}{kr} \frac{d}{dr} (r h_n^{(1)}(kr)) \right) \cdot \frac{d}{d\theta} P_n^1(\cos \theta) \cdot \sin \phi \right\}. \quad (\text{E.14})
\end{aligned}$$

$$\begin{aligned}
H_{s\phi} &= \frac{k_2}{\omega \mu_2} \sum_{n=1}^{\infty} \frac{i^n(2n+1)}{n(n+1)} \left\{ b_n^{sh} (-h_n^{(1)}(kr)) \cdot \frac{d}{d\theta} P_n^1(\cos \theta) \cdot \sin \phi \right. \\
&\quad \left. - i a_n^{sh} \left(\frac{1}{kr} \frac{d}{dr} (r h_n^{(1)}(kr)) \right) \cdot \frac{P_n^1(\cos \theta)}{\sin \theta} \cdot \cos \phi \right\}. \quad (\text{E.15})
\end{aligned}$$

Therefore,

$$\begin{aligned}
E_{s\theta} \cdot H_{s\phi}^* &= \frac{k_2}{\omega \mu_2} \left[\sum_{n=1}^{\infty} \frac{i^n(2n+1)}{n(n+1)} \left\{ a_n^{sh} h_n^{(1)}(kr) \cdot \frac{P_n^1(\cos \theta)}{\sin \theta} \cdot \cos \phi \right. \right. \\
&\quad \left. \left. + i b_n^{sh} \frac{1}{kr} \frac{d}{dr} (r h_n^{(1)}(kr)) \cdot \frac{d}{d\theta} P_n^1(\cos \theta) \cdot \cos \phi \right\} \right] \times \\
&\quad \left[\sum_{n'=1}^{\infty} \frac{(-i)^{n'}(2n'+1)}{n'(n'+1)} \left\{ b_{n'}^{*sh} (-z_{n'}^*(kr)) \cdot \frac{d}{d\theta} P_{n'}^1(\cos \theta) \cdot \cos \phi \right. \right. \\
&\quad \left. \left. + i a_{n'}^{*sh} \left(\frac{1}{kr} \frac{d}{dr} (r z_{n'}^*(kr)) \right) \cdot \frac{P_{n'}^1(\cos \theta)}{\sin \theta} \cdot \cos \phi \right\} \right] \quad (\text{E.16})
\end{aligned}$$

$$\begin{aligned}
E_{s\phi} \cdot H_{s\theta}^* &= \frac{k_2}{\omega\mu_2} \left[\sum_{n=1}^{\infty} \frac{i^n(2n+1)}{n(n+1)} \left\{ a_n^{sh}(-h_n^{(1)}(kr)) \cdot \frac{d}{d\theta} P_n^1(\cos\theta) \cdot \sin\phi \right. \right. \\
&\quad \left. \left. + i b_n^{sh} \left(-\frac{1}{kr} \frac{d}{dr} (r h_n^{(1)}(kr)) \right) \cdot \frac{P_n^1(\cos\theta)}{\sin\theta} \cdot \sin\phi \right\} \right] \times \\
&\quad \left[\sum_{n'=1}^{\infty} \frac{(-i)^{n'}(2n'+1)}{n'(n'+1)} \left\{ b_{n'}^{*sh}(-z_{n'}^*(kr)) \frac{P_{n'}^1(\cos\theta)}{\sin\theta} \cdot \sin\phi \right. \right. \\
&\quad \left. \left. + i a_{n'}^{*sh} \left(\frac{1}{kr} \frac{d}{dr} (r z_{n'}^*(kr)) \right) \right\} \cdot \frac{d}{d\theta} P_{n'}^1(\cos\theta) \cdot \sin\phi \right].
\end{aligned} \tag{E.17}$$

The ϕ integration over $[0, 2\pi]$ gives

$$\int_0^{2\pi} d\phi \cos^2\phi \quad \text{or} \quad \int_0^{2\pi} d\phi \sin^2\phi \tag{E.18}$$

which evaluate to π . The θ -integrations involve:

$$\begin{aligned}
\int_0^\pi d\theta \sin\theta \left(\frac{dP_n^1}{d\theta} \cdot \frac{dP_{n'}^1}{d\theta} + \frac{1}{\sin^2\theta} \cdot P_n^1 P_{n'}^1 \right) &= 0 \quad (n \neq n') \\
&= \frac{2n(n+1)}{2n+1} \cdot \frac{(n+1)!}{(n-1)!} \quad (n = n')
\end{aligned} \tag{E.19}$$

$$\begin{aligned}
\int_0^\pi d\theta \sin\theta \left(\frac{P_n^1}{\sin\theta} \cdot \frac{dP_{n'}^1}{d\theta} + \frac{P_{n'}^1}{\sin\theta} \cdot \frac{dP_n^1}{d\theta} \right) &= \int_0^\pi d\theta \frac{d}{d\theta} (P_n^1 P_{n'}^1) \\
&= P_n^1(\cos\theta) P_{n'}^1(\cos\theta) \Big|_0^\pi \\
&= 0 \quad (\text{since } P_n^1(\pm 1) = 0).
\end{aligned} \tag{E.20}$$

Thus we have

$$\begin{aligned}
\int_0^{2\pi} d\phi (E_{s\theta} H_{s\phi}^* - E_{s\phi} H_{s\theta}^*) &= \\
\frac{\pi k_2}{\omega\mu_2} \sum_{n=1}^{\infty} \sum_{n'=1}^{\infty} &\left[\frac{i^n (-i)^{n'} (2n+1)(2n'+1)}{n(n+1)n'(n'+1)} \times \right. \\
&\left\{ \left(-a_n^{sh} b_{n'}^{*sh} \cdot h_n^{(1)}(kr) \cdot h_{n'}^{(1)*}(kr) \frac{P_n^1(\cos\theta)}{\sin\theta} \cdot \frac{d}{d\theta} P_{n'}^1(\cos\theta) \right. \right. \\
&+ i a_n^{sh} a_{n'}^{*sh} h_n^{(1)}(kr) \left(\frac{1}{kr} \frac{d}{dr} (r h_{n'}^{(1)}(kr)) \right)^* \frac{P_n^1(\cos\theta)}{\sin\theta} \cdot \frac{P_{n'}^1(\cos\theta)}{\sin\theta} \\
&- i b_n^{sh} b_{n'}^{*sh} \left(\frac{1}{kr} \frac{d}{dr} (r h_n^{(1)}(kr)) \right) \cdot h_{n'}^{(1)*}(kr) \cdot \frac{d}{d\theta} P_n^1(\cos\theta) \cdot \frac{d}{d\theta} P_{n'}^1(\cos\theta) \\
&\left. \left. - b_n^{sh} a_{n'}^{*sh} \left(\frac{1}{kr} \frac{d}{dr} (r h_n^{(1)}(kr)) \right) \left(\frac{1}{kr} \frac{d}{dr} (r h_{n'}^{(1)}(kr)) \right)^* \frac{d}{d\theta} P_n^1(\cos\theta) \frac{P_{n'}^1(\cos\theta)}{\sin\theta} \right) \right\}
\end{aligned} \tag{E.21}$$

$$\begin{aligned}
& - \left(a_n^{sh} b_{n'}^{*sh} h_n^{(1)}(kr) h_{n'}^{(1)*}(kr) \frac{d}{d\theta} P_n^1(\cos \theta) \cdot \frac{P_{n'}^1(\cos \theta)}{\sin \theta} \right. \\
& - i a_n^{sh} a_{n'}^{*sh} h_n^{(1)}(kr) \cdot \left(\frac{1}{kr} \frac{d}{dr} (r h_{n'}^{(1)}(kr)) \right)^* \frac{d}{d\theta} P_n^1(\cos \theta) \cdot \frac{d}{d\theta} P_{n'}^1(\cos \theta) \\
& + i b_n^{sh} b_{n'}^{*sh} \left(\frac{1}{kr} \frac{d}{dr} (r h_n^{(1)}(kr)) \right) \cdot h_{n'}^{(1)*}(kr) \cdot \frac{P_n^1(\cos \theta)}{\sin \theta} \cdot \frac{P_{n'}^1(\cos \theta)}{\sin \theta} \\
& \left. + b_n^{sh} a_{n'}^{*sh} \left(\frac{1}{kr} \frac{d}{dr} (r h_n^{(1)}(kr)) \right) \left(\frac{1}{kr} \frac{d}{dr} (r h_{n'}^{(1)}(kr)) \right)^* \cdot \frac{P_n^1(\cos \theta)}{\sin \theta} \cdot \frac{d}{d\theta} P_{n'}^1(\cos \theta) \right) \Bigg]
\end{aligned}$$

Due to the θ -integrals just discussed, we have the $a_n^{sh} b_{n'}^{*sh}$ and the $b_n^{sh} a_{n'}^{*sh}$ terms vanish when the θ -integration is carried out. The $i a_n^{sh} a_{n'}^{*sh}$ and $i b_n^{sh} b_{n'}^{*sh}$ terms have the same r -dependence, and on θ -integration, only the $n = n'$ terms survive, so one of the infinite summation drops out and we can write $i a_n^{sh} a_{n'}^{*sh} = i |a_n^{sh}|^2$ and $i b_n^{sh} b_{n'}^{*sh} = i |b_n^{sh}|^2$. Thus we have

$$\begin{aligned}
& \int_0^{2\pi} d\phi \int_0^\pi d\theta \sin \theta \left(E_{s\theta} H_{s\phi}^* - E_{s\phi} H_{s\theta}^* \right) = \tag{E.22} \\
& \frac{\pi k_2}{\omega \mu_2} \sum_{n=1}^{\infty} \left[\frac{(2n+1)}{n(n+1)} \right]^2 \left\{ i |a_n^{sh}|^2 h_n^{(1)}(kr) \left(\frac{1}{kr} \frac{d}{dr} (r h_n^{(1)}(kr)) \right)^* \times \right. \\
& \quad \int_0^\pi d\theta \sin \theta \left(\frac{P_n^1 P_n^1}{\sin^2 \theta} + \frac{dP_n^1}{d\theta} \frac{dP_n^1}{d\theta} \right) \\
& \quad \left. - i |b_n^{sh}|^2 z_n^*(kr) \left(\frac{1}{kr} \frac{d}{dr} (r h_n^{(1)}(kr)) \right)^* \int_0^\pi d\theta \sin \theta \left(\frac{dP_n^1}{d\theta} \frac{dP_n^1}{d\theta} + \frac{P_n^1 P_n^1}{\sin^2 \theta} \right) \right\} \\
& = \frac{\pi k_2}{\omega \mu_2} \sum_{n=1}^{\infty} 2(2n+1) \left\{ |a_n^{sh}|^2 \left(i h_n^{(1)}(kr) \left(\frac{1}{kr} \frac{d}{dr} (r h_n^{(1)}(kr)) \right)^* \right) \right. \\
& \quad \left. + |b_n^{sh}|^2 \left(h_n^{*(1)}(kr) \left(\frac{1}{kr} \frac{d}{dr} (r h_n^{(1)}(kr)) \right)^* \right)^* \right\}
\end{aligned}$$

Now the asymptotic behavior of $h_n^{(1)}(kr)$ is given by

$$h_n^{(1)}(kr) \simeq \frac{1}{kr} (-i)^{n+1} e^{ikr} \tag{E.23}$$

$$h_{n-1}^{(1)}(kr) \simeq \frac{(-i)^n}{kr} e^{ikr} \tag{E.24}$$

$$h_{n+1}^{(1)}(kr) \simeq \frac{(-i)^{n+2}}{kr} e^{ikr}. \tag{E.25}$$

Therefore.

$$\begin{aligned}
& ih_n^{(1)}(kr) \cdot \left(\frac{1}{kr} \frac{d}{dr} (rh_n^{(1)}(kr)) \right)^* \\
&= ih_n^{(1)}(kr) \cdot \left(\frac{(n+1)h_{n-1}^{(1)}(kr) - nh_{n+1}^{(1)}(kr)}{(2n+1)} \right)^* \\
&= \frac{i(-i)^{n+1}}{kr} \frac{e^{ikr}}{(2n+1)} \left(\frac{(n+1)(-i)^n e^{ikr} - (-i)^{n+2} n e^{ikr}}{kr} \right)^* \\
&= \frac{i(-i)^{n+1}}{(kr)^2} \frac{1}{(2n+1)} [(n+1)(i)^n + n(i)^n] \\
&= \frac{(-i)^{n+1}(i)^{n+1}}{(kr)^2} = \frac{1}{(kr)^2} \tag{E.26}
\end{aligned}$$

Thus the total scattered energy at the sphere at radius R is

$$\begin{aligned}
W_s &= \frac{1}{2} R \epsilon \int_0^\pi d\theta \sin \theta \int_0^{2\pi} d\phi (E_{s\theta} H_{s\phi}^* - E_{s\phi} H_{s\theta}^*) \cdot R^2 \\
&= \frac{\pi k_2}{\omega \mu_2} \frac{R^2}{(k_2 R)^2} \sum_{n=1}^{\infty} (2n+1) (|a_n^{sh}|^2 + |b_n^{sh}|^2) \tag{E.27}
\end{aligned}$$

$$= \frac{\pi}{k_2^2} \sqrt{\frac{\epsilon_2}{\mu_2}} \sum_{n=1}^{\infty} (2n+1) (|a_n^{sh}|^2 + |b_n^{sh}|^2). \tag{E.28}$$

The **scattering cross section** is defined as the ratio of the total scattered energy per second to the energy density of the incident wave. For an incident plane wave of unit amplitude, the mean energy flow per unit area is

$$\langle \mathbf{E} \times \mathbf{H} \rangle = \frac{E_0^2}{2} \sqrt{\epsilon_2 \mu_2} = \frac{1}{2} \sqrt{\epsilon_2 \mu_2} \quad (\text{since } E_0 = 1) \tag{E.29}$$

Thus the scattering cross section, Q_s is

$$Q_s = \frac{2\pi}{k_2^2} \sum_{n=1}^{\infty} (2n+1) (|a_n^{sh}|^2 + |b_n^{sh}|^2) \tag{E.30}$$

Let us now find the sum of absorbed and scattered energies, W_t :

$$W_t = -\frac{1}{2} R \epsilon \int_0^\pi d\theta \sin \theta \int_0^{2\pi} d\phi (E_{i\theta} H_{s\phi}^* + E_{s\theta} H_{i\phi}^* - E_{i\phi} H_{s\theta}^* - E_{s\phi} H_{i\theta}^*) R^2 \tag{E.31}$$

Here we have the two combination terms:

$$E_{i\theta}H_{s\phi}^* - E_{i\phi}H_{s\theta}^* \quad \text{and} \quad E_{s\theta}H_{i\phi}^* - E_{s\phi}H_{i\theta}^*. \quad (\text{E.32})$$

The expressions for $E_{i\theta}$, $E_{i\phi}$, $H_{i\theta}$ and $H_{i\phi}$ are similar to the ones derived explicitly for $E_{s\theta}$, $E_{s\phi}$, $H_{s\theta}$ and $H_{s\phi}$, with a_n^{sh} replaced by a_n^i and b_n^{sh} replaced by b_n^i . Also the spherical Hankel functions are replaced by the spherical Bessel functions. Let us evaluate the two terms separately.

$$\begin{aligned} I_1 = & \int_0^{2\pi} d\phi \left(E_{i\theta}H_{s\phi}^* - E_{i\phi}H_{s\theta}^* \right) = \quad (\text{E.33}) \\ & \frac{\pi k_2}{\omega \mu_2} \sum_{n=1}^{\infty} \sum_{n'=1}^{\infty} \left[\frac{i^n (-i)^{n'} (2n+1)(2n'+1)}{n(n+1)n'(n'+1)} \times \right. \\ & \left\{ \left(-a_n^i b_{n'}^{*sh} \cdot j_n(kr) \cdot h_{n'}^{(1)*}(kr) \frac{P_n^1(\cos \theta)}{\sin \theta} \cdot \frac{d}{d\theta} P_{n'}^1(\cos \theta) \right. \right. \\ & + i a_n^i a_{n'}^{*sh} j_n(kr) \left(\frac{1}{kr} \frac{d}{dr} (r h_{n'}^{(1)}(kr)) \right)^* \frac{P_n^1(\cos \theta)}{\sin \theta} \cdot \frac{P_{n'}^1(\cos \theta)}{\sin \theta} \\ & - i b_n^i b_{n'}^{*sh} \left(\frac{1}{kr} \frac{d}{dr} (r j_n(kr)) \right) \cdot h_{n'}^{(1)*}(kr) \cdot \frac{d}{d\theta} P_n^1(\cos \theta) \cdot \frac{d}{d\theta} P_{n'}^1(\cos \theta) \\ & - b_n^i a_{n'}^{*sh} \left(\frac{1}{kr} \frac{d}{dr} (r j_n(kr)) \right) \left(\frac{1}{kr} \frac{d}{dr} (r h_{n'}^{(1)}(kr)) \right)^* \frac{d}{d\theta} P_n^1(\cos \theta) \frac{P_{n'}^1(\cos \theta)}{\sin \theta} \\ & - \left(a_n^i b_{n'}^{*sh} j_n(kr) h_{n'}^{(1)*}(kr) \frac{d}{d\theta} P_n^1(\cos \theta) \cdot \frac{P_{n'}^1(\cos \theta)}{\sin \theta} \right. \\ & - i a_n^i a_{n'}^{*sh} j_n(kr) \cdot \left(\frac{1}{kr} \frac{d}{dr} (r h_{n'}^{(1)}(kr)) \right)^* \frac{d}{d\theta} P_n^1(\cos \theta) \cdot \frac{d}{d\theta} P_{n'}^1(\cos \theta) \\ & + i b_n^i b_{n'}^{*sh} \left(\frac{1}{kr} \frac{d}{dr} (r j_n(kr)) \right) \cdot h_{n'}^{(1)*}(kr) \cdot \frac{P_n^1(\cos \theta)}{\sin \theta} \cdot \frac{P_{n'}^1(\cos \theta)}{\sin \theta} \\ & \left. \left. + b_n^i a_{n'}^{*sh} \left(\frac{1}{kr} \frac{d}{dr} (r j_n(kr)) \right) \left(\frac{1}{kr} \frac{d}{dr} (r h_{n'}^{(1)}(kr)) \right)^* \cdot \frac{P_n^1(\cos \theta)}{\sin \theta} \cdot \frac{d}{d\theta} P_{n'}^1(\cos \theta) \right) \right\} \right]. \end{aligned}$$

Clearly, the only surviving terms after θ -integration will be the $a_n^i a_{n'}^{*sh}$ and $b_n^i b_{n'}^{*sh}$ terms with only $n = n'$ surviving.

$$\begin{aligned} I_1 = & \int_0^{2\pi} d\phi \int_0^\pi d\theta \sin \theta \left(E_{i\theta}H_{s\phi}^* - E_{i\phi}H_{s\theta}^* \right) \\ = & \frac{\pi k_2}{\omega \mu_2} \sum_{n=1}^{\infty} 2(2n+1) \left\{ a_n^i a_n^{*sh} \left(i j_n(kr) \left(\frac{1}{kr} \frac{d}{dr} (r h_n^{(1)}(kr)) \right)^* \right) \right. \\ & \left. + b_n^i b_n^{*sh} \left(i h_n^{(1)}(kr) \left(\frac{1}{kr} \frac{d}{dr} (r j_n(kr)) \right)^* \right) \right\} \quad (\text{E.34}) \end{aligned}$$

Now we consider the second term,

$$\begin{aligned}
I_2 = & \int_0^{2\pi} d\phi \left(E_{s\theta} H_{i\phi}^* - E_{s\phi} H_{i\theta}^* \right) = \tag{E.35} \\
& \frac{\pi k_2}{\omega \mu_2} \sum_{n=1}^{\infty} \sum_{n'=1}^{\infty} \left[\frac{i^n (-i)^{n'} (2n+1)(2n'+1)}{n(n+1)n'(n'+1)} \times \right. \\
& \left\{ \left(-a_n^{sh} b_{n'}^{*i} \cdot h_n^{(1)}(kr) \cdot j_{n'}^*(kr) \frac{P_n^1(\cos \theta)}{\sin \theta} \cdot \frac{d}{d\theta} P_{n'}^1(\cos \theta) \right. \right. \\
& + i a_n^{sh} a_{n'}^{*i} h_n^{(1)}(kr) \left(\frac{1}{kr} \frac{d}{dr} (r j_{n'}(kr)) \right)^* \frac{P_n^1(\cos \theta)}{\sin \theta} \cdot \frac{P_{n'}^1(\cos \theta)}{\sin \theta} \\
& - i b_n^{sh} b_{n'}^{*i} \left(\frac{1}{kr} \frac{d}{dr} (r h_n^{(1)}(kr)) \right) \cdot j_{n'}^*(kr) \cdot \frac{d}{d\theta} P_n^1(\cos \theta) \cdot \frac{d}{d\theta} P_{n'}^1(\cos \theta) \\
& - b_n^{sh} a_{n'}^{*i} \left(\frac{1}{kr} \frac{d}{dr} (r h_n^{(1)}(kr)) \right) \left(\frac{1}{kr} \frac{d}{dr} (r j_{n'}(kr)) \right)^* \frac{d}{d\theta} P_n^1(\cos \theta) \frac{P_{n'}^1(\cos \theta)}{\sin \theta} \\
& - \left(a_n^{sh} b_{n'}^{*i} h_n^{(1)}(kr) j_{n'}^*(kr) \frac{d}{d\theta} P_n^1(\cos \theta) \cdot \frac{P_{n'}^1(\cos \theta)}{\sin \theta} \right. \\
& - i a_n^{sh} a_{n'}^{*i} h_n^{(1)}(kr) \cdot \left(\frac{1}{kr} \frac{d}{dr} (r j_{n'}(kr)) \right)^* \frac{d}{d\theta} P_n^1(\cos \theta) \cdot \frac{d}{d\theta} P_{n'}^1(\cos \theta) \\
& + i b_n^{sh} b_{n'}^{*i} \left(\frac{1}{kr} \frac{d}{dr} (r h_n^{(1)}(kr)) \right) \cdot j_{n'}^*(kr) \cdot \frac{P_n^1(\cos \theta)}{\sin \theta} \cdot \frac{P_{n'}^1(\cos \theta)}{\sin \theta} \\
& \left. \left. + b_n^{sh} a_{n'}^{*i} \left(\frac{1}{kr} \frac{d}{dr} (r h_n^{(1)}(kr)) \right) \left(\frac{1}{kr} \frac{d}{dr} (r j_{n'}(kr)) \right)^* \cdot \frac{P_n^1(\cos \theta)}{\sin \theta} \cdot \frac{d}{d\theta} P_{n'}^1(\cos \theta) \right) \right\} \Bigg].
\end{aligned}$$

So the second integral is

$$\begin{aligned}
I_2 &= \int_0^{2\pi} d\phi \int_0^\pi d\theta \sin \theta \left(E_{s\theta} H_{i\phi}^* - E_{s\phi} H_{i\theta}^* \right) \\
&= \frac{\pi k_2}{\omega \mu_2} \sum_{n=1}^{\infty} 2(2n+1) \left\{ a_n^{*i} a_n^{sh} \left(i h_n^{(1)}(kr) \left(\frac{1}{kr} \frac{d}{dr} (r j_n(kr)) \right)^* \right) \right. \\
&\quad \left. + b_n^{*i} b_n^{sh} \left(i j_n(kr) \left(\frac{1}{kr} \frac{d}{dr} (r h_n^{(1)}(kr)) \right)^* \right)^* \right\} \tag{E.36}
\end{aligned}$$

Now let us consider the asymptotic behavior of the spherical Bessel functions:

$$\begin{aligned}
j_n(kr) &\simeq \frac{1}{kr} \cos \left(kr - \frac{n+1}{2} \pi \right) \\
&\simeq \frac{1}{kr} \left\{ \frac{e^{i(kr - \frac{n+1}{2} \pi)} + e^{-i(kr - \frac{n+1}{2} \pi)}}{2} \right\} \\
&\simeq \frac{1}{2kr} \left\{ e^{ikr} \cdot e^{-i(\frac{n+1}{2} \pi)} + e^{-ikr} \cdot e^{i(\frac{n+1}{2} \pi)} \right\}
\end{aligned}$$

$$\simeq \frac{1}{2kr} \left\{ e^{ikr} \cdot (-i)^{n+1} + e^{-ikr} (i)^{n+1} \right\} \quad (\text{E.37})$$

Similarly,

$$j_{n-1}(kr) \simeq \frac{1}{2kr} \left\{ e^{ikr} (-i)^n + e^{-ikr} (i)^n \right\}. \quad (\text{E.38})$$

$$j_{n+1}(kr) \simeq -\frac{1}{2kr} \left\{ e^{ikr} (-i)^n + e^{-ikr} (i)^n \right\}. \quad (\text{E.39})$$

Therefore,

$$\begin{aligned} \frac{1}{kr} \frac{d}{dr} (rj_n(kr)) &= \frac{1}{(2n+1)} \left\{ (n+1)j_{n-1}(kr) - nj_{n+1}(kr) \right\} \\ &\simeq \frac{1}{2kr} \left\{ (-i)^n e^{ikr} + (i)^n e^{-ikr} \right\} \end{aligned} \quad (\text{E.40})$$

Similarly,

$$\begin{aligned} \frac{1}{kr} \frac{d}{dr} (rh_n^{(1)}(kr)) &= \frac{1}{(2n+1)} \left\{ (n+1)h_{n-1}^{(1)}(kr) - nh_{n+1}^{(1)}(kr) \right\} \\ &\simeq \frac{i^n e^{-ikr}}{kr}. \end{aligned} \quad (\text{E.41})$$

Therefore,

$$\begin{aligned} ij_n(kr) \left[\frac{1}{kr} \frac{d}{dr} (rh_n^{(1)}(kr)) \right]^n &= \frac{i^{n+1}}{2(kr)^2} \left\{ (-i)^{n+1} + (i)^{n+1} + e^{-2ikr} \right\} \\ &= \frac{1}{2(kr)^2} \left\{ 1 + e^{-2ikr} \cdot (i)^{2n+2} \right\} \\ &= \frac{1}{2(kr)^2} \left\{ 1 + (-1)^{n+1} e^{-i2kr} \right\}. \end{aligned} \quad (\text{E.42})$$

Similarly,

$$\begin{aligned} ih_n^{(1)}(kr) \cdot \left[\frac{1}{kr} \cdot \frac{d}{dr} (rj_n(kr)) \right]^n &= \frac{i(-1)^{n+1}}{kr} \cdot e^{ikr} \cdot \frac{1}{2kr} \cdot \left\{ (i)^n e^{-ikr} + (-i)^n e^{ikr} \right\} \\ &= \frac{1}{2(kr)^2} \cdot \left[1 + i(-i) \cdot (-1)^{2n} e^{i2kr} \right] \\ &= \frac{1}{2(kr)^2} \left[1 + (-1)^n e^{i2kr} \right]. \end{aligned} \quad (\text{E.43})$$

So, adding I_1 and I_2 , we obtain:

$$\begin{aligned} I_1 + I_2 &= \frac{\pi k_2}{\omega \mu_2} \frac{1}{(kr)^2} \cdot \sum_{n=1}^{\infty} (2n+1) \times \\ &\quad \left[a_n^i a_n^{*sh} (1 + (-1)^{n+1} e^{-i2kr}) + b_n^i b_n^{*sh} (1 + (-1)^n e^{-i2kr}) \right. \\ &\quad \left. + a_n^{i*} a_n^{sh} (1 + (-1)^n e^{i2kr}) + b_n^{i*} b_n^{sh} (1 + (-1)^{n+1} e^{i2kr}) \right] \end{aligned} \quad (\text{E.44})$$

If we let $a_n^i a_n^{*sh} = a$, $b_n^i b_n^{*sh} = b$ and $(-1)^n e^{-i2kr} = c$, then we can write the expression within the square brackets as:

$$\begin{aligned} & a(1-c) + b(1+c) + a^*(1+c^*) + b^*(1-c^*) \\ &= (a+a^*) + (b+b^*) + c(b-a) - c^*(b^*-a^*) \end{aligned} \quad (\text{E.45})$$

$$= 2\text{Re}(a) + 2\text{Re}(b) + 2i\text{Im}(c(b-a)). \quad (\text{E.46})$$

Since,

$$W_t = -\frac{R^2}{2} \text{Re}[I_1 + I_2]. \quad (\text{E.47})$$

we obtain

$$W_t = -\frac{\pi}{k_2^2} \sqrt{\frac{\epsilon_2}{\mu_2}} \text{Re} \sum_{n=1}^{\infty} (2n+1) (a_n^i a_n^{*sh} + b_n^i b_n^{*sh}). \quad (\text{E.48})$$

and since the **total cross section** is defined as

$$Q_t = \frac{W_t}{\frac{1}{2} \sqrt{\frac{\epsilon_2}{\mu_2}}}. \quad (\text{E.49})$$

therefore:

$$Q_t = -\frac{2\pi}{k_2^2} \text{Re} \sum_{n=1}^{\infty} (2n+1) (a_n^i a_n^{*sh} + b_n^i b_n^{*sh}) \quad (\text{E.50})$$

Appendix F

A Vector Identity

We give the proof that the following vector identity holds good in the spherical polar coordinate system:

$$\nabla \times \nabla \times \mathbf{A} = \nabla(\nabla \cdot \mathbf{A}) - \nabla^2 \mathbf{A} \quad (\text{F.1})$$

In spherical polar coordinates, (r, θ, ϕ) , unit vectors at point \mathbf{P} are \mathbf{e}_r , \mathbf{e}_θ and \mathbf{e}_ϕ . Unlike the unit vectors in rectangular coordinates $(\mathbf{e}_x, \mathbf{e}_y, \mathbf{e}_z)$, \mathbf{e}_r , \mathbf{e}_θ , \mathbf{e}_ϕ are not constant vectors:

$$\begin{aligned} \mathbf{e}_r &= (\mathbf{e}_r \cdot \mathbf{e}_x)\mathbf{e}_x + (\mathbf{e}_r \cdot \mathbf{e}_y)\mathbf{e}_y + (\mathbf{e}_r \cdot \mathbf{e}_z)\mathbf{e}_z \\ \mathbf{e}_r &= \sin\theta \cos\phi \mathbf{e}_x + \sin\theta \sin\phi \mathbf{e}_y + \cos\theta \mathbf{e}_z \\ \mathbf{e}_r &= (\sin\theta \cos\phi, \sin\theta \sin\phi, \cos\theta) \quad (\text{Cartesian components}) \end{aligned} \quad (\text{F.2})$$

Similarly,

$$\mathbf{e}_\theta = (\cos\theta \cos\phi, \cos\theta \sin\phi, -\sin\theta) \quad \text{and} \quad (\text{F.3})$$

$$\mathbf{e}_\phi = (-\sin\phi, \cos\phi, 0) \quad (\text{F.4})$$

Thus,

$$\frac{\partial \mathbf{e}_r}{\partial r} = \mathbf{0} \quad \frac{\partial \mathbf{e}_\theta}{\partial r} = \mathbf{0} \quad \frac{\partial \mathbf{e}_\phi}{\partial r} = \mathbf{0}$$

$$\frac{\partial \mathbf{e}_r}{\partial \theta} = (\cos\theta \cos\phi, \cos\theta \sin\phi, -\sin\theta) = \mathbf{e}_\theta$$

$$\frac{\partial \mathbf{e}_r}{\partial \phi} = (-\sin\theta \sin\phi, \sin\theta \cos\phi, 0) = \sin\theta \mathbf{e}_\phi$$

$$\frac{\partial \mathbf{e}_\theta}{\partial \theta} = (-\sin\theta \cos\phi, -\sin\theta \sin\phi, -\cos\theta) = -\mathbf{e}_r$$

$$\frac{\partial \mathbf{e}_\theta}{\partial \phi} = (-\cos\theta \sin\phi, \cos\theta \cos\phi, 0) = \cos\theta \mathbf{e}_\phi$$

$$\frac{\partial \mathbf{e}_\phi}{\partial \theta} = (0, 0, 0) = \mathbf{0}$$

$$\frac{\partial \mathbf{e}_\phi}{\partial \phi} = (-\cos\phi, -\sin\phi, 0) = -\sin\theta \mathbf{e}_r - \cos\theta \mathbf{e}_\theta$$

Let us define an arbitrary vector function \mathbf{A} :

$$\mathbf{A} = A_r(r, \theta, \phi) \mathbf{e}_r + A_\theta(r, \theta, \phi) \mathbf{e}_\theta + A_\phi(r, \theta, \phi) \mathbf{e}_\phi.$$

The **Laplacian** operator ∇^2 in spherical polar coordinates is given by:

$$\nabla^2 \equiv \frac{1}{r^2 \sin\theta} \left[\frac{\partial}{\partial r} \left(r^2 \sin\theta \frac{\partial}{\partial r} \right) + \frac{\partial}{\partial \theta} \left(\sin\theta \frac{\partial}{\partial \theta} \right) + \frac{\partial}{\partial \phi} \left(\frac{1}{\sin\theta} \frac{\partial}{\partial \phi} \right) \right]$$

The first term(operator) does not *act* on \mathbf{e}_r , \mathbf{e}_θ or \mathbf{e}_ϕ by virtue of Eqn F.5. If we carry out straight forward differentiation, we obtain:

$$\frac{\partial}{\partial r} \left(r^2 \sin\theta \frac{\partial}{\partial r} (A_r \mathbf{e}_r) \right) = \left\{ \frac{\partial}{\partial r} \left(r^2 \sin\theta \frac{\partial A_r}{\partial r} \right) \right\} \mathbf{e}_r \quad (\text{F.5})$$

$$\frac{\partial}{\partial r} \left(r^2 \sin\theta \frac{\partial}{\partial r} (A_\theta \mathbf{e}_\theta) \right) = \left\{ \frac{\partial}{\partial r} \left(r^2 \sin\theta \frac{\partial A_\theta}{\partial r} \right) \right\} \mathbf{e}_\theta \quad (\text{F.6})$$

$$\frac{\partial}{\partial r} \left(r^2 \sin\theta \frac{\partial}{\partial r} (A_\phi \mathbf{e}_\phi) \right) = \left\{ \frac{\partial}{\partial r} \left(r^2 \sin\theta \frac{\partial A_\phi}{\partial r} \right) \right\} \mathbf{e}_\phi \quad (\text{F.7})$$

Similarly for the θ and ϕ parts, we obtain:

$$\begin{aligned} \frac{\partial}{\partial \theta} \left(\sin\theta \frac{\partial}{\partial \theta} (A_r \mathbf{e}_r) \right) &= -\sin\theta A_r \mathbf{e}_r + \sin\theta \frac{\partial A_r}{\partial \theta} \mathbf{e}_\theta \\ &\quad + \left\{ \frac{\partial}{\partial \theta} (\sin\theta A_r) \right\} \mathbf{e}_\theta + \left\{ \frac{\partial}{\partial \theta} \left(\sin\theta \frac{\partial A_r}{\partial \theta} \right) \right\} \mathbf{e}_r \end{aligned} \quad (\text{F.8})$$

$$\begin{aligned} \frac{\partial}{\partial \theta} \left(\sin\theta \frac{\partial}{\partial \theta} (A_\theta \mathbf{e}_\theta) \right) &= -\left\{ \frac{\partial}{\partial \theta} (\sin\theta A_\theta) \right\} \mathbf{e}_r - \sin\theta A_\theta \mathbf{e}_\theta \\ &\quad - \sin\theta \frac{\partial A_\theta}{\partial \theta} \mathbf{e}_r + \left\{ \frac{\partial}{\partial \theta} \left(\sin\theta \frac{\partial A_\theta}{\partial \theta} \right) \right\} \mathbf{e}_\theta \end{aligned} \quad (\text{F.9})$$

$$\frac{\partial}{\partial \theta} \left(\sin\theta \frac{\partial}{\partial \theta} (A_\phi \mathbf{e}_\phi) \right) = \left\{ \frac{\partial}{\partial \theta} \left(\sin\theta \frac{\partial A_\phi}{\partial \theta} \right) \right\} \mathbf{e}_\phi \quad (\text{F.10})$$

$$\begin{aligned} \frac{\partial}{\partial \phi} \left(\frac{1}{\sin \theta} \frac{\partial}{\partial \phi} (A_r \mathbf{e}_r) \right) &= -\sin \theta A_r \mathbf{e}_r - \cos \theta A_r \mathbf{e}_\theta \\ &+ 2 \frac{\partial A_r}{\partial \phi} \mathbf{e}_\phi + \left\{ \frac{\partial}{\partial \phi} \left(\frac{1}{\sin \theta} \frac{\partial A_r}{\partial \phi} \right) \right\} \mathbf{e}_r \end{aligned} \quad (\text{F.11})$$

$$\begin{aligned} \frac{\partial}{\partial \phi} \left(\frac{1}{\sin \theta} \frac{\partial}{\partial \phi} (A_\theta \mathbf{e}_\theta) \right) &= -\cos \theta A_\theta \mathbf{e}_r - \frac{\cos^2 \theta}{\sin \theta} A_\theta \mathbf{e}_\theta \\ &+ 2 \frac{\cos \theta}{\sin \theta} \frac{\partial A_\theta}{\partial \phi} \mathbf{e}_\phi + \left\{ \frac{\partial}{\partial \phi} \left(\frac{1}{\sin \theta} \frac{\partial A_\theta}{\partial \phi} \right) \right\} \mathbf{e}_\theta \end{aligned} \quad (\text{F.12})$$

$$\begin{aligned} \frac{\partial}{\partial \phi} \left(\frac{1}{\sin \theta} \frac{\partial}{\partial \phi} (A_\phi \mathbf{e}_\phi) \right) &= -\sin \theta A_\phi \mathbf{e}_\phi - \frac{\cos^2 \theta}{\sin \theta} A_\phi \mathbf{e}_\phi - 2 \frac{\partial A_\phi}{\partial \phi} \mathbf{e}_r \\ &- 2 \frac{\cos \theta}{\sin \theta} \frac{\partial A_\phi}{\partial \phi} \mathbf{e}_\theta + \left\{ \frac{\partial}{\partial \phi} \left(\frac{1}{\sin \theta} \frac{\partial A_\phi}{\partial \phi} \right) \right\} \mathbf{e}_\phi \end{aligned} \quad (\text{F.13})$$

Thus we observe that $\nabla^2 \mathbf{A} = \nabla^2 (A_r \mathbf{e}_r + A_\theta \mathbf{e}_\theta + A_\phi \mathbf{e}_\phi)$ will have components along \mathbf{e}_r , \mathbf{e}_θ and \mathbf{e}_ϕ . Therefore $(\nabla^2 \mathbf{A}) \cdot \mathbf{e}_r$ will be given by the sum of all the \mathbf{e}_r components obtained above (Eqns F.5.F.8.F.11):

$$\begin{aligned} (\nabla^2 \mathbf{A}) \cdot \mathbf{e}_r &= \left[\frac{\partial^2 A_r}{\partial r^2} + \frac{2}{r} \frac{\partial A_r}{\partial r} + \frac{\cos \theta}{r^2 \sin \theta} \frac{\partial A_r}{\partial \theta} + \frac{1}{r^2} \frac{\partial^2 A_r}{\partial \theta^2} - \frac{2}{r^2} A_r \right. \\ &\quad \left. - \frac{2}{r^2} \frac{\partial A_\theta}{\partial \theta} - \frac{2 \cos \theta}{r^2 \sin \theta} A_\theta + \frac{1}{r^2 \sin^2 \theta} \frac{\partial^2 A_r}{\partial \phi^2} - \frac{2}{r^2 \sin \theta} \frac{\partial A_\phi}{\partial \phi} \right] \end{aligned} \quad (\text{F.14})$$

Similarly,

$$\begin{aligned} (\nabla^2 \mathbf{A}) \cdot \mathbf{e}_\theta &= \frac{2}{r^2} \frac{\partial A_r}{\partial \theta} + \frac{2}{r} \frac{\partial A_\theta}{\partial r} + \frac{\partial^2 A_\theta}{\partial r^2} - \frac{A_\theta}{r^2} + \frac{\cos \theta}{r^2 \sin \theta} \frac{\partial A_\theta}{\partial \theta} \\ &+ \frac{1}{r^2} \frac{\partial^2 A_\theta}{\partial \theta^2} - \frac{\cos^2 \theta}{r^2 \sin^2 \theta} A_\theta + \frac{1}{r^2 \sin^2 \theta} \frac{\partial^2 A_\theta}{\partial \phi^2} - \frac{2 \cos \theta}{r^2 \sin^2 \theta} \frac{\partial A_\phi}{\partial \phi} \end{aligned} \quad (\text{F.15})$$

and

$$\begin{aligned} (\nabla^2 \mathbf{A}) \cdot \mathbf{e}_\phi &= \frac{2}{r^2 \sin \theta} \frac{\partial A_r}{\partial \phi} + \frac{2 \cos \theta}{r^2 \sin^2 \theta} \frac{\partial A_\theta}{\partial \phi} + \frac{2}{r} \frac{\partial A_\phi}{\partial r} + \frac{\partial^2 A_\phi}{\partial r^2} \\ &+ \frac{\cos \theta}{r^2 \sin^2 \theta} \frac{\partial A_\phi}{\partial \theta} + \frac{1}{r^2} \frac{\partial^2 A_\phi}{\partial \theta^2} + \frac{1}{r^2 \sin^2 \theta} \frac{\partial^2 A_\phi}{\partial \phi^2} - \frac{A_\phi}{r^2 \sin^2 \theta} \end{aligned} \quad (\text{F.16})$$

Now, since

$$\nabla \cdot \mathbf{A} = \frac{\partial A_r}{\partial r} + \frac{2}{r} A_r + \frac{\cos \theta}{r \sin \theta} A_\theta + \frac{1}{r} \frac{\partial A_\theta}{\partial \theta} + \frac{1}{r \sin \theta} \frac{\partial A_\phi}{\partial \phi} \quad (\text{F.17})$$

Therefore, $[\nabla(\nabla \cdot \mathbf{A})] \cdot \mathbf{e}_r = \frac{\partial}{\partial r}(\nabla \cdot \mathbf{A})$ is given by:

$$[\nabla(\nabla \cdot \mathbf{A})] \cdot \mathbf{e}_r = \frac{\partial^2 A_r}{\partial r^2} - \frac{2}{r^2} A_r + \frac{2}{r} \frac{\partial A_r}{\partial r} - \frac{\cos \theta}{r^2 \sin \theta} A_\theta + \frac{\cos \theta}{r \sin \theta} \frac{\partial A_\theta}{\partial r} - \frac{1}{r^2} \frac{\partial A_\theta}{\partial \theta} + \frac{1}{r} \frac{\partial^2 A_\theta}{\partial r \partial \theta} - \frac{1}{r^2 \sin \theta} \frac{\partial A_\phi}{\partial \phi} + \frac{1}{r \sin \theta} \frac{\partial^2 A_\phi}{\partial \phi \partial r} \quad (\text{F.18})$$

Similarly, $[\nabla(\nabla \cdot \mathbf{A})] \cdot \mathbf{e}_\theta = \frac{1}{r} \frac{\partial}{\partial \theta}(\nabla \cdot \mathbf{A})$ is given by:

$$[\nabla(\nabla \cdot \mathbf{A})] \cdot \mathbf{e}_\theta = \frac{1}{r} \frac{\partial^2 A_r}{\partial \theta \partial r} + \frac{2}{r^2} \frac{\partial A_r}{\partial \theta} + \frac{\cos \theta}{r^2 \sin \theta} \frac{\partial A_\theta}{\partial \theta} - \frac{1}{\sin^2 \theta} \frac{A_\theta}{r^2} + \frac{1}{r^2} \frac{\partial^2 A_\theta}{\partial \theta^2} + \frac{1}{r^2 \sin \theta} \frac{\partial^2 A_\phi}{\partial \theta \partial \phi} - \frac{\cos \theta}{r^2 \sin^2 \theta} \frac{\partial A_\phi}{\partial \phi}. \quad (\text{F.19})$$

and, $[\nabla(\nabla \cdot \mathbf{A})] \cdot \mathbf{e}_\phi = \frac{1}{r \sin \theta} \frac{\partial}{\partial \phi}(\nabla \cdot \mathbf{A})$ is given by:

$$[\nabla(\nabla \cdot \mathbf{A})] \cdot \mathbf{e}_\phi = \frac{1}{r \sin \theta} \left[\frac{\partial^2 A_r}{\partial \phi \partial r} + \frac{2}{r} \frac{\partial A_r}{\partial \phi} + \frac{\cos \theta}{r \sin \theta} \frac{\partial A_\theta}{\partial \phi} + \frac{1}{r} \frac{\partial^2 A_\theta}{\partial \phi \partial \theta} + \frac{1}{r \sin \theta} \frac{\partial^2 A_\phi}{\partial \phi^2} \right] \quad (\text{F.20})$$

Now,

$$\begin{aligned} \nabla \times \mathbf{A} = & \left\{ \left[\frac{1}{r} \frac{\partial A_\phi}{\partial \theta} + \frac{\cos \theta}{r \sin \theta} A_\phi - \frac{1}{r \sin \theta} \frac{\partial A_\theta}{\partial \phi} \right] \mathbf{e}_r \right. \\ & + \left[\frac{1}{r \sin \theta} \frac{\partial A_r}{\partial \phi} - \frac{A_\phi}{r} - \frac{\partial A_\phi}{\partial r} \right] \mathbf{e}_\theta \\ & \left. + \left[\frac{\partial A_\theta}{\partial r} + \frac{A_\theta}{r} - \frac{1}{r} \frac{\partial A_r}{\partial \theta} \right] \mathbf{e}_\phi \right\} \quad (\text{F.21}) \end{aligned}$$

Therefore,

$$[\nabla \times \nabla \times \mathbf{A}] \cdot \mathbf{e}_r = \left[\frac{1}{r} \frac{\partial^2 A_\theta}{\partial \theta \partial r} + \frac{\cos \theta}{r \sin \theta} \frac{\partial A_\theta}{\partial r} + \frac{1}{r^2} \frac{\partial A_\theta}{\partial \theta} + \frac{\cos \theta}{r^2 \sin \theta} A_\theta - \frac{1}{r^2} \frac{\partial^2 A_r}{\partial \theta^2} - \frac{\cos \theta}{r^2 \sin \theta} \frac{\partial A_r}{\partial \theta} - \frac{1}{r^2 \sin^2 \theta} \frac{\partial^2 A_r}{\partial \phi^2} + \frac{1}{r^2 \sin \theta} \frac{\partial A_\phi}{\partial \phi} + \frac{1}{r \sin \theta} \frac{\partial^2 A_\phi}{\partial \phi \partial r} \right] \quad (\text{F.22})$$

and,

$$[\nabla \times \nabla \times \mathbf{A}] \cdot \mathbf{e}_\theta = \left[\frac{1}{r^2 \sin \theta} \frac{\partial^2 A_\phi}{\partial \phi \partial \theta} + \frac{\cos \theta}{r^2 \sin^2 \theta} \frac{\partial A_\phi}{\partial \phi} - \frac{1}{r^2 \sin^2 \theta} \frac{\partial^2 A_\theta}{\partial \phi^2} - \frac{1}{r} \frac{\partial A_\theta}{\partial r} - \frac{\partial^2 A_\theta}{\partial r^2} - \frac{1}{r} \frac{\partial A_\theta}{\partial r} + \frac{1}{r} \frac{\partial^2 A_r}{\partial r \partial \theta} \right] \quad (\text{F.23})$$

and

$$\begin{aligned}
 [\nabla \times \nabla \times \mathbf{A}] \cdot \mathbf{e}_\phi &= \left[\frac{1}{r \sin \theta} \frac{\partial^2 A_r}{\partial r \partial \phi} - \frac{2}{r} \frac{\partial A_\phi}{\partial r} - \frac{\partial^2 A_\phi}{\partial r^2} - \frac{1}{r^2} \frac{\partial^2 A_\phi}{\partial \theta^2} \right. \\
 &\quad \left. - \frac{\cos \theta}{r^2 \sin \theta} \frac{\partial A_\phi}{\partial \theta} + \frac{A_\phi}{r^2 \sin^2 \theta} - \frac{\cos \theta}{r^2 \sin^2 \theta} \frac{\partial A_\theta}{\partial \phi} + \frac{1}{r^2 \sin \theta} \frac{\partial^2 A_\theta}{\partial \theta \partial \phi} \right] \quad (\text{F.24})
 \end{aligned}$$

Therefore we find, by comparing term by term, that:

$$\begin{aligned}
 [\nabla \times \nabla \times \mathbf{A}] \cdot \mathbf{e}_r &= [\nabla(\nabla \cdot \mathbf{A}) - \nabla^2 \mathbf{A}] \cdot \mathbf{e}_r \\
 [\nabla \times \nabla \times \mathbf{A}] \cdot \mathbf{e}_\theta &= [\nabla(\nabla \cdot \mathbf{A}) - \nabla^2 \mathbf{A}] \cdot \mathbf{e}_\theta \\
 [\nabla \times \nabla \times \mathbf{A}] \cdot \mathbf{e}_\phi &= [\nabla(\nabla \cdot \mathbf{A}) - \nabla^2 \mathbf{A}] \cdot \mathbf{e}_\phi
 \end{aligned}$$

Hence the proof.